İSTANBUL TECHNICAL UNIVERSITY ★ INSTITUTE OF SCIENCE AND TECHNOLOGY

THE IMPACT OF DIFFERENT FORMS OF SINGLE NATURAL VEGETATIVE ELEMENTS ON FLOW CHARACTERISTICS IN OPEN CHANNELS

Ph.D. Thesis by
Oral YAĞCI, M.Sc.

Department : **Civil Engineering**

Programme: **Water Engineering**

JULY 2006

İSTANBUL TECHNICAL UNIVERSITY ★ INSTITUTE OF SCIENCE AND TECHNOLOGY

THE IMPACT OF DIFFERENT FORMS OF SINGLE NATURAL VEGETATIVE ELEMENTS ON FLOW CHARACTERISTICS IN OPEN CHANNELS

Ph.D. Thesis by

Oral YAĞCI, M.Sc.

(501992421)

Date of submission : **11 May 2006**

Date of defence examination: **3 July 2006**

Supervisor (Chairman): **Prof. Dr. M. Sedat KABDAŞLI**

Members of the Examining Committee: **Prof.Dr. İsmail DURANYILDIZ**

Prof.Dr. İlhan AVCI

Prof.Dr. Yalçın YÜKSEL (YTÜ)

Prof.Dr. Lütfi SALTABAŞ (SÜ)

JULY 2006

ACKNOWLEDGEMENT

This doctoral thesis was prepared at the Hydraulics Laboratory of Istanbul Technical University under the supervision of Prof. Dr. M. Sedat Kabdaşlı. I am deeply indebted to my supervisor Prof. Dr. Kabdaşlı whom supported and helped me throughout my PhD study with his invaluable comments and advices. It was a great fortune and opportunity for me to studying under the supervision of him. I am always pleased to be his student and closely work with him.

I wish to thank the members of my committee, Prof. Dr. Yalçın Yüksel and Prof. Dr. İsmail Duranyıldız for their precious support and encouragement.

I had opportunity to conduct a part of my research in Environmental Management Research Center of Cardiff University in UK for a year. In this context I would express thanks to the institutions British Council and TUBITAK which supported my staying in UK for 8 months. I wish to thank to Dr. Catherine A.M.E. Wilson who supervised me during my staying in Cardiff University for her invaluable contributions. The friendly welcome of Dr. Wilson and her group made my stay both worthwhile and pleasant. Additionally the comments of my colleagues whom I met in Cardiff University Dr. Hans Peter Rauch from Universtity of Natural Resources and Applied Life Sciences in Vienna and Dr. Ingo Schnauder from Karlsruhe University were highly appreciated.

I would very much like to thank Phyllis Randall for editing and polishing the text with her native English.

I would express heartfelt thanks to my dear friends Tanju Akar, Nilay Elginöz Yaşa, Özgür V.Ş. Kırca, Avni Büyüközer, Alparslan Aydıngakko, Yalçın Işığaner Ahmet Ozan Çelik, Atakan Yüce, Adil Akgül, and Kutlu Darılmaz for all their help, interest and precious suggestions. Also I present my sincere thanks to Assoc. Prof. Şevket Çokgör for his valuable comments and encouragement during the study.

I received great support from the laboratory staff throughout the laboratory studies, and I would like to express my thanks to Hasan Yalçın, Mevlüt Uluçınar and Yaşar Aktaş. Especially without the valuable support and friendship of Hasan Yalçın completing the experimental stage could have been much more difficult.

Last but not least I would like to extend my hearty thanks to my mother Sezer Yağcı. Her love, support and encouragement were extremely important during my study. I would also like to present my deepest appreciation to my wife Nevin for her love, understanding and patience.

May, 2006 Oral YAGCI

TABLE OF CONTENTS

LIST OF TABLES

LIST OF FIGURES

NOMENCLATURE

γ	: Specific weight of the liquid
β	: Dimensionless measure of effective plant form
ϕ	: Constant to account for leaf incidence angle
α	: Density of vegetation
μ	: Fluid dynamic viscosity
ρ	: Mass density of water
μ	: Dynamic viscosity
λ	: Vegetal area coefficient
κ	: Von Karman's turbulance coefficient
τ_0	: Average boundary shear stress
ΔS	: Mean spacing between cylinders
τ_w	: Shear force per unit area on the channel boundary
ξ	: Vegetation intensity parameter
a	: Vegetation density
A	: Cross-sectional area of flow; MAA (momentum absorbing area)
A_0	: One side of leaf size
A_{frond}	: Frond surface area
A_h	: Projected area of vegetation onto horizontal plane
A_{stipe}	: Stipe area
a_z	: Approximate height of frond
B	: Channel width
C_D	: Drag coefficient for the vegetation
d	: Water depth
D	: Cylinder diameter
D_v	: Projection diameter
E	: Modulus of elasticity
F_D	: Drag force exerted on the vegetation
F_G	: Gravitational force
F_S	: Surface friction of the sidewalls and bottom
F_X	: Forces in the x direction
g	: Gravitational constant
H	: Average height of the vegetation in canopy
h	: Roughness height
h_{stipe}	: Stipe length
I	: Second increment of area of its cross-section
J	: Flexural rigidity of the vegetation
K	: Deflected height of the roughness elements
L	: Length of the channel
l_1	: Cross-wise length occupied by a tree
l_2	: Flow-wise length occupied by a tree
l_n	: Characteristic lengths defining spacing of plants
L_v	: Spacing of vegetation

m	: Number of roughness elements per unit area of channel bed
n	: Number of cylinders per unit area
$\mathbf{n_b}$	: Manning's boundary roughness coefficient
$\mathbf{n_w}$	: Sidewall resistance
P	: Wetted perimeter of channel
Q	: Flow discharge
R	: Hydraulic radius
$\mathbf{R_b}$	: Hydraulic radius of the bed
$\mathbf{R_w}$	: Hydraulic radius of walls
S	: Uniform flow friction slope
$\mathbf{S_e}$	: Energy gradient
U	: Mean velocity of the flow
$\mathbf{U}_u$	: Time averaged velocity in streamwise direction measured at the upstream of vegetative element
$\mathbf{U}_d$	: Time averaged velocity in streamwise direction obtained at the downstream of vegetative element
$\mathbf{U}_{mean}$	: Time averaged velocity in the streamwise direction
u_*	: Shear velocity
u	: Instantaneous velocity
$\mathbf{u'}$	: Fluctuation velocity
$\mathbf{u_{rms}}$	: Streamwsie turbulence intensity
$\mathbf{(u_{rms})_u}$	: Streamwise turbulence intensity measured at the upstream side of vegetative element
$\mathbf{(u_{rms})_d}$	: Streamwise turbulence intensity measured at the downstream side of vegetative element
$\mathbf{(w_{rms})_u}$	: Vertical turbulence intensity measured at the upstream side of vegetative element
$\mathbf{(w_{rms})_d}$	: Vertical turbulence intensity measured at the downstream side of vegetative element
$\mathbf{V_{veg}}$	: Occupied volume by vegetation for the given depth
Z	: Spanwise coordinate
$\mathbf{z_0}$	: Water depth

AÇIK KANALLARDAKİ FARKLI ŞEKİLLERE SAHİP TEKİL DOĞAL BİTKİLERİN HİDROLİK KARAKTERİSTİKLER ÜZERİNDEKİ ETKİSİ

ÖZET

Son yirmi yıldır artan çevre bilinci ile birlikte akarsu yatağındaki bitkilerin akım alanı üzerine etkisini araştıran çalışmalara olan ilgi oldukça artmıştır. Ancak bu alanda farklı türde bitki topluluklarının akım alanı üzerine etkisini araştıran pek çok araştırma yapılmış olmasına rağmen geniş gövdeli tekil ağaçlar gibi bitki türlerinin akım alanı üzerine etkisi henüz yeterince anlaşılmış değildir. Bu çalışmada bir akım ortamındaki tekil doğal bitkilerin akımın hız ve türbülans karakteristikleri üzerine etkisini araştırmayı amaçlayan iki boyutlu deneyler gerçekleştirilmiştir. Deneylerin tamamı 26 m uzunluğunda, 0.98 m genişliğinde ve 0.85 m derinliğindeki akım kanalında gerçek bitki fidanları kullanılarak gerçekleştirilmiştir. Taşkın yataklarında sıkça rastlanan bu doğa olayını analiz etmek amacıyla, geniş gövdeli ağaçlar hacim yükseklik değişimleri gözönüne alınarak üç başlıca sınıfa ayrılmıştır. Hız ölçümlerinde üç adet akustik Doppler velocimeter kullanılmıştır. Analiz aşamasında akım doğrultusundaki ve düşeydeki zamansal ortalama hız bileşenleri, akım doğrultusundaki ve düşeydeki türbülans bileşenleri ve türbülans kinetik enerjileri araştırılmıştır. Buna ilave olarak bitkinin mansab tarafında, bitkiden belirli bir mesafeye sahip konumda, bitkinin mimari özelliklerinin bir fonksiyou olarak hız profilini veren bir eşitlik elde edilmiştir. Elde edilen eşitliğin geçerliliği deney verileri aracılığı ile sınanmıştır. Deneyler sonucunda geçirimli yapılarına rağmen akım ortamındaki bitkilerin akımı kayda değer ölçüde etkilediği ve neden oldukları türbülans ile önemli miktarda enerjiyi kırdıkları görülmüştür.

THE IMPACT OF DIFFERENT FORMS OF SINGLE NATURAL VEGETATIVE ELEMENTS ON HYDRAULIC CHARACTERISTICS IN OPEN CHANNELS

SUMMARY

In the last two decades with the increasing environment awareness there is a growing interest on studies which attempt to understand the impact of vegetation on flow field in river and estuarine systems. Although in the past great attention has been devoted to explore the impact of vegetation community on flow pattern, the effect of singular vegetative element, such as trees with large trunk, on flow and turbulence pattern is not yet known.

In this study two dimensional experimental measurements, which aim to explore the impact of presence of natural singular vegetative elements on velocity and turbulence characteristics, were conducted. All the experiments were conducted in the flume with the size of 26m in length, 0.98m in width and 0.85m in depth and real tree saplings were utilized to represent the vegetative effect. In order to analyze this commonly observed nature phenomenon, trees with large trunk were classified into three groups on the basis of their volume versus height relation. Throughout the velocity measurements three Acoustic Doppler Velocimeters were employed. During the analysis time averaged streamwise and vertical velocity components, streamwise and vertical turbulence intensities and turbulence kinetic energy parameters were examined. Additionally a formulation, which gives the velocity profile at a certain downstream distance of vegetation, was introduced and the validity of the proposed formulation was verified with experimental data. Furthermore it was seen that despite their porous structures, the presence of vegetation considerably disturbs the flow field and dissipate a remarkable amount of energy by turbulence.

1. INTRODUCTION

1.1. Introduction

When the history of river engineering is examined, it is seen that there are two major concepts that is adopted by hydraulic researchers. Practitioners' designed straight and concrete lining channels for long years since it is uncomplicated to describe and solve the problem and also easier to construct the project in the field. However, this concept brought along with some problems. For instance, it was noted that in these sorts of straight channels, flow velocity considerably increases and this leads to potential risk of flood (**Mas, 2004**). As an alternative to this approach, in recent years a new concept called "river restoration" appeared. The primary objective of river restoration is to revitalize aquatic ecosystem and to minimize flood hazard as riverbanks are often considered as valuable agricultural lands (**Mas, 2004**). Further, Stephan and Gutknecht (2002) pointed out that natural roughness such as bank and floodplain vegetation, irregular cross-sections as well as bed roughness of different textures are often recommended for enhancing the variability in stream bed morphology and for improving habitat development. Furthermore, emergent vegetation along rivers and in floodplains consumes great momentum from flow and is often found to be in the region with the most roughness (**Fathi-Maghadam and Kouwen, 1997)**. On the other hand, presence of vegetation in bank and floodplains remarkably reduce channel capacity. **Stephan and Gutknecht (2002)** emphasized that in addition to ecological improvements due to macrophyte growth, there are also unfavourable hydraulic effects such as reduced cross-sectional area and increased river roughness**.** Increased roughness, that is, increased resistance causes a higher water level in vegetated regions compared to unvegetated regions. However, today the current environmental river restoration approach prefers to keep the natural riverbank and floodplain vegetation (**Jarvela, 2002a**). Estimation of the roughness coefficient with a sufficient accuracy in natural channel and flood plain systems is extremely important in many construction and river engineering problems. The depth of flow is mainly function of present vegetation specie, density etc. where flow passes through a vegetated field. In areas where the flow is through vegetation, the depth may be largely determined by the existing type of vegetation (**Fathi-Maghadam and Kouwen, 1997**).

In addition to these arguments, presence of vegetation in flow areas is an important element at the design stage of water resources. Examples where vegetation plays a major role are 1) rivers with heavily vegetated floodplains 2) roadside drainage ditches with thick tall vegetation; and 3) channels choked with aquatic weeds (**Petryk and Bosmajian, 1975**). Another aspect of the problem that determination of sediment transport in open channels is vital issue for hydraulic structures such as dams, power plants and turbines since sediment transport rate control the life of these hydraulic structures. It has been generally agreed that vegetation increases flow resistance, changes backwater profiles, and modifies sediment transport and deposition (**Yen, 2002**) Estimation of life of a dam correctly is quite important issue in terms of engineering concept. The flow and sediment transport characteristics in vegetated channels largely determined by vegetation depending on the vegetation type, density, branch pattern and flexural rigidity etc. Similarly, in civil and landscape engineering in order to mitigate soil erosion, vegetation is commonly used to attenuate the velocity of the wind (**Bache and MacAskill, 1984**). According to **Sellin (2003)**, from a practical point of view, it is advisable that the vegetation on bank and floodplain should be trimmed from their base in autumn and should be left them as are during the year. In this way, whilst vegetation increases the stabilization of the bottom they do not reduce the conveyance capacity of the channel.

1.2. Objectives

Some of the different aspects of the issue are discussed above. In the light of these facts, there is a growing interest on studies which effort to understand the impact of vegetation on flow field in river and floodplain systems. This explosion of interest is yield of the new concept described above. On the basis of this concept, many attempts have been undertaken to explore the interaction between flow and vegetation where flow through vegetation. Even though in the past large effort has been devoted to further understand the influence of a plant community on flow domain, the impact of a single vegetative elements on flow is not fully understood yet. Based on this idea, an experimental study was performed in Hydraulic

Laboratory of Istanbul Technical University. The major goal of this study was to further understand the effect of different forms of natural vegetative elements on flow characteristics.

2. LITERATURE REVIEW

2.1 Hydraulic Resistance in Vegetated Channels

Estimation of the flow resistance with an acceptable accuracy has great importance in river management, as it significantly affects the conveyance capacity of the channel, depth of the flow, velocity profile and hence sediment transport. Flow resistance problems in vegetated flow areas may be roughly classified into two groups: flow over submerged, short vegetation and flow through non-submerged, tall vegetation. Recent approaches in experimental studies as well as two and three-dimensional numerical models have used a drag force approach to model the stem drag imposed by plants. **Li and Shen (1973)** described four different factors that should be accounted in determining the drag coefficient: (1) the effects of open channel turbulence; (2) the effect of non-uniform velocity profile; (3) the free surface effects; and (4) the effects of blockage. Later on, **Linder (1982)** concluded that in densely vegetated channels, first two of these are of minor importance and can be neglected. In fact, the contribution of different vegetative roughness types to the total flow resistance largely depends on the type and combination of vegetation and exhibits considerable variability in time and space (**Jarvela, 2004a**). **Jarvela (2004a)** illustrated this by two examples considering a floodplain growing dense willows and grasses. First, in middle of a growing season, leaves on willows are likely to dominate the total drag, and bottom grasses may be only a minor source of flow resistance. Second, in winter, when the willows are leafless, the bottom grasses may contribute more than the willow stems to the total flow resistance.

The flow resistance through a given vegetated area is a function of many variables, i.e. velocity, distribution of vegetation in the streamwise vertical and lateral directions, roughness of the channel boundary as well as structural and hydrodynamic properties associated with the stems and leaves of the plants. In large number of studies, vegetative roughness were modeled or formulated treating plants as rigid cylinders (**Nepf and**

Vivoni, 2000; Nezu and Onitsuka, 2001, Shimuzu and Tsujimoto, 1994; Lopez and Garcia, 2001, Fisher-Antze et al., 2001; Cui and Neary, 2002; Choi and Kang; 2004). Another group of researchers (**Kouwen and Unny, 1973; Wu at al., 1999; Wilson et al., 2003, Baptist, 2003**) have used different artificial flexible elements to simulate plants in laboratory conditions. Owing to difficulties in simulating plants in the limited laboratory conditions, fewer experimental studies have been conducted with real plants (**Hasegawa et al., 1999; Jarvela, 2002a; Stephan and Gutknecht, 2001; Wilson and Horritt 2002; Fathi-Maghadam and Kouwen, 1997; Kouwen and Fathi, 2000; Carollo et al., 2002; Rauch, 2005**). However, representing the vegetative roughness with rigid stems has some drawbacks. Normally, for rigid stems, the drag is expected to increase with the square of the velocity. However, **Fathi-Maghadam and Kouwen (1997)** found that drag appears to have a linear relationship due to deflection of plant foliage area and reduction of drag coefficient with increasing the flow velocity for flexible roughness such as real tree models. **Erduran and Kutija (2003)** have introduced a quasi-three dimensional numerical solution and in order to take into account vegetation deflection they used cantilever beam theory. Further, **Çelik and Kabdaşlı (2004)** investigated the bending effect of the plants on velocity profiles. This is followed by **Wilson et al. (2006a)**, who investigated the influence of the applied simulation techniques (i.e. rigid stem or natural plant) on drag force and on velocity profiles. **Wilson et al. (2006a)** found that usage of uniform cylinder analogy resulted in an underestimation of the drag force in the region close to the bed and hence overestimation of both the velocity and the bed shear stress. In this section, the studies focused on hydraulic resistance in vegetated channels will be summarized as concise as possible.

In the literature one of the other first studies on vegetation - flow interaction is presented by **Petryk and Bosmajian (1975).** In their study, **Petryk and Bosmajian (1975)** proposed an analytical expression solving Manning Equation for the control volume where the flow occurs through vegetation. Considering the importance of understanding the assumptions and derivations of analytical solutions for practicing engineers, the derivation and assumptions of this expression is presented herein. Moreover it should be kept in mind that the assumptions limit the utilization of this proposed formula.

Petryk and Bosmajian (1975) used a relatively simple method to derive the flow resistance properties of emergent vegetation. In order to simplify the solution they assumed that the velocity is small enough to prevent a large degree of plant bending. Therefore, the projected area in the streamwise direction is not a function of the velocity. In fact, this assumption makes valid the solution only for where the vegetation is large woods **(Freeman et al., 2000)**. Besides, normally drag is expected to increase with the square of velocity. However, **Fathi and Kouwen (1997)** showed that for flexible roughness, drag appears to be linear relationship due to deflection of the plant foliage area (momentum absorbing area) and reduction of drag coefficient C_D with increasing velocity. **Petryk and Bosmajian (1975)** assumed the vegetation is distributed relatively uniformly in the lateral direction and large variations in average velocity do not occur laterally across the channel. Another assumption which was adopted by the researchers was that maximum flow depth is less than or equal to the average height of the vegetation, and large variations in flow velocity do not occur over the flow depth.

From momentum considerations, they equated the sum of the forces in the x direction to zero (see Figure 2.1).

$$\sum F_x = 0 \qquad \textbf{(2.1)}$$

In this case pressure forces in the x direction cancel, and the remaining forces are gravity, shear forces on the boundary caused by viscosity, wall roughness and drag forces on the plants. Equation 2.1 expands to give:

$$\gamma ALS - \sum D_i - \tau_w PL = 0 \qquad \textbf{(2.2)}$$

in which γ = specific weight of the liquid; A = cross-sectional area of flow; L = length of the channel; S = bed slope of channel; F_D = drag force on the *i*th plant; τ_w = shear force per unit area on the channel boundary; and P = the wetted perimeter of channel.

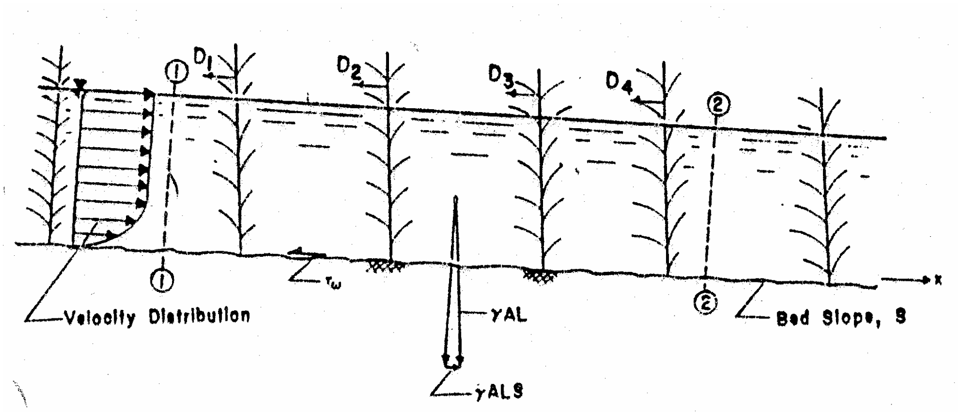

Figure 2.1: Flow resistance model which was written by **Petryk and Bosmajian (1975)**

The drag force on each plant may be described by

$$F_D = \frac{1}{2} C_D \frac{\gamma}{g} V_i^2 A_i = \frac{1}{2} C_D \rho V_i^2 A_i \qquad \textbf{(2.3)}$$

in which C_D = the drag coefficient for the vegetation; V_i = the average approach velocity to the i_{th} plant in the streamwise direction; and g = gravitational constant. The average boundary shear stress, τ_w, is conventionally derived in the form

$$\tau_w = \gamma \left(\frac{A}{P} \right) S_e \qquad \textbf{(2.4)}$$

in which S_e = the energy gradient due to the average shear stress on the boundary. Substituting the Manning formula which has the following form in English unit system

$$V = \frac{1{,}49}{n_b} \left(\frac{A}{p} \right)^{2/3} S_e^{1/2} \qquad \textbf{(2.5)}$$

into Equation 2.4, the following result is obtained for shear stress:

$$\left. \begin{aligned} \tau_w &= \gamma \left(\frac{A}{P} \right) V^2 \left(\frac{n_b}{1{,}49} \right)^2 \left(\frac{P}{A} \right)^{4/3} \\ \tau_w &= \gamma V^2 \left(\frac{n_b}{1{,}49} \right)^2 \left(\frac{P}{A} \right)^{1/3} \end{aligned} \right\} \qquad \textbf{(2.6)}$$

in which V = the area mean velocity; and n_b = Manning's boundary roughness coefficient excluding the effect of vegetation.

Substitution of Equations 2.3 and 2.6 into Equation 2.2, and assuming the approach velocity to each plant is V,

$$\gamma ALS - \frac{\gamma C_d V^2 \sum A_i}{2g} - \gamma V^2 \left(\frac{n_b}{1{,}49}\right)^2 \left(\frac{P}{A}\right)^{1/3} PL = 0 \qquad \textbf{(2.7)}$$

Dividing by γAL and solving for V^2, the following expression is obtained.

$$V^2 = \frac{S}{\dfrac{C_d \sum A_i}{2gAL} + \left(\dfrac{n_b^2}{1{,}49}\right)\left(\dfrac{P}{A}\right)^{4/3}} \qquad \textbf{(2.8)}$$

Expressing the average velocity according to the conventional Manning formula, and equating to Equation 2.10, one obtains

$$V^2 = \left(\frac{1{,}49}{n}\right)^2 \left(\frac{A}{P}\right)^{4/3} S = \frac{S}{\dfrac{C_d \sum A_i}{2gAL} + \left(\dfrac{n_b^2}{1{,}49}\right)\left(\dfrac{P}{A}\right)^{4/3}} \qquad \textbf{(2.9)}$$

in which n is the total roughness coefficient including boundary and vegetation effects. Solving for n from Equation 2.9, the required result for n is

$$\left.\begin{aligned} n &= n_b \sqrt{1 + \frac{C_d \sum A_i}{2gAL}\left(\frac{1{,}49}{n_b}\right)^2 \left(\frac{A}{P}\right)^{4/3}} \\ &\text{or} \\ n &= n_b \sqrt{1 + \frac{C_d \sum A_i}{2gAL}\left(\frac{1{,}49}{n_b}\right)^2 R^{4/3}} \end{aligned}\right\} \qquad \textbf{(2.10)}$$

in which R = the hydraulic radius.

Equation 2.10 which was proposed by **Petryk and Bosmajian (1975)** presents the "n" value in terms of the boundary roughness, n_b, the hydraulic radius, R, and the vegetation characteristics, $Cd\sum Ai/(AL)$. The expression $Cd\sum Ai/(AL)$ represents the vegetation area per unit length of channel per unit area of flow.

Petryk and Bosmajian (1975) noted two limiting solutions for Equation 2.10: 1) for the case of no vegetation, i.e. $Cd\sum Ai/(AL) = 0$, and the expected result $n = n_b$, 2) for the case in which most of the flow resistance is caused by vegetation, the second term in Equation 2.10 is much greater than 1 or

$$\frac{Cd\sum Ai}{2gAL}\left(\frac{1,49}{n_b}\right)^2 R^{4/3} >> 1 \qquad \textbf{(2.11)}$$

and Equation 2.10 reduces to

$$n = nb\sqrt{\frac{C_d\sum A_i}{2gAL}\left(\frac{1,49}{n_b}\right)^2 R^{4/3}} \qquad \textbf{(2.12)}$$

or

$$n = 1,49R^{2/3}\sqrt{\frac{C_d\sum A_i}{2gAL}} \qquad \textbf{(2.13)}$$

As it may be seen from the Equation 2.13, the equation is valid for constant vegetation density. According to **Petryk and Bosmajian (1975)**, this occurs in floodplains where the tree trunk is constant over the flow depth, or as the depth increases, the decrease in the trunk area is compensated by an increase in effective area due to branches and foliages. Furthermore, **Petryk and Bosmajian (1975)** found mean velocity by substituting Equation 2.13 into Manning formula, has a constant value of

$$V = \sqrt{\frac{2gAL}{C_d\sum A_i}}S^{1/2} \qquad \textbf{(2.14)}$$

and as expected, it is independent of the depth of flow.

In "flow-vegetation interaction" one of the primary complications is that there are different alternatives to define the reference area (e.g. wetted area, plan area), which can significantly influence the computed drag force. Among the other researchers, Wu et al. (1999) coupled the drag coefficient with the reference area into a bulk drag coefficient $C_D^{'}$, and used the concept "projected plant area per unit volume". Considering the practical importance of the study of **Wu et al. (1999),** the procedure briefly summarized below.

Wu et al (1999) proposed the method for emergent and submerged vegetation which may be employed during the investigation of variation of roughness coefficient. They developed a simplified model based on force equilibrium to evaluate the drag coefficient of vegetal elements. The Manning's equation is employed to convert the drag coefficient into the roughness coefficient. This process briefly as is described below.

Wu et al. (1999) conceptually divided the cross-section into sub-areas corresponding to sidewalls (A_w) and the bed (A_b). In other words:

$$A = A_w + A_b \qquad \textbf{(2.15)}$$

and

$$A = BD$$

where B = channel width and D = flow depth for a rectangular channel.

Further, they assumed that the average velocity is uniformly distributed over the entire cross-section. In this case for the metric system the Manning equation is as given below.

$$V = \frac{1}{n_w} R_w^{2/3} S^{1/2} \qquad \textbf{(2.16)}$$

$$V = \frac{1}{n_b} R_b^{2/3} S^{1/2} \qquad \textbf{(2.17)}$$

in which V = Q/A = the average velocity, Q = the flow discharge, S = for uniform flow friction slope or water surface slope or bed slope; n_w and n_b are the sidewall and bottom resistance respectively, R_w and R_b are the hydraulic radius corresponding to the walls and the bed respectively, and their expressions are:

$$R_w = \frac{A_w}{2D} \quad \textbf{(2.18)}$$

$$R_b = \frac{A_w}{B} \quad \textbf{(2.19)}$$

Employing $n_w = 0.01$ value which was given by **Chow (1959)** in the literature, R_w can be calculated. According to **Fathi-Maghadam and Kouwen (1997)** bed resistance, n_w, dominated by the vegetative roughness rather than surface friction of the bottom. Therefore in their study, **Wu et al. (1999)** represented vegetative roughness coefficient employing n_b. After calculating R_w, A_w, A_b, R_b, and n_b, can be obtained.

In order to estimate the drag coefficient for emergent condition of vegetation **Wu et al. (1999)** wrote force balance in the streamwise direction (Figure 2.2).

$$F_G=F_D+F_S \quad \textbf{(2.20)}$$

In which,

$$F_G = C_D(TBL)\frac{\rho V^2}{2} \quad \textbf{(2.21)}$$

Where F_D = drag force exerted on the vegetation; F_S = surface friction of the sidewalls and bottom; F_G = the gravitational force; ρ = mass density of water; g = gravity constant. Further in their study **Wu et al. (1999)** based on the study of **Fenzl (1962)** suggested that F_S is negligible. In such a case the drag of vegetation can be equated to the gravitational force (Equation 2.22), as shown in Figure 2.2.

$$F_G=F_D \quad \textbf{(2.22)}$$

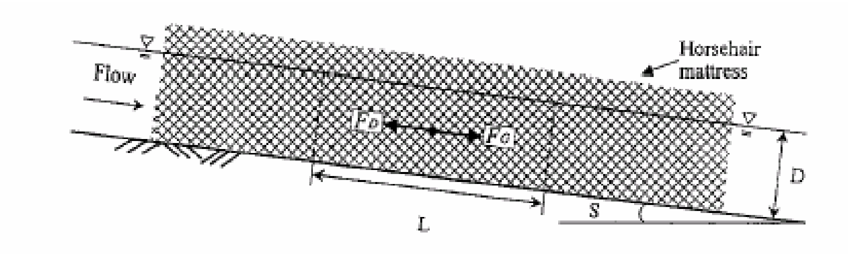

Figure 2.2: Definition Sketch of Force Balance for Emergent Vegetation Condition (**Wu et al., 1999**)

Wu et al. (1999) formulated classical drag force for vegetation:

$$F_D = C_D(\lambda LA)\frac{\rho V^2}{2} \quad \textbf{(2.23)}$$

where C_D = drag coefficient; λ = vegetal area coefficient representing the area fraction per unit length of channel and the magnitude of λ is dependent upon the vegetation type, density, and configuration; and λAL = total frontal area of vegetation in the channel reach L. Equating F_G and F_D gives

$$C'_D = \frac{2gS}{V^2} \quad \textbf{(2.24)}$$

in which C'_D=λC_D.

Also, **Wu et al. (1999)** obtained another drag coefficient expression for the submerged condition of vegetation. The derivation of the drag coefficient for submerged case is as given below.

According to **Wu et al. (1999)** for the submerged case differing from the emergent case there is a shear force, F_τ , between the vegetation and the overflow to balance the gravitational force, F_{G1}, for uniform flow (see Figure 2.3). In such a case the following expression is obtained.

$$F\tau = \rho g(BHL)S \quad \textbf{(2.25)}$$

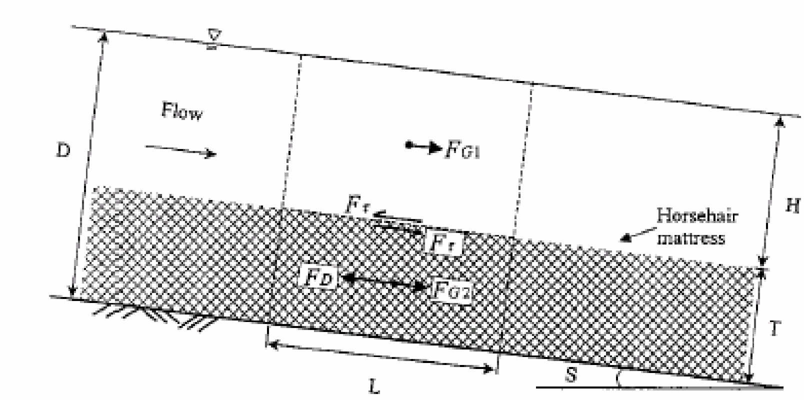

Figure 2.3: Definition Sketch of Force Balance for Submerged Vegetation Condition (**Wu et al., 1999**)

On the other hand, for the flow through the vegetation force balance becomes

$$F_D = F_{G2} + F_\tau \qquad \textbf{(2.26)}$$

In which T = height of vegetation. Equation 2. 26 leads to

$$F_D = C_D (TBL\lambda)\frac{\rho V^2}{2} \qquad \textbf{(2.27)}$$

Using force equilibrium the following equation is obtained.

$$C'_D = \left(\frac{D}{T}\right)\frac{2gS}{V^2} \qquad \textbf{(2.28)}$$

In their study, **Wu et al. (1999)** stated that their channel width-depth ratios are greater than 10 in most of the experiments. Further they also showed that the percentages of A_b/A are far far beyond those of A_w/A. This will lead to an immediate result of Rb ≅ D. Using Equation 2.17 as well as Equation 2.24 or Equation 2.28, one can convert the vegetal drag coefficient C'_D to the roughness coefficient n_b, i.e.

$$n_b = \left(\frac{D^{2/3}}{\sqrt{2g}}\right)\sqrt{C'_D}\ ; \qquad n_b = \left(\frac{D^{1/6}T^{1/2}}{\sqrt{2g}}\right)\sqrt{C'_D} \qquad \textbf{(2.29a,b)}$$

Equations 2.29a and 2.29b are used for emergent and submerged vegetation, respectively. One may notice that Equation 2.29a coincides with the results of **Petryk and Bosmajian (1975)** for heavily vegetated situation due to the fact that C'_D contains a factor of vegetation density λ.

However the assumptions which were used by **Wu et al. (1999)** such "F_s is negligible compared with F_D" and "bending of the mattress can be ignored" limit validity of the results for the real vegetation.

Jarvela (2002a) experimentally investigated the resistance of natural grasses, sedges and willows for various combinations of these species (i.e. the combinations: only sedges, sedges with leafy willows, sedges with leafless willows, only leafless willows, grasses, grasses with leafless willows) and different density and spacing. He mainly explored how type density, placement, depth and velocity influence friction losses. During the tests, the head losses were determined via differential pressure transducer and based on those experimental data it was claimed that the friction factor decreased with increasing Reynolds number, except in the series of leafless willows on bare bottom soil (Figure 2.4). As may be concluded form the Figure 2.4, sedges and leafy willows give the highest values of *f*, and produce the most scattered plot, but distinctive patterns are found when the data are classified according to flow depth. **Jarvela (2002a)** summarized the most notable experimental results as: the friction factor was dependent mostly on (1) the relative roughness in the case of grasses; (2) the flow velocity in the case of willows and sedges/grasses combined; and (3) the flow depth in the case of leafless willows on bare bottom soil. In his another studies, **Jarvela (2004a and b)** claimed that when compared to leafless conditions, the presence of leaves increased the friction factor up to seven fold and this is strongly dependent on the flow velocity.

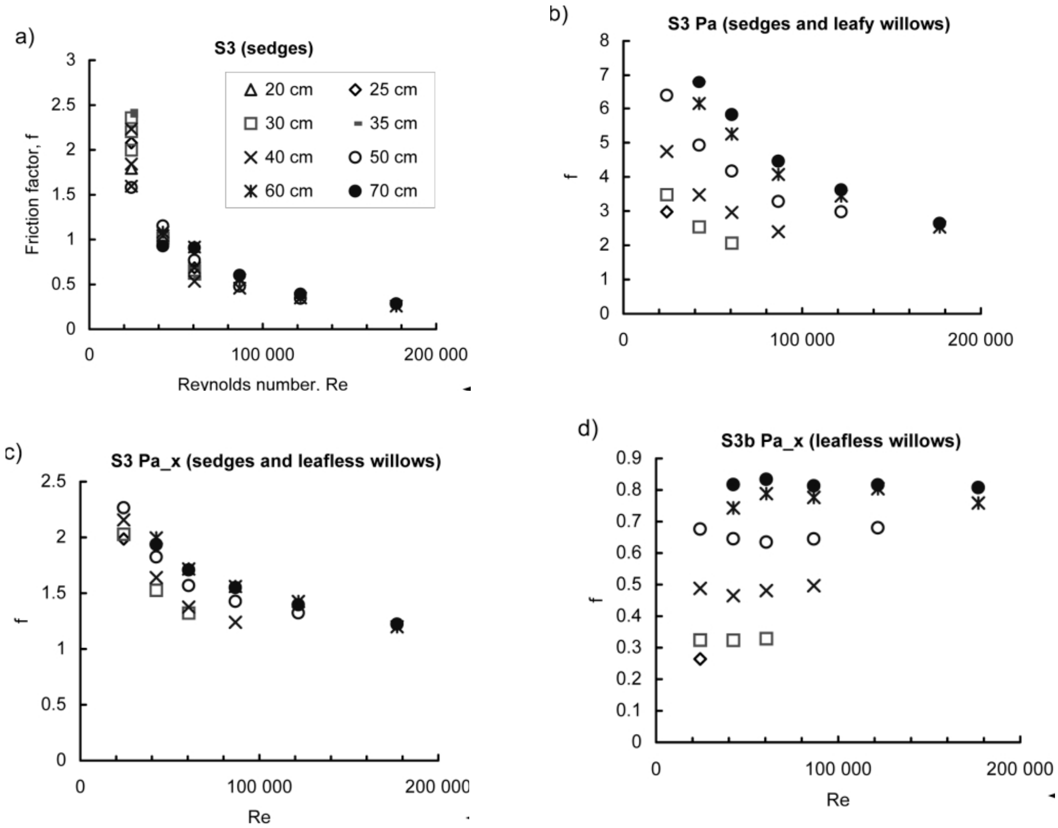

Figure 2.4: Friction factor versus Reynolds number for various sedges-willow combinations (**Jarvela, 2002**).

Fathi-Maghadam and Kouwen (1997) explored roughness of nonrigid nonsubmerged vegetation on floodplains and they pointed out that assuming vegetation on floodplains as rigid cylinders leads to large errors in the relationship between velocity and drag force. In their study in order to characterize the effect of vegetation on flow they used a dimensional analysis (Buckhingham $\prod$ theorem) and support it by experimental data.

They determined the parameters affecting the flow structure in a nonsubmerged non rigid vegetated channel for the dimensional analysis. The parameters proposed by **Fathi-Maghadam and Kouwen (1997)** are presented below.

$$f=(C_D, A_0, V, \rho, y_n, J, g, \mu, h, \phi, l_1....l_n) \quad \textbf{(2.30)}$$

in which; C_D = drag coefficient; A = MAA (momentum absorbing area) , which is closely related to the one-side area of leaves and stems; A_0 = One side of leaf size; V = mean channel stream velocity; ρ = mass density of water; y_n = depth of flow; J = flexural rigidity; g = gravitational constant; μ = fluid dynamic viscosity; h = average height of the vegetation in canopy; ϕ = constant to account for leaf incidence angle and l_n = characteristic lengths defining spacing of plants. Also for Equation 2.28 they employed the following assumptions.

1) Soil surface shear is negligible compared to the total plant drag.

2) Distribution of plant foliage and stems are randomly uniform in a horizontal plane.

3) Considerable change of biomass density can exist in the vertical direction.

Fathi-Maghadam and Kouwen (1997) considering C_D and ϕ are already dimensionless parameters they stated that C_D and ϕ are the first and the second dimensionless parameters. In their dimensional analysis, they assigned y_n, V and ρ parameters as repeated variables and obtained the following dimensionless parameters.

$$f_1(C_D, \phi, \frac{A_0}{y_n^2}, \frac{l_1}{y_n}, \frac{l_2}{y_n}, \frac{h}{y_n}, \frac{\rho V^2 y_n^4}{J}, \frac{V^2}{g y_n}, \frac{\rho V y_n}{\mu}) = 0 \qquad \textbf{(2.31)}$$

Further, considering A_0/y_n^2, l_1/y_n and l_2/y_n are independent of C_D, they obtained second dimensionless parameter A/a, which takes into consideration for the effect of density of vegetation, combining these three parameters with ϕ. Then they simplified that expression introducing the MAA of the tree, defined as A = ϕA_0. Then Equation 2.31 becomes

$$f_1(C_D, \frac{A}{a}, \frac{h}{y_n}, \frac{\rho V^2 y_n^4}{J}, \frac{V^2}{g y_n}, \frac{\rho V y_n}{\mu}) = 0 \quad \text{(for } y_n<h) \qquad \textbf{(2.32)}$$

The another assumption which was adopted **by Fathi-Maghadam and Kouwen (1997)** was that all individual uniformly shaped and spaced trees were placed in equal volume boxes in the canopy with horizontal surface of $a = l_1 l_2$ and vertical height of *h*, where l_1 and l_2 are cross and flow-wise lengths occupied by a tree.

Further **Fathi-Maghadam and Kouwen (1997)** highlighted that the friction factor is much more closely related to the ratio of MAA per unit volume of the canopy flow $\left[A/(ay_n)\right]$than with MAA per unit horizontal area (A/a). Then they assumed that MAA linearly increases with the increase of flow depth. Finally they multiplied the first three dimensionless parameters in Equation 2.32 and obtained the following combined expression.

$$C_d\left(\frac{A}{\forall}\right)h \qquad \textbf{(2.33)}$$

where $\forall = ay_n$.

In Equation 2.30 last two parameters are the Froude and Reynolds number, respectively. **Fathi-Maghadam and Kouwen (1997)** pointed out that since for practically all cases of interest, flow through dense nonsubmerged vegetation is in the fully turbulent zone, the flow is considered to be independent of the Reynolds number. Also **Koloseus and Davidian (1966)** have shown that resistance to flow in a uniform open channel is independent of the Froude number when the flow is stable [i.e. when no roll waves are present] **(Fathi-Maghadam and Kouwen, 1997)**. **Koloseus and Davidian, (1966)** have shown that for supercritical flow, the friction factor *f* for a rough channel of this type is independent of gravitational effects when the Froude number is less then 1.6, and is independent of viscous effect when flow is completely turbulent **(Fathi-Maghadam and Kouwen, 1997)**.

As a final point **Fathi-Maghadam and Kouwen (1997)** by limiting their study to subcritical and turbulent flow conditions and eliminating the Reynolds number and Froude number they gave the final relationship between dimensionless parameters for estimation of resistance to flow for non-submerged , tall, densely vegetated channels.

$$C_D\left(\frac{A}{\forall}\right)h = f_4\left(\frac{\rho V^2 y_n^4}{J}\right) \qquad \textbf{(2.34)}$$

According to the classical drag equation for rigid roughness the drag is expected to increase with the square of the velocity. However, in their study **Fathi-Maghadam and**

Kouwen (1997) concluded that for flexible roughness such as the tree models tested in their study, drag appears to be a linear relationship due to deflection of plant foliage area (MAA) and reduction of drag coefficient C_D with increasing the flow velocity.

2.2 Description of Velocity Profile in Vegetated Channels

In the existing literature, one of the first studies is presented by **Fenzl (1962)**. **Fenzl (1962)** presented a dimensional analysis for the conditions of uniform flow in a channel with constant bottom slope and no filtration **(Kouwen and Unny, 1973)**. In their study **Kouwen and Unny (1973)** gave this functional relationship, which was proposed by **Fenzl (1962)** as follow. However, that expression excludes surface tension.

$$\phi\left(\frac{\tau_0}{\rho U^2},\frac{U}{\sqrt{g y_n}},\frac{U y_n \rho}{\mu},\frac{\rho U^2 y_n^4}{J},\frac{k}{y_n},\frac{\lambda_1}{y_n},.....\frac{\lambda_n}{y_n},\beta\right)=0 \qquad \textbf{(2.35)}$$

Where τ_0 = the average boundary shear stress; ρ = the mass density; U_{mean} = the time averaged velocityin the streamwsie direction; g = the acceleration due to gravity; y_n = the normal depth; μ = the bdynamic viscosity; J = the flexural rigidity of the vegetation; k = the deflected height of the roughness elements; λ_1 λ_2 …λ_n = characteristic lengths defining spacing of plants; and β = a dimensionless measure of effective plant form. The assumptions which were adopted by **Fenzl (1962)** were 1) the soil characteristics are not important because of their small contribution to the drag; 2) the distribution of vegetation is random and uniformly dense **(Kouwen and Unny, 1973)**.

Using similar approaches, which were given above by **Fathi-Maghadam and Kouwen (1997)**, **Kouwen and Unny (1973)** neglected second and third terms (Froude number and Reynolds number) in the Equation 2.33. Also considering geometrical dimensionless parameters λ_1/y_n, … λ_n/y_n, vary within a small range due to the variation of y_n, they neglected λ_1/y_n, … λ_n/y_n parameters. Then they obtained the following expression.

$$\phi\left(\frac{\tau_0}{\rho U^2},,\frac{\rho U^2 y_n^4}{J},\frac{k}{y_n}\right)=0 \qquad \textbf{(2.36)}$$

Where J = EI = the flexural rigidity in bending; E = the modulus of elasticity; I = the second increment of area of its cross-section. Further they introduced the shear velocity $u_* = \sqrt{\tau_0 / \rho}$ as a new parameter in Equation 2.36 and rearranged the equation as below.

$$\frac{U}{u_*} = \phi\left(\frac{k}{\left(\frac{EI}{\rho u_*^2}\right)^{1/4}}, \frac{k}{y_n}\right) \tag{2.37}$$

Finally, **Kouwen and Unny (1973)** incorporated k/*h* and *m* terms into Equation 2.37 and proposed the final form of this equation as below.

$$\frac{U}{u_*} = \phi\left(\frac{h}{\left(\frac{mEI}{\rho u_*^2}\right)^{1/4}}, \frac{k}{h}, \frac{k}{y_n}\right) \tag{2.38}$$

Where h = the roughness height and m = the number of roughness elements per unit area of channel bed and thus represents the roughness density. Based on these findings **Kouwen and Unny (1973)** pointed out that the velocity distribution over natural and artificial flexible roughness can be represented by

$$\frac{u}{u_*} = \frac{u_k}{u_*} + \frac{1}{\kappa}\ln\left(\frac{y}{k}\right) \tag{2.39}$$

where u =the velocity at a distance, y, from the bed; u_* = the shear velocity, u_k =a characteristic or slip velocity at a distance y =k; κ = von Karman's turbulance coefficient. They integrated Equation 2.39 to yield the flow formula.

$$\frac{U}{u_*} = C_1 + C_2 \ln\frac{y_n}{k} \tag{2.40}$$

in which U = the mean velocity of the flow; y_n = the normal depth of the flow; and C_1 and C_2 are coefficients. If Equation 2.40 is valid then the factor. $1 / \left(\frac{mEI}{\rho u_*^2} \right)^{1/4}$ in Equation 2.38 should be a constant.

2.3 Characterization of Vegetation Density in Open Channels

Another crucial aspect of the problem is that the selected plant characterization method in representation of vegetative roughness. Various plant characterization methods were adopted by different researchers (**Petryk and Bosmajian, 1975; Nepf, 1999; Wilson et al., 2004**).

Nepf (1999) employed a different dimensionless parameter to describe a relationship between vegetation densities and drag force. The vegetation density description (Equation 2.37), which was proposed by **Nepf (1999)** excludes effect of stem morphology and flexibility and considers vegetations as rigid cylinders.

$$a = nd = \frac{dh}{\Delta S^2 h} = \frac{d}{\Delta S^2} \quad \textbf{(2.41)}$$

in which a = vegetation density (the projected plant area per unit volume (per meter)); n = the number of cylinders per unit area; ΔS = the mean spacing between cylinders; d = the cylinder diameter and h = the flow depth.

From Equation 2.41, **Nepf (1999)** defined a dimensionless population density as described below.

$$ad = \frac{d^2}{\Delta S^2} \quad \textbf{(2.42)}$$

For the rigid cylinder models *ad* represents the fractional volume of the domain occupied by plants.

Fischer-Antze et al. (2001) numerically modelled the submerged vegetation-flow interaction in a given open channel. They gave drag on a vegetative element, with unity height, as below.

$$F_{D,i} = \frac{1}{2}\rho U_i^2 C_D \lambda \qquad \textbf{(2.43)}$$

Where $F_{D,i}$ = the drag force; ρ = the mass density of water; U_i = the average velocity in time; C_D = the drag coefficient and λ = the vegetative coefficient. In their study Fischer-**Antze et al (2001)** described the vegetative coefficient, λ, as given below.

$$\lambda = \frac{\text{projected area of plant}}{\text{total volume}} = \frac{D}{s^2} \text{ or } \lambda_s = \frac{D}{sl} \qquad \textbf{(2.44)}$$

Where D = the diameter of a plant; s and l = the lengths of the control volume (Figure 2.5). Further **Fischer-Antze et al (2001)** pointed out that the experimental drag coefficient C_D, which corresponds to the shape and diameter of the vegetational elements, could be approximated as 1.0 for Reynolds numbers above 10^3 for a round shape of the projected area of the stems of bushes and trees.

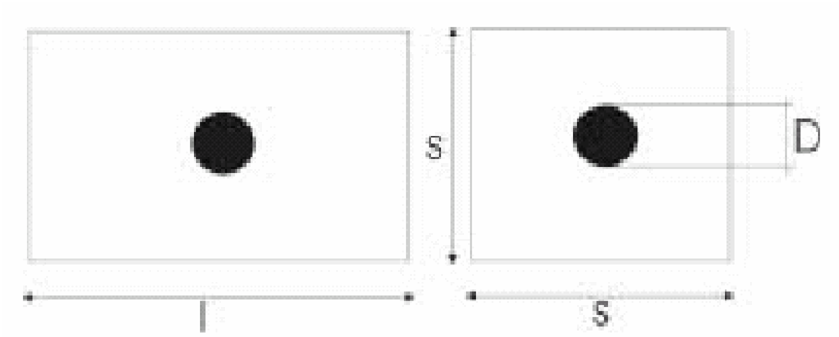

Figure 2.5: Definition of plant density λ

In their study **Wilson et al. (2003)** extended this definition and incorporated the effect of fronds into Equation 2.44. The expression proposed by **Wilson et al. (2003)** as given below.

$$\lambda_p = \frac{\text{Total Momentum Absorbing Area}}{\text{Total volume}} = \frac{A_{frond} + A_{stipe}}{s^2(a_z + h_{stipe})} \qquad \textbf{(2.45)}$$

Where, A_{frond} = the frond surface area; A_{stipe} = the stipe area; a_z = approximate height of frond when stretched and h_{stipe} = stipe length.

Nezu and Onitsuka (2001) and Nezu, (2005) investigated turbulent structures in partly vegetated open channel flows using LDA (laser doppler anemometer) and PIV (particle image velocimeter). In their study they used the following expression in order to characterize the vegetated area.

$$\alpha = \frac{H_v D}{L_v^2} \quad \textbf{(2.46)}$$

Where α=density of vegetation; H_v=flow depth; D=vegetation diameter; L_v=spacing of vegetation.

2.4 Turbulence in Flow through Vegetation

Turbulent transport of momentum, heat and mass dominates many of the fluid flows investigated in physics, fluid mechanics, hydraulic engineering and environmental engineering **(Nezu and Nakagawa, 1993)**. Furthermore, turbulent transport processes strongly influence the velocity distribution, the bed shear stress, sediment movement, and contaminant transport **(Nezu and Nakagawa, 1993)**. In this context understanding the turbulence where flow passes through vegetation is necessary in terms of hydraulic engineering. **Fairbanks and Diplas (1998)**, conducted experiments to investigate the turbulence structure of flow through rigid vegetation. They simulated the vegetation by a uniform array of acrylic dowels mounted to the bed of a hydraulic flume. During the analysis of the data **Fairbanks and Diplas (1998)** explored the skew of the longitudinal and vertical velocity histograms. In this way they endeavoured to detect the asymmetry in probability density function of the turbulent fluctuations. Skewed histograms are typically found in flows with strong gradients of turbulence intensity; in their study **Nezu and Onitsuka (2001)** investigated turbulent structures in partly vegetated open channels using PIV and LDA. They simulated vegetation by bronze cylinder rods with D=2mm. They performed the experiments in 10m long, 40cm wide and 30cm deep tilting flume. As is shown in Figure 2.6 they found that span-wise Reynolds stress $-\overline{uw}$

increases with an increase of z/B in the vegetated zone, and attains a peak near the junction between vegetated zone and non-vegetated zone. Where B=channel width; z=spanwise coordinate. **Nezu and Onitsuka (2001)** pointed out that a mutual interaction between these two zones becomes significant and suggests that horizantal vortices are generated.

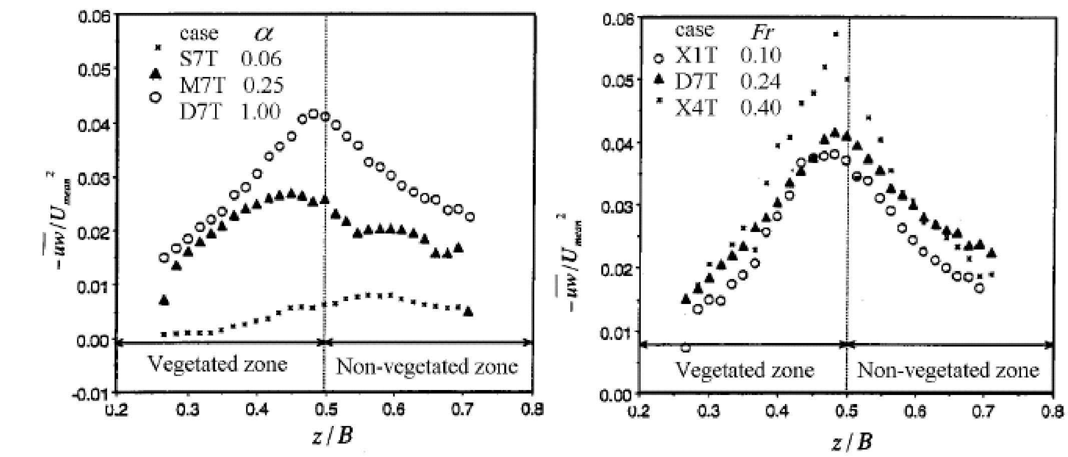

Figure 2.6: (a) Spanwise Reynolds stress for Fr=0.24 (vegetation density is changed) (b) Spanwise Reynolds stress for a=1.0 (Froude number is changed) (**Nezu and Onitsuka, 2001**)

Another important experimental result obtained by **Nezu and Onitsuka (2001)** is about instantaneous velocity fluctuations. As it may be seen from Figure 2.7 , researchers observed quasi-periodical velocity fluctuations and explained this by the horizontal vortex based on the studies which were carried out by **Naot et.al (1996), Nezu and Nakayama (1997)**. As it can be seen for the Figure 2.7 $\tilde{u}(t)$ takes a minimum value $\tilde{w}(t)$ tends to take the associated maximum value, and vice verse. **Nezu and Onitsuka (2001)** emphasized that in such situation spanwise Reynolds stress –u(t)w(t) is generated.

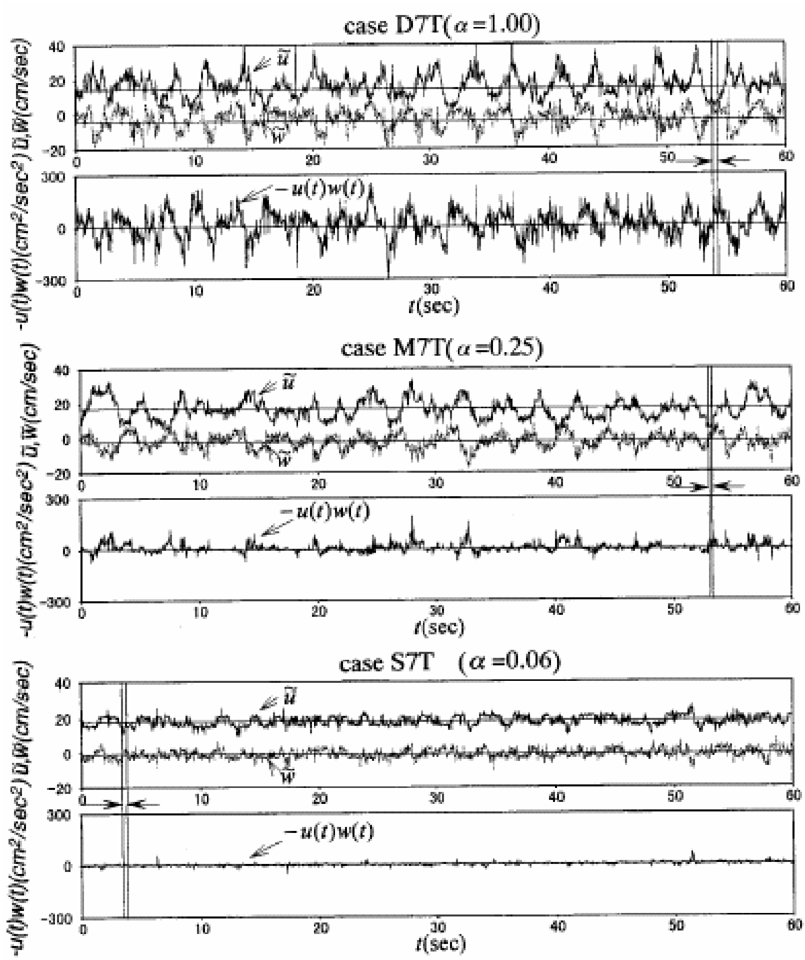

Figure 2.7: Instentaneous Velocity Fluctuations (**Nezu and Onitsuka, 2001**)

Further in their study, as it is seen in Figure 2.8, **Nezu and Onitsuka (2001)** observed the horizontal vortex, which has a central pivot in the non-vegetated zone, moves downstream. The vector in front of the horizontal vortex points from the vegetated zone to non-vegetated zone. Also another important result of the study, which was conducted by **Nezu and Onitsuka (2001)**, is that as judged from Figure 2.9 isolevel lines of the instantaneous streamwise velocity $\widetilde{u}(t)$ in the non-vegetated zone, which has high velocity values, bulge out ahead of the horizantal vortex towards the vegetated zone diagonally and also that the isolevel lines in the vegetated zone which has low velocity values, bulge out from the vegetated zone towards the region behind the horizontal vortex diagonally. The instantaneous spanwise velocity $\widetilde{w}(t)$ has a negative value in front of the horizontal vortex and has a positive value behind the vortex, as judged from

Figure 2.9. Therefore, the high momentum fluid is transported from the non-vegetated zone to the vegetated zone before the horizontal vortex passes and the low momentum fluid is transported from the vegetated zone to the non-vegetated zone after the horizontal vortex passes.

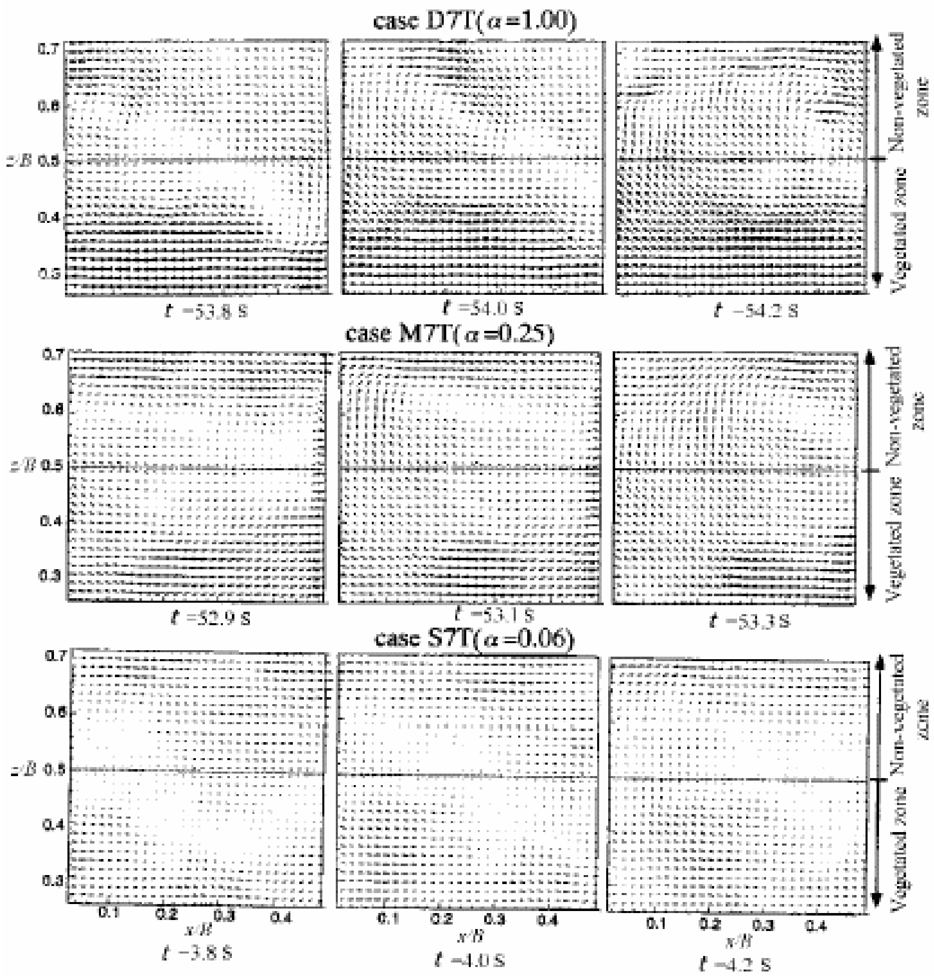

Figure 2.8: Vector Description of instantaneous velocity components (**Nezu and Onitsuka, 2001**)

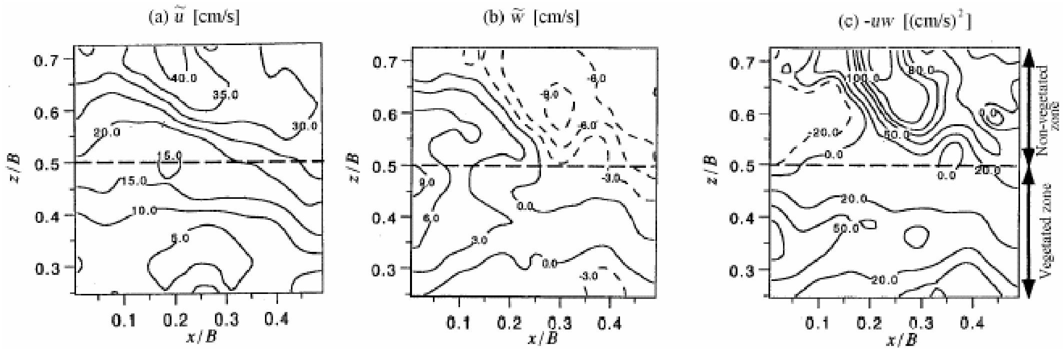

Figure 2.9: Contour lines of instantaneous velocities and Reynolds stress at t=54.0(s) in the case of D7T (a=1.0) (**Nezu and Onitsuka, 2001**).

2.5 Vegetation Architecture

Based on the explanations above, it is obvious that determination of the drag force imposed by vegetation has a special importance to describe the problem and the accompanying solution. There are basically three primary parameters in drag force expression (Equation 2.43) that need to be quantified with an acceptable accuracy: 1) drag coefficient, 2) velocity profile and 3) projected (or reference) area. In this context, projected (or reference) area of vegetation is closely related to architectural properties of the vegetation. This situation makes the problem further complicated since each species has a unique architectural property. Therefore, it might be a good approach to establish the species which are commonly observed in riverbank and floodplains as a first step.

Vegetation can be regarded as the objects with complex and porous structure. Owing to this complex structure, the crucial question is that what kind of method or procedure should be employed in the characterization of the vegetation. Thus, knowledge about the plant architecture helps better understanding the impact of vegetation on flow, depending on the geometric and biomechanical (flexural rigidity) properties of the plant specie. In this field, one of the first studies on this issue were undertaken by **McMohan (1975)** and **McMohan and Kronauer (1976)**. Based on their extensive experimental studies, the researchers have claimed that the branching pattern is approximately stationary within a plant specimen and a tree’s structure is elastically self similar. Hence, any patch of the structure is a model of the entire tree, and even whole species. Thanks to this result, the requirement of elastic similarity between models and prototypes, which is the most important similarity with respect to behaviour of a tree, is automatically satisfied. During their research, **McMohan and Kronauer (1976)** have applied the **Strahler (1952)** hierarchical ordering system to classify the branches in terms of their relationship with the trunk. **Jarvela (2002b)** found that the projected area of the willows appeared to increase linearly (R^2=98%) with the increasing flow depth excluding the base and tip zones of the plant. Branches contributed 2/3 to the total leafless projected area. Later on (**Wilson et al., 2006a**) found that the cumulative plant volume increases linearly with increasing basal diameter. If the velocity profile is fairly constant with plant height the projected area-plant height relationship may govern the drag force-height profile.

2.6 Summary and Conclusion

In the last couple of decades many studies have been undertaken attempting to explore the effect of vegetation on flow characteristics where the flow passes through vegetation. These studies may be classified as numerical and experimental studies. Probably due to the difficulties in simulating plants in the limited laboratory conditions, there have been fewer experimental studies conducted with real plants (**Hasegawa et al., 1999; Jarvela 2002a; Stephan 2001; Wilson and Horritt 2002; Fathi-Maghadam and Kouwen, 1997; Kouwen and Fathi-Maghadam, 2000; Carollo et al., 2002**).

Recent approaches in two and three-dimensional numerical models have used a drag force term in the momentum equations to model the stem drag imposed by plants (**Fischer-Antze et al., 2001; Stoesser et al., 2003; Choi and Kang, 2004, Wilson et al., 2006b**). As stated above, in most studies vegetative roughness were simulated by artificial rigid stems (**Nepf and Vivoni, 2000; Nezu and Onitsuka, 2001**) or different artificial flexible elements (**Kouwen and Unny, 1973; Wu at al., 1999; Baptist, 2003; Wilson et al., 2003**). Nevertheless representing the vegetative roughness with rigid stems has some drawbacks. Normally, for rigid stems, the drag is expected to increase with the square of the velocity. However, **Fathi-Maghadam and Kouwen (1997)** found that drag appears to have a linear relationship due to deflection of plant foliage area and reduction of drag coefficient with increasing the flow velocity for flexible roughness such as real tree models. Further, **Çelik and Kabdaşlı (2004)** investigated the bending effect of the plants on velocity profiles. This is followed by **Wilson et al. (2006a)**, who investigated the influence of the applied simulation techniques (i.e. rigid stem or natural plant) on drag force and on velocity profiles. They found that using the uniform cylinder analogy resulted in an underestimation of the drag force in the region close to the bed and hence overestimation of both the velocity and the bed shear stress. Another crucial aspect of the problem is that the selected plant characterization method in representation of vegetative roughness. Various plant characterization methods were adopted by different researchers (**Petryk and Bosmajian, 1975; Nepf, 1999; Wilson et al., 2004**).

The new concept, which tries to solve hydraulic engineering problems taking ecological balance into account, entails better knowledge about architectural and biomechanical properties of the plants since the impact of vegetation on flow field largely depend on these properties.

In the current situation, since there is no reliable method to select the proper roughness coefficient and no analytical way to determine velocity distribution of vegetated open channels, the current studies, which attempt to understand the impact of vegetation on flow field, use numerical (**Wilson et al., 2004; Stoesser et al., 2003; Fischer-Antze et al., 2001**) and experimental methods (**Petryk and Bosmajian, 1975; Tsujimoto et.al, 1991; Maghadam and Kouwen, 1997; Kouwen and Fathi-Maghadam, 2000; Carollo et al., 2002; Wilson and Horritt, 2002; Stephan and Gutknecht 2002; Jarvela, 2002a; Nepf and Vivoni, 2000; Nezu and Onitsuka, 2001; Fairbanks and Diplas, 1998; Nepf, 1999**).

3. THEORETICAL APPROACH

3.1 Introduction

In the previous chapter some of the examples from former researches were presented and discussed. As was seen there, in the last two decades a large number of attempts have been undertaken to further understand the interaction between flow and vegetation where the flow passes through a vegetated field. In these experimental studies, mostly researchers have preferred to simplify the problem employing a group of rigid stems or artificial elements in the experiments to model the vegetation group. Probably as a consequence of the complexity of the problem, only a few of these researchers were performed their experiments with real vegetation community. However, the effect of a singular vegetative element such as trees on flow and turbulence patterns is not yet known although in the past great attention has been devoted to explore the impact of a plant community on flow patterns. Knowledge about the relationship between an individual vegetative element and flow characteristics helps better the understanding of flow in floodplains. More specifically, only in this way is the impact of a singular vegetative element on transformation of velocity profile and turbulence structure clarified. This was the motivation for conducting a set of experimental studies which aimed to describe the effect of single vegetal elements such as trees with large trunks on flow domain characteristics. In this context, the decision about the goals and methods are crucial in terms of determining the scope and limits of the conducted study. The primary objective of the study was to experimentally investigate the impact of the presence of singular vegetation, such as a tree a large trunk, on flow field characteristics. In order to achieve the objective stated above, two dimensional experimental measurements were conducted in this study. The further details about the experimental details are presented in Chapter 4. The characterization method of the vegetal element and the scope of the study are presented and discussed in the following two chapters.

3.2 Classification of Vegetation

The importance of categorization and characterization of the vegetation is emphasized above. Vegetation can be classified by any number of criteria. However, in this study it is assumed that this classification may be carried out only based upon the architectural properties of vegetation (e.g., volume, height, diameter, canopy density, seasonal leaf area index LAI, submergence degree etc.) since it the unique property for a species and it directly affects the flow pattern where flow passes through a vegetated area. In the light of these facts, this classification was carried out considering principally the relationship between the parameters “volume” with “height” and this approach was called as “volumetric approach” hereafter. In order to introduce this classification in a more intelligible way Figure 3.1 is illustrated. As given in Figure 3.1, the vegetation types were classified as Type 1, Type 2 and Type 3 and hereafter this notation will be adopted. As a matter of fact the primary difference between those introduced types is the volume increment gradient along the height of the vegetation. The classification of different vegetation types were carried out based on this criteria. In this study, three tree species were selected to represent Type 1, Type 2 and Type 3 to simplify the problem. These species are *Pinus Pinea, Thuja Orientalis,* and *Cupressus Macrocarpa* respectively. In the controlled laboratory conditions, the variation of volume of Type 1, Type 2 and Type 3 with respect to height were determined by cutting trees into consecutive parts and measuring their volumes using measuring cylinders. Figure 3.2 presents the cumulative volume measuring procedures. Based on those measurements the variation of cumulative volume with height was obtained and depicted in Figure 3.3. Highlighting the difference “volume versus height” variation between three classes of vegetation is important in terms of further understanding the characterization and distinguishing properties of these there types. Basically, the main difference between the curves belonging to representative types is the variation of gradient of curves along the height. The gradient of Type 1 decreases along the height. In other words, the second derivation of curve for Type 1 is negative. In a way, this indicates that for given successive height intervals, the vegetation volume belonging to any interval is always larger than the volume of the interval belonging to the earlier one (the one closer to bed). For Type 3, the gradient of the curve increases through the height. On the other hand, the gradient belonging to Type 2 exhibit relatively constant appearance along the height.

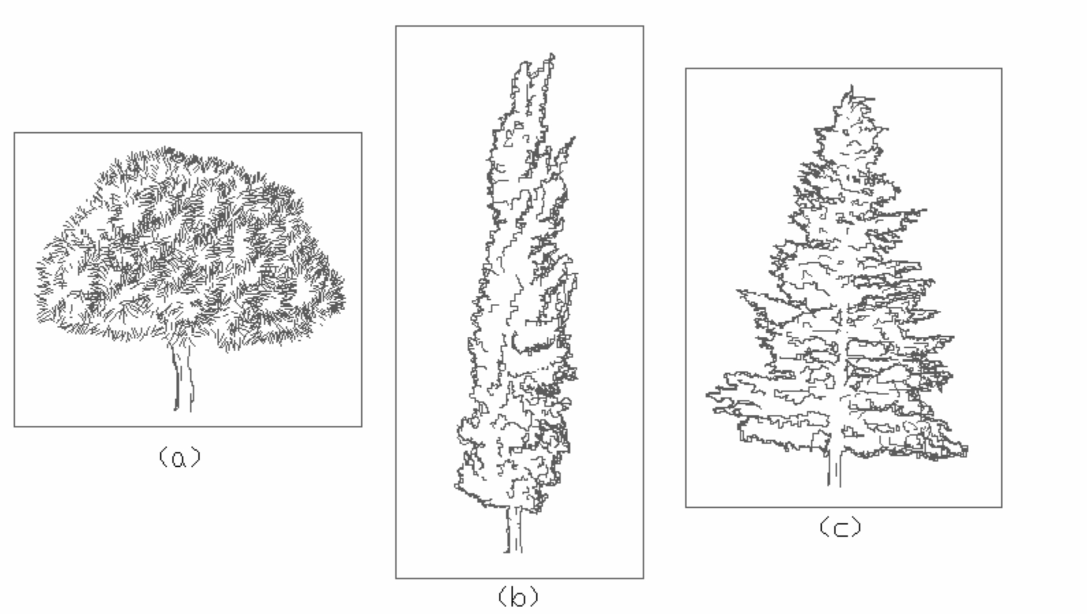

Figure 3.1: The classification of trees with large trunk based on the "volume versus height" variation. a) Type 1, b) Type 2, c) Type 3.

Establishing a relationship between flow field and parts of vegetation is necessary to identify and describe the impact of the presence of vegetation on flow characteristics. In order to facilitate the expression of this relation, the illustration in Appendix A were presented for 25 cm water depth. In these illustrations, as could be seen the submerged region is divided into two parts one is below and the other above $z/z_0=0.4$. The lower part of $z/z_0=0.4$ was named as "Zone 1", the upper of $z/z_0=0.4$ was called as "Zone 2" and the border between Zone 1 and Zone 2 was called the "interface". Hereafter, this classification was employed to facilitate the analysis.

(a)

(b)

Figure 3.2: Views of pine tree taken during the process of "cumulative volume versus height" measurements a) cutting process b) measuring the volume process

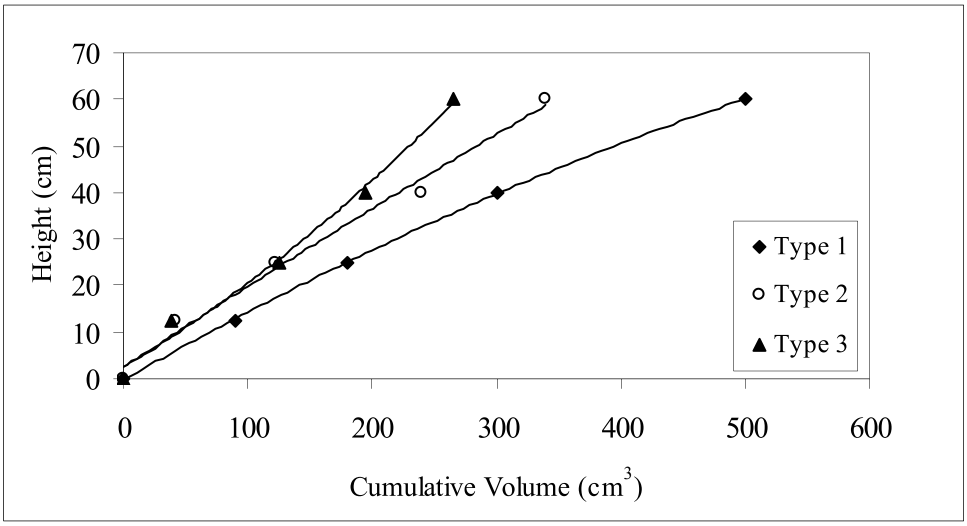

Figure 3.3: The variation of cumulative volume of with respect to height for Type 1, Type 2 and Type 3.

3.3 Characterization of Vegetation

As emphasized above, most of the studies in the literature were performed for a community of vegetation. Since each species has a unique architectural property, the obtained solutions were limited only for the specie which was exposed to the tests. The methods for characterization of vegetation density which were adopted by the earlier studies were presented and discussed in the previous chapter. However, since those studies were performed for a vegetation community, in those studies the characterization of vegetation was carried out mostly considering the intervals between vegetation and the density of vegetal community. Also, in most of those studies the projected area (onto vertical plane) of vegetation was used to identify the vegetated zone. Differing from the earlier works, in this study a new parameter which is called hereafter as "vegetation intensity parameter" (VIP) was introduced. The expression of vegetation intensity parameter (VIP) is given below.

$$\xi = \frac{\frac{V_{veg}}{z_0}}{A_h} \tag{3.1}$$

Where ξ= vegetation intensity parameter (VIP); V_{veg}=occupied volume by vegetation for the given depth; z_0= water depth; A_h=the projected area of vegetation onto horizontal plane. The expression of projected area was substituted in Equation 3.2 and 3.3. Dimensionless V_{veg}/z_0 explains the volume of vegetation occupied at unit depth. Dividing it by the area of projection of vegetation onto horizontal plane, vegetation intensity parameter obtained. In physical speaking, this gives the occupied volume by vegetation at unit projection area for the unit depth.

$$\xi = \frac{\frac{V_{veg}}{z_0}}{\frac{\pi D_v^2}{4}} = \qquad \textbf{(3.2)}$$

$$\xi = \frac{4V_{veg}}{\pi D_v^2 z_0} \qquad \textbf{(3.3)}$$

where D_v=the projection diameter which was quantified before the experiments for the projected area calculation. The projection diameters belong to tree saplings which were used through the projection area calculation are 48 cm, 39 cm, 36 cm for 25 cm depth (water depth condition 1) and 55 cm, 39 cm, 36 cm for 40 cm depth (water depth condition 2) respectively. Based on these values the average tree diameter can be calculated and given as 41cm for 25 cm depth and 43.3 cm for 40 cm depth. The VIP values of the three tree sapling were ξ_1=0.00398; ξ_2=0.00409; ξ_3=0.00492 for 25 cm depth and ξ_1=0.00316 and ξ_3=0.00480 for 40 cm water depth.

3.4 Analysis Method

In order to achieve the objectives of the study explained above, a set of experiments were conducted by following the procedure which is described in Chapter 4. Concisely, the comparisons were undertaken between the flow characteristics at the upstream and downstream of the singular vegetation. The velocity measurements were employed at the locations which have the name of c100 and c360 (Figure 4.4) to check the velocity characteristics belong to upstream and downstream side of the vegetative element. The location of the vegetative element was at c320 (Figure 4.4) which means that there was a 220 cm between upstream measurement point and axis of vegetal element and it is assumed that the flow characteristics measured at this point characterize the non-disturbed flow. Additionally, there was 40 cm between downstream measurement point and axis of base pertains to vegetal element. Unless this length is expressed in terms of vegetative characteristics it does not make any sense. In the light of this fact it would be convenient to express these distance values in terms of vegetative characteristics. It was considered that using the projection diameters was adequate expressive for this purpose and could constitute a reference for the future studies. When it is considered that average projection diameter is 41 cm and 43.3 cm for the water depth values of 25 cm and 40 cm respectively, it may be stated that the downstream measurements were performed approximately at one projection diameter. In summary, the velocity measurements which were preformed at 220 cm upstream side of the vegetation were used to characterize the non disturbed flow at the upstream. The velocity data which were obtained from the point located circa at the $1D_v$ downstream side of the vegetation were used to characterize the downstream flow. As explained in the next chapter, in addition to these two characterizing points, further velocity measurements were performed in 13 other vertical profiles at the centerline of the flume.

After the data acquisition and processing, the time averaged mean velocity values were plotted for the upstream and downstream of vegetation. In this context, it was sensible to focus on transformation of velocity profile in consequence of presence of vegetation. Based on this idea, the velocity difference parameter was described as given in Equation 3.4.

$$VDP = U_u - U_d \qquad \textbf{(3.4)}$$

Where U_u= the time averaged velocity in streamwise direction obtained at the upstream of vegetative element; U_d= the time averaged velocity in streamwise direction obtained at the downstream of vegetative element; VDP=velocity difference parameter.

In most textbooks, instantaneous velocity "u" may be described as is given in Equation 3.5. Here, the quantity U_{mean} denotes the time averaged velocity and u′ is the fluctuation component. In most general forms, time average value is then defined by Equation 3.6 (**Sümer et al, 1982; Hinze, 1959; Stanisic, 1988**). However the definition of time averaged velocity, U_{mean}, may be described using Equation 3.7 for a finite number of data sampling. Throughout the experiments the sampling frequency was 200Hz and the duration of data collection for each individual measurement point was 1 minute, hence the "n" was equal to 12000 for each single measurement point which can be regarded as large sampling number from the statistical point of view. The analysis method of turbulence due to vegetative element is considered in the following paragraphs.

$$u = U_{mean} + u' \qquad \textbf{(3.5)}$$

$$U_{mean} = \lim_{T \to \infty} \frac{1}{T} \int u dt \qquad \textbf{(3.6)}$$

$$U_{mean} = \frac{1}{n} \sum_{i=1}^{n} u(t_i) \qquad \textbf{(3.7)}$$

Where U_{mean}= time averaged velocity in streamwise direction; n=sampling number; u= instantaneous velocity. However, the results obtained via VDP were not dimensionless and thus those were not adaptable for the future studies. With the normalization of VDP, the obtained results would be expressed in a more applicable form in terms of future studies. For this purpose normalized velocity difference parameter (NVDP) which is given in Equation 3.8 was utilized through the analysis given below.

$$NVDP = 1 - \frac{U_d}{U_u} \qquad \textbf{(3.8)}$$

In physical speaking, Equation 3.8 gives the retaining percentage of time averaged velocity due to presence of vegetation. Although NVDP has a dimensionless form, it is not a function of the vegetation characteristics. In other words, the obtained results are conclusive only for the vegetation which was exposed to the tests. Hence the NVDP also should be expressed in terms of vegetal element characteristics to convert the results to more applicable, comparable and transferable form for the future studies. For this purpose Equation 3.9 was introduced which takes the vegetation intensity parameter into account to characterize the vegetation.

$$NVVDP = \frac{\left(1 - \frac{U_d}{U_u}\right)}{\xi} \qquad \textbf{(3.9)}$$

Where U_u= the time averaged velocity in streamwise direction obtained based on the measurements undertaken at the upstream of vegetative element; U_d= the time averaged velocity in streamwise direction obtained based on the measurements undertaken at the downstream of vegetative element; NVVDP= normalized vegetative velocity difference parameter; ξ= vegetation intensity parameter. During the analysis the variation of NVVDP with respect to relative depth for different test conditions were plotted. In order to describe the impact of vegetation on primary characteristic of flow domain such as time average velocity, logarithmic velocity profile was modified based on the obtained relationship between "NVVDP versus relative depth" and a new formulation was introduced. The proposed formulation allows predicting transformed time averaged mean velocity values due to vegetation as a function of vegetation characteristics. The verification of the proposed formulation was checked by the experimental data. The derivation of the formulization and the verification is given in Chapter 5 together with the analyzing of the data.

In addition to understanding the deflection of velocity profile due to vegetation, knowledge about the disturbance length of flow due to existence of vegetation is also important. Based on this fact, the velocity field at the downstream side of vegetation was also further explored through the centerline of flow. This was carried out by using experimentally obtained 15 velocity profile located at the downstream of vegetative element. At this stage the software named "Tecplot v10.0" was utilized for the interpolation process.

Knowledge about the influence of vegetation on neighbor velocity profiles is required in terms of describing the influence of placement interval of vegetative elements in a floodplain on conveyance capacity. Moreover, these measurements are essential so as to assure whether continuity is satisfied or not. For this purpose, additional velocity measurements were executed along the depth at the consecutive locations denoted as c300, r300, r320, and r360 in Figure. 4.4. It was considered that expressing the lateral distance between these measurement points and the vegetative element in terms of vegetative characteristics is necessary due to the similar reasons explained above. The lateral distance between these measuring points was 25 cm and this value approximately corresponds to $0.6D_v$. The non-disturbed velocity profiles and the velocity profile which is located at the same cross-section with vegetative element were compared and analyzed to asses the influence of vegetative element in spanwise direction.

The variation of time averaged vertical velocity due to vegetation was also explored. In order to make a comparison possible the time averaged vertical velocity versus relative depth were plotted for the non-disturbed case. Next, the relationships between the same parameters were attained for the downstream of vegetation. Similar normalization procedures, which are carried out for time averaged mean velocity, were applied for time averaged vertical velocity as well.

With regard to additional turbulence which occurs due to presence of vegetation where the flow passes through vegetative element, similar analysis methods were implemented for both streamwise and vertical component of the turbulence. Thus, the descriptions presented in this paragraph are given for both streamwise and vertical turbulence assessment. So as to facilitate the explanations, the schematic representation of a time series belonging to a velocity record is illustrated in Figure 3.4. From the statistical point of view, the variance of a time series is a measure of the scattering of data around the mean value. In this context, this scattering corresponds to velocity fluctuation around a mean value for a time series obtained by velocity record. In a way, the increment of this scattering indicates increasing turbulence. Based on Figure 3.4 and Equation 3.5 the fluctuation part of the velocity can be rewritten as given in Equation 3.10. The variance of fluctuation component of the velocity is given in Equation 3.11. Equation 3.12 is acquired substituting Equation 3.10 into 3.11. However, the unit of Equation 3.12 is not in velocity dimension. Hence, to provide the uniformity between the units, the square root of the Equation 3.12 is taken and the standard deviation of fluctuation is attained (**Nezu and Onitsuka, 2001**). The obtained expression of standard deviation (Equation 3.13) is the definition of streemwise “u_{rms}” and vertical “w_{rms}” turbulence intensity.

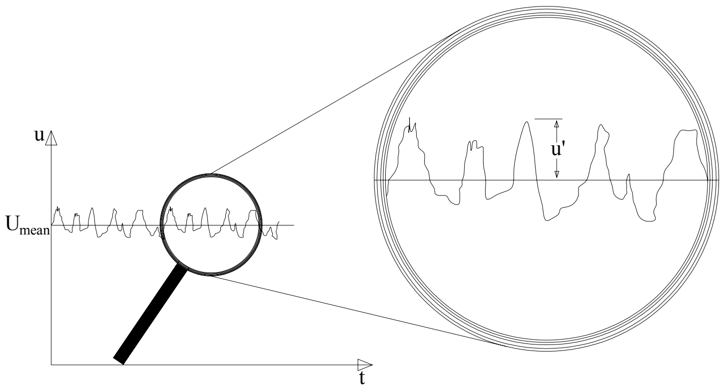

Figure 3.4: The schematic representation of a time series belonging to a velocity record

$$u' = u - U_{mean} \quad \textbf{(3.10)}$$

$$Var(u) = \frac{1}{n-1}\sum_{i=1}^{n-1} u'(t_i)^2 \quad \textbf{(3.11)}$$

$$Var(u) = \frac{1}{n-1}\sum_{i=1}^{n-1} (u - U_{mean})^2 \quad \textbf{(3.12)}$$

$$\sigma_u = \sqrt{Var(u)} = \overline{u'^2} = u_{rms} \quad \textbf{(3.13)}$$

The expression of turbulence intensity (i.e. u_{rms} and w_{rms}) was utilized throughout the analysis of additional streamwise and vertical turbulence which occurs owing to flowing through a vegetative element. For this purpose the variations of streamwise and vertical turbulence intensity with respect to relative depth were plotted and those were compared between non-disturbed case and comparisons of turbulence intensity (i.e. in both streamwise and vertical directions) belong to non-disturbed and disturbed by vegetation were carried out to further understand the influence of vegetal elements on turbulence structure. However, the acquired results were not in dimensionless form. Thus, in order to make the results more comparable, transferable and adaptable for future studies a normalization of turbulence intensity was carried out using $[(u_{rms})_d - (u_{rms})_u]/(u_{rms})_u$ and $[(w_{rms})_d - (w_{rms})_u]/(w_{rms})_u$ for the streamwise and vertical turbulence intensity respectively. Physically speaking, $[(u_{rms})_d - (u_{rms})_u]/(u_{rms})_u$ and $[(w_{rms})_d - (w_{rms})_u]/(w_{rms})_u$ give the additional turbulence occurrence due to presence of vegetation in terms of percentage.

Where $(u_{rms})_u$= the streamwise turbulence intensity measured at the upstream side of vegetative element; $(u_{rms})_d$= the streamwise turbulence intensity measured at the downstream side of vegetative element; $(w_{rms})_u$= the vertical turbulence intensity measured at the upstream side of vegetative element; $(w_{rms})_d$= the vertical turbulence intensity measured at the downstream side of vegetative element. Nevertheless, $\left[(u_{rms})_d-(u_{rms})_u\right]/(u_{rms})_u$ and $\left[(w_{rms})_d-(w_{rms})_u\right]/(w_{rms})_u$ were not the function of vegetative characteristics. In order to incorporate the vegetative characteristics into the expression of $\left[(u_{rms})_d-(u_{rms})_u\right]/(u_{rms})_u$ and $\left[(w_{rms})_d-(w_{rms})_u\right]/(w_{rms})_u$ vegetation intensity parameter "ξ" was employed and $\left\{\left[(u_{rms})_d-(u_{rms})_u\right]/(u_{rms})_u\right\}/\xi$ and $\left\{\left[(w_{rms})_d-(w_{rms})_u\right]/(w_{rms})_u\right\}/\xi$ were obtained for streamwise and vertical turbulence intensity respectively.

In order to further understand the role of presence of vegetation in the flow domain on turbulence structure, the turbulence kinetic energies which are measured at the upstream and downstream side of vegetation were compared.The expression of turbulence kinetic energy as is given by Equation 3.14 (**Nezu and Onitsuka, 2001**). After the comparison of turbulence kinetic energy, the variation between normalized kinetic energy (Equation 3.15) and relative depth was taken into assessment for the purpose of comparison. Equation 3.15 gives the contribution of the presence of vegetation into the turbulence kinetic energy in terms of percentage. Moreover, Equation 3.16 was acquired by incorporating the vegetation intensity parameter into Equation 3.16 and the variation between this parameter and relative depth was also considered. In this context, it should be also kept in mind that determination of "vegetation intensity parameter", which is used throughout the analysis, with an acceptable accuracy, is vital. The details and further discussion about the vegetation intensity parameter is presented in the Chapter 5 together with the experimental results.

$$k=\frac{1}{2}\left(\sigma_u^2+\sigma_v^2+\sigma_w^2\right)=\frac{1}{2}\left(\overline{u'^2}+\overline{v^2}+\overline{w^2}\right)=\frac{1}{2}\left(u_{rms}^2+v_{rms}^2+w_{rms}^2\right) \quad \textbf{(3.14)}$$

$$1-\frac{k_u}{k_d} \qquad \textbf{(3.15)}$$

$$\frac{\left(1-\frac{k_u}{k_d}\right)}{\xi} \qquad \textbf{(3.16)}$$

4. EXPERIMENTAL SETUP and PROCEDURE

4.1 The Experimental Set-Up and the Measurement Devices

All the experiments were conducted in the flume, which is capable of supplying steady flow and regular wave, located in Hydraulic Laboratory of Technical University of Istanbul. The size of the flume is 26m in length, 0.98m in width and 0.85 m in depth. In the flume, steady flow is provided by an interior re-circulating system. Two pipes each has 200 mm in diameter supplied the re-circulation and two pumps positioned at the downstream of the flume, each has 2x50 kW, were employed for the power supply. In order to reduce fluctuation, a flow straighter system was placed at the entrance of the flume. The flume had Plexiglas sidewalls in order to facilitate the observation and the bottom was made of smooth concrete. A sketch and picture of the flume are given in Figure 4.1 and Figure 4.2 respectively.

For the velocity measurements three Acoustic Doppler Velocimeters were used. Two of the ADVs were new generation ADV Vectrinos which are capable of data acquisition with 200 Hz, the other one was ADV which can collect data with a sampling frequency of 25 Hz. In Figure 4.3, the centreline view of the flume and three Acoustic Doppler Velocimeters is given. The ADV is a high precision instrument that measures all three flow velocity components. ADV consists of three modules: the measuring probe, the conditioning module and processing module. The acoustic sensor of the 3D down-looking probe is mounted on a rigid stem 0.4 m long and is composed of one transmit transducer and three receive transducers. These technical specification are quoted form the ADV Manuel (**Nortek, 2004**). Differing from the earlier versions, new generation ADV Vectrinos have four receive transducers and in comparison with the earlier generation have a thinner arm.

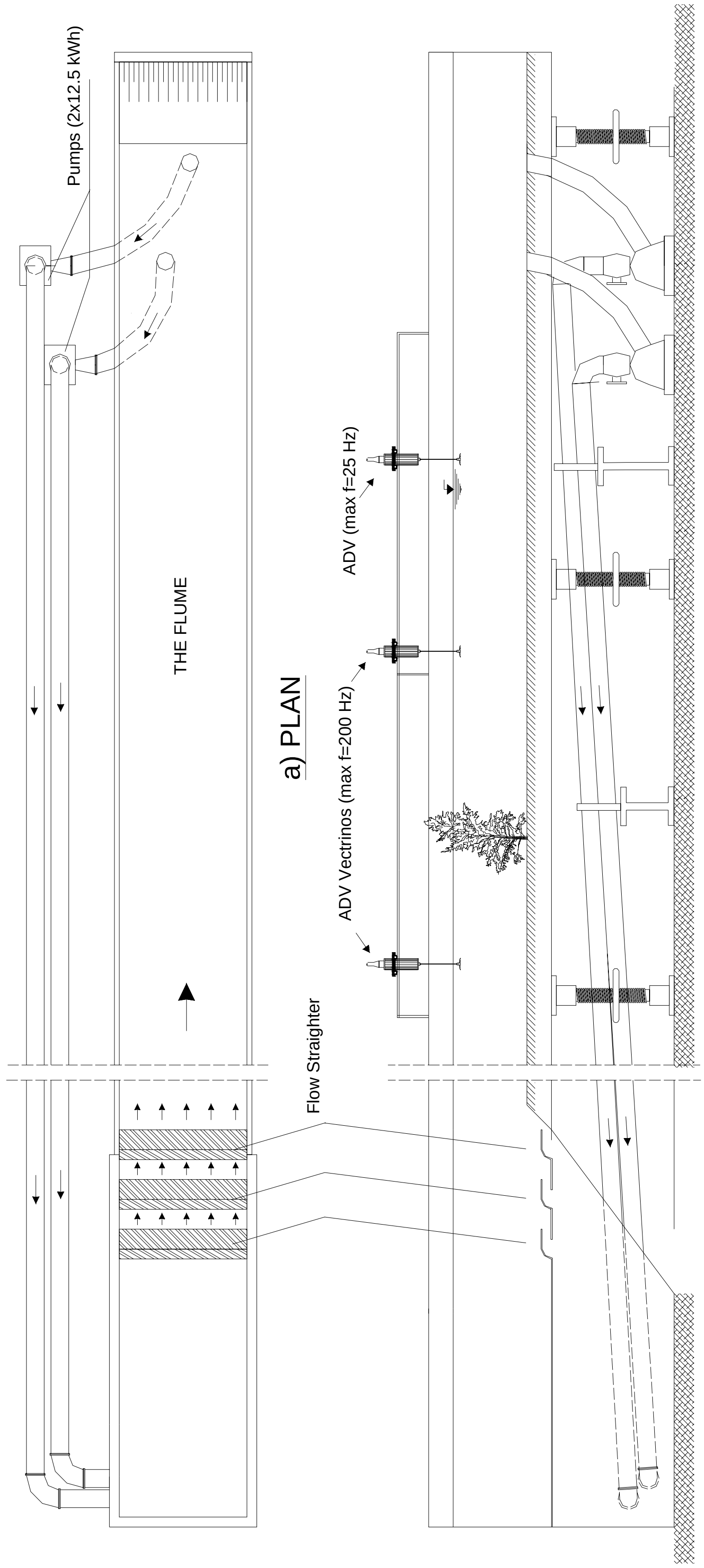

Figure 4.1: The sketch of the flume (no scale)

An ADV measures the velocity in a sampling volume of 0.125 cm^3 which is 5 cm from the sensing elements. On the other hand the sampling volume range of the ADV Vectrino is set to between 0,085cm^3 or 0.425 cm^3 which is 5 cm away from sensing elements. These properties are user selectable. The ADV processing module consists of a PC card, installed in a PC, and data acquisition software. However, the ADV Vectrino does not require a PC card. In order to mount and move the ADV vector velocimeters in three direction (in the streamwise, vertical and lateral), a traverse system, which has 6 m length (in streamwise direction), with a width which is equal to channel width was constructed on the top of the flume.

Figure 4.2: The side view of the flume

Figure 4.3: The centerline view of the flume and the Acoustic Doppler Velocimeters

4.2 Procedure

The details of the flume and instrumentation as are given above. The experiments planned to serve the objects which are aforementioned in the earlier chapter. In order to achieve those goals explained above, velocity measurements were performed. In Figure 4.4 the velocity measurement points are denoted on the area occupied by the traverse system which was 6 m in length.

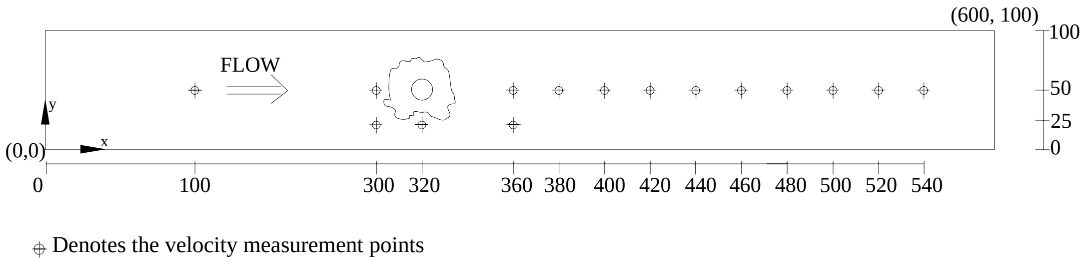

Figure 4.4: The location of the points where the velocity measurements were performed (in terms of coordinate values; all coordinates are in cm).

In this sketch, it must be noted that the velocity measurement points were given in terms of coordinate values. In this study, all the tests were conducted for the case of relatively low velocity values and emergent real vegetation since those conditions are commonly observed in low-gradient valleys and floodplains (**Jarvela, 2004a**). The experiments that aimed to examine the variation of velocity profile at the downstream of vegetation were conducted for the different combinations of water depth, velocity values, and representative “type” of the vegetation. More specifically, the experiments on velocity profile measurements along the flume were planned to be run for the combination of 2 depth values, 5 consecutive discharge (Q1>Q2>Q3>Q4>Q5) values and 3 vegetation species. Table 4.1 summerizes the test conditions.

Table 4.1: Experimental Schedule

Exp. No	Experiment Name	Water Depth (in cm)	Discharge Condition	Representative Vegetation Type	How Many Vertical Velocity Profile Obtained
1	D25-Q1-T1	25	Q1	Type 1	15
2	D25-Q2-T1	25	Q2	Type 1	15
3	D25-Q3-T1	25	Q3	Type 1	15
4	D25-Q4-T1	25	Q4	Type 1	15
5	D25-Q5-T1	25	Q5	Type 1	15
6	D40-Q1-T1	40	Q1	Type 1	15
7	D40-Q2-T1	40	Q2	Type 1	15
8	D40-Q3-T1	40	Q3	Type 1	15
9	D40-Q4-T1	40	Q4	Type 1	15
11	D25-Q1-T2	25	Q1	Type 2	10
12	D25-Q2-T2	25	Q2	Type 2	10
13	D25-Q3-T3	25	Q3	Type 2	10
15	D25-Q1-T3	25	Q1	Type 3	17
16	D25-Q2-T3	25	Q2	Type 3	17
17	D25-Q3-T3	25	Q3	Type 3	17
18	D25-Q4-T3	25	Q4	Type 3	17
19	D40-Q1-T3	40	Q1	Type 3	17
20	D40-Q2-T3	40	Q2	Type 3	17
21	D40-Q3-T3	40	Q3	Type 3	17
22	D40-Q4-T3	40	Q4	Type 3	17

4.3 Preliminary Tests

Several controls were carried out in order to make sure of the quality and the reliability of the data. These are briefly summarized in the next two subchapters.

4.3.1 The effect of sampling number on the data collected by ADV

Before starting the experiments, it was considered that the measurement results obtained from the Acoustic Doppler Velocimeter could be affected by the sampling number of the data recorded. Collecting too many samples could be redundantly effort and time consuming. On the other hand, collecting data with insufficient sampling numbers could lead to misleading results. In the light of these arguments, before starting the point measurements, a set of preliminary experiments were performed to decide the sampling number for the data. For this purpose, point measurements were undertaken at the upstream and downstream of the vegetation. More specifically, those measurements were performed at the points denoted with the coordinate values of (300, 50) and (360, 50) in Figure 4.4. In order to determine the effect of sampling numbers on measurement results, data collection was repeated at the same locations given above, for the duration of 5, 10, 15, 20, 25, 30, 40, 50, 60, 90, 120, 150, and 180 seconds with a sampling frequency of 200 Hz. All these measurements were carried out at the point which had a 30 cm distance from the bottom for the depth of SWL (still water level) 40 cm.

Throughout the analysis, the variations of mean velocity components in the three directions (i.e. u, v, w) with sampling duration were considered. Additionally, their variance versus sampling duration was taken into consideration for the points at the both upstream and downstream side of the vegetative element. In Figure 4.5 the variations of U_{mean} (time averaged mean velocity value in the streamwise direction) with respect to corresponding sampling duration are presented.

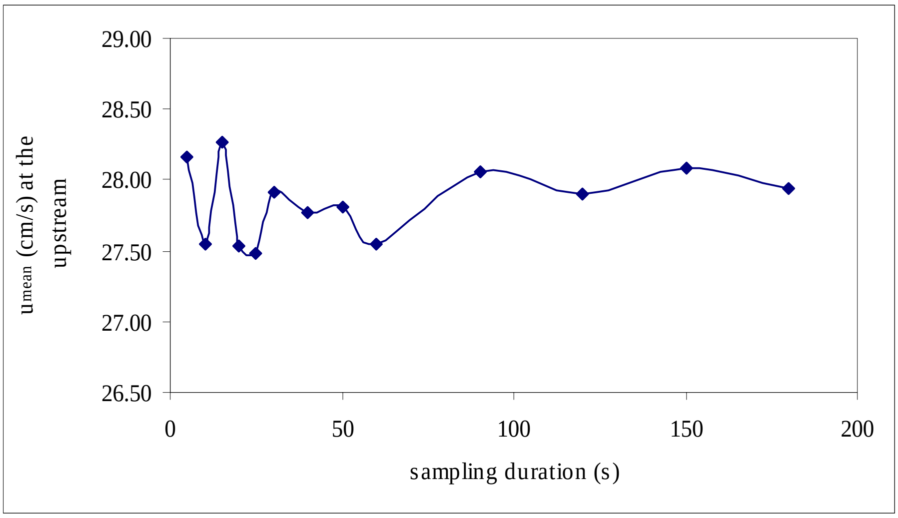

(a)

Figure 4.5: The variation of u_{mean} with respect to sampling duration a) at the upstream side of the vegetative element b) at the downstream side of the vegetative element

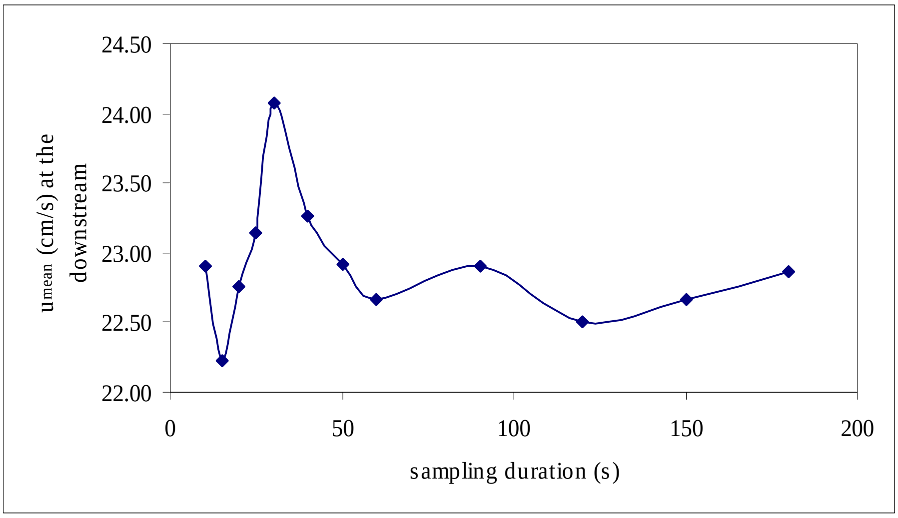

(b)

Figure 4.5 (continued): The variation of u_{mean} with respect to sampling duration a) at the upstream side of the vegetative element b) at the downstream side of the vegetative element

As may be judged from the Figure 4.5, for the short sampling durations, U_{mean} values scatter in a narrow range. Nevertheless, even this small uncertainty in velocity measurement is important in the turbulence measurements. This scattering is clearer at the downstream side of the vegetative element as expected since the turbulence intensity is expected to increase at the downstream of the flume in consequence of vegetation. Further, with the increasing number of sampling duration these values stabilized in the vicinity of a certain velocity value. With the intention of gain better knowledge about the effect of sampling number on quality of measurement data, the variation of v_{mean} and w_{mean} with respect to sampling number were also taken into consideration. Here v_{mean} and w_{mean} denote time averaged lateral and vertical velocity respectively. In Figure 4.6 and Figure 4.7, the variation of v_{mean} and w_{mean} as a function of sampling number were depicted respectively.

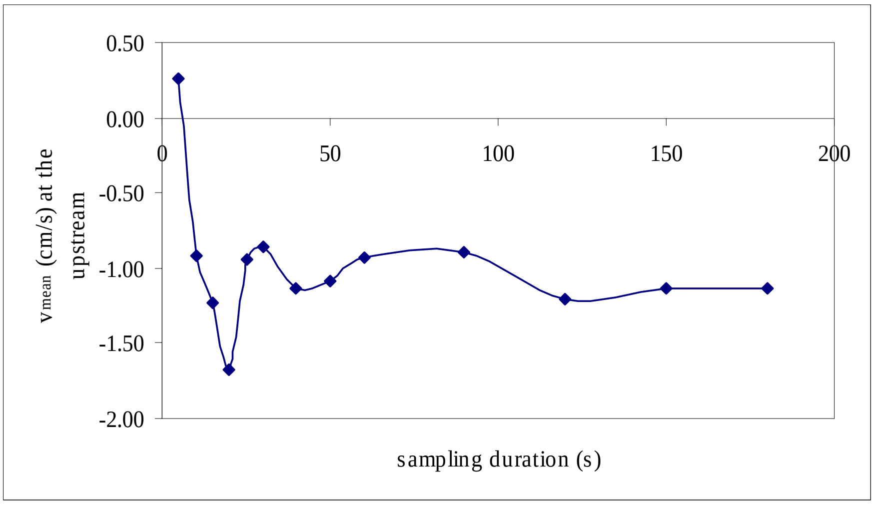

(a)

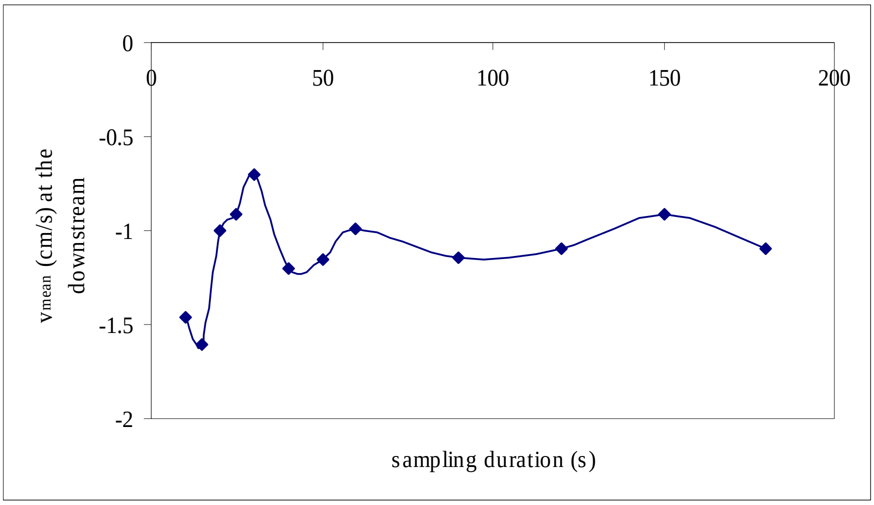

(b)

Figure 4.6: The variation of v_{mean} with respect to sampling duration a) at the upstream side of the vegetative element b) at the downstream side of the vegetative element

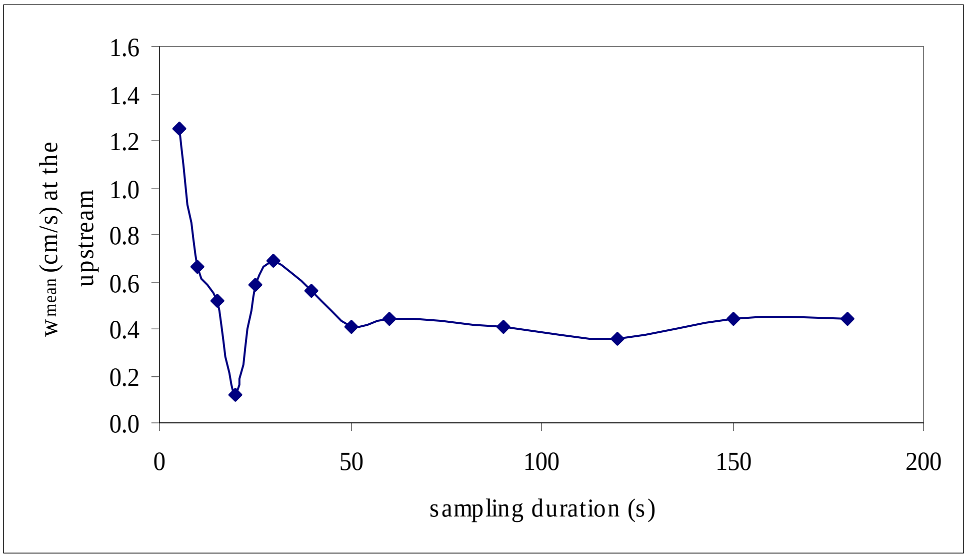

(a)

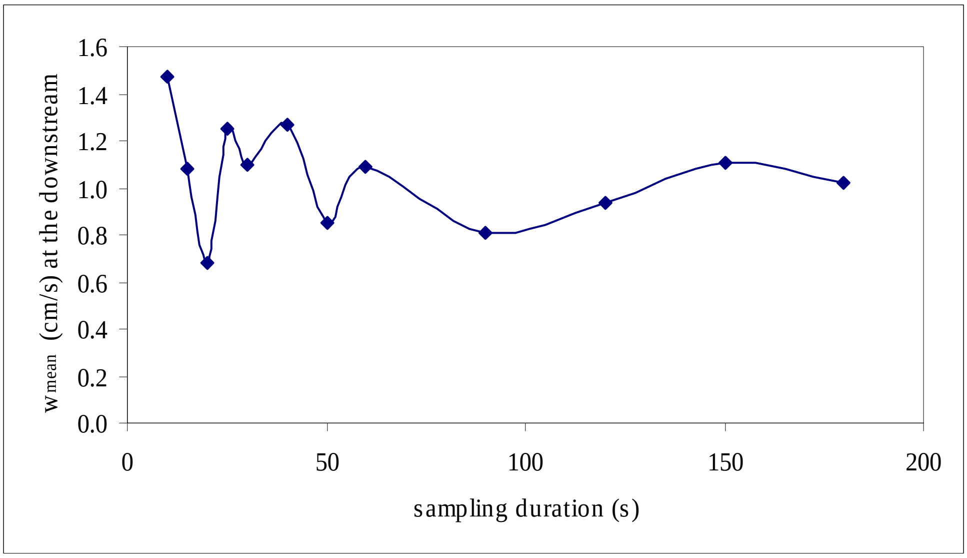

(b)

Figure 4.7: The variation of w_{mean} with respect to sampling duration a) at the upstream side of the vegetative element b) at the downstream side of the vegetative element

Based on the Figures 4.6 and 4.7, it may be claimed that for sampling duration shorter than 30 seconds, the instability in the velocity values are relatively higher compared to the velocity values having sampling duration longer than 60 seconds. Also, as may be concluded from same figures, the velocity values which have sampling duration longer than 60 seconds stabilized. Moreover, the variation of variance values of the U_{mean}, v_{mean}, and w_{mean} (it represent the square of turbulence intensity for the related direction) with respect to sampling numbers were further analyzed to confirm the idea attained above (Figure 4.8). As may be seen from Figure 4.8, collecting data with a sampling duration shorter than 30 seconds gave instable results in terms of turbulence intensity as well. However, the variance values of velocity records stabilized for the sampling duration longer than 60 seconds. In other words, variance values of velocity records which have longer than 60 seconds leads to a constant value and this means that collecting data longer than 60 seconds does not make any extra contribution in terms of data quality. Based on these findings, sampling duration was chosen as 60 seconds and throughout the experiments this sampling duration was satisfied.

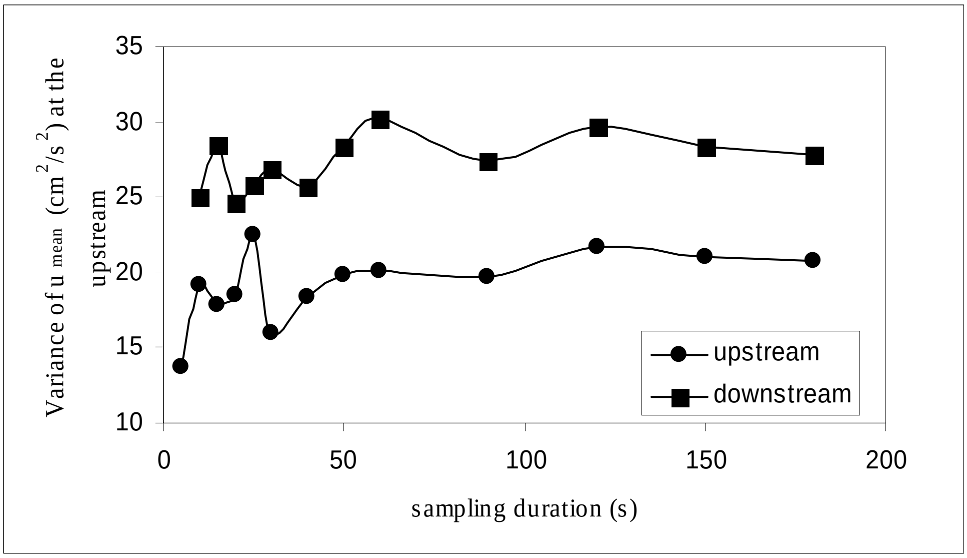

(a)

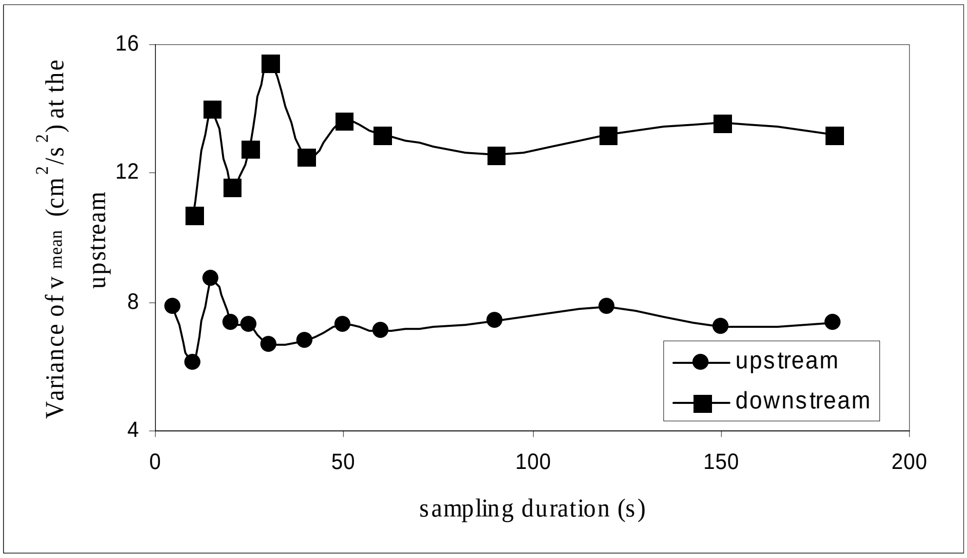

(b)

Figure 4.8: The variation of the variance values belong to mean velocities with respect to different sampling durations a) U_{mean}, b)v_{mean}, c)w_{mean}

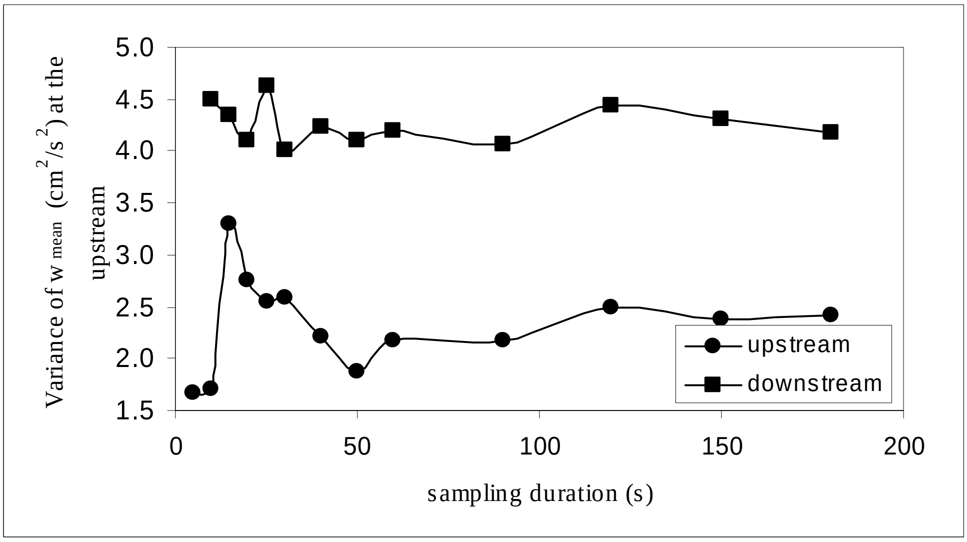

(c)

Figure 4.8 (continued): The variation of the variance values belong to mean velocities with respect to different sampling durations a) U_{mean}, b)v_{mean}, c)w_{mean}

4.3.2 The verification of the logarithmic velocity profile

The validities of the obtained results are misleading unless the velocity profile of the non-disturbed flow satisfied the logarithmic velocity profile. Thus, to make sure that the velocity profiles of the non-disturbed flow fit the logarithmic velocity profile a set of analyses were undertaken. For this purpose, the velocity profiles were plotted in semi-logarithmic form (i.e. only the ordinate was in natural logarithmic form) for different test conditions. In Figure 4.9 velocity profiles are presented for three tests conditions belong to three different vegetation conditions (i.e. Type 1, 2, and 3) and denoted in Table 4.1 with experiment no: 1, 12, and 17. As could be seen from Figure 4.9, the velocity profiles fit logarithmic velocity distribution properly.

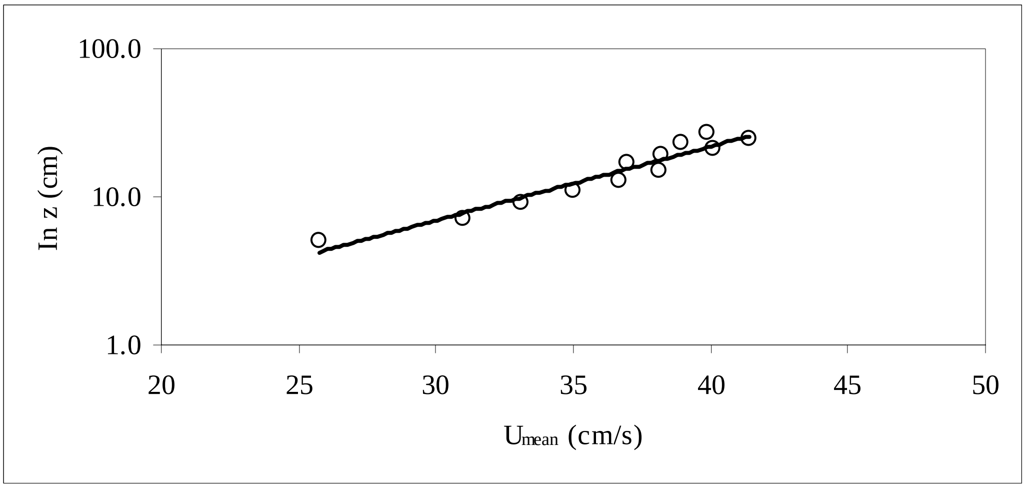

(a)

Figure 4.9: Example velocity profiles in semi-logarithmic form a) Experiment no:1 b) Experiment no:12 c) Experiment no:17

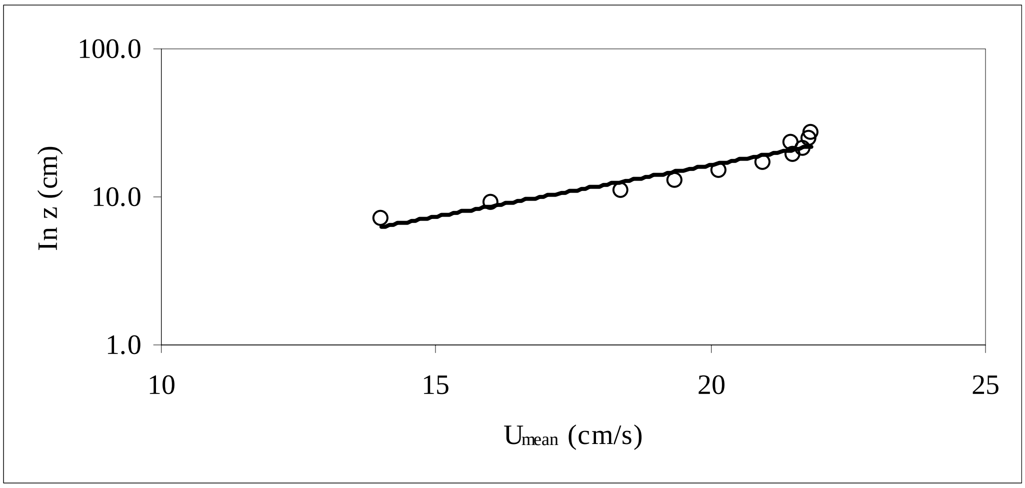

(b)

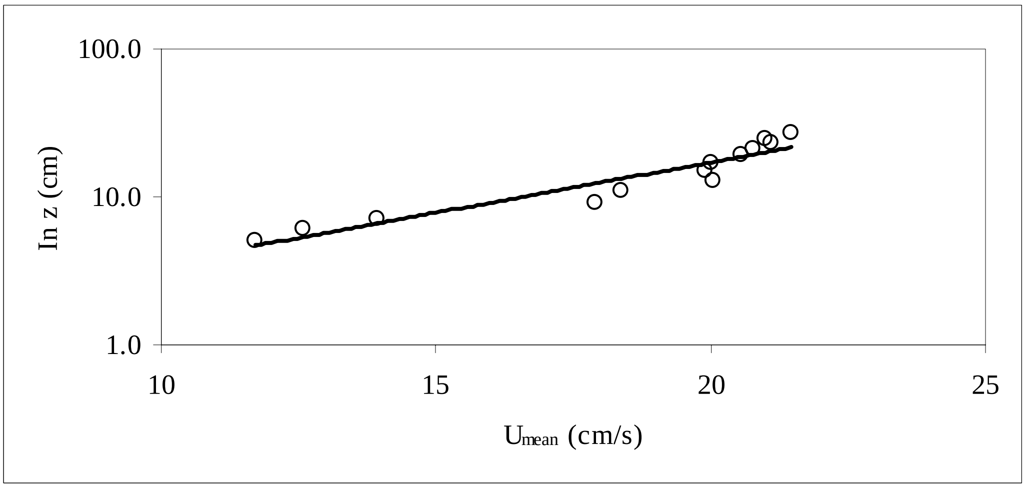

(c)

Figure 4.9: Example velocity profiles in semi-logarithmic form a) Experiment no:1 b) Experiment no:12 c) Experiment no:17

4.4. Data Collection and Processing

Collecting data for 60 seconds with a sampling frequency of 200 Hz sampling frequency in a measurement point provided 12000 data per minute for just a singular measurement point for one flow direction. When the total number of the data collection point is taken into consideration, which is around 4000, it is seen that there is mass of data that need to be processed and converted into a meaningful form. In order to do this, the steps which are presented in Figure 4.10 were followed for the data processing.

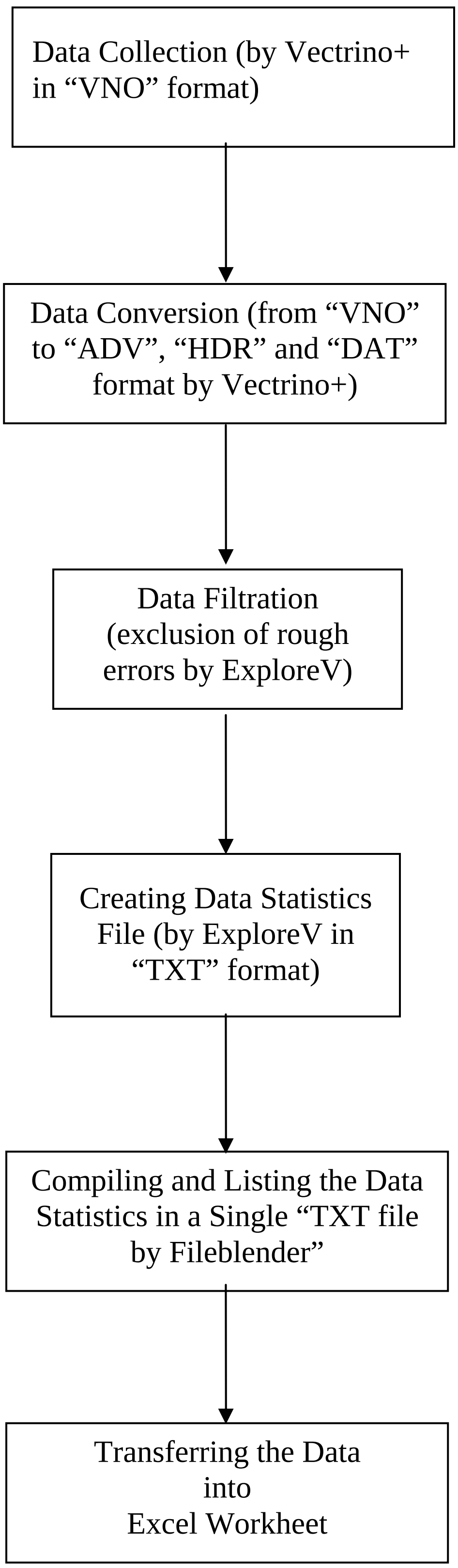

Figure 4.10: Flow chart of data processing

The steps which were given in Figure 4.10 were repeated for each measurement point. As stated in the previous paragraph, since velocity measurements were carried out at roughly 4000 points, those steps were repeated circa 4000 times. During the data acquisition, software named "Vectrino+" was employed. This software has been developed by Nortek AS for the aim of data collection in high sampling frequencies using Vectrino Velocimeter. Vectrino+ creates a file with extension of "VNO" for a single point measurement. After data acquisition was completed, this file converted into three different file formats. These were "ADV", "HDR" and "DAT" formats. The obtained ADV files were opened by software named ExploreV. ExploreV is a program for post processing data collected by NORTEK acoustic Doppler velocimeter. It allows viewing, editing and analyzing large data sets to print and export results (Nortek, 2000). The crude data collected from a point measurement needs to be refined and filtered to remove the spikes and outlier values. ExploreV provides the user with various methods to exclude rough errors in time series associated with velocity sampling (Nortek, 2000). In this study, two of those methods were adopted and utilized during the exclusion of rough errors and outliers. These were 1) correlation score threshold method, 2) velocity threshold method. Correlation score threshold replaces velocity values for which the correlation scores are lower than the threshold value. The user can optionally specify averaged threshold values for all three components or minimum correlation values among all three components (Nortek, 2000). During the post-processing process correlation score threshold set to 80 averaged one. Values to replace the bad samples might be linearly interpolated or excluded from the time series according to the selected option. Velocity threshold method replaces the samples in which the magnitude exceeds the defined threshold. The threshold value is expressed as a multiplied of the standard deviation of each velocity component. Values to replace bad samples are calculated in the same manner as for the correlation score threshold method or excluded from the time series according to the selected option (Nortek, 2000). During the post-processing this value was set as 4. After exclusion of rough errors and outliers, the statistics of the data were generated in text format by ExploreV. However the format of these created statistics needed to be rearranged. Considering large number of the measurement point, a code named "fileblender" was written to rearrange the statistics. In this way, the data statistics belong to different measurement points were compiled for each vertical profile. These compiled sets were transferred into Microsoft Excel Worksheets to start analyses.

5. EXPERIMENTAL RESULTS AND DISCUSSION

5.1 Introduction

In the light of the background presented in Chapter 3, an experimental study was performed based on the procedure described in Chapter 4. For this purpose the forms of vegetation were classified into three representative groups and called as Type 1, Type 2, and, Type 3 as explained in Chapter 3. Then the related results were presented on the basis of this classification. In this chapter, the results of the experimental investigation are presented and discussed.

5.2 General Remarks on Flow Field Disturbed by Vegetation

The velocity measurements were undertaken for three different forms of real vegetation (i.e. representative vegetation of Type 1, 2, and 3) both at the upstream and downstream of the vegetated section. The measured velocity profiles at the upstream and downstream for the three types of vegetation were presented in Appendix B. When all experimental cases are taken into assessment, based on the velocity profiles belonging to Type 1, 2, and, 3 (Appendix B); it can be said that the presence of vegetation leads to considerable amount of sub-canopy flow. This is much more significant for Type 2 and 3. Type 3 causes weaker sub-canopy flow compared to Type 2. In other words, Type 2 and 3 have a larger influence on flow compared to Type 1 in terms of retaining the flow. However it should be noted that heavy sub-canopy flow may lead to undesirable possible erosion. Unexpectedly, for Type 2 (Figure B.11, B.12, B.13) some negative time averaged velocity values were observed at the downstream of vegetation in the region closer to the water surface. This is because Type 2 is more compact in terms of the foliage and branch structure, hence it retains the flow more significantly. This is an important outcome in terms of habitat as it indicates this sort of compact vegetation structure in naturally vegetated rivers provides stream variability, which is vital for the improvement of fish habitat **(Odeh and Cada, 2002)**.

Further understanding about the disturbance length due to presence of vegetation gains importance in terms of describing the influence of placement interval of vegetation in floodplain. Moreover, yet the relationship between disturbance length and vegetative characteristics are unknown. For this purpose, as explained in Chapter 4, velocity measurements were conducted employing three ADV's at the locations denoted in Figure 4.4 along centerline of the flow. Based on those data, contour plots of time averaged velocity profiles were drawn. The software named Tecplot 10.0 was used as a tool for this procedure. The obtained velocity contours under the effect of vegetation for three representative types are as given in Appendix C. In these illustrations the abscissa value of location of vegetal element is "0". As may be concluded from Appendix C, in spite of their porous structures, the existence of any type of representative vegetation considerably disturbs the flow field at the downstream. However, this effect is more notable for Type 2 since it has relatively more compact foliage, branch structure. Also for Type 2 negative velocity values were observed in the downstream of vegetation at the area closer to water surface. Similarly, extremely low velocity values were observed at the same region for Type 1, as well. As mentioned above, it was observed that (Appendix C) the presence of vegetation leads to strong sub-canopy flow, and this effect is more remarkable for the denser form of vegetation as seen in Type 2.

5.3 Formulating the Effect of Vegetation on Velocity Profile

The discussion on the effect of presence of vegetation on velocity profile where flow through vegetation as presented above. However, those discussions are verbal and needed to be expressed in dimensionless and numerical form to make it more applicable and adaptable for the later studies. Since the dimensionless numbers are introduced in Chapter 3, no more discussions were given here. Instead, only the relationships between introduced parameters and the relative depth were interpreted below. Nevertheless, in order to facilitate the following text, it would be convenient to remind the short form of introduced parameters first: ξ=VIP (Vegetation Intensity Parameter); U_u-U_d=VDP (Velocity Difference Parameter); $(U_u-U_d)/U_u$= NVDP (Normalized Velocity Difference Parameter); $[(U_u-U_d)/U_u]/\xi$=NVVDP (Normalized Vegetative Velocity Difference Parameter).

In Figure 5.1, the distributions of "velocity difference parameter" (VDP) along the depth were presented for the three types of representative vegetative elements respectively. As could be concluded from Figure 5.1, the negative VDP values were appeared around the region closer to the bed. Negative VDP values indicate the sub-canopy flow occurrence in this region. Conversely, in the region towards water surface VDP take positive values. Positive values point out the flow retaining in consequence of existence of vegetation. This retaining effect is highly remarkable and clear for Type 2 and Type 3 since those two have higher vegetative intensity parameter (VIP) values. However, as could be drawn a conclusion from Figure 5.1a, 5.1b and Figure 5.1d, 5.1e belonging to Type 1 and 3 respectively, this effect diminishes with the increasing water depth. Another outcome that may be drawn from Figure 5.1 is that, the retaining effect of the vegetative element increases with the increasing flow velocity. This statement is comparatively clearer for Type 2 and 3 as those have higher VIP value in comparison with Type 1.

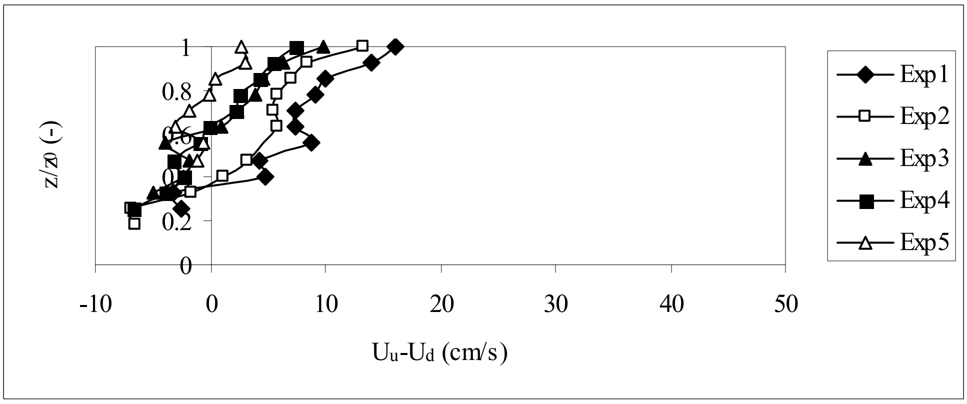

(a)

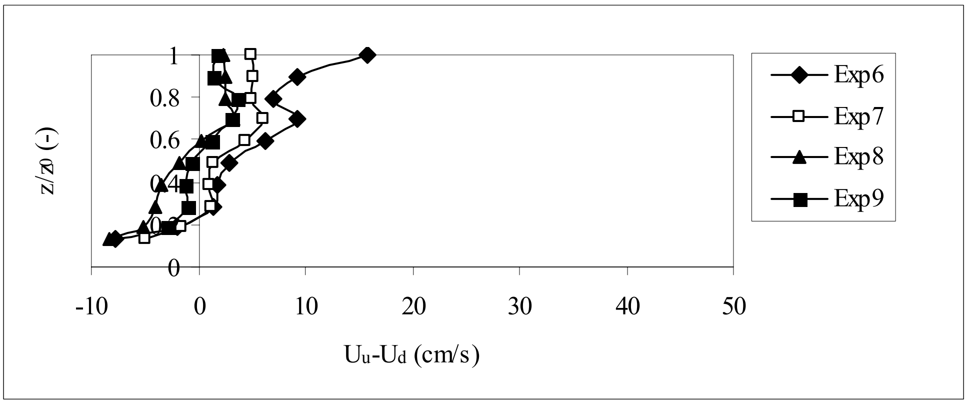

(b)

Figure 5.1: The distributions of "velocity difference parameter" along the relative depth for a) Type 1, Depth=25cm; b) Type 1, Depth=40cm; c) Type 2, Depth=25cm; d) Type 3, Depth=25cm; e) Type 3, Depth=40cm

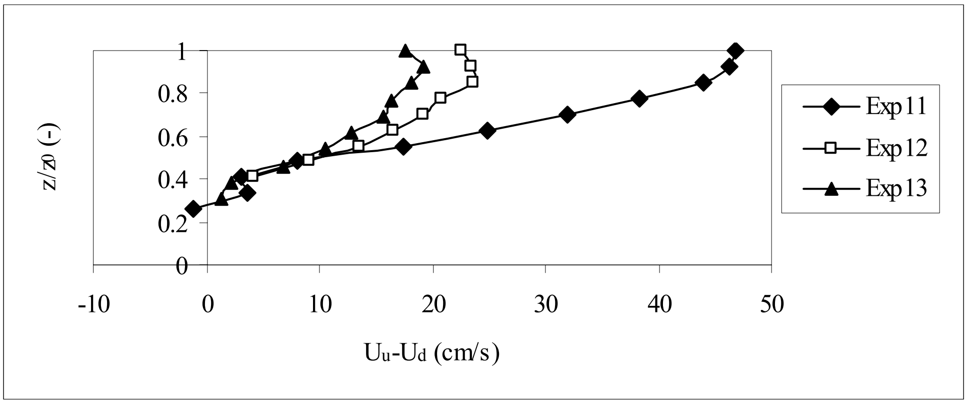

(c)

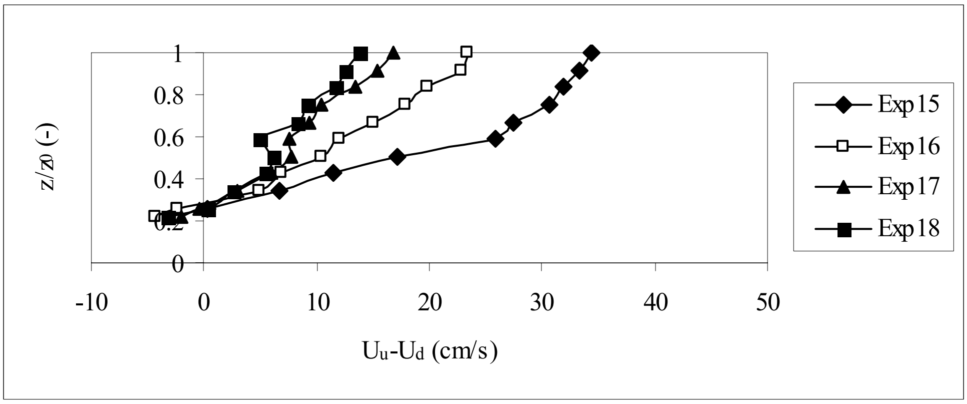

(d)

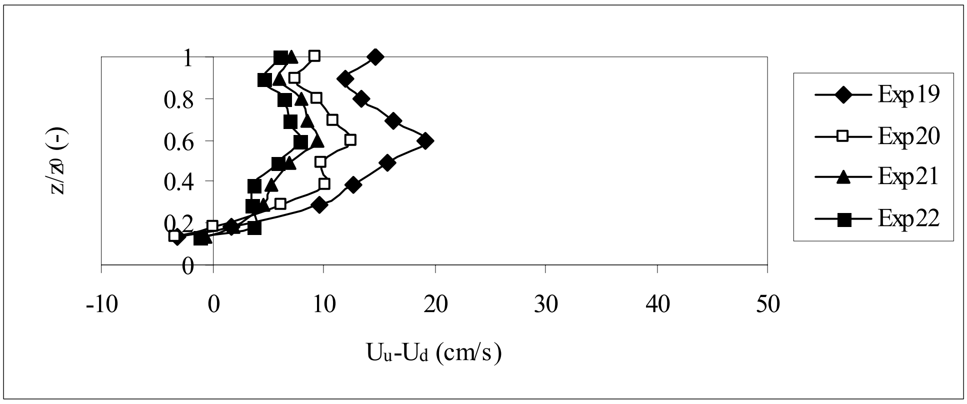

(e)

Figure 5.1 (continued): The distributions of "velocity difference parameter" along the relative depth for a) Type 1, Depth=25cm; b) Type 1, Depth=40cm; c) Type 2, Depth=25cm; d) Type 3, Depth=25cm; e) Type 3, Depth=40cm

The variation of VDP against relative depth is discussed above. However, with the aim of deriving a relationship between velocity values non-disturbed flow and downstream of vegetation, those parameters need to be represented in dimensionless forms. In this way, the obtained results would be expressed in a more applicable and adaptable form in terms of future studies. For this purpose, normalized velocity difference parameter (NVDP) was introduced as given in the earlier chapter. This parameter gives the retaining percentage of the flow. Figure 5.2 illustrates the variation of NVDP versus relative depth for three types of vegetation respectively. In the region where the NVDP has minus value, the velocity value at the downstream of vegetation is higher than the one at the upstream. This occurs where the sub-canopy flow is observed. Based on the Figure 5.2, it may be claimed that NVDP shows 50 % flow retaining due to presence of the vegetation in the region closer to the water surface for Type 1. For the same region NVDP takes its maximum value for Type 2 which is 110 %. This could be explained by the VIP parameter belonging to Type 2. The VIP value of Type 2 is highest among the three types of vegetation and therefore highest flow retaining is observed in Type 2. In Type 3, 70-90% flow retaining occurs for the same region. However, when the area closer to bed was examined it was seen that maximum minus values belong to Type 1. In other words, the severest sub-canopy flow was observed for Type 1.

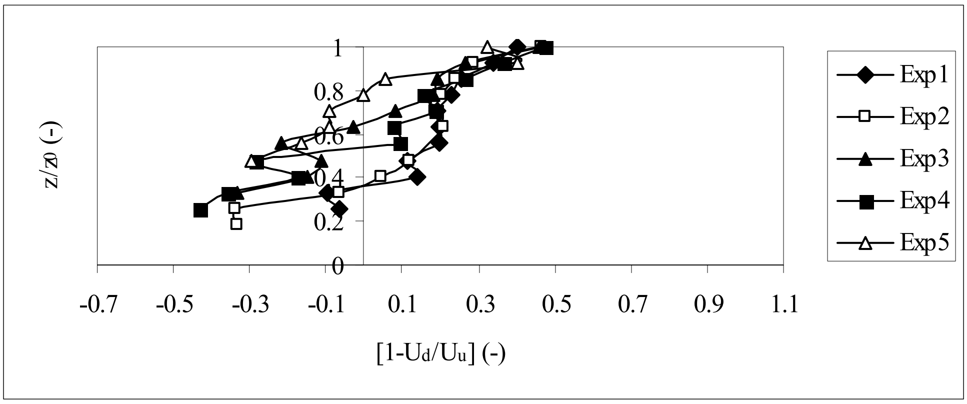

(a)

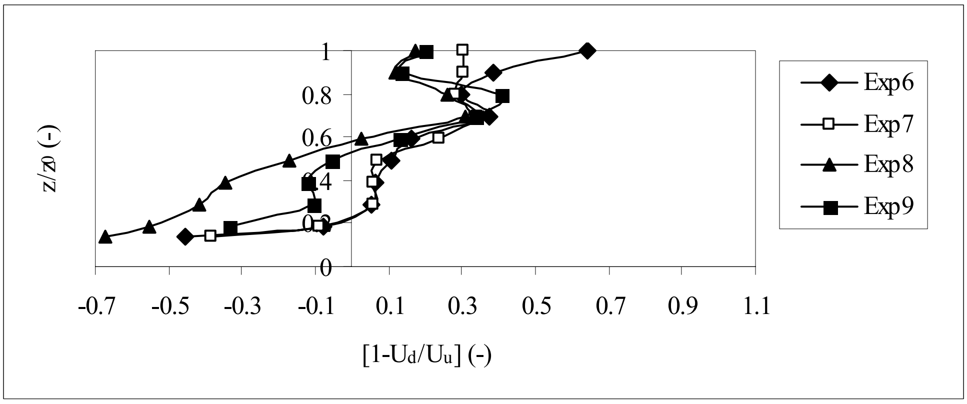

(b)

Figure 5.2: The distributions of “normalized velocity difference parameter” along the relative depth for a) Type 1, Depth=25cm; b) Type 1, Depth=40cm; c) Type 2, Depth=25cm; d) Type 3, Depth=25cm; e)Type 3, Depth=40cm

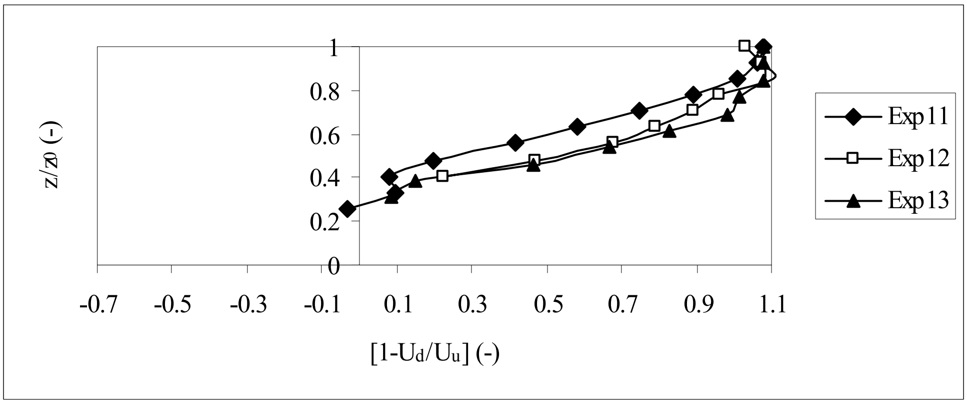

(c)

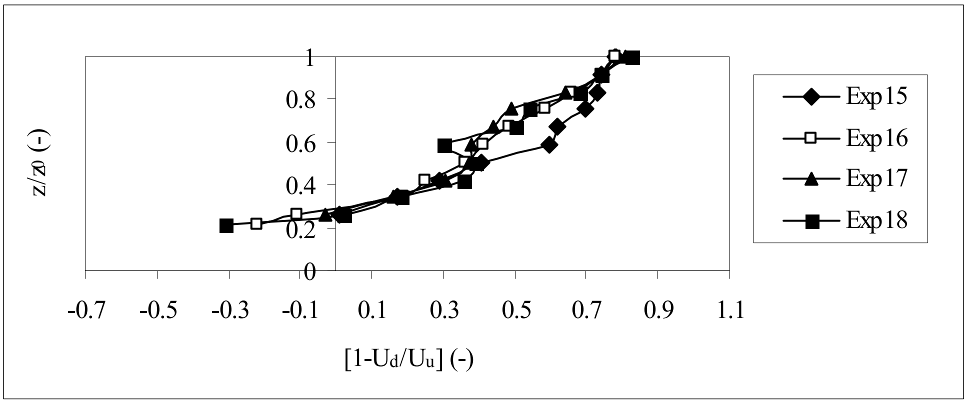

(d)

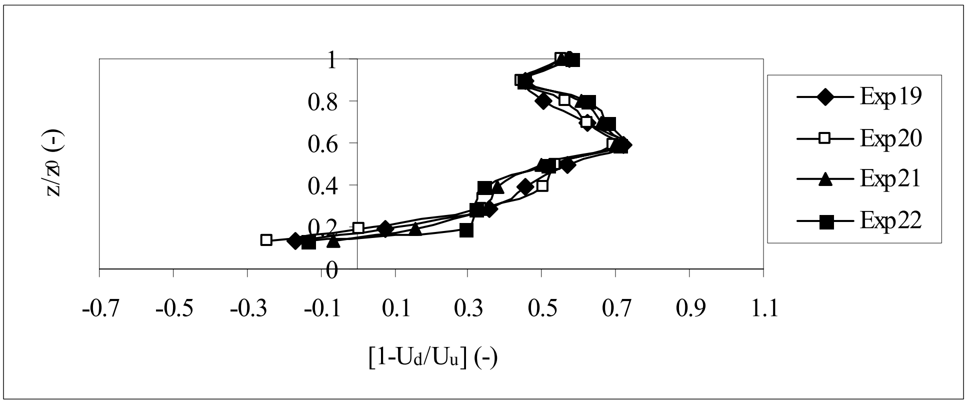

(e)

Figure 5.2 (continued): The distributions of "normalized velocity difference parameter" along the relative depth for a) Type 1, Depth=25cm; b) Type 1, Depth=40cm; c) Type 2, Depth=25cm; d) Type 3, Depth=25cm; e)Type 3, Depth=40cm

The variations of VDP and NVDP with respect to relative depth are analyzed above. However, these expressions are not functions of vegetative characteristics. In other words, the obtained results are representative only for the vegetative bodies tested.

Therefore those experimental results need to be expressed in terms of vegetative characteristics to make the data more applicable and comparable for the future studies. Vegetative intensity parameter (VIP) which is introduced in the earlier chapter was incorporated into NVDP expression for this purpose. The variation of the parameters belonging to flow (i.e. streamwise mean velocity measured at the upstream and downstream side of vegetation) and vegetative elements were taken into account and "normalized vegetative velocity difference parameter" (NVVDP) was derived. In Figure 5.2, the distribution of NVVDP along the relative depth was illustrated for three types of vegetative element. Since three types of vegetation have approximately close VIP values in terms of magnitude, the appearance of Figure 5.3 is not dramatically differing from Figure 5.2. Hence not to repeat the comments given in the previous paragraph, no additional interpretation is presented in this paragraph.

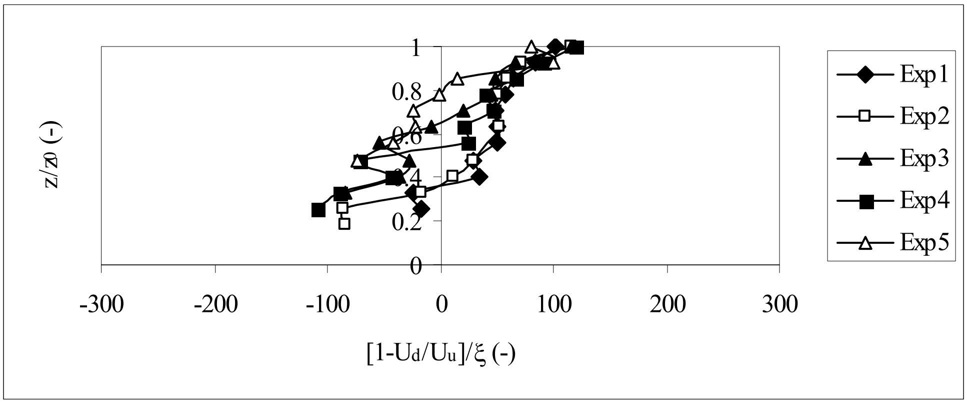

(a)

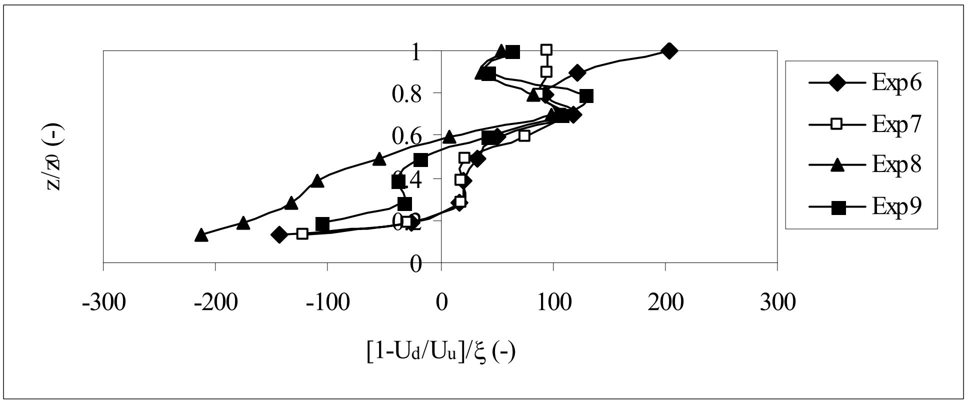

(b)

Figure 5.3: The distributions of "normalized vegetative velocity difference parameter" along the relative depth for a) Type 1, Depth=25cm; b) Type 1, Depth=40cm; c) Type 2, Depth=25cm; d) Type 3, Depth=25cm; e)Type 3, Depth=40cm

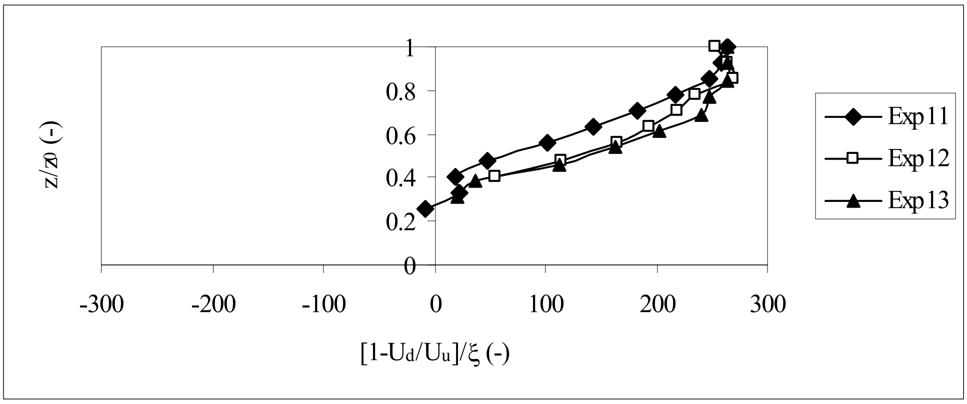

(c)

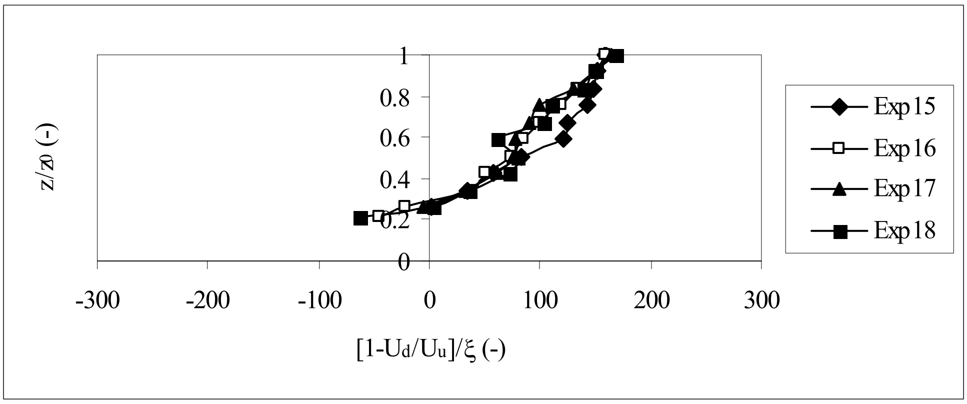

(d)

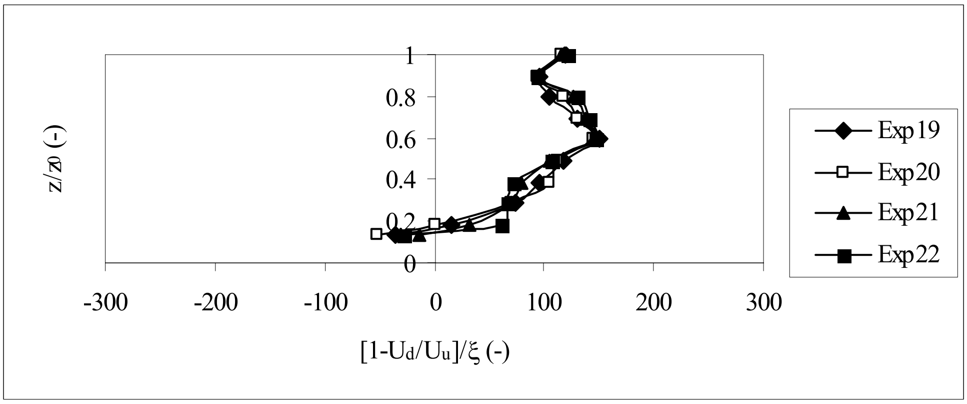

(e)

Figure 5.3 (continued): The distributions of "normalized vegetative velocity difference parameter" along the relative depth for a) Type 1, Depth=25cm; b) Type 1, Depth=40cm; c) Type 2, Depth=25cm; d) Type 3, Depth=25cm; e)Type 3, Depth=40cm

Several assessments were carried out so far in the light of the experimental data in order to further understand the effect of different vegetative elements with different architectural properties on streamwise mean velocity profiles. Nevertheless, it is considered that generating a simplified formulation which gives the relationship between velocity profile and relative depth would aid river engineers during the calculation of the velocity profile at the upstream of vegetation. In order to accomplish this, firstly all the data belonging to Figure 5.3a, 5.3b, 5.3c, 5.3d, 5.3e were marked on the same graph i.e. Figure 5.4 below. The relationship between NVVDP and relative depth is nearly linear in Figure 5.3 but Figure 5.3e. Considering this aspect, linear regression lines and corresponding regression equations were generated based on the marked experimental data in Figure 5.4a. In order to facilitate the observing of Figure 5.4a, same linear curves are presented again without data marks in Figure 5.4b. The gradient, the intercept and some major statistics of the regression lines belonging to three types of vegetation are summarized in Table 5.1. As may be judged from Figure 5.4 and Table 5.1, each linear regression has different gradient and intercept in consequence of their unique architectural properties. Because of this reason, the formulation which gives the velocity profile at the downstream of vegetation is presented below in a generalized form as a function of flow characteristics (i.e. velocity values at the upstream of vegetation) and vegetative characteristics (i.e. distribution of volume of vegetation in vertical and projection area of vegetation in plane).

Table 5.1: The gradient and the intercept of the regression lines belong to three type of vegetation

Type	Gradient	Intercept	Correlation Coefficient
1 (Depth=25cm)	0.0034	0.561	0.78
1 (Depth=40cm)	0.0025	0.516	0.82
2 (Depth=25cm)	0.0024	0.240	0.93
3 (Depth=25cm)	0.0039	0.280	0.95
3 (Depth=40cm)	0.0039	0.202	0.72
Mean	0.0032	0.360	0.84
St. Dev.	0.0007	0.166	-

A common form of a linear equation in two variables is given in Equation 5.1.

$$y = mx + c \qquad \textbf{(5.1)}$$

Where x and y = the variables of abscess and ordinate respectively; m = gradient; c = intercept. Substituting abscissa and ordinate parameters given in Figure 5.4 into Equation 5.1 the new form of the equation becomes:

$$\frac{z}{z_0} = m\frac{\left(1-\frac{U_d}{U_u}\right)}{\xi} + c \qquad \textbf{(5.2)}$$

Where U_u and U_d=the streamwise mean velocity at the upstream and downstream of vegetation respectively; ξ= vegetation intensity parameter (VIP); rearranging Equation 5.2:

$$\frac{z}{z_0} - c = m\left(1-\frac{U_d}{U_u}\right)\frac{1}{\xi} \qquad \textbf{(5.3)}$$

Multiplying both sides of Equation 5.3 by the vegetation intensity parameter (VIP) it becomes:

$$\xi\left(\frac{z}{z_0} - c\right) = m\left(1-\frac{U_d}{U_u}\right) \qquad \textbf{(5.4)}$$

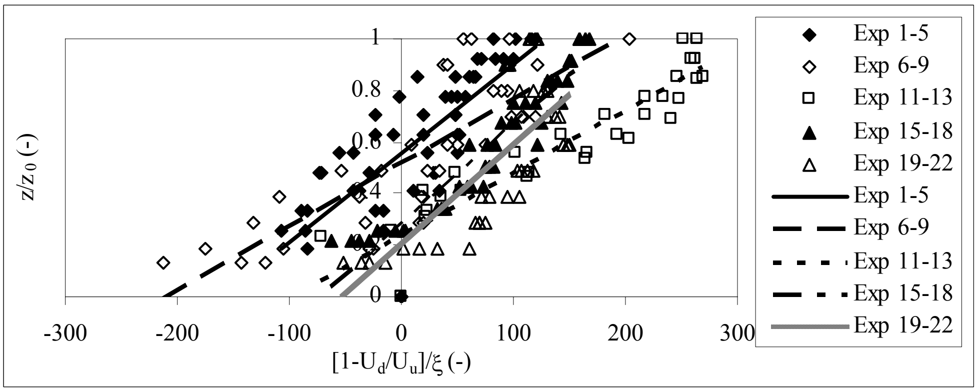

(a)

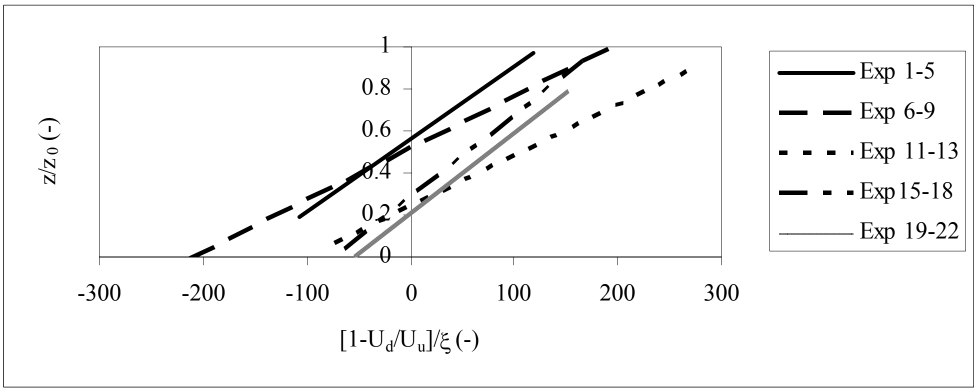

(b)

Figure 5.4: The distributions of "normalized vegetative velocity difference parameter" along the "relative depth" for all types of vegetation a) with data markers b) without data markers

Dividing both sides of Equation 5.4 by 0.0032 constant and rearranging it, the new form of the expression could be given as:

$$\left[\xi\left(\frac{z}{z_0}-c\right)\right]/m=1-\frac{U_d}{U_u} \qquad \textbf{(5.5)}$$

Multiplying both sides of Equation 5.5 by -1 and rearranging it, the expression takes the following form:

$$\frac{U_d}{U_u}=1-\xi\frac{\frac{z}{z_0}-c}{m} \qquad \textbf{(5.6)}$$

Considering to leave U_d alone on the one side of Equation 5.6 may facilitate the interpretation of the expression, both sides of Equation 5.6 was multiplied by U_u and rearranged.

$$U_d=U_u\left[1-\left(\frac{(V_{veg}/h)}{A}\right)\left(\frac{z-cz_0}{mz_0}\right)\right] \qquad \textbf{(5.7)}$$

Lastly, the expanded form of vegetative intensity parameter (ξ) was substituted in Equation 5.7 and the final form of the equation was obtained. The last form of the equation is presented below (Equation 5.8).

$$U_d=U_u\left[1-\left(\frac{V_{veg}}{Ah}\right)\left(\frac{z-cz_0}{mz_0}\right)\right] \qquad \textbf{(5.8)}$$

The final form of the Equation 5.8 could be applied for the different types of vegetation (i.e. Type 1, 2, and 3) by substituting the related gradient and intercept (Table 5.1) values into Equation 5.8. This form of the equation will be called as “specific equation” hereafter. However, the obtained formulation would be questionable unless the validity of the formulation was verified. So as to verify the proposed formulation, the velocity profiles at the downstream of the vegetation were predicted employing Equation 5.8 for each type of vegetation and compared with the experimentally measured ones. In Figure 5.5 the comparisons were illustrated for the vegetation of Type 1, 2 and 3 respectively. Since experiments were carried out in two depths for Type 1 and 3, two examples are presented for the verification charts. Nevertheless, in some circumstances it may be more convenient to define a singular equation not to lead any misusage of formulation for practitioners. Therefore, based on the gradient and intercept values belonging to different test conditions given in Table 5.1, mean gradient and intercept values were calculated. Those values are underlined in Table 5.1. Equation 5.8 is described based upon the mean values which are given in Table 5.1 and this form of Equation 5.8 will be named as “generalized equation” hereafter. In the following paragraph a discussion on the performance of the Equation 5.8 is presented. In Figure 5.5, “measured velocity values” and “predicted velocity values” which was calculated by “specific equation” is given together with “generalized equation”. For the verification of the proposed formulation, Experiment 3, 6, 11, 15 and 19 (Table 4.1) was taken into assessment. In order to observe how the velocity profiles deflected in consequence of presence of vegetation, the non-disturbed velocity profile is also added into the charts. Figure 5.5a and 5.5b showed that in general speaking the introduced formulation Equation 5.8 provides quite satisfactory results in terms of velocity profile prediction performance for Type 1. When measured values and the values obtained by “specific equation” are compared, it is seen that the performance of “specific equation” is quite satisfactory for the value of lower water depth. For higher depth, the “specific equation” gives slightly overestimated velocity values at the region closer to the bed. In the vicinity of water surface, “specific equation” gives fairly satisfactory outcomes. When the performance of “generalized equation” is taken into consideration, it is seen that for shallower case “generalized equation” gives underestimated velocity values along the depth. It has better performance than “specific equation” for the higher depth value. When Figure 5.3 carefully examined it is seen that this is not a surprising outcome since the NVVDP values are highly scattered through the depth. Thus proposing one equation may provide better or worse results depending on the location of NVVDP curve.

In Figure 5.5c the predicted and measured velocity values at the downstream of vegetation are presented together with non-disturbed velocity profiles for Type 2. As seen from Figure 5.5b, the predicted velocity profiles by “specific equation” at the downstream of vegetation are in well agreement with the one experimentally measured. On the other hand, the “generalized equation” leads to slightly overestimated velocity values through the depth. Additionally, the outcomes showed that the trend of the velocity profile is predicted well by the proposed equation.

The variation of measured velocity values and those predicted by different form of proposed equation are illustrated in Figure 5.5d and 5.5e. The velocity values at the downstream of the vegetation predicted by both "specific equation" and "generalized equation" are in well agreement with the ones experimentally measured along the vertical for the lower value of depth. In spite of the fact that the velocity values which are predicted by "specific equation" and "generalized equation" are fairly close to each other but the region close to the bed. In the region close to the bed, the "generalized equation" gives relatively higher velocity values compared to the form of "specific equation". When the two equations are taken into consideration, it is clearly seen that both lead to overestimate velocity values in the region close to bed and underestimate velocity values in the area close to water surface. However, when the trend of measured velocity profile carefully examined it is seen that the profile has "s" shape and this profile could not be regarded as general behavior for all vegetation. Therefore it would be more appropriate to take the general trend of velocity profile into account.

In conclusion, the proposed equation (Equation 5.8) provides reasonable outcomes during the calculation of anticipated velocity profile at the $1D_v$ downstream of vegetation. However it should be noted the success of the results largely depend on the estimation of the volume of the plant in the field with an acceptable accuracy. In this context, the theorem which was firstly introduced by **McMohan and Kronauer (1976)** may be utilized. According to **McMohan and Kronauer (1976)**, branching pattern is approximately stationary within a plant specimen (**Fathi-Maghadam and Kouwen, 1997**). In other words there is a self similarity between the plant and its branch pattern. This similarity may be used as a reference during the calculation vegetation intensity parameter.

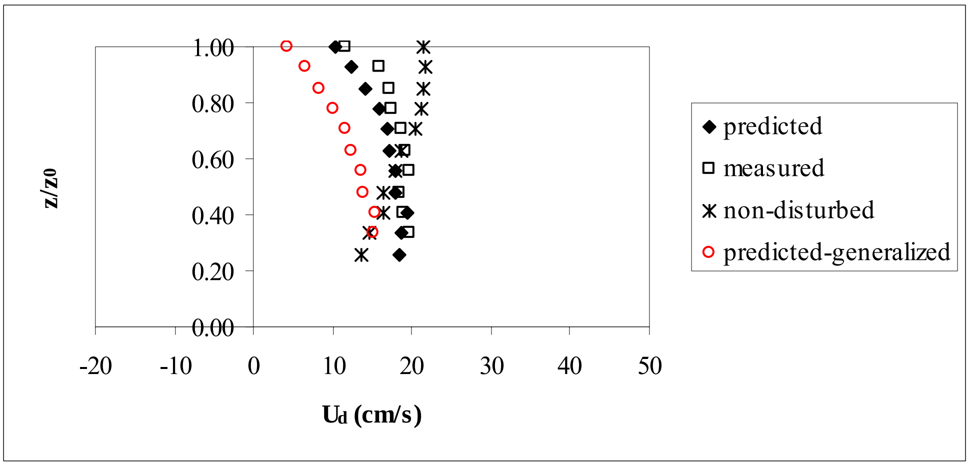

(a)

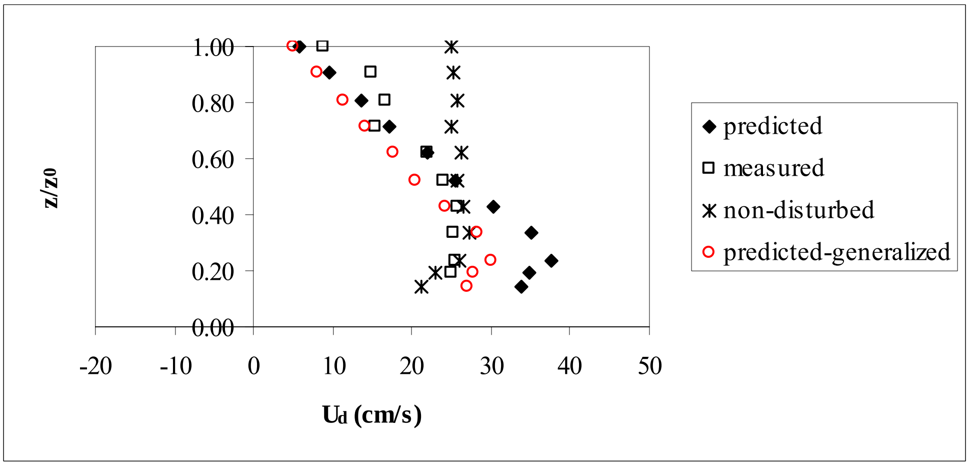

(b)

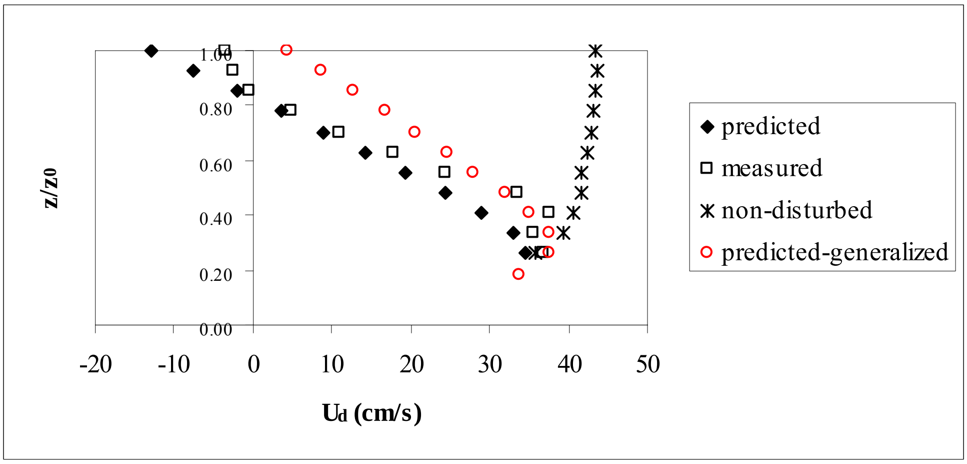

(c)

Figure 5.5: Comparison between measured and predicted velocity profiles at the downstream of vegetative element a) for Experiment no:3; b) for Experiment no:6; c) for Experiment no:11; d) for Experiment no:15; e) for Experiment no:19

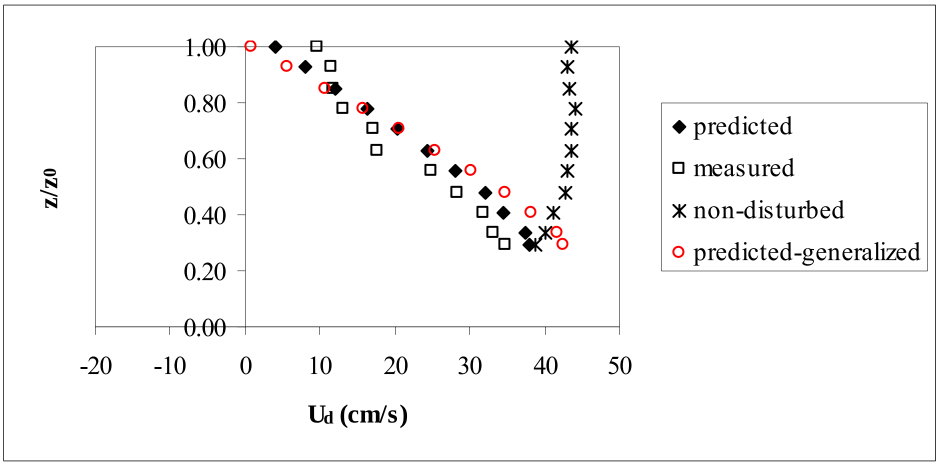

(d)

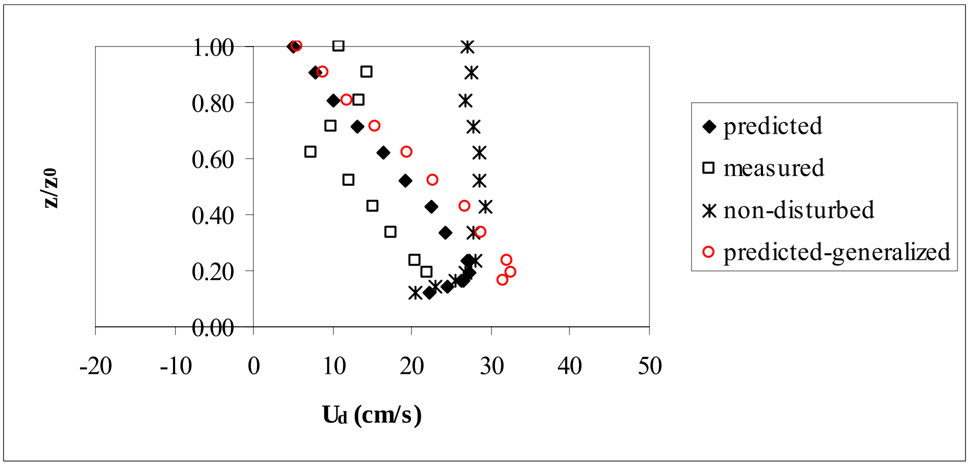

(e)

Figure 5.5 (continued): Comparison between measured and predicted velocity profiles at the downstream of vegetative element a) for Experiment no:3; b) for Experiment no:6; c) for Experiment no:11; d) for Experiment no:15; e) for Experiment no:19

5.4 The Influence of Vegetation on Neighbor Velocity Profiles

The influence of vegetative element in lateral direction was explored based on the experimental data in the light of the method given in Chapter 3. The graphs belong to variations of time averaged velocity along the depth at the measurement locations (Figure 4.4) are given in Appendix D section for all the test conditions. The one of the most important conclusion may be drawn from Appendix D is that the neighbor velocity profiles clearly fit to logarithmic velocity profile differing from the one at the downstream of vegetation along the centerline. When all the plots were taken into consideration in Appendix D, it may be clearly said that the vegetative element leads to considerable velocity increment along the depth at the neighbor locations of vegetation. As explained in Chapter 3, the lateral distance between axis of vegetal element and neighbor velocity profiles is $0.6D_v$. As seen from Figure D.1 to D.9, due to the presence of vegetation the time averaged velocity profiles are literally identical at the successive neighbor cross sections (i.e. at r300, r320, and r360) for Type 1. This is clearer for the shallower case (i.e. depth=25cm) (Figure D.1 to Figure D.9). Differing from Type 1, velocity profiles are fairly different from each other at the consecutive locations (i.e. r300, r320, and r360) for Type 2 (Figure D.11, D.12 and D.13). When those successive neighbor locations are taken into assessment, it is seen that unexpectedly the highest velocity profile is not at the vertical that is positioned at the same cross-section with vegetation. Surprisingly, the highest velocity profiles are observed at the locations “r360” which is at the 40 cm downstream of vegetative element. In spite of the fact that it is not as clear as Type 2, same circumstance was observed for Type 3 too (Figure D.15 to D.22). This is more noticeable for lower water depth in Type 3 (Figure D.15 to D.18). In summary, the presence of vegetation induces higher streamwise mean velocity at the neighbor locations of vegetative element. However, these assessments are verbal and it would be convenient to express it in numerical and dimensionless form. For this purpose, the non-disturbed velocity profiles and the velocity profile which is located at the same cross-section with vegetative element were compared and illustrated in dimensionless form in Figure 5.6 below. Since the details about the dimensionless expression were discussed in earlier chapter, no more discussion is presented in this chapter. However, it could be suitable to repeat in this connection that the dimensionless number belong to abscissa defines the ratio of increment in velocity in terms of percentage due to presence of vegetation. As may be seen from Figure 5.6a, when all the representative cases are considered it is seen that 10-30% velocity increment occurs at $0.6D_v$ cm neighbor locations in area closer to water surface of vegetative element. However, this percentage (10-30%) increases towards to depth. At the region closer to bed this ratios take the values of 20-60 %. Nevertheless, considering it is necessary to represent these ratios in terms of vegetative characteristics, Figure 5.6b was illustrated below.

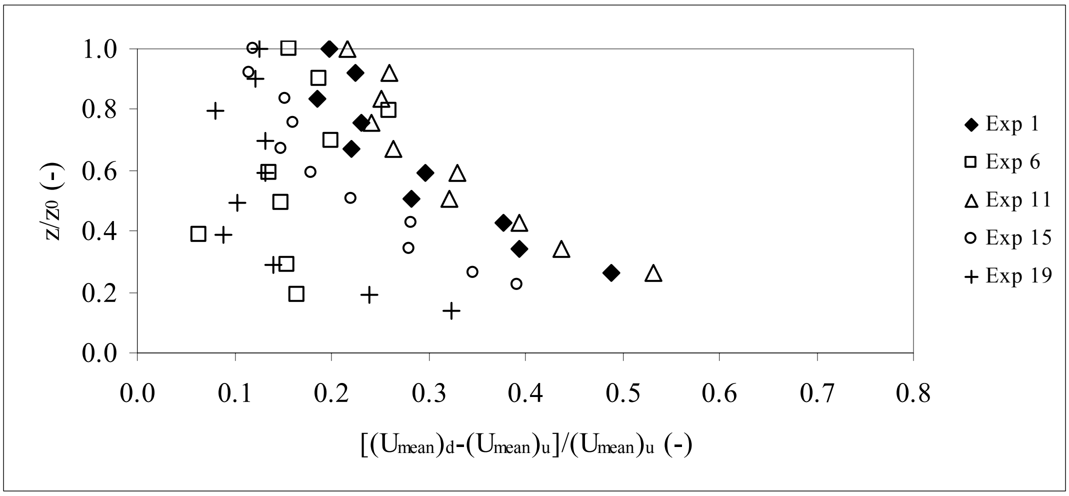

(a)

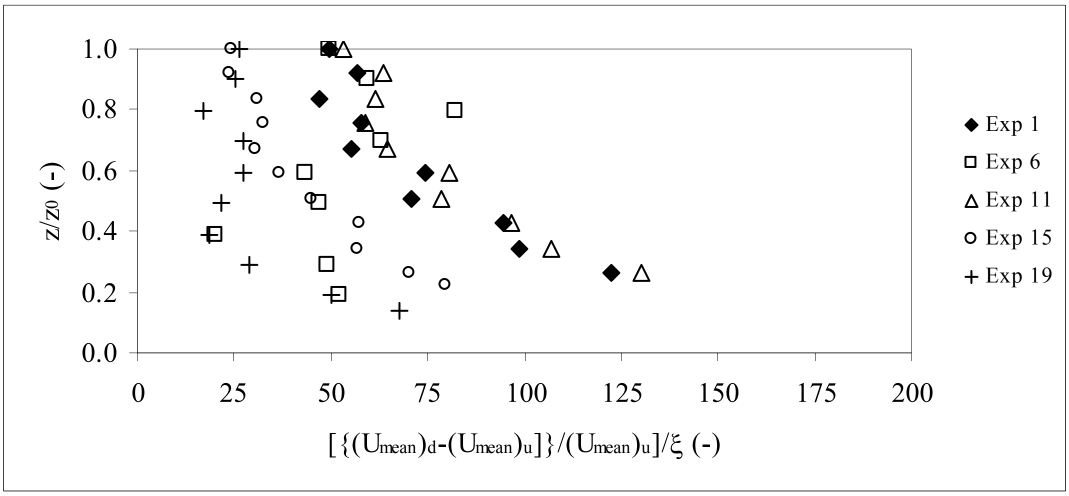

(b)

Figure 5.6: Comparison of velocity profiles which are located at the same cross-section with vegetative element and which has $0.6D_v$ cm lateral distance from the element a) normalized velocity difference parameter versus relative depth b) normalized vegetative velocity difference parameter versus relative depth

5.5 The Impact of Vegetation on Time Averaged Vertical Velocity

Non-disturbed case:

Time averaged vertical velocity versus relative depth is depicted in Figure 5.7 for non-disturbed flow for the test for Type 1, 2, and 3. As seen from Figure 5.7, around the region where z/z_0>0.2-0.3 time averaged vertical velocity take negative values for the non-disturbed case. In other words, vertical component towards to water surface in this region. Below the interface (which correspond to $z/z_0<0.4$) time averaged vertical velocity values leads to either zero or positive values.

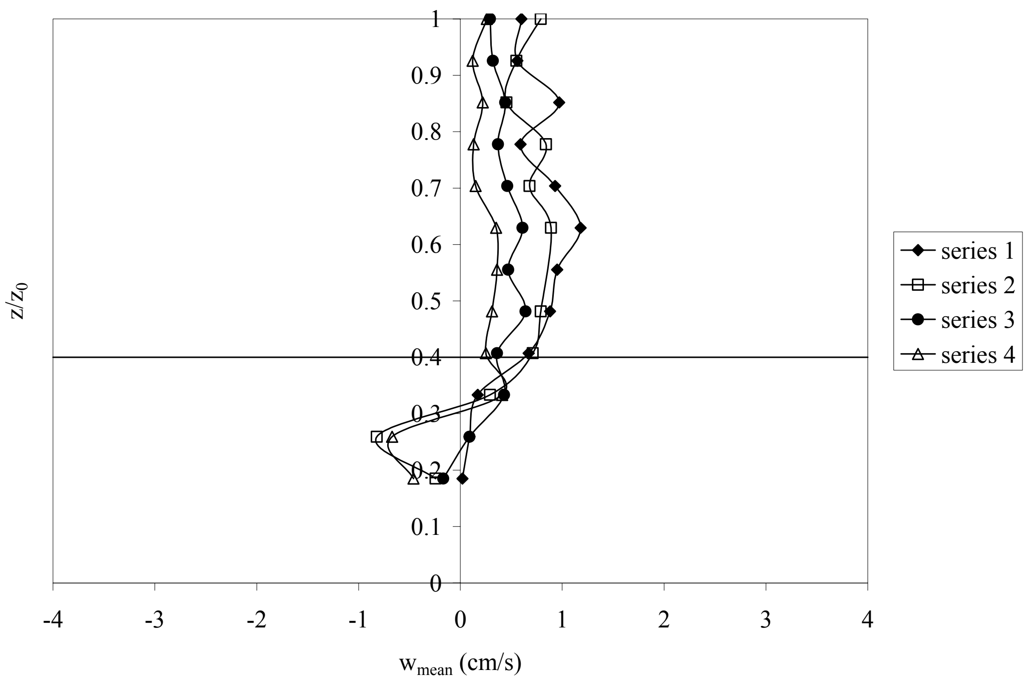

(a)

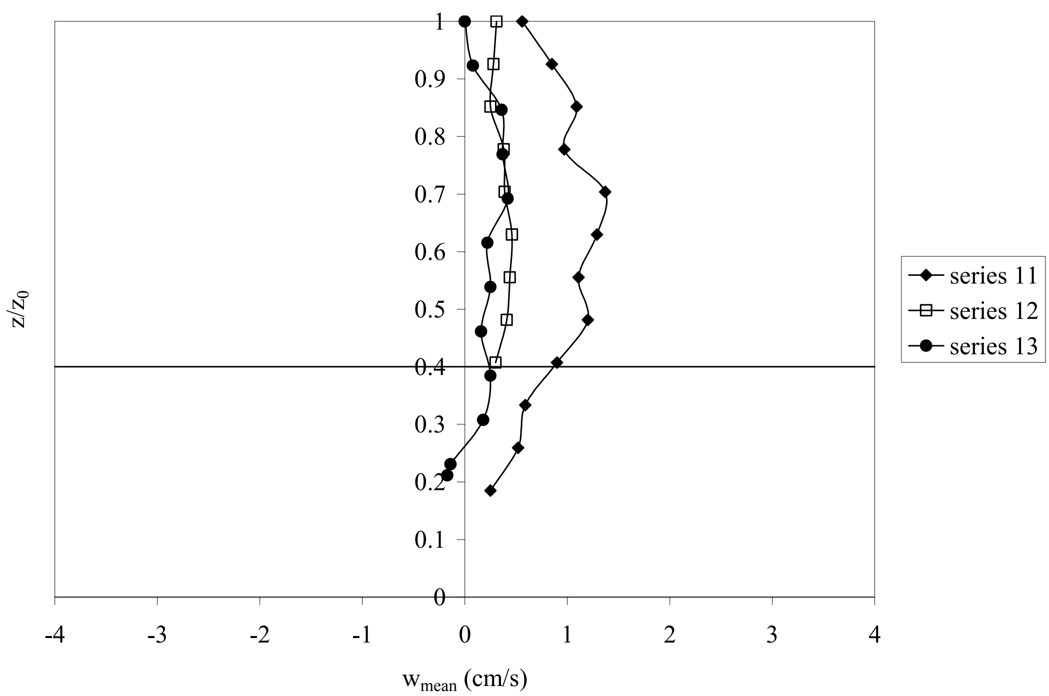

(b)

Figure 5.7: The variation of time averaged vertical velocity values against to relative depth belong to non-disturbed flow for a) Type 1, b) Type 2, c) Type 3

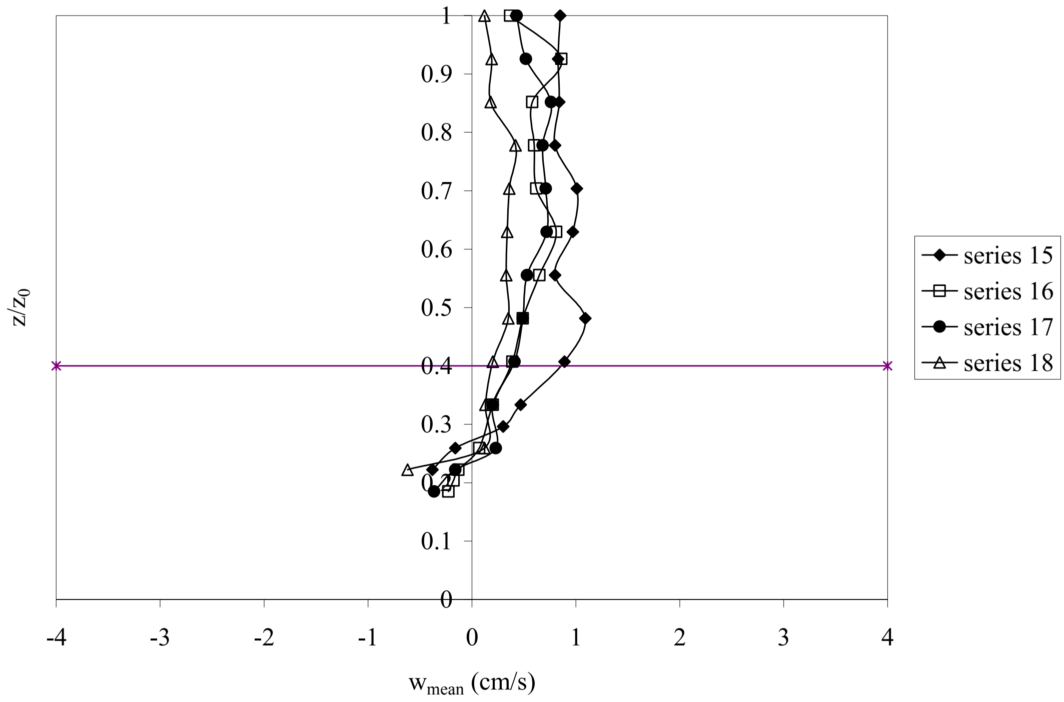

(c)

Figure 5.7 (continued): The variation of time averaged vertical velocity values against to relative depth belong to non-disturbed flow for a) Type 1, b) Type 2, c) Type 3

Type 1

Time averaged vertical velocity measured at the downstream of vegetation is plotted against to relative depth and presented in Figure 5.8. As could be seen from Figure 5.8, time averaged vertical velocity values is not significantly different from non-disturbed case in terms of magnitude for Type 1. Furthermore, the magnitude of time averaged vertical velocity is fairly low. In parallel with non-disturbed case, time averaged vertical velocity values are mostly positive along the depth but the region closer to bed. Despite of the fact that it is not rather obvious, time averaged vertical velocity has tends to increase around the interface between Zone 1 and Zone 2. This is very characteristic for all cases i.e. Type 1, 2 and, 3.

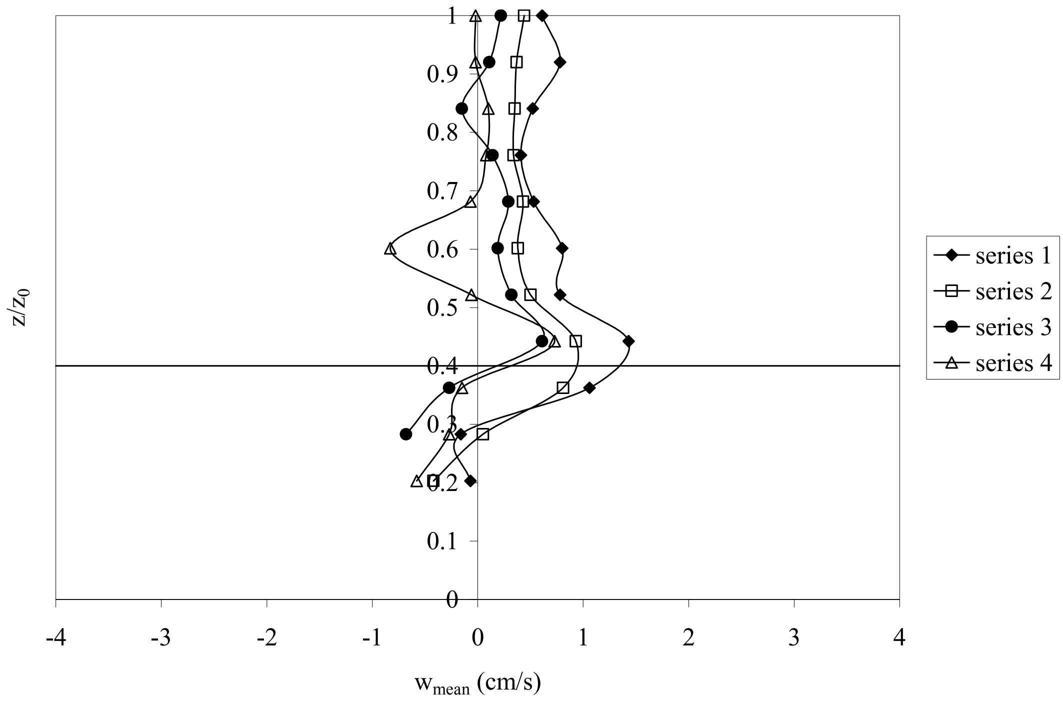

Figure 5.8: Time averaged vertical velocity measured at the downstream of vegetation versus relative depth for Type 1

The abscess of Figure 5.9 gives the additional time averaged vertical velocity percentage due to presence of vegetation. As may be seen from the Figure 5.9, at the downstream side of the vegetation the time averaged vertical velocity mostly take lower values compared to one at the upstream for Type 1. This situation can be explained with the foliage structure of the vegetation. As may be seen from the Figure A.1, *Pinus Pinea* foliages are fairly skinny and long. Thanks to this property the foliages adapt streamlines very easily and mitigate the vertical component of the flow. In addition to normalized vertical velocity difference parameter for Type 1, also is the variation of normalized vegetative vertical velocity difference parameter with respect to relative depth for Type 1 is given in Appendix E.1.

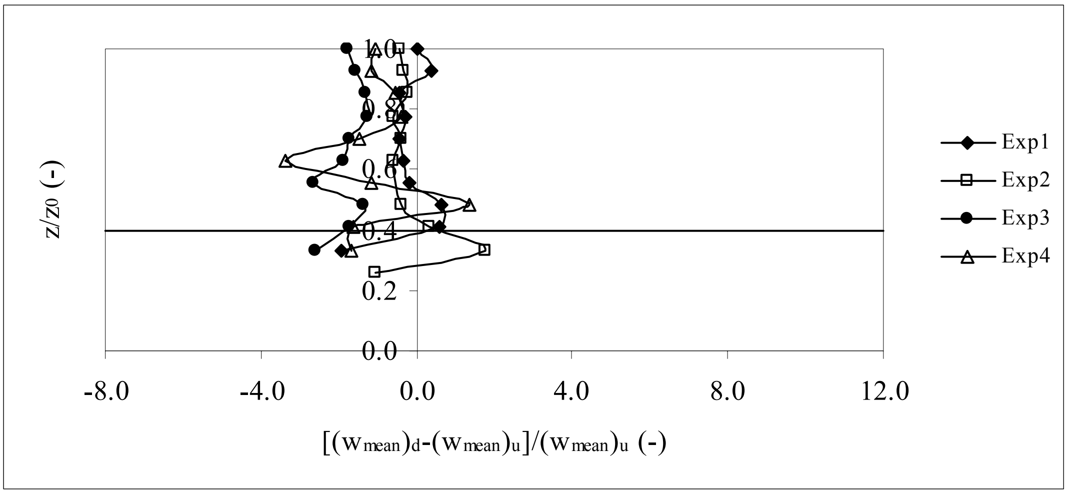

Figure 5.9: The variation of normalized vertical velocity difference parameter with respect to relative depth for Type 1

Type 2

The time averaged vertical velocity observed at the downstream of vegetation versus relative depth is depicted in Figure 5.10 for Type 2. In Type 2, stronger time averaged vertical velocity values were observed compared to Type 1 around the interface between Zone 1 and Zone 2. This could be explained by the stronger under canopy flow that occurs owing to plant architecture of Type 2. In other words, depending on the vegetation architecture more severe under canopy flow occurs in Type 2. Above the interface, time averaged vertical velocity does not differentiate along the depth for Type 2. Nevertheless, it should be also kept in mind that the magnitude of the time averaged vertical velocity is not quite high along the depth compared to streamwise time averaged mean velocity values.

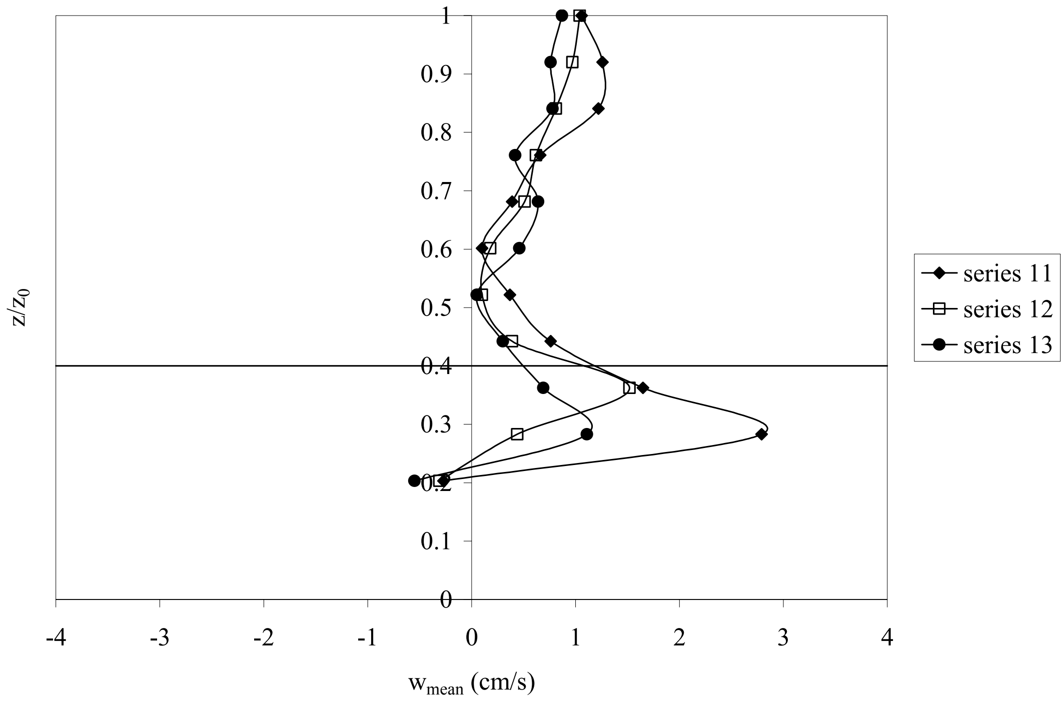

Figure 5.10: Time averaged vertical velocity measured at the downstream of vegetation versus relative depth for Type 2

In Figure 5.11, additional time averaged vertical velocity percentage due to presence of vegetation versus relative depth is given for Type 2. As may be concluded from Figure 5.11 that the existence of vegetation induces approximately 200-300 % additional time averaged vertical velocity at the upper part of $z/z_0=0.8$ for Type 2. At the location of $0.5<z/z_0<0.8$ the additional time averaged vertical velocity values take negative values which means the presence of vegetation reduce the time averaged vertical velocity. In the vicinity of the interface between Zone1 and Zone 2, the vertical velocity addition due to the vegetation dramatically increases and indicates 300-400% additional time averaged vertical velocity. The variation of normalized vegetative vertical velocity difference parameter with respect to relative depth for Type 2 is given in Appendix (E.2).

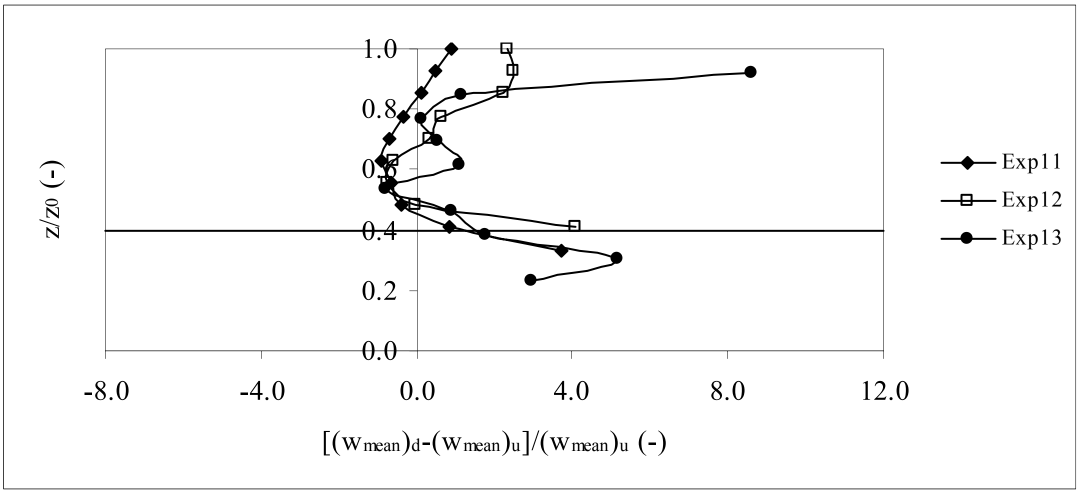

Figure 5.11: The variation of normalized vertical velocity difference parameter with respect to relative depth for Type 2

Type 3

Time averaged vertical velocity values are slightly larger in Type 3 compared to Type 1 and Type 2 around the interface between Zone 1 and Zone 2. More specifically, approximately 2-4 cm/s velocity values were observed towards to water surface around the region interface. This situation could be explained with the strong under canopy flow. In fact, as could be seen from contour plots (Figure D.15 to D.18) though there is a strong under canopy flow in Type 3, the time averaged mean velocity in the streamwise direction is pretty low in the region Zone 2. Because of this reason, a strong momentum transfer occurs towards to water surface direction.

In Zone 2, around the region z/z_0=0.5-0.6 time averaged mean vertical velocity is in the vicinity of zero value. Above z/z_0=0.5-0.6 towards to water surface time averaged mean vertical velocity has values between-1cm/s and -2cm/s. Here it should be noticed that negative values indicate the flow direction towards bed,

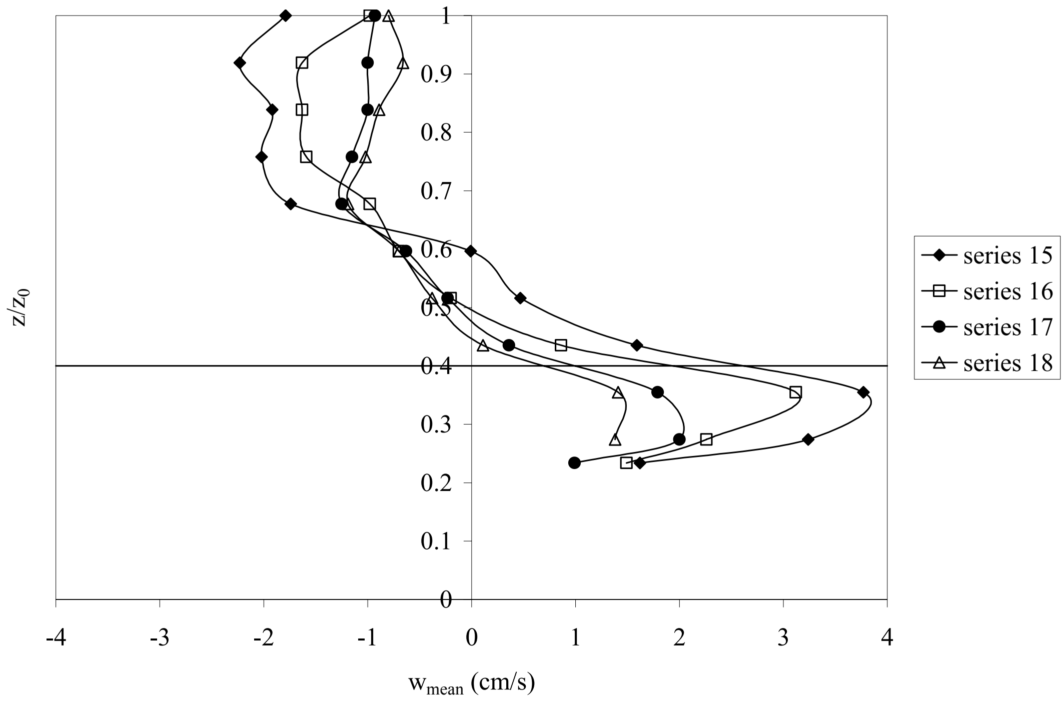

Figure 5.12: Time averaged vertical velocity measured at the downstream of vegetation versus relative depth for Type 3

The relationship between relative depth and the additional time averaged vertical velocity due to presence of vegetation for Type 3 is given in Figure 5.13. As may be seen from Figure 5.12, at the upper part of $z/z_{0=}0.5$ (i.e. $z/z_0>0.5$), the additional time averaged vertical velocity ratios has negative values since at the downstream of the vegetation time averaged vertical velocity is already negative (Figure 5.12). Negative vertical velocity values indicate the flow direction is towards to water surface. It can be judged from Figure 5.12 that at the lower part of $z/z_{0=}0.5$ (i.e. $z/z_0<0.5$) up to 8 times higher time averaged vertical velocity values were observed at the downstream side of the vegetation. Especially when the interface between zone1 and zone2 is considered, it may be seen that 6-10 times larger values are occurred due to under canopy flow. In addition to normalized vertical velocity difference parameter for Type 3, also the variation of normalized vegetative vertical velocity difference parameter with respect to relative depth for Type 3 is given in Appendix (E.3).

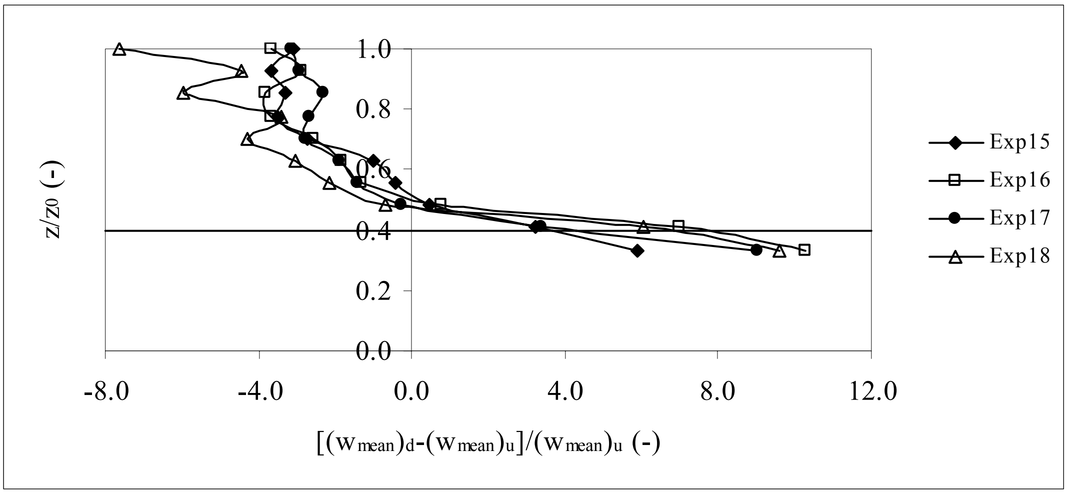

Figure 5.13: The variation of normalized vertical velocity difference parameter with respect to relative depth for Type 3

The relationship between “distances from bottom” versus “vegetation volume” is depicted in Figure 3.3. When the results from Figure 3.3 and the results given in the paragraph above both considered, strangely it was seen that flow is less disturbed by Type 3 though the occupied volume of Type 3 is higher compared to Type 1 and 2. This could be explained by the plant architecture of vegetation which has relatively high trunk and first order branch volume and low foliage volume.

Despite of the fact that Type 2 and 3 have close values of volume for the given depth, more severe under-canopy flow was observed in Type 3. This could be explained by more stiff foliage nature of Cupressus Macrocarpa (which characterizes Type 3) compared to Thuja Oriantalis (which characterizes Type 2).

5.6 The Effect of Vegetation on Streamwise Turbulence Intensity

The variation of streamwise turbulence intensity with relative depth is shown below for Type1, 2 and 3. As could be seen from Figure 5.14, 5.16, and 5.17, streamwise turbulence intensity increases towards to bed for all cases. Furthermore, when flow velocities are also taken into consideration, it may be said that with the increasing of flow velocity the gradient of $[(dz/z_0)/du'_{rms}]$ prone to decrease.

Based on the Figure 5.14 to 5.19, it may be said that streamwise turbulence intensity increases towards to bed for non-disturbed case. Furthermore, it was seen that with the decreasing time averaged mean velocity $[(dz/z_0)/du_{rms}]$ gradient prone to decrease.

Type 1

The variation of streamwise turbulence intensity with relative depth is given at downstream of vegetation and the non-disturbed case. When the streamwise turbulence intensity at the downstream of vegetation and non-disturbed case are compared it was seen that there is no significant difference between those two in terms of magnitude. This result is in agreement with the time averaged mean vertical velocity values measured for non disturbed case and at the downstream of vegetation.

It would be convenient to analyze the streamwise turbulence intensity in two parts; those are above and below of z/z_0=0.84. Above z/z_0=0.84, the streamwise turbulence intensity values dramatically increase towards to water surface. This part corresponds to the area where foliage and branch volume is significantly high (Figure A.1) compared to below part of it. This could be attributed to time averaged mean velocity. As may be seen form Figure B.1, B.2, B.3 and B.4, the gradient of time averaged mean velocity with depth is higher around the region closer to water surface compared to below part since the blockage of the vegetation is pretty high in this region. In other words, in this part $[d(z/z_0)/dU_{mean}]$ ratio is lower behind the vegetation compared to non-disturbed case.

Below the z/z_0=0.84, streamwise turbulence intensity increases linearly towards to the bed. As is seen from Figure 5.14 , with the increasing flow velocity the gradient of this linear part decreases. Additionally, below z/z_0=0.84 there is no dramatic difference between streamwise turbulence intensity at the downstream of vegetation and non-disturbed case. In fact, this is a surprising outcome as the time averaged mean velocities are quite different from each other at these two locations. On the other hand, when the time averaged mean vertical velocities are considered (Figure B.1, B.2, B.3 and B.4) it may be seen that this parameter takes lower values for Type 1 compared to Type 2 and 3 which indicates lower momentum transfer between layers for Type 1. This result is in an agreement with observed streamwise turbulence intensity.

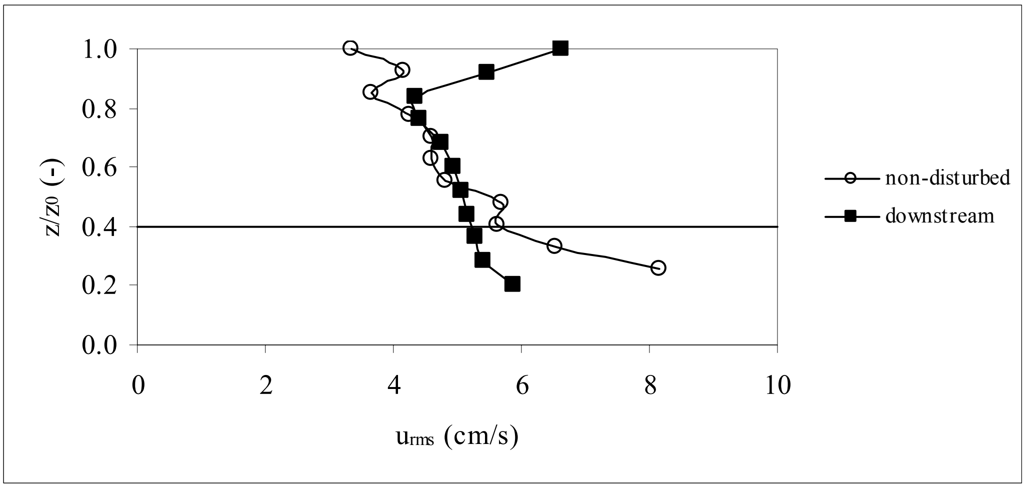

(a)

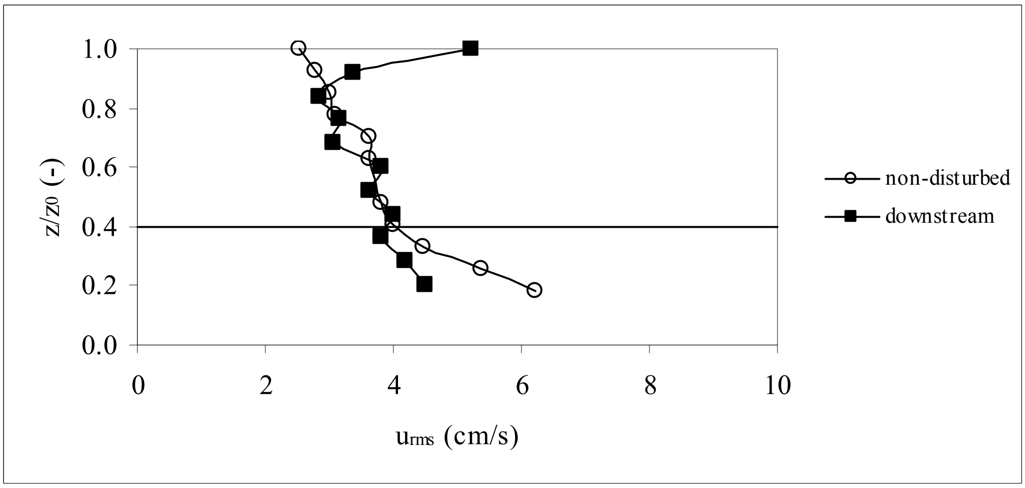

(b)

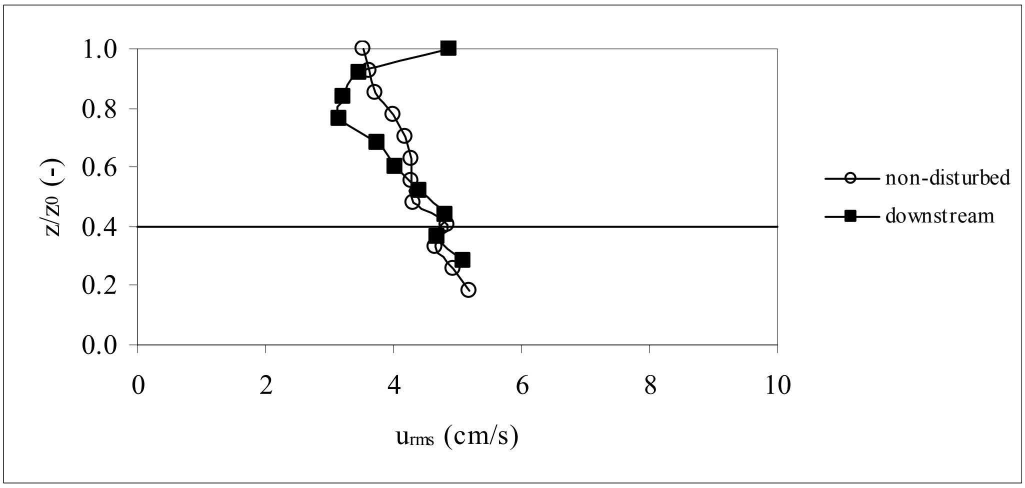

(c)

Figure 5.14: The variation of streamwise turbulence intensity with relative depth for Type1 a) Experiment 1, b) Experiment 2, c) Experiment 3

The relationship between relative depth and additional streamwise turbulence intensity owing to existence of vegetation is given in Figure 5.15. As it may be concluded from Figure 5.15, the highest contribution to additional streamwise turbulence intensity is at the location where the vegetation block the flow relatively more (z/z_0>0.9). However, even at this location the additional turbulence intensity ratio is not larger than 100%. On the other hand, as could be concluded form Figure 5.15, at the lower part of z/z_0<0.9 the additional turbulence intensity values may take either negative or positive values. More specifically, the presence of vegetation induces ±20 % additional streamwise turbulence intensity. In other words, for Type 1 the contribution of vegetation on additional streamwise turbulence intensity is not distinctive accept at the location of z/z_0>0.9. This situation can be explained by comparatively low blockage ratio for Type 1 at the location of z/z_0<0.9. Additionally, the variation of normalized vegetative streamwise turbulence intensity parameter with respect to relative depth for Type 1 is given in Appendix (F.1).

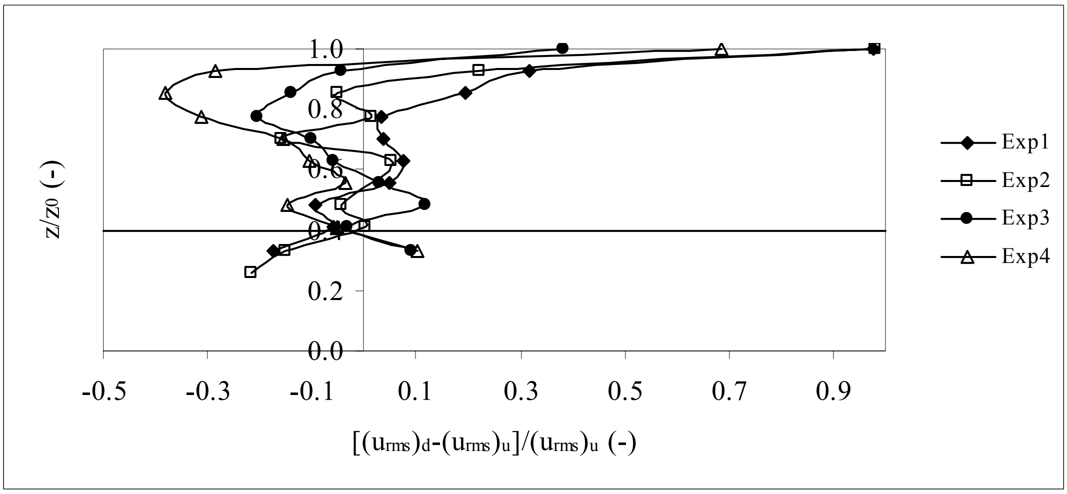

Figure 5.15: The variation of normalized streamwise turbulence intensity parameter with respect to relative depth for Type 1

Type 2

The streamwise turbulence intensity could be considered in two parts at the downstream of the vegetation (Figure 5.16). These are above and below z/z_0=0.4 which correspond to interface between Zone 1 and 2. In general speaking, as could be seen from Figure 5.16 extra streamwise turbulence intensity due to presence of vegetation is relatively stronger along the depth in Type 2. In a way, this situation indicate the existence of vegetation largely dissipate the energy in Type 2. Above z/z_0=0.4, when the streamwise turbulence intensity examined it is seen that for Type 2 the values of this parameter are relatively smaller compared to Type 1. The turbulence at the downstream has lower values around water surface and it increases towards to interface. In the vicinity of interface it reaches peak values. In other words, maximum turbulence is appeared around the level where the second degrees of branches are appeared. A relationship could be established between this result and time averaged mean vertical velocity observed at the same level. In fact, around the same level time averaged mean vertical velocity values reach the peak values as well. These prove that there is a high momentum transfer between the vertical layers. The results obtained from "vertical turbulence intensity" versus "relative depth" variation are supportive for these conclusions. Below z/z_0=0.4 streamwise turbulence intensity decreases towards to bed.

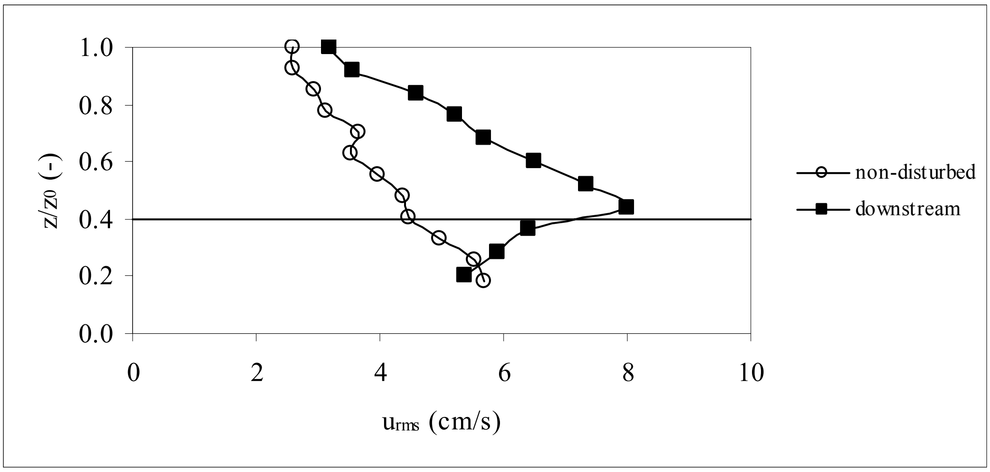

(a)

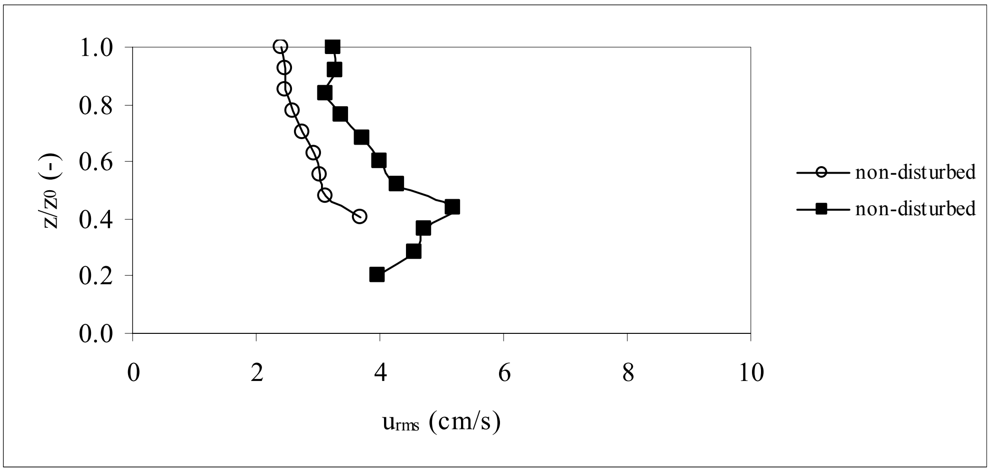

(b)

Figure 5.16: The variation of streamwise turbulence intensity with relative depth for Type 2 a) Experiment 11, b) Experiment 12, c) Experiment 13

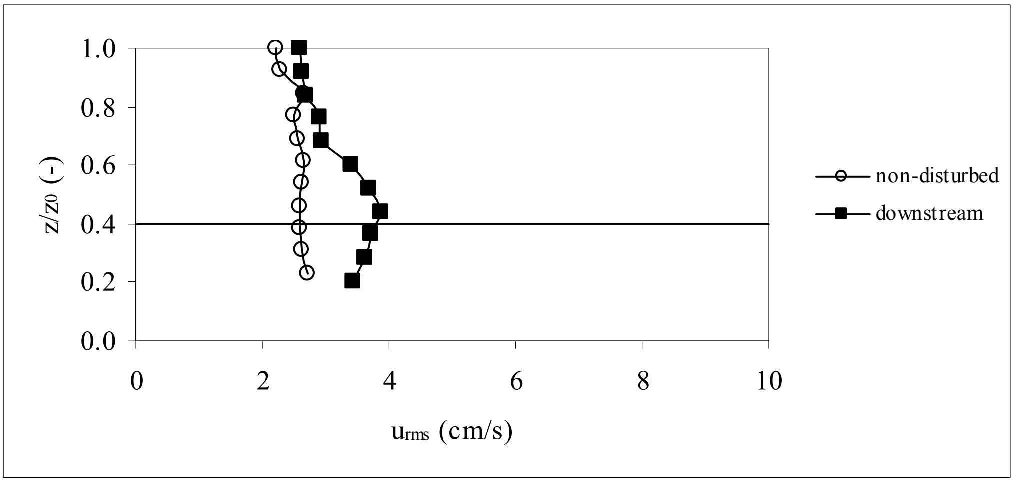

(c)

Figure 5.16 (continued): The variation of streamwise turbulence intensity with relative depth for Type 2 a) Experiment 11, b) Experiment 12, c) Experiment 13

Figure 5.17, presents the variation between relative depth and additional streamwise turbulence intensity owing to vegetation for Type 2. In Type 2, differing from Type 1 the additional turbulence intensity due to vegetation is always positive. This situation may be associated with the dense foliage structure of Type 2. In fact also for Type 1, in parallel with Type 1, where the foliage density is high (z/z_0>0.9) the additional turbulence intensity is fairly high. When the scale of additional streamwise turbulence due to vegetation is considered it may be concluded that, up to 90 % additional streamwise turbulence occurred (Figure 5.17). Further when each of the experiment is individually examined, it may be seen that slightly higher additional turbulence occurred in the vicinity of interface between Zone1 and Zone2. Moreover, at the lower part of this interface additional turbulence tends to decrease. Also, based on the Figure 5.17 it may be claimed that with the increasing flow velocity, the additional turbulence increases. Additionally, the variation of normalized vegetative streamwise turbulence intensity parameter with respect to relative depth for Type 2 is given in Appendix (F.2).

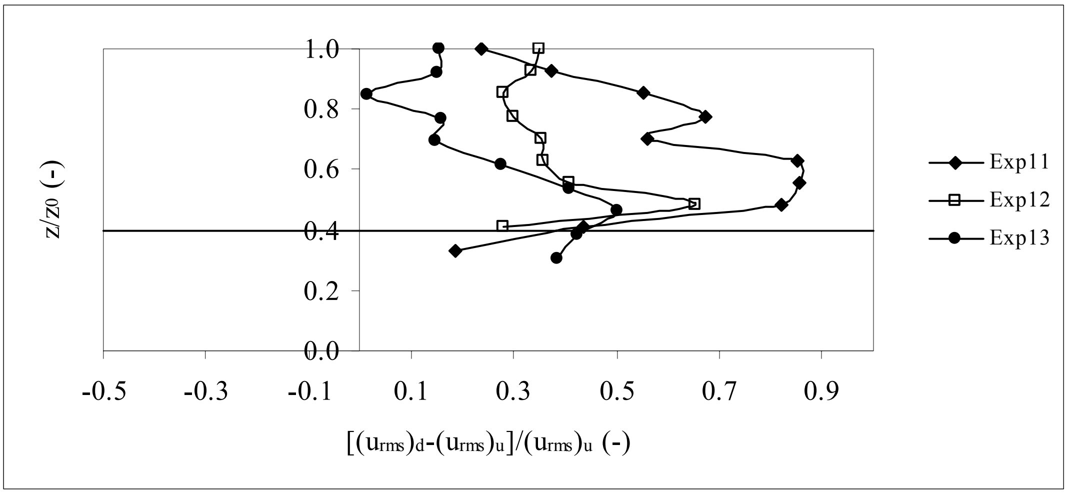

Figure 5.17: The variation of normalized streamwise turbulence intensity parameter with respect to relative depth for Type 2

Type 3

In Figure 5.18 the variation of streamwise turbulence intensity owing to presence of vegetation with relative depth is given for non-disturbed case. Figure 5.18 showed that streamwise turbulence intensity between non-disturbed case and measured at the downstream of vegetation is not dramatically different from each other in terms of magnitude. However as is seen in Figure 5.18, when the time averaged mean velocity is high the streamwise turbulence intensity is relatively higher than the one belong to non-disturbed case.

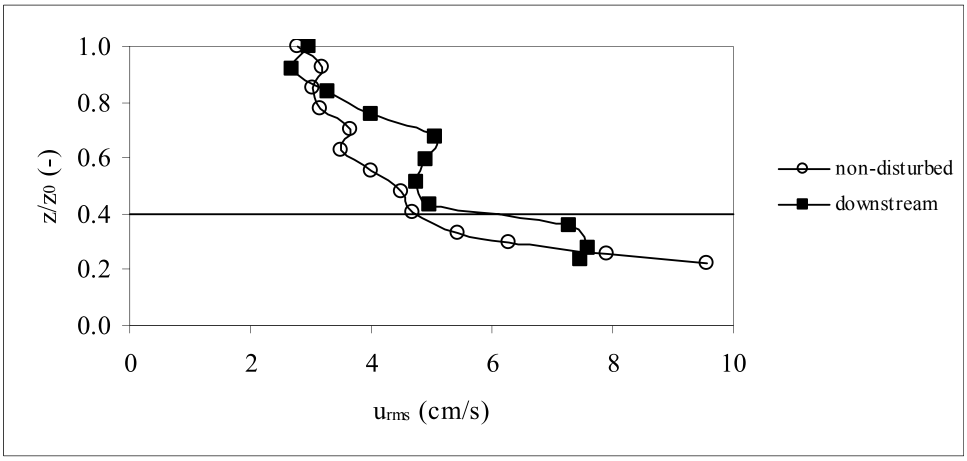

(a)

Figure 5.18: The variation of streamwise turbulence intensity with relative depth for Type 3 a) Experiment 15, b) Experiment 16, c) Experiment 17, d) Experiment 18

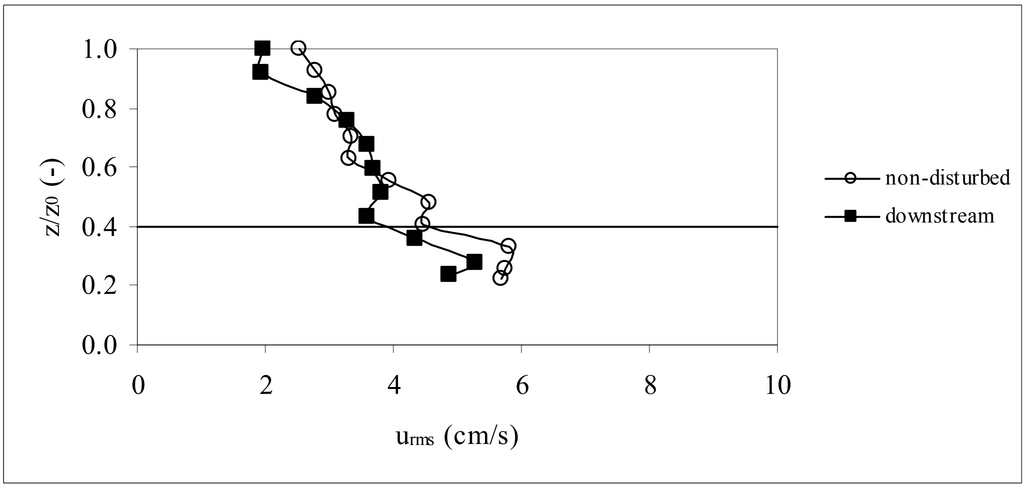

(b)

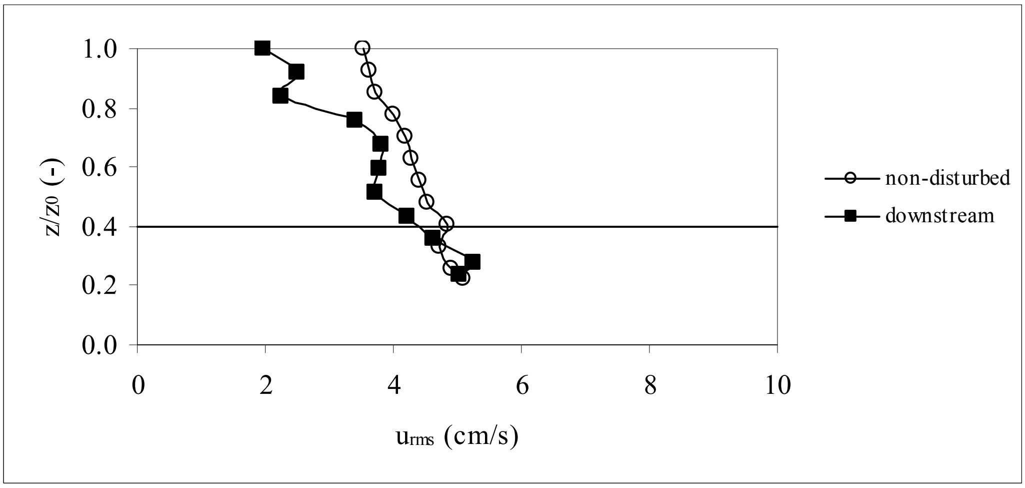

(c)

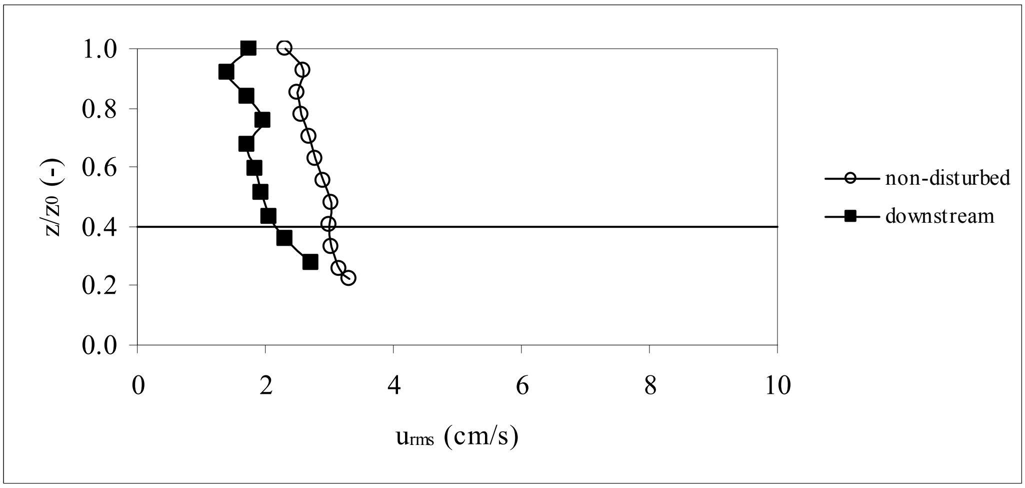

(d)

Figure 5.18 (continued): The variation of streamwise turbulence intensity with relative depth for Type 3 a) Experiment 15, b) Experiment 16, c) Experiment 17, d) Experiment 18

When the variation of the streamwise turbulence intensity with depth is examined it is seen that differing from Type 1 and 2, the curve of Type 3 has a more smooth character. In other words, any peak value was not observed along the depth in Type 3 like observed in Type 1 at closer to surface or like observed in Type 2 around the interface.

In Figure 5.19, relative depth versus additional streamwise turbulence due to vegetation is given for Type 3. In parallel with Type2, Type 3 point out that when the flow velocity increases, the additional turbulence intensity due to vegetation increases. Another conclusion that may be drawn from Figure 5.19 that variation of additional streamwise turbulence intensity along the depth is not very characteristic for Type3. When the size of the additional turbulence is taken into consideration, it can be seen from Figure 5.19 that approximately ± 50 % additional turbulence occurred due to presence of vegetation. In other words, vegetation increases or decreases the streamwise turbulence depending on the magnitude of velocity for Type3. The variation of normalized vegetative streamwise turbulence intensity parameter with respect to relative depth for Type 3 is given in Appendix (F.3)

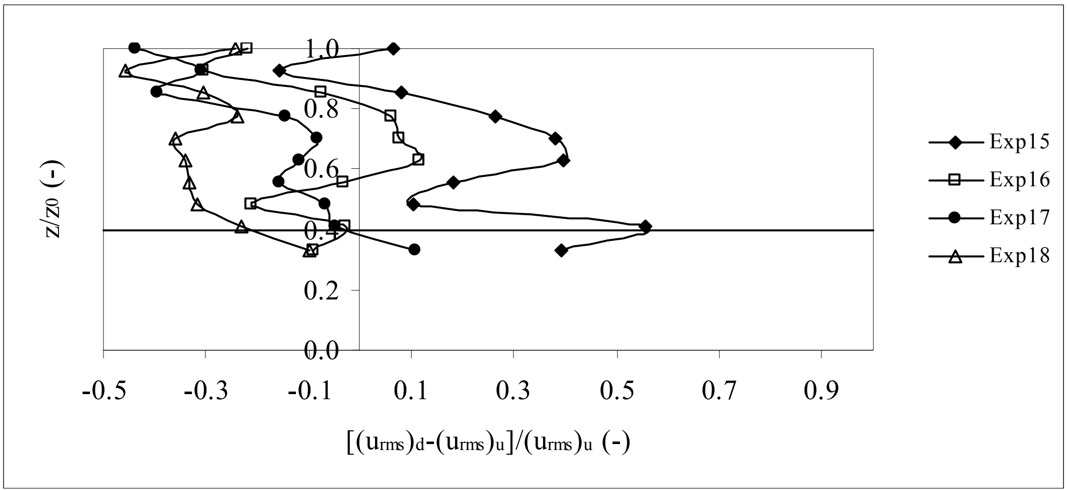

Figure 5.19: The variation of normalized streamwise turbulence intensity parameter with respect to relative depth for Type 3

When all experimental results belong to three types of vegetation are taken into consideration, it was seen that the sizes of additional streamwise turbulence intensities vary depending on the vegetation type. Furthermore, it was observed that additional turbulence intensity due to vegetation is relatively high where the blockage of the vegetation is high in all types of vegetation. However, the size of the additional streamwise turbulence is not considerably high even for the locations where the additional turbulence intensity is comparatively high. The highest additional streamwise turbulence intensity observed in the tests is not larger than 100 %. On the other hand, as may be judged from the following section, this ratio takes much higher values for vertical turbulence intensity. Another general conclusion that may be drawn from the experimental result is that with the increasing flow velocity additional streamwise turbulence increases.

The variation of “additional turbulence intensity due to vegetation” versus “relative depth” for three types of vegetation was analyzed in this section. The additional streamwise turbulence intensity is combined with vegetative parameter and given by Figure (E.2).

5.7 The Effect of Vegetation on Vertical Turbulence Intensity

The performed measurements showed that vertical turbulence intensity is not a function of depth and it takes a constant value along the water depth for non-distrubed flow (Figure 5.20, 5.22 and 5.24). However, in all cases differing from streamwise turbulence intensity, vertical turbulence intensity takes much higher values in comparison with non-disturbed case. When all cases are taken into consideration it could be claimed that at the downstream of vegetation vertical turbulence intensity is two or three times bigger than the non-disturbed case. In a way this situation indicates that presence of vegetation leads to much extra larger vertical turbulence intensity compared to streamwise turbulence intensity. Another common side of three type of vegetation is that vertical turbulence intensity reaches the peak values in the vicinity of interface.

Type 1

The variation of vertical turbulence intensity with relative depth is illustrated in Figure 5.20. As is seen from Figure 5.20 the curve has “S” shape with a maximum appeared around the interface. In parallel with streamwise turbulence intensity, vertical turbulence intensity is also takes maximum values at the region close to the water surface. This part corresponds to the region where the foliage and branch volume is significantly high (Figure A.1) compared to below part of it. In other words, in this part the resistance to flow is the highest. It is a well known fact that between two points, how the energy difference is high, energy flux between those two is that much high. Based on this fact, when the time averaged mean velocities belong to Type 1 are checked (Figure B.1, B.2, B.3, (B.4)) it is seen that at the points closer to the water surface, the velocity differences between layers are high. This induces larger degree of momentum transfer between the layers and this leads to larger degree of streamwise and vertical turbulence intensity. Another location where the maximum vertical turbulence intensity occurs is the vicinity of the interface between Zone 1 and 2. In parallel with observing peak vertical turbulence intensity around the interface, time averaged velocities are also takes the peak values around this region. For the other types (for both Type 2 and 3), maximum vertical turbulence intensity observed around this region as well.

The lowest value of vertical turbulence intensity is appeared at the locations of $z/z_0=0.76$; $z/z_0=0.76$; $z/z_0=0.76$ and, $z/z_0=0.68$ for the subsequent four experiments respectively. This observed low value of vertical turbulence intensity at this region could be explained by further understanding time averaged mean velocity belong to this location (Figure B.1, B.2, B.3, 3.4). As could be seen from Figure B.1, B.2, B.3, B.4, at the just above and below neighbour measurement points, time averaged mean velocity values are not substantially different than the values at aforementioned locations above. As is stated in previous paragraph, how the magnitude of energy difference is high between two points, the energy flux between those two is that much high. In this connection, when the time averaged mean velocities represent flow energy in away, the reason of low value of vertical intensity is better understood for the locations aforementioned.

When it is considered that the magnitude of occurred energy transfer between flow layers is dependent on the magnitude of the difference of energy between those layers this outcome could be more easily understood.

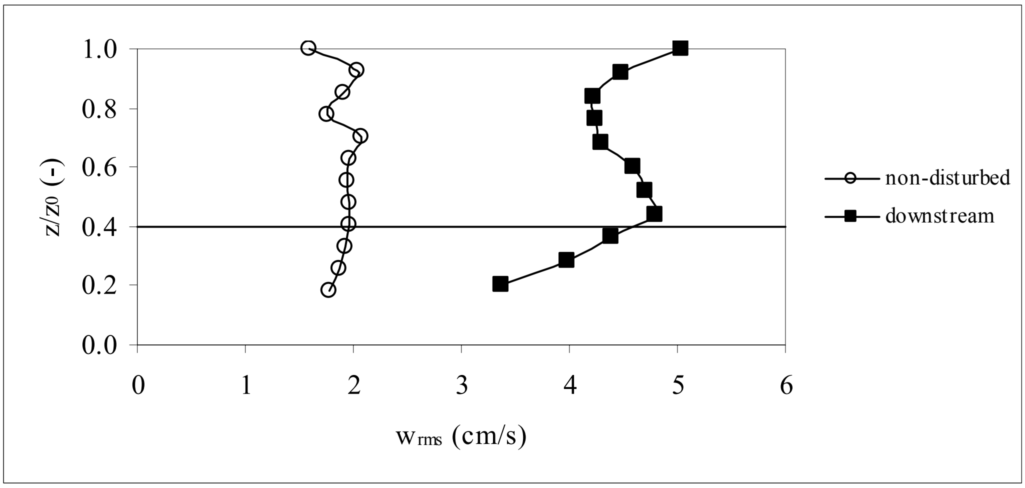

(a)

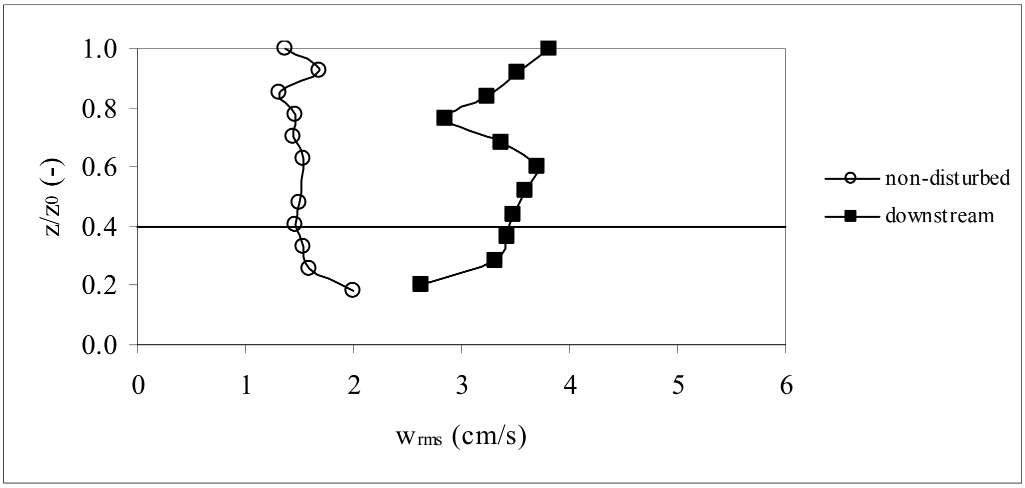

(b)

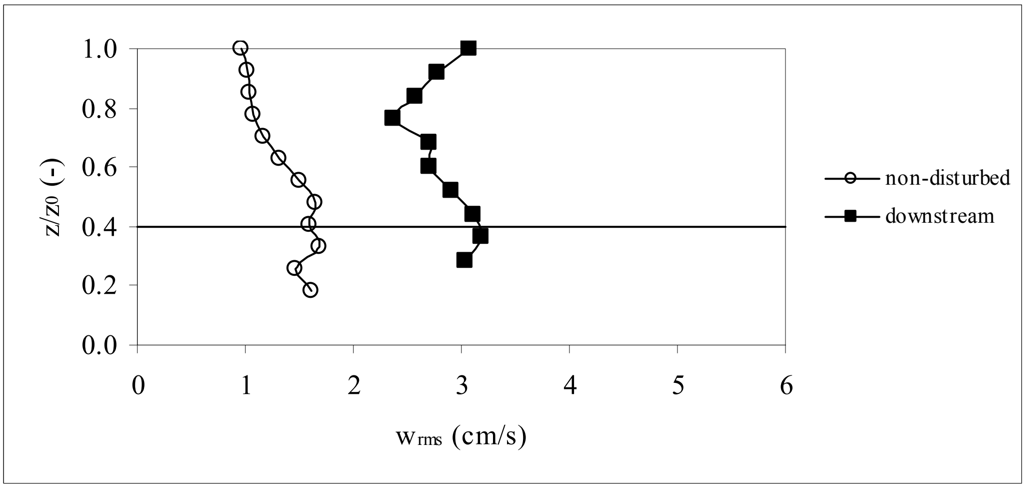

(c)

Figure 5.20: The variation of vertical turbulence intensity with relative depth for Type 1; a) Experiment 1, b) Experiment 2, c) Experiment 3, d) Experiment 4

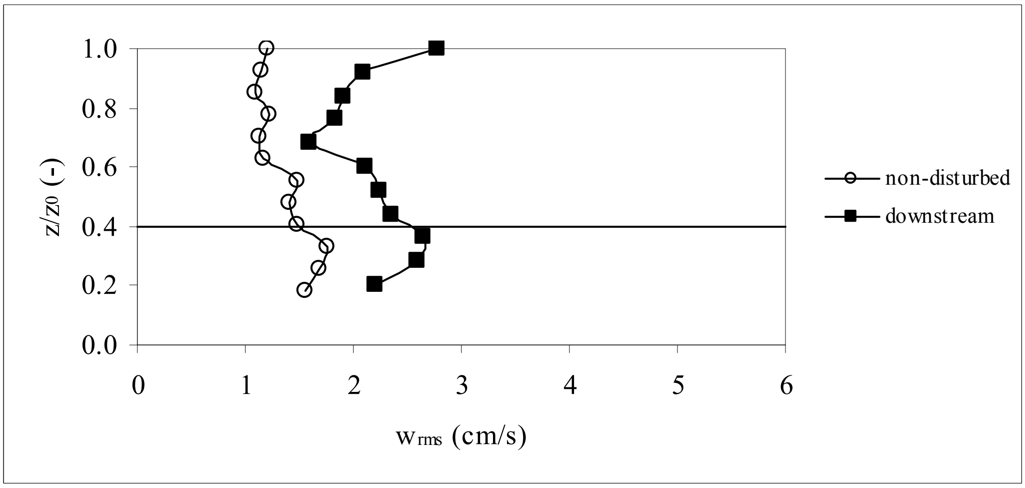

(d)

Figure 5.20 (continued): The variation of vertical turbulence intensity with relative depth for Type 1; a) Experiment 1, b) Experiment 2, c) Experiment 3, d) Experiment 4

The variation of “additional vertical turbulence intensity percentage due to existence of vegetation versus relative depth is given below (Figure 5.21). Figure 5.21 showed that the presence of vegetation leads to dramatic increment of the additional vertical turbulence intensity for Type 1. More specifically, presence of vegetation produces circa 220 % extra vertical turbulence. This value is almost double of additional streamwise turbulence due to vegetation. In spite of the fact that it is not quite distinctive, it may be said that with the increasing flow velocity, vegetation induced additional vertical turbulence intensity ratio prone to increase. In parallel with the earlier results above, the highest extra turbulence intensity due to vegetation is in the region of water surface. The variation of normalized vegetative vertical turbulence intensity parameter with respect to relative depth for Type 1 is given in Appendix (G.1).

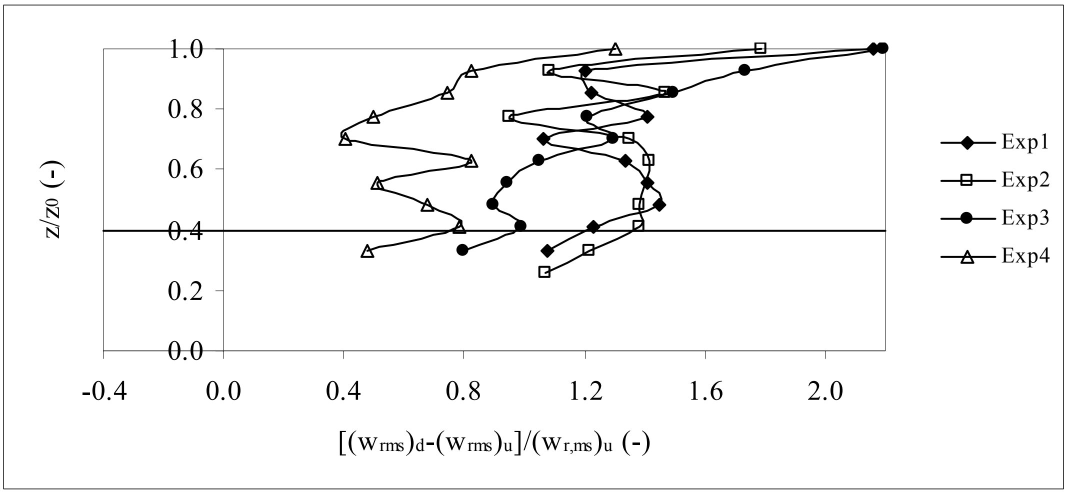

Figure 5.21: The variation of normalized vertical turbulence intensity difference parameter with respect to relative depth for Type 1

Type 2

The variation of vertical turbulence intensity with respect to relative depth is as given in Figure 5.22. As seen from Figure 5.22, vertical turbulence intensity has smoother curve for Type 2 compared to Type 1. Furthermore, it is seen that maximum values of this parameter along the depth is located in the vicinity of interface. When the variation of time averaged mean velocity against to relative depth examined (Figure B.11, B.12 and B.13) it is seen that at the location where the vertical turbulence intensity high, time averaged mean velocity is high. In other words, at that locations severe under-canopy flow occurrence has been observed. Time averaged vertical velocity get maximum values around the same region along the depth (Figure 5.10. As seen from Figure 5.22, vertical turbulence intensity linearly increases along depth towards to interface. In spite of the fact that there is no substantial number of data below interface it may be claimed that vertical turbulence intensity prone to decrease towards to bed.

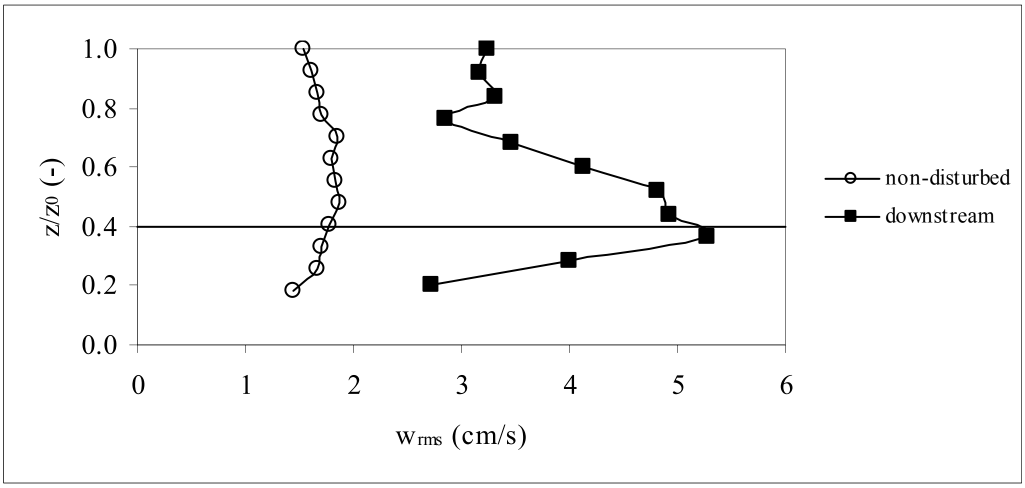

(a)

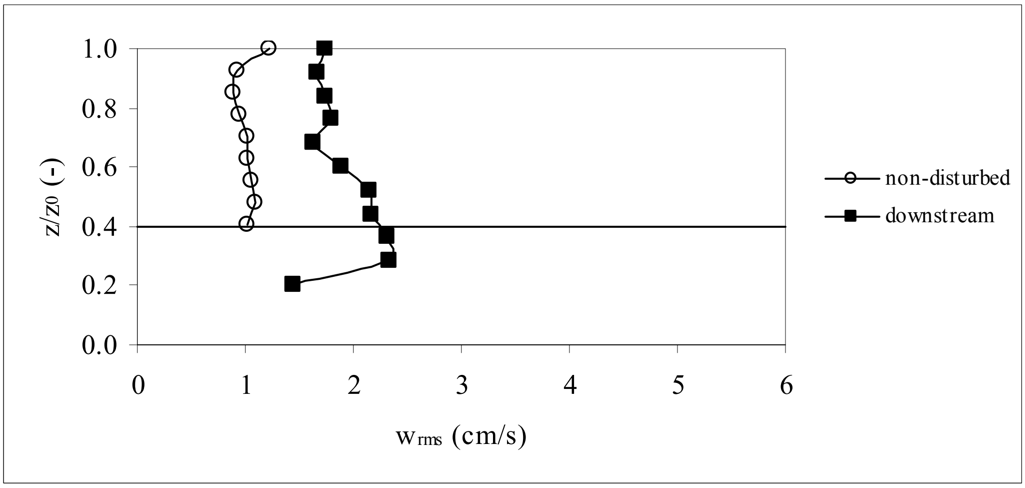

(b)

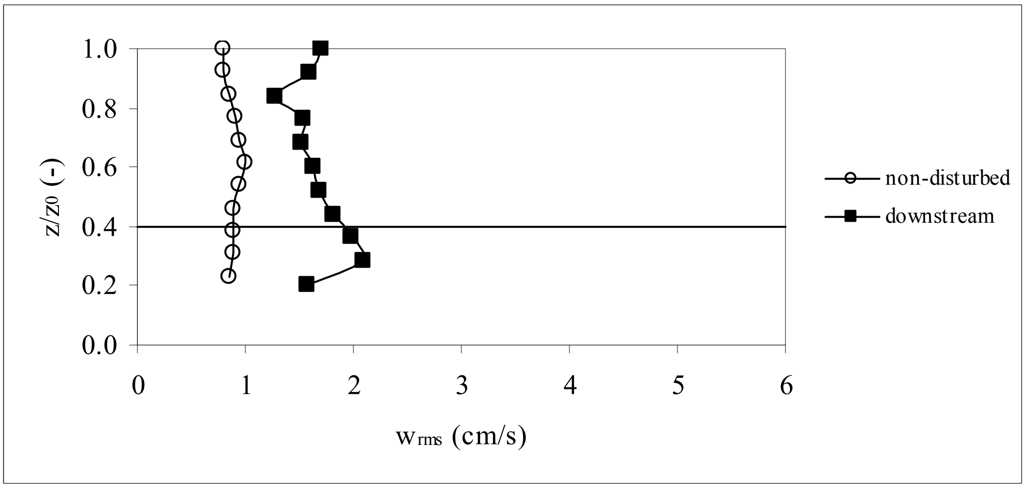

(c)

Figure 5.22: The variation of vertical turbulence intensity with relative depth for Type 2; a) Experiment 11, b) Experiment 12, c) Experiment 13

Figure 5.23 depicts the variation between "additional vertical turbulence intensity due to vegetation" and "relative depth". When Figure 5.23 considered, it is said that up to 200 % extra vertical turbulence intensity occurred in consequence of presence of vegetation. Another conclusion that could be drawn from Figure 5.23 that with the increasing flow velocity, the additional turbulence ratio increases. Furthermore, it was seen that maximum additional turbulence intensity ratio occur around z/z_0=0.4 value. This point corresponds to interface between Zone 1 and Zone 2. The variation of normalized vegetative vertical turbulence intensity parameter with respect to relative depth for Type 2 is given in Appendix (G.2).

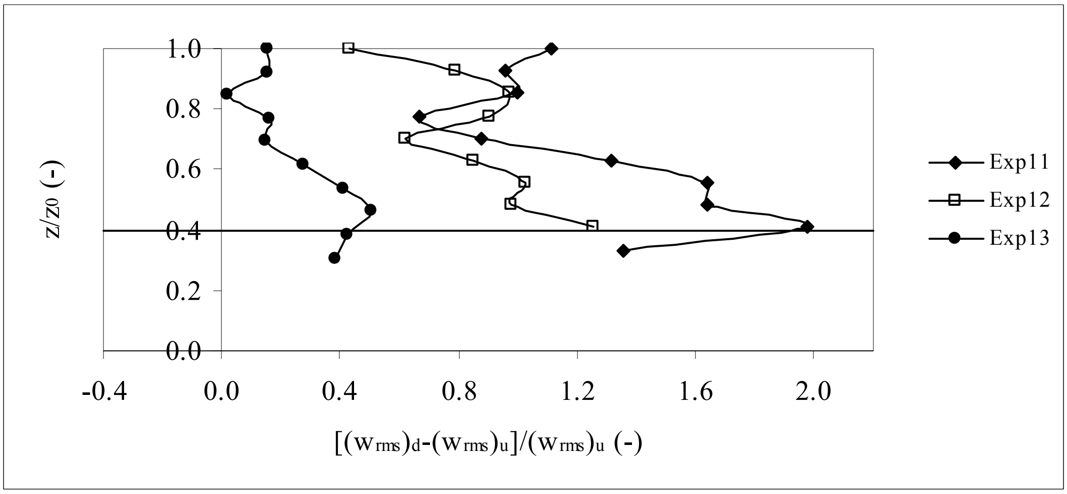

Figure 5.23: The variation of normalized vertical turbulence intensity difference parameter with respect to relative depth for Type 2

Type 3

Vertical turbulence intensity versus relative depth variation is depicted in Figure 5.24. The curves belong to Type 3 composed of two parts. Vertical turbulence intensity increase towards to interface from the region close to the water surface. At the slightly below of interface, maximum vertical turbulence intensity values were observed. From this point to bed, this parameter tends to decrease. This circumstance could be associated with time averaged vertical velocity. In agree with vertical turbulence intensity, time averaged vertical velocity has the maximum around the interface; and below the interface that prone to decrease.

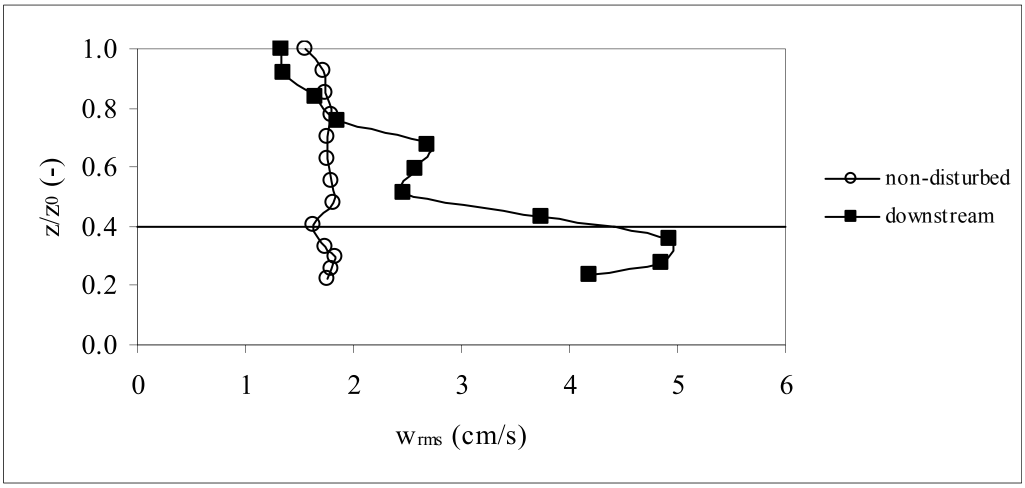

(a)

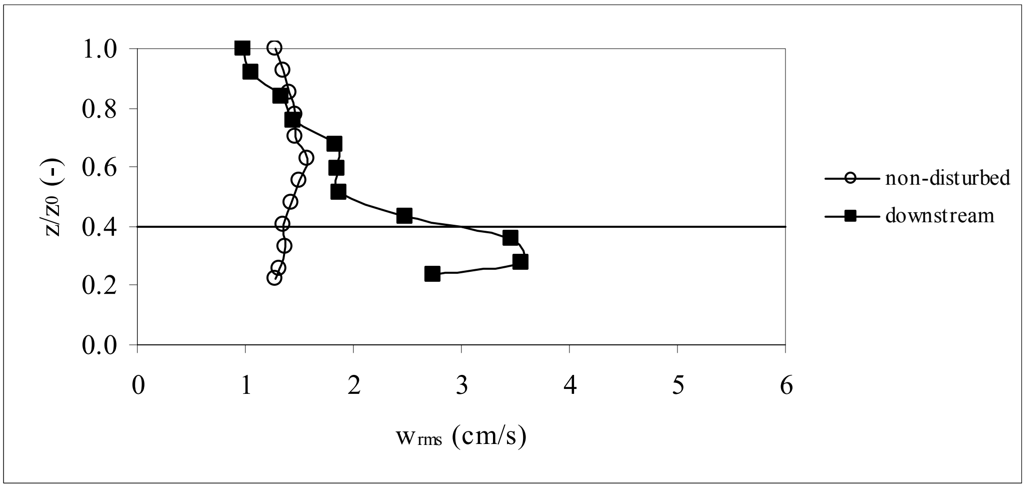

(b)

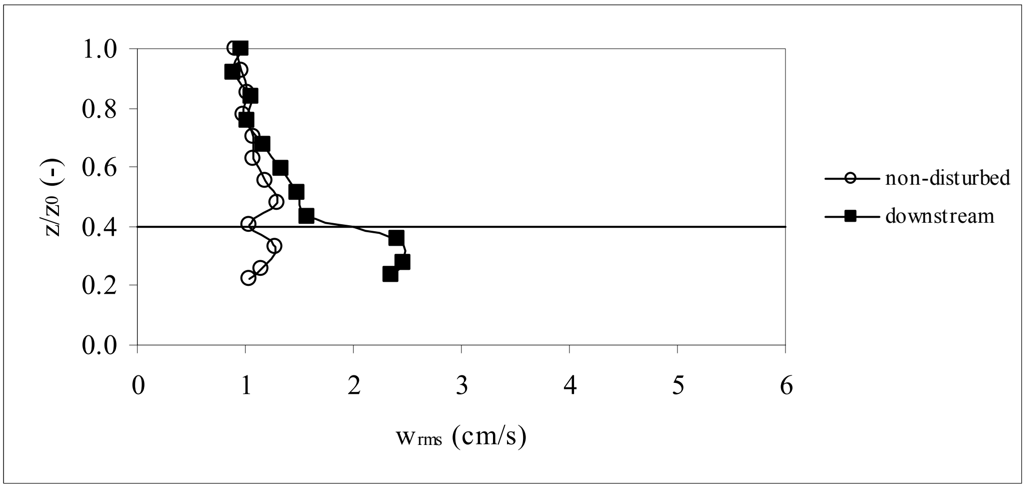

(c)

Figure 5.24: The variation of vertical turbulence intensity with relative depth for Type 3; a) Experiment 15, b) Experiment 16, c) Experiment 17, d) Experiment 18

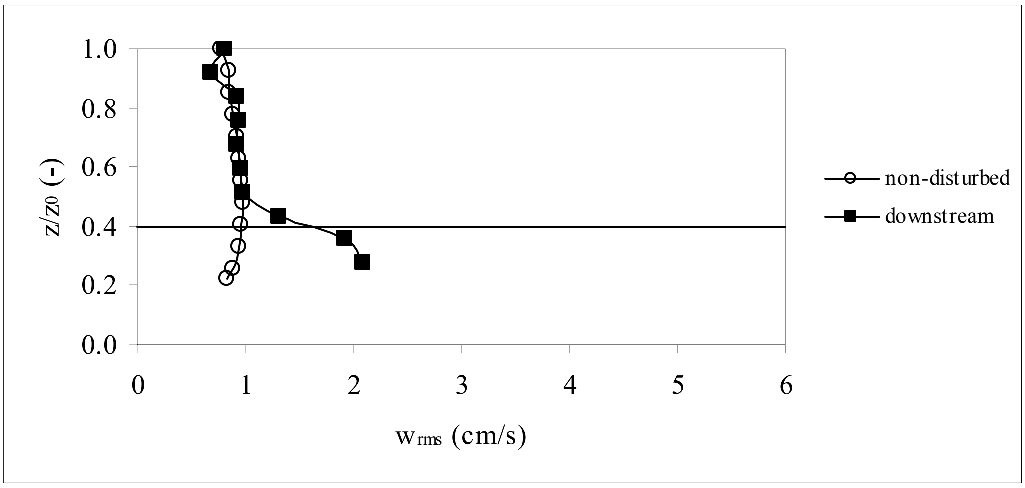

(d)

Figure 5.24 (continued): The variation of vertical turbulence intensity with relative depth for Type 3; a) Experiment 15, b) Experiment 16, c) Experiment 17, d) Experiment 18

The distribution of additional vertical turbulence intensity ratio due to vegetation is as given in Figure 5.25. Figure 5.25 clearly showed that maximum additional vertical turbulence intensity occurs in the vicinity of interface between Zone 1 and Zone 2. More specifically, this additional vertical turbulence ratio takes the value of between 100% and 200%. Though there is no enough large number of substantial data, it may be roughly said that additional vertical turbulence intensity ratio has a tendency to decrease below the interface. On the other hand, additional vertical turbulence intensity ratio decreases towards to water surface above the interface. The variation of normalized vegetative vertical turbulence intensity parameter with respect to relative depth for Type 3 is given in Appendix (G.3).

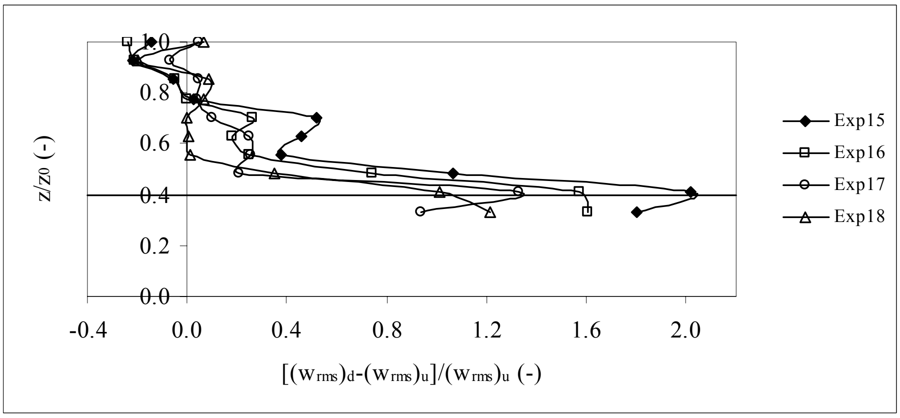

Figure 5.25: The variation of normalized vertical turbulence intensity difference parameter with respect to relative depth for Type 3

5.8 The Impact of Vegetation on Turbulence Kinetic Energy

The variation between turbulence kinetic energy observed at the downstream and upstream of vegetation is given below for Type 1, 2 and 3. In the light of these data it was seen that considerably higher turbulence kinetic energy occurs at the downstream of plant in consequence of presence of vegetation. In a way this result indicates the presence of vegetation leads to dissipation of energy. Further, the variation of "additional turbulence kinetic energy ratio owing to existence of vegetation" versus "relative depth" is examined for each type below as well.

Type 1

Turbulence kinetic energy versus relative depth is depicted in Figure 5.26 for Type 1. Based on Figure 5.26 it may be said that the vegetation produce considerably high turbulence kinetic energy at the downstream of vegetation for Type 1. At the region closer to the water surface, the turbulence kinetic energy is relatively higher compared to lower part of this area. This is the most distinctive property of Type 3. When Figure (A.1) is carefully examined it may be seen that vegetation density is comparatively higher where the turbulence kinetic energy is relatively higher. In parallel with non-disturbed case, turbulence kinetic energy increases towards to bed where disturbed by vegetation.

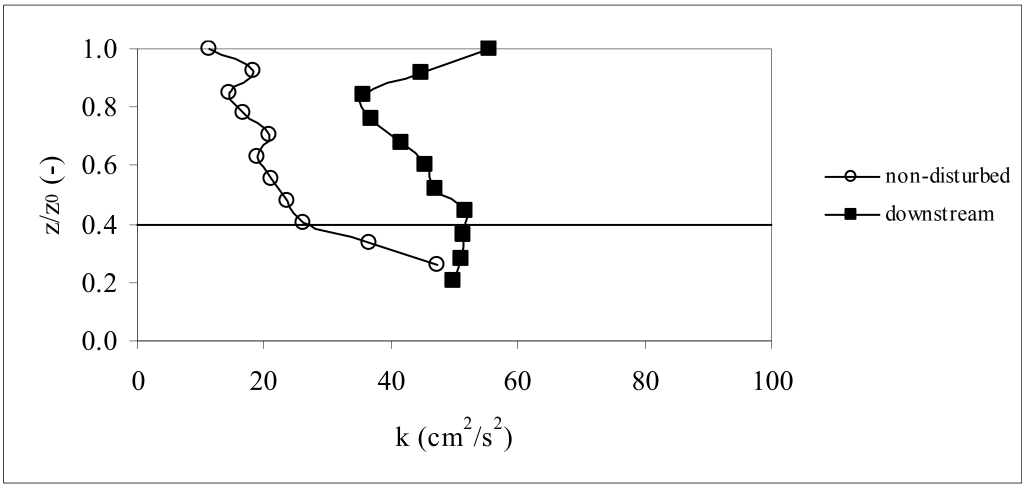

(a)

Figure 5.26: The variation of vertical turbulence intensity with relative depth for Type 1; a) Experiment 1, b) Experiment 2, c) Experiment 3, d) Experiment 4

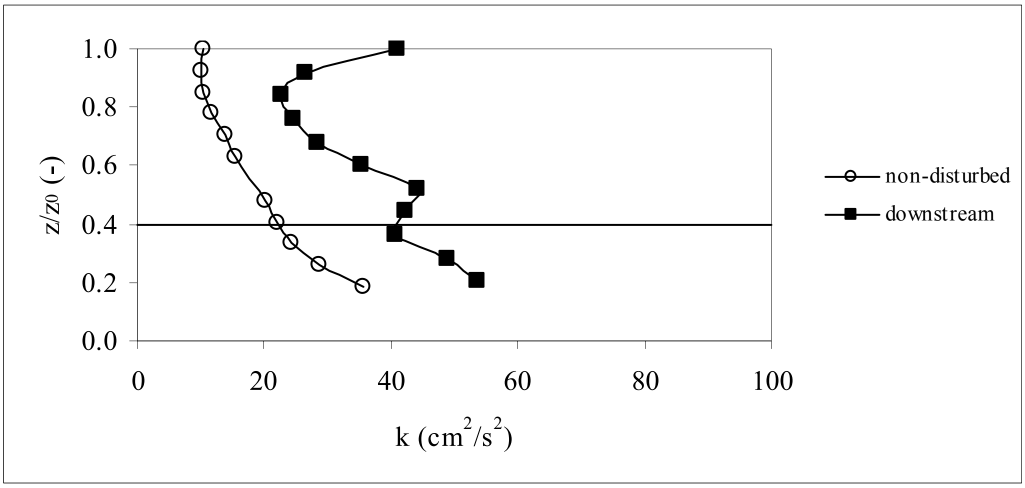

(b)

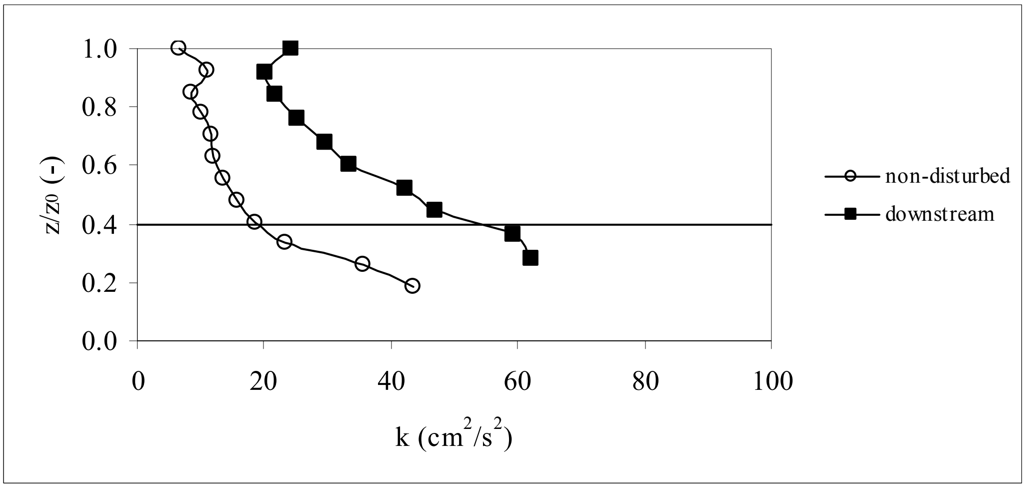

(c)

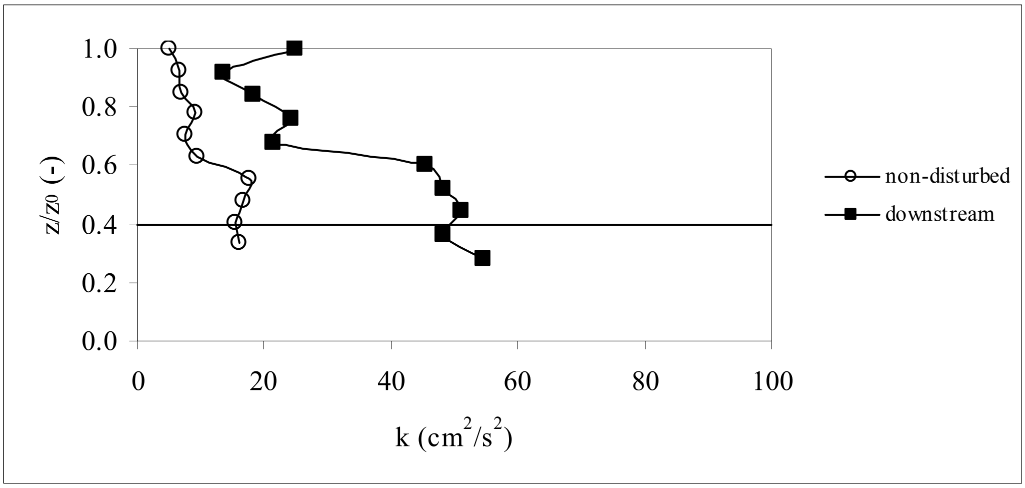

(d)

Figure 5.26 (continued): The variation of vertical turbulence intensity with relative depth for Type 1; a) Experiment 1, b) Experiment 2, c) Experiment 3, d) Experiment 4

The variation of “additional turbulence kinetic energy ratio owing to existence of vegetation” versus “relative depth” is depicted for Type 1 in Figure 5.27 based on the four different experiments. As could be concluded from Figure 5.27, the most significant part of extra turbulence kinetic energy occurs in the vicinity of water surface. This point correspond to area where the flow highly obstructed by vegetation. More precisely, the additional turbulence kinetic energy ratio takes the value of 270% and 400% depending on the mean velocity flow. This result overlapped with the result obtained from streamwise turbulence intensity ratio for Type 1 (Figure (5.15). In other words, the component of streamwise turbulence intensity dominates the additional turbulence kinetic energy for Type 1. The variation of normalized vegetative turbulence kinetic energy parameter with respect to relative depth for Type 1 is given in Appendix (H.1)

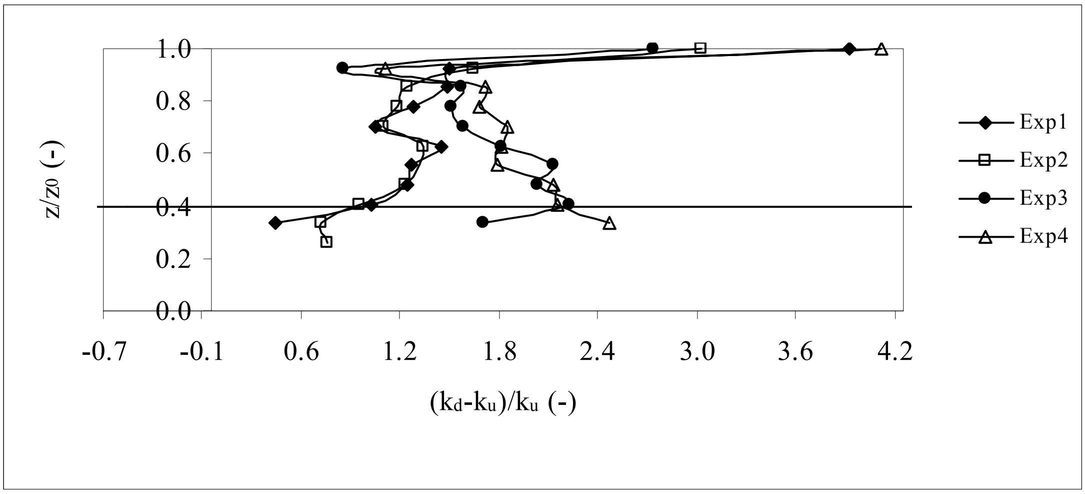

Figure 5.27: The variation of turbulence kinetic energy difference parameter difference parameter with respect to relative depth for Type 1

Type 2

In Figure 5.28, the variation of turbulence kinetic energy with relative depth is presented. With reference to Figure 5.28, it could stated that presence of vegetation bring about higher turbulence kinetic energy at the downstream of vegetation along the depth. Maximum turbulence kinetic energy was observed around the interface between Zone 1 and Zone 2. This situation is a characteristic property for Type 2. Streamwise turbulence intensity and vertical turbulence intensity take the maximum values for each individual experiment at the same region. In spite of the fact that there is no enough large number of substantial data below the region, it may be said that below the interface turbulence kinetic energy prone to decrease towards to bed.

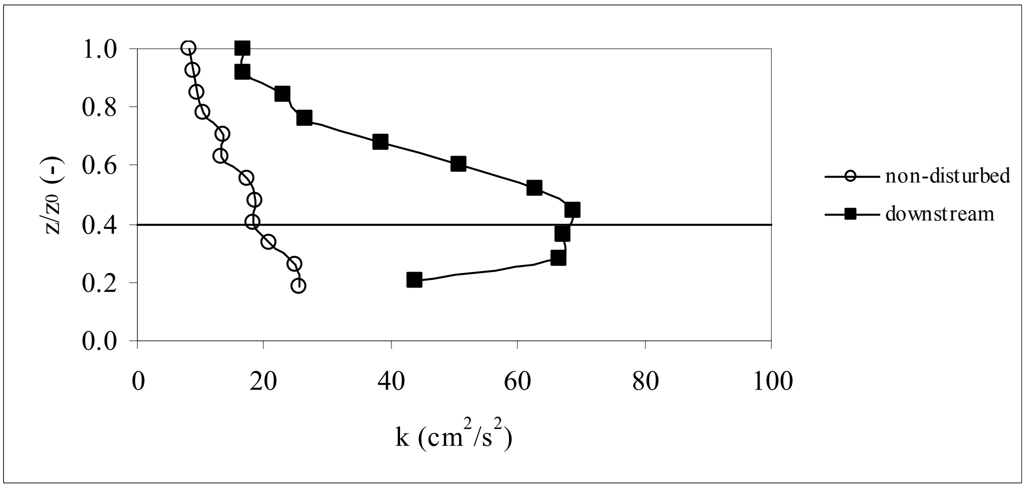

(a)

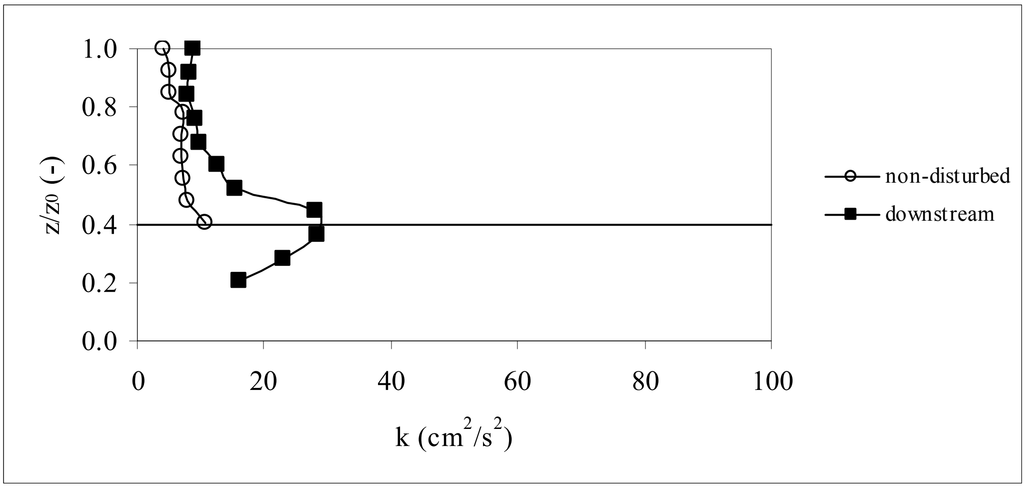

(b)

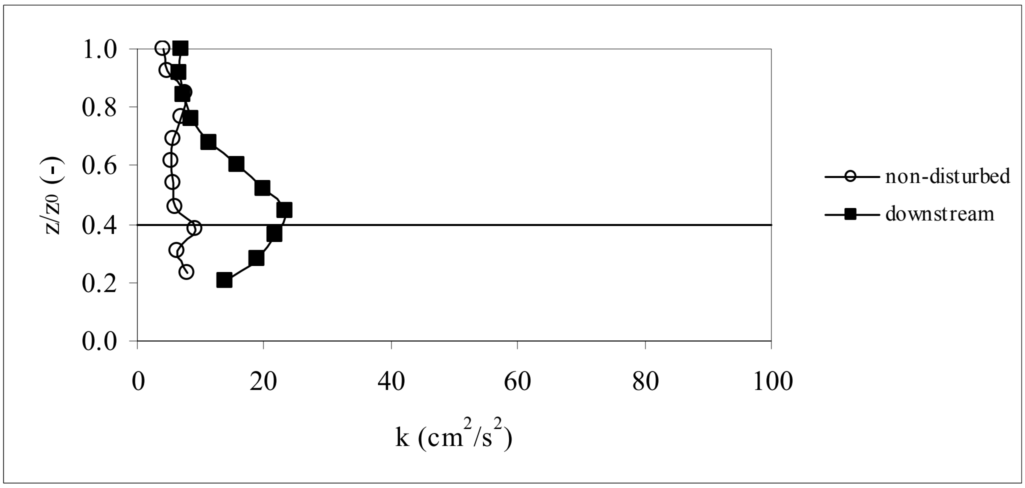

(c)

Figure 5.28: The variation of vertical turbulence intensity with relative depth for Type 2; a) Experiment 11, b) Experiment 12, c) Experiment 13

In Figure 5.29 the relationship between "additional turbulence kinetic energy ratio in consequence of presence of vegetation" and "relative depth" was illustrated for Type 2 based on the three different experiments. As can be seen from Figure 5.29, the highest additional turbulence occurrence appeared around the region of interface between Zone 1 and Zone 2 at the downstream of vegetation. At the same region streamwise turbulence intensity and vertical turbulence intensity take the maximum values along the depth. In numerical speaking, approximately 150%-300% additional turbulence kinetic energy occurs at the downstream of vegetation. On the other hand, the additional turbulence kinetic energy ratio decreases towards to water surface along the depth for Type 2. The variation of normalized vegetative turbulence kinetic energy parameter with respect to relative depth for Type 2 is given in Appendix (H.2).

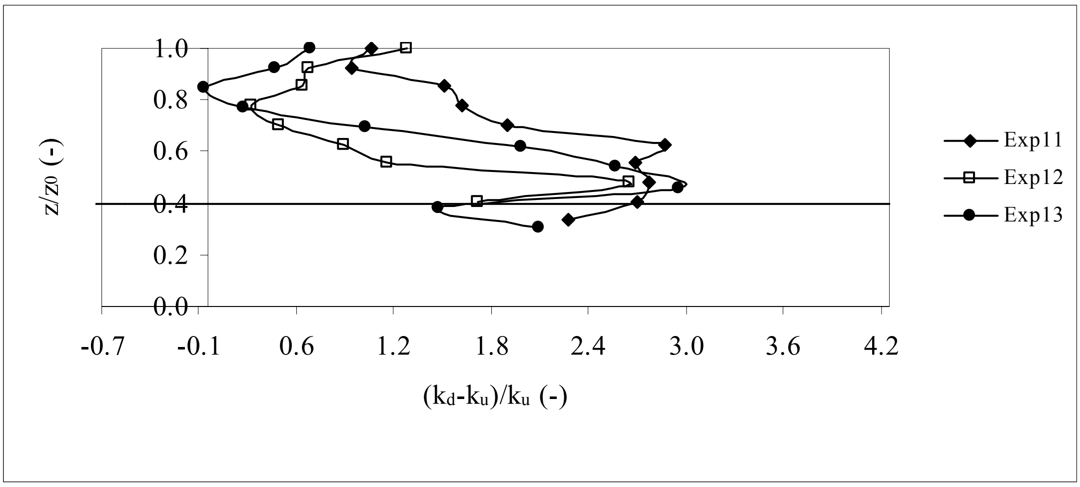

Figure 5.29: The variation of turbulence kinetic energy difference parameter difference parameter with respect to relative depth for Type 2

Type 3

"Turbulence kinetic energy due to presence of vegetation" against to "relative depth" is as given in Figure 5.30. In general speaking, Figure 5.30 showed that existence of vegetation generates considerable extra turbulence kinetic energy at the downstream of vegetation for Type 3. Nevertheless around the region closer to water surface, relatively lower turbulence kinetic energy values were observed compared to non disturbed case for four experiments in Type 3. This is fairly distinguishing feature for Type 3 since this situation has been observed neither in Type 1 nor in Type 2. At the region towards to the bed, turbulence kinetic energy exhibit similar character with non-disturbed case but take relatively higher values.

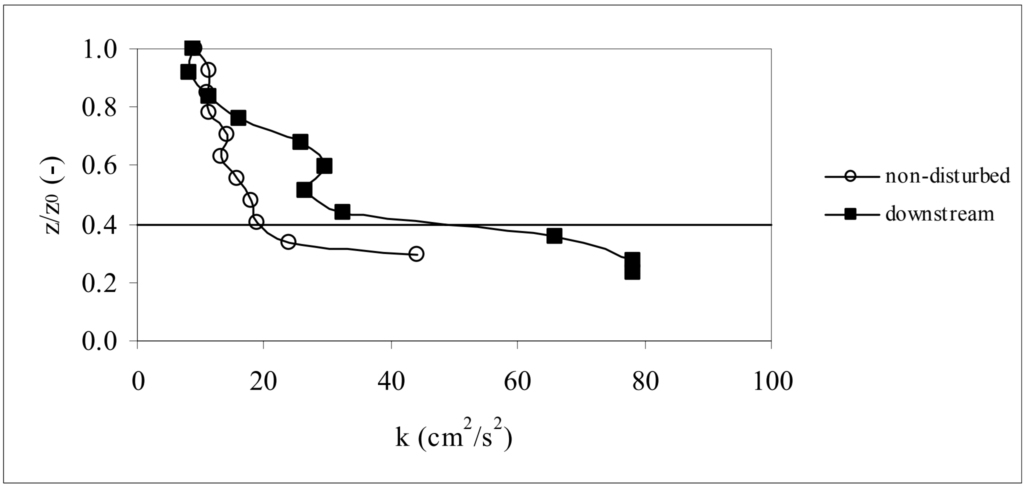

(a)

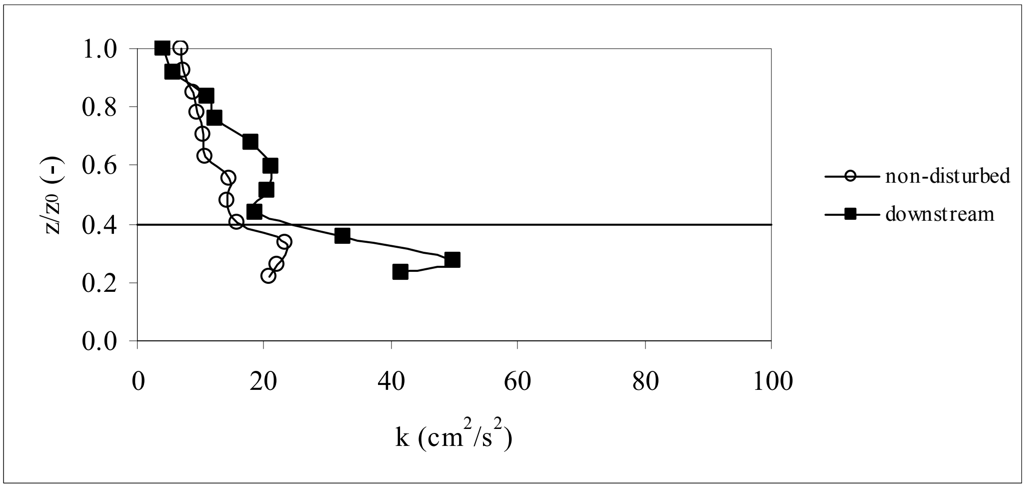

(b)

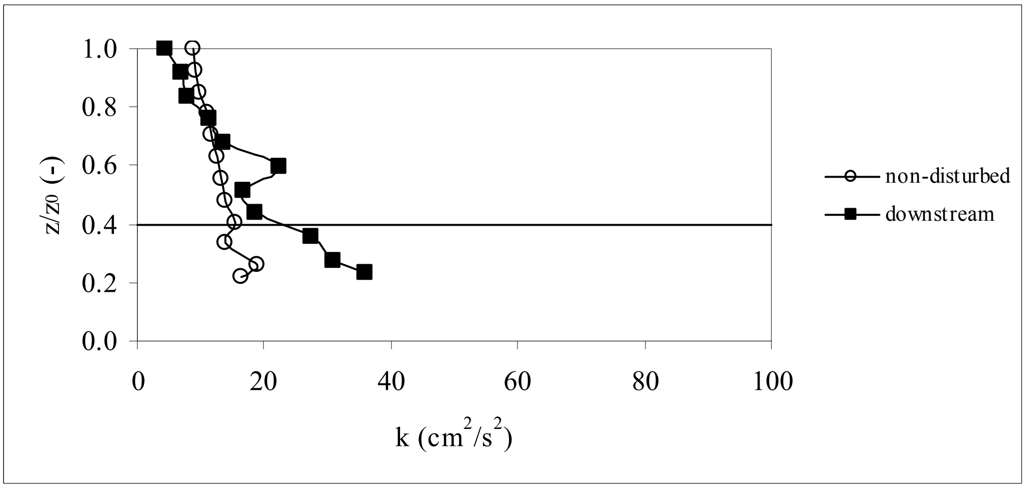

(c)

Figure 5.30: The variation of vertical turbulence intensity with relative depth for Type 3; a) Experiment 15, b) Experiment 16, c) Experiment 17, d) Experiment 18

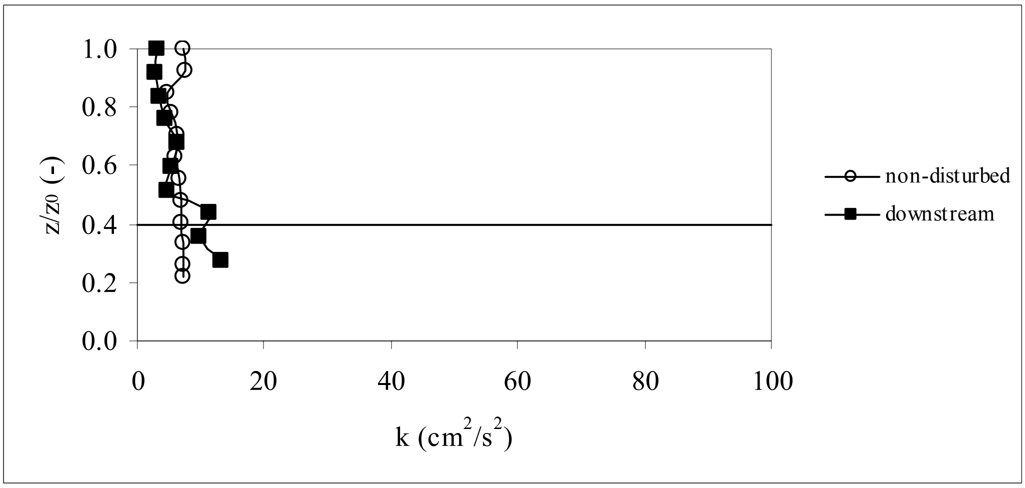

(d)

Figure 5.30 (continued): The variation of vertical turbulence intensity with relative depth for Type 3; a) Experiment 15, b) Experiment 16, c) Experiment 17, d) Experiment 18

In Figure 5.30, the variation of "additional turbulence kinetic energy ratio as a result of presence of vegetation" with "relative depth" is illustrated in Figure 5.30 for the downstream side of vegetation. Based on the Figure 5.30 it could be claimed that presence of vegetation bring about negative additional turbulence kinetic energy ratio closer to water surface which means the existence of vegetation leads to less turbulence around the region closer to water surface. As pointed out above, this is very distinctive feature for Type 3 and any negative additional turbulence kinetic energy ratio values closer to water surface was observed in none of the experiments but Type 3. In the vicinity of this region, up to 70% less "additional turbulence kinetic energy values" were observed. The additional turbulence kinetic energy ratio exhibit augmentation from water surface to bed and take the maximum value around the region closer to interface. The variation of normalized vegetative turbulence kinetic energy parameter with respect to relative depth for Type 3 is given in Appendix (H.3)

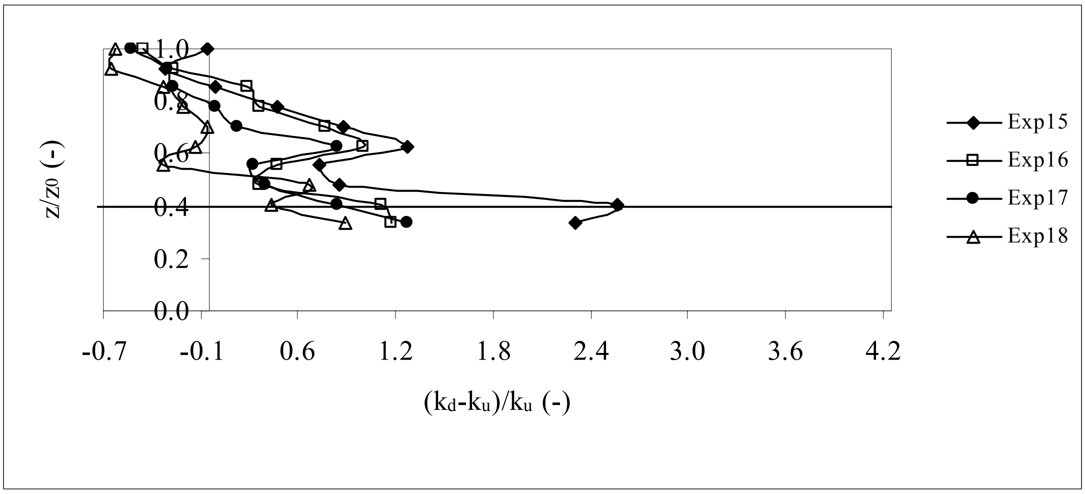

Figure 5.31: The variation of turbulence kinetic energy difference parameter difference parameter with respect to relative depth for Type 3

6. CONCLUSIONS

The major goal of the study was to explore the impact of presence of singular vegetation in flow domain, such as a tree with large trunk, on flow characteristics. For this purpose an experimental study was conducted under controlled laboratory conditions using real vegetative elements. In order to analyze this commonly observed phenomenon, trees with large trunks were classified into three groups on the basis of their volume versus height relation. The primary difference between those introduced three types was the volume increment gradient along the height. For given successive height intervals, the volume of vegetation that belongs to any interval is always larger than the volume of the interval that belongs to the one closer to bed for Type 1 (*Pinus Pinea)*, approximately constant for Type 2 (*Thuja Orientalis)*, smaller for Type 3 (*Cupressus Macrocarpa)*. In other words, this definition could be also summarised as $\left[\left\{\left(\partial V / \partial h\right)/ \partial h\right\} < 0\right]$ for Type 1; $\left[\left\{\left(\partial V / \partial h\right)/ \partial h\right\} \cong 0\right]$ for Type 2 and $\left[\left\{\left(\partial V / \partial h\right)/ \partial h\right\} > 0\right]$ for Type 3. The conclusions given in this chapter are dependent upon the vegetation types and therefore it is definitely necessary to interpret the results considering the architectural and foliage structure properties of three types of tree models. Based on this classification and the experimental data, the following conclusions were drawn.

Experimental findings revealed that flow at the downstream of vegetation is significantly retarded by vegetative element and the velocity profile no longer follows the logarithmic law profile. Additionally, a gap was detected in the literature that there is still not any method or formulation which gives the velocity profile at the downstream of vegetation depending on the vegetative characteristics. It was considered that generating a simplified formulation which gives the velocity profile at the downstream of vegetation is necessary for river engineers. Based on the experimental data, an empirical equation was derived. The proposed formulation gives the velocity values at the downstream of vegetation depending on the distance from the bottom. The formulation was derived for the distance of $1D_v$ between vegetation and predicted velocity profile. The validity of the formulation was examined by the experimental data and it was seen that the formulation gives quite satisfactory results. The parameters “m” and “c” take different values depending on the type of vegetation. However, the results also showed that generalized form of the equation gives fairly reasonable predictions and this makes the usage of the formula easier. In this context, estimating the volume of vegetation in the field with an acceptable accuracy is crucial for the success of the equation. The self-similarity between the plant and its branch can be employed as a reference during the calculation of volume of vegetation.

The experimental data of time averaged velocity showed that sub-canopy flow occurs at the downstream of vegetation in the region close to bed for all three types of vegetation. With increasing compactness of vegetation the magnitude of sub-canopy flow increases. This may lead to undesirable effects such as additional erosion. On the other hand, with the increasing compactness of vegetation, relatively lower and in some cases negative time averaged velocity values are observed in the area closer to water surface at the downstream of vegetation. This brings about some favorable consequences in terms of habitat and ecology as it indicates that such a compact vegetation structure providing stream variability in naturally vegetated rivers which is vital for the improvement of fish population. Another aspect of the issue is that in a flood event the presence of vegetation with a compact foliage and branch structure reduces streamwise mean velocity. However, this situation also leads to decrease of conveyance capacity and thus elevated water depth values are expected.

Three types of representative vegetation caused different percentages of sub-canopy flow at the downstream of vegetation in the region close to bed. More specifically, Type 1 leads to 50-70 %, Type 3 caused to 10-30 % sub-canopy flow. Nevertheless the magnitude of sub-canopy flow for Type 2 is extremely limited. The experiments showed that the flow is retained by presence of vegetation in the region close to the water surface at the downstream of vegetation. More clearly, flow is retained by Type 1 30-50 %, 90-110 % by Type 2 and 60-90 % by Type 3. In overall assessment, it was concluded that presence of any type of tree with large trunk leads to 0-70 % extra sub-canopy flow at the bottom and 30-110 % retaining effect close to the water surface. It should be kept in mind that these results should be taken into consideration together with the architectural branch and foliage properties of the related vegetation.

Differing from the results obtained for the centerline of the downstream of vegetation, the velocity profiles clearly fit to logarithmic velocity profile at the $0.6D_v$ lateral neighborhood of vegetation axis. Data from the successive neighboring locations (at the $0.6D_v$ lateral neighborhood of vegetation axis) showed unpredictably that the highest velocity profile is not at the vertical which is positioned at the same cross-section with vegetation. Surprisingly, the highest velocity profiles are observed at the further downstream of vegetative element. Additionally, 10-30 % velocity increase occurs at $0.6D_v$ cm neighboring locations in the area closer to water surface of vegetative element. However, this percentage increases towards to depth up to 50 %.

It was observed that presence of vegetation leads to additional vertical time averaged velocity around the interface between Zone 1 and 2 for all types of representative vegetation. However, the variation of additional time averaged vertical velocity along the depth significantly alters depending on the vegetation type. Generallly speaking, Type 1 mitigates time averaged vertical velocity thanks to their long and skinny foliages. Type 2 causes to circa 400 % extra time average vertical velocity around the interface and 200 % around the water surface. These ratios are approximately 400 % and 1000 % for Type 3 around the water surface and interface respectively. As could be concluded form these values, the most significant contribution to additional time averaged vertical velocity is by Type 3. This circumstance can be explained by the extremely stiff foliage nature of Type 3.

In addition to mean part of velocity characteristics, turbulent components (streamwise turbulence intensity, vertical turbulence intensity and turbulence kinetic energy) of flow were also examined. In the light of the experimental data it was concluded that the variation of streamwise turbulence intensity along the depth is significantly different from each other for the three types of vegetation. The magnitude of this parameter is not remarkably different from the non-disturbed case for Type 1 and Type 3. This could be explained by architectural properties of these species (*Pinus Pinea* and *Cupressus Macrocarp).* However, Type 1 induces 30-100 % extra streamwise turbulence intensity around the water surface; in the middle part of depth this value takes ±20 %. Type 2 leads to extra streamwise turbulence intensity approximately 30-70 % along the depth around the interface that reaches the peak of 90 %. Additionally Type 2 is the unique species among the three which causes substantially extra streamwise turbulence intensity. It was observed that Type3 may diminish or intensify the streamwise turbulence intensity depending on the flow rate in the percentage of ±50 %. With the increasing flow velocity Type 3 tends to aggravate the turbulence intensity. In conclusion, presence of vegetation can mitigate or aggravate the streamwise turbulence intensity depending on the architectural characteristics of vegetation.

The experimental findings showed that, differing from the streamwise turbulence intensity, presence of vegetation always remarkably increases the vertical turbulence intensity. It was seen that the most intense vertical turbulence occurs about the region of the interface for all types of vegetal elements. Also it tends to decrease for all three types of vegetation towards to water surface. It could be claimed that turbulence intensity is prone to decrease towards to the bed though there was no considerably large number of data below the interface. More specifically, presence of vegetation produces approximately 50-220 % extra vertical turbulence intensity. This ratio takes a value between 10-200 % for Type 2. Type 3 exhibits a different character in terms of production of additional vertical turbulence intensity. In the region around the water surface, the presence of vegetation lessens or intensifies the vertical turbulence intensity (± % 20). However, towards to bed the additional turbulence intensity increases and around the interface it reaches the peak and takes the value of approximately 200 %.

So as to acquire more conclusive results about the turbulence component of the flow, the turbulence kinetic energy produced by vegetal element was also examined. Experimental findings clearly revealed that presence of vegetation produces a remarkable degree of additional turbulence kinetic energy which indicates the energy dissipative role of vegetative element in a flow field. Furthermore, it was concluded that the most significant part of turbulence kinetic energy dissipated around the interface for three representative vegetative elements. More precisely, depending on the flow rate 100-250 % additional turbulence kinetic energy occurs due to vegetation for Type 1 in the middle part of depth. However, this value reaches the climax and takes the values between 300-420 % around the water surface. With regard to Type 2, additional turbulence kinetic energy is approximately 150-300 % around the interface. On the other hand, the additional turbulence kinetic energy ratio decreases towards water surface and the magnitude of it is 60-120 %. As for Type 3, the existence of vegetation diminishes turbulence kinetic energy with a percentage of 10-60 around the region closer to water surface. This is a very distinctive feature for Type 3. The additional turbulence kinetic energy ratio exhibits increment from water surface to bed and reaches the maximum value around the region closer to interface (50-250 %).

In conclusion, the experimental findings point out that the issue has different aspects and those aspects should be rigorously considered during flood plain and bank restoration studies. In the light of the data, it was seen that in spite of their porous structures, the existence of any type of vegetation considerably disturbs the flow field at the downstream of vegetal elements and they dissipate a remarkable amount of energy by turbulence. As expected, this effect is more remarkable for the species which has relatively more compact foliage, branch structure that has higher vegetation intensity parameter. Therefore restoration and designing of floodplains without considering these aspects could bring about some unfavorable outcomes.

REFERENCES

Bache, D.H., and MacAskill, A., 1984. Vegegation in civil and landscape engineering, Technical Books, Granada, London.

Baptist, M.J., 2003. A flume experiment on sediment transport with flexible, submerged vegetation, *International workshop on Riparian Forest vegetated channels: Hydraulic Morphological and Ecological Aspects*, February 20-22, Trento, Italy.

Carollo, F.G., Ferro, V. and Termini, D., 2002. Flow velocity measurements in vegetated channels, *Journal of Hydraulic Engineering*, **128**(7), 664-673.

Çelik, A.O. and Kabdaşlı, M.S., 2004. Effect of bending of vegetation on flow resistance, *Proceedings in 5th International Conference on Ecohydraulics*, Madrid, Spain, September 12-17.

Choi, S-U. and Kang H., 2004. Reynolds stress modeling of vegetated open channel flows, *Journal of Hydraulic Research*, IAHR, **42**, 3-12.

Chow, V.T., 1959. Open channel hydraulics, McGraw-Hill, New York.

Cui, J. and Neary V.S., 2002. Large eddy simulation (LES) of fully developed flow through Vegetation, *Proceedings in IAHR 5th International Conference on Hydroinformatics*, Cardiff, UK, July 1-5

Erduran, K.S. and Kutija, V., 2003. Quasi-three-dimensional numerical model for flow through flexible, rigid, submerged and non-submerged vegetation, *Journal of Hydroinformatics*, **5**(3), 189-202.

Fairbanks, J.D. and Diplas, P., 1998. Turbulence characteristics of flows through partially and fully submerged vegetation, *Proceedings in Wetlands Engineering and River Restoration Conference,* Denver, Colorado, March 22-27, 865-870.

Fathi-Maghadam, M. and Kouwen, N., 1997. Nonrigid, nonsubmerged, vegetative roughness on floodplains, *Journal of Hydraulic Engineering*, ASCE, **123**(1), 51-57.

Fenzl, R.N., 1962. Hydraulic resistance of broad shallow vegetated channels, *PhD Thesis*, University of California, Davis, California.

Fischer-Antze, T., Stoesser, T., Bates, P. and Olsen, N.R.B., 2001. 3D Numerical modelling of open-channel flow with submerged vegetation, *Journal of Hydraulic Research*, **39**(3), 303-310.

Freeman, G.E., Rahmeyer, W.J. and Copeland, R.R., 2000. Determination of resistance due to shrubs and woody vegetation, *US Army Corps of Engineers, ERDC/CHL*, No: TR-00-25.

Hasegawa, K., Asai, S., Kanetaka, S. and Baba, H., 1999. Flow properties of a deep open experimental channel with a dense vegatation bank, *Journal of Hydroscience and Hydraulic Engineering*, **17**(2), 59-70.

Hinze, J.O., 1959. Turbulence, McGraw-Hill, New York.

Jarvela, J., 2002a. Flow resistance of flexible and stiff vegetation: A flume study with natural plants, *Journal of Hydrology*, **269**, 44-54.

Jarvela, J., 2002b. Determination of flow resistance of vegetated channel banks and floodplains, *International Conference on Fluvial Hydraulics*, Louvain-la-Neuve, Belgium, September 4-6, 311-318.

Jarvela, J., 2004a. Flow resistance in environmental channels: Focus on vegetation, *PhD Thesis*, Helsinki University of Technology, Helsinki.

Jarvela, J., 2004b. Determination of flow resistance caused by non-submerged woddy vegetation, *International Journal of River Basin Management*, **2**(1), 61-70.

Koloseus, M.J. and Davidian, J., 1966. Free surface instability corelations. Laboratory Studies in Open Channel Flows, Water-supply paper 1952-C, U.S. Geological Survey, Washington D.C.

Kouwen, N. and Unny, T.E., 1973. Flexible roughness in open channels, *Journal of Hydraulic Division*, ASCE, **99**, 713-728.

Li, R.M. and Shen, H.W., 1973**.** Effects of tall vegetations on flow and sediment, *Journal of Hydraulic Division*, ASCE, **99**(5), 793-814.

Linder, K, 1982. Der strömungswiderstand von Pflanzenbestannden, *PhD Thesis,* Mitteilungen 75, Leichtweiss-Institut fur Wasserbau, TU Braunschweig.

Lopez, F. and Garcia M., 2001. Mean flow and turbulence structure of open channel flow through non-emergent vegetation,. *Journal of Hydraulic Engineering*, ASCE, **127**, 392-402.

Mas, J., 2005. Measuring the hydraulic resistance on real vegetation, *MSc Thesis*, Cardiff University, Cardiff.

McMohan, T.A. and Kronauer, R.E., 1976. Tree structures: deducing the principal of mechanical design, *Journal of Theoretical Biology*, **59**, 443-466.

McMohan, T.A., (1975). The mechanical design of trees, *Scientific Am*., **233**(1), 92-102.

Naot, D., Nezu, I. and Nakagawa, H., 1996. Hydrodynamic behavior of partly vegetated open channels, *Journal of Hydraulic Engineering*, ASCE, **122**, 625-633.

Naot, D., Nezu, I. and Nakagawa, H., 1996. Unstable patterns in partly vegetated channels, *Journal of Hydraulic Engineering*, ASCE, **122**, 671-673.

Nepf, H.M. and Vivoni, E.R., 2000. Flow structure in depth-limited, vegetated flow, *Journal of Geophysical Research,* **105**(28), 547-28, 557.

Nepf, H.M., 1999. Drag, turbulance, and diffusuion in flow through emergent vegetation, *Water Resources Research*, **35**(2), 479-489.

Nezu, I. and Nakagawa, H., 1993. Turbulence in open channel flows, Balkema, Roterdam, The Netherlands.

Nezu, I. and Nakagawa, T., 1997. Space-time correlation structures of horizontal coherent vortices in compound open channel flows by using particle-tracking velocimetry, *Journal of Hydraulic Research*, IAHR, **35**(2), 191-208.

Nezu, I. and Onitsuka, K., 2001.Turbulent structures in partly vegetated open channel flows with LDA and PIV measurements, *Journal of Hydraulic Research*, **39**(6), 629-642.

Nezu, I., 2005. Open channel turbulence and its reserach prospect in the 21st century. *Journal of Hydraulic Engineering*, ASCE, **131**(4), 229-246.

Nortek, 2004. ADV operation manual, Nortek AS, Vollen, Norway.

Odeh, M., Noreika, J.F., Haro, A., Maynard, A., Castro-Santos, T. and Cada, G.F., 2002. Evaluation of the effects of turbulence on the behaviour of migratory fish. U:S: Department of energy Bonneville power administration division of fish and wildlife, project number: 2000-057-00, contract number: 00000022.

Petryk, S. and Bosmajian, G., 1975. Analysis of flow through vegetation, *Journal of Hydraulic Division*, ASCE, **101**(7), 871-884.

Rauch, H.P., 2005. Hydraulic impact of a vegetated river bank exemplified by the soil bioengineering test flume of the river Wien. Ph.D. Thesis, Institute of Soil Bioengineering and Landscape Construction, University of Natural Resources and Applied Life Sciences, Vienna, Austria.

Schnauder, I, 2004. Strömungsstruktur und Impulsaustausch in Gegliederten Gerinnen Mit Vorlandvegetation, *PhD thesis*, University of Karlsruhe, Karlsruhe.

Sellin, R.H.J., 2003. Personal contact in University of Cardiff, UK.

Shimizu Y. and Tsujimoto T., 1994. Numerical analysis of turbulent open channel flow over a vegetation layer using a k-epsilon turbulence model, *Journal of Hydroscience and Engineering,* **11,** 57-67.

Stanisic, M.M., 1988. The mathematical theory of turbulence, Springer-Verlag, New York.

Stephan, U. and Gutknecht, D., 2002. Hydraulic resistance of submerged flexible vegetation, *Journal of Hydrology*, Elsevier Science, **269**(1-2), 27-43.

Stoesser, T, Wilson, C.A.M.E., Bates, P.D. and Dittrich, A., 2003. Application of a 3D numerical model to a river with vegetated floodplains.IAHR/IWA Journal of Hydroinformatics **5**: 99-112.

Strahler A. N., 1952. Hypsometric (area-altitude) analysis of erosional topography. *Bull. Geolog. Soc. Amer.,* **63**, 1117-1142.

Sümer, M., Ünsal, İ. and Bayazıt, M., 1982. Hidrolik, Birsen Yayınevi, İstanbul.

Tsujimoto, T., Shimuzu, Y., Kitamura, T. and Okada, T., 1992. Turbulent open-channel flow over bed by rigid, *Journal of Hydroscience and Hydraulic Engineering*, **10**(2), 13-25.

Wilson, C.A.M.E. ve Horrit, M.S., 2002. Measuring flow resistance of submerged grass, *Hydrological Process*, **16**, 2589-2598.

Wilson C.A.M.E., Stoesser, T., Bates, P.D. and Batemann Pinzen, A., 2004. Open channel flow through different forms of submerged flexible vegetation. *Journal of Hydraulic Engineering*, ASCE, **129** (11), 847-853.

Wilson C.A.M.E., Yagci, O., Rauch, H.P. & Stoesser, T. 2006a**.** Application of the drag force approach to model the flow interaction of natural vegetation, *Journal of River Basin Management* **4**(2), 137-146.

Wilson, C.A.M.E., Yagci, O, Rauch, H.P and Olsen, N.R.B., 2006b. 3D Numerical modelling of a willow vegetated river/floodplain system, *Journal of Hydrology*, **327**(1-2), 13-21.

Wu, F.C., Shen, H. W. and Chou, Y. J., 1999. Variation of roughness coefficient for unsubmerged and submerged vegetation, *Journal of Hydraulic Engineering*, ASCE, **125**(9), 934-942.

Yen, B.C., 2002. Open channel flow resistance, *Journal of Hydraulic Engineering*, ASCE, **128**(1), 20-39.

APPENDIXES

APPENDIX A: THE SIDE VIEW OF PLANTS

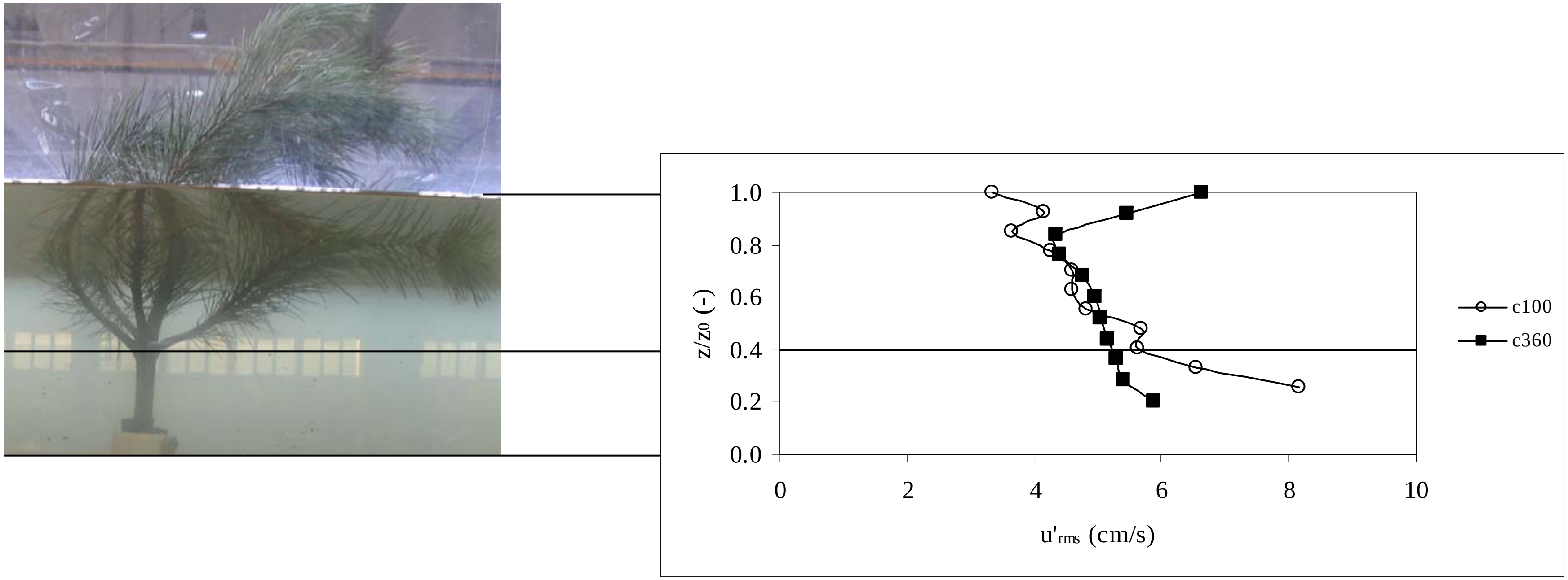

Figure A.1: The side view of Type 1 (*Pinus Pinea)*

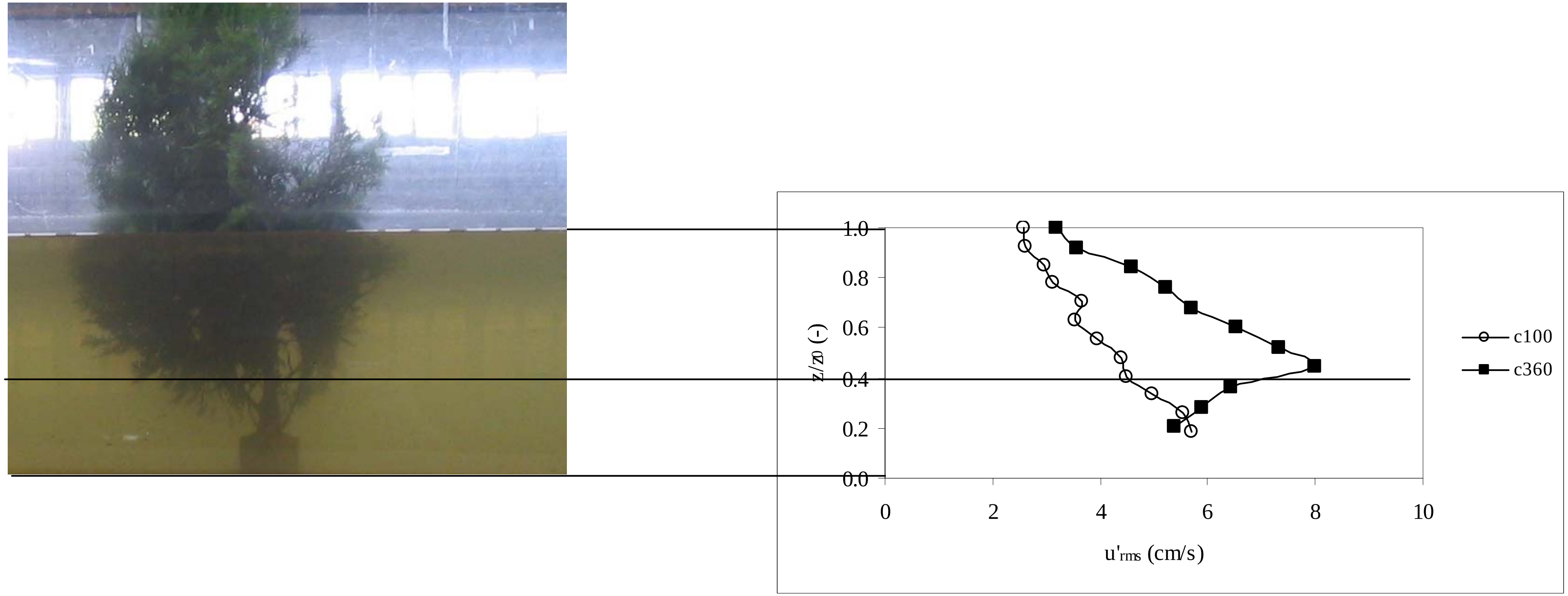

Figure A.2: The side view of Type 2 (*Thuja Orientalis)*

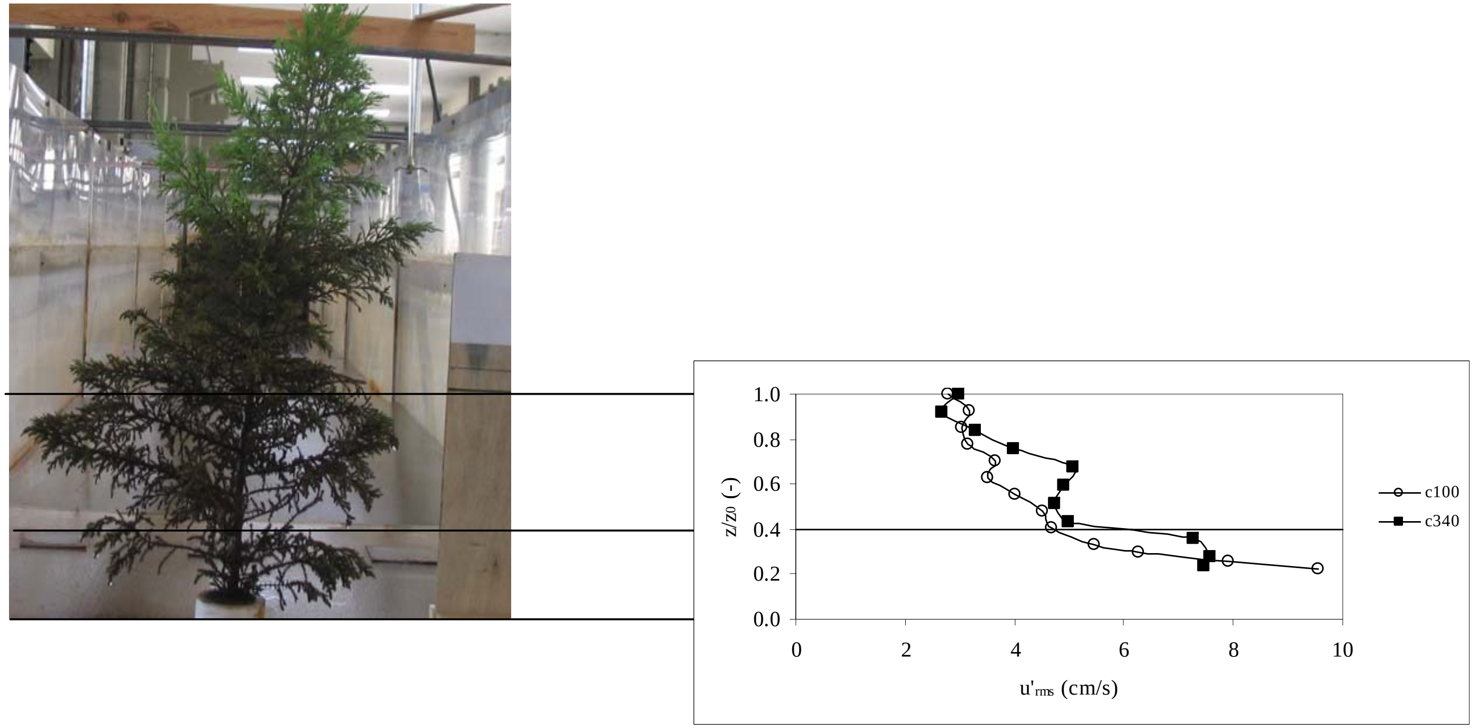

Figure A.3: The side view of Type 2 (*Cupressus Macrocarpa)*

APPENDIX B: THE MEASURED VELOCITY PROFILE OF NON-DISTURBED CASE AND MEASURED VELOCITY PROFILE AT THE DOWNSTREAM OF VEGETATIVE ELEMENT FOR DIFFERENT EXPERIMENTS

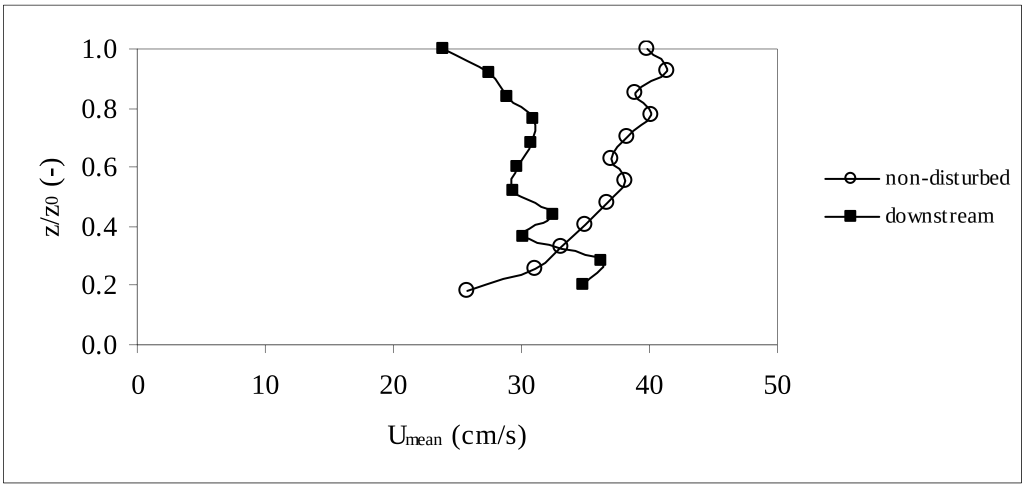

Figure B.1: The measured velocity profile of non-disturbed case and measured velocity profile at the downstream of vegetative element for Experiment no: 1 (Type 1, d=25 cm)

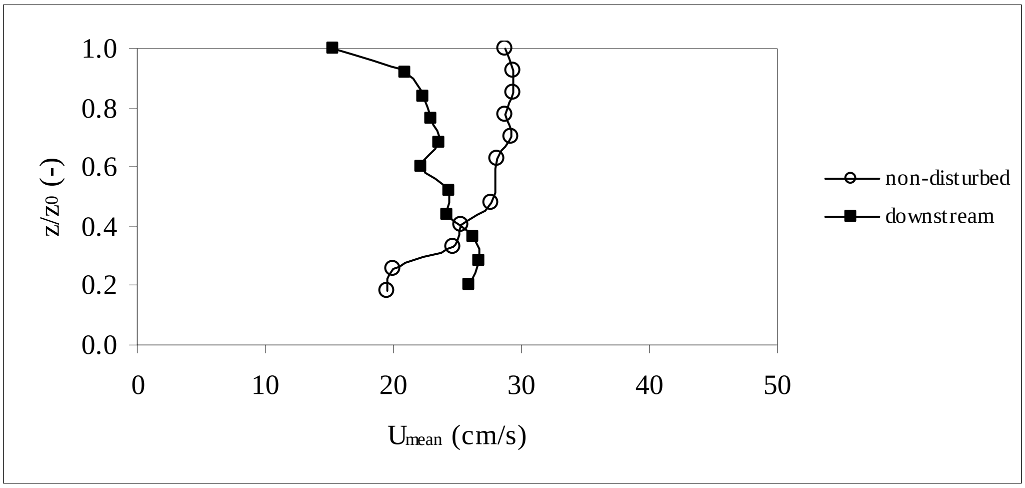

Figure B.2: The measured velocity profile of non-disturbed case and measured velocity profile at the downstream of vegetative element for Experiment no: 2 (Type 1, d=25 cm)

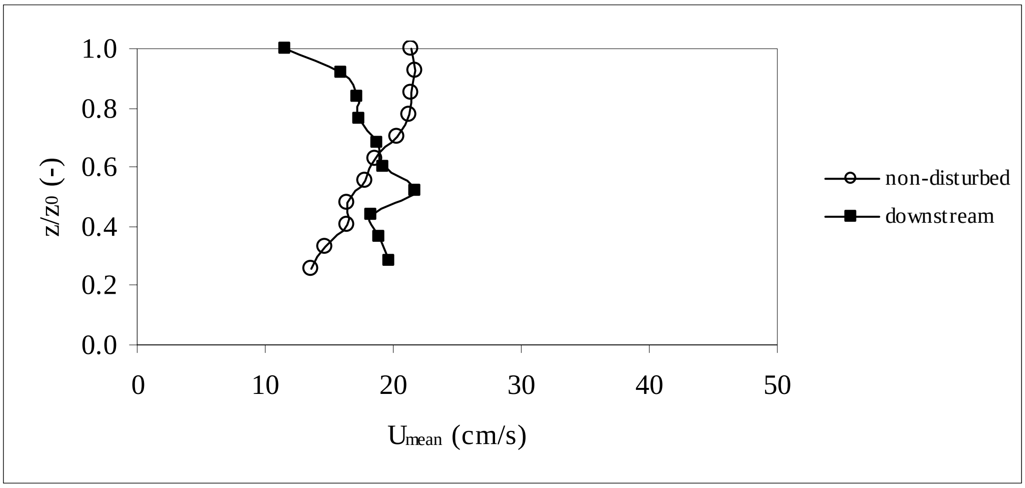

Figure B.3: The measured velocity profile of non-disturbed case and measured velocity profile at the downstream of vegetative element for Experiment no: 3 (Type 1, d=25 cm)

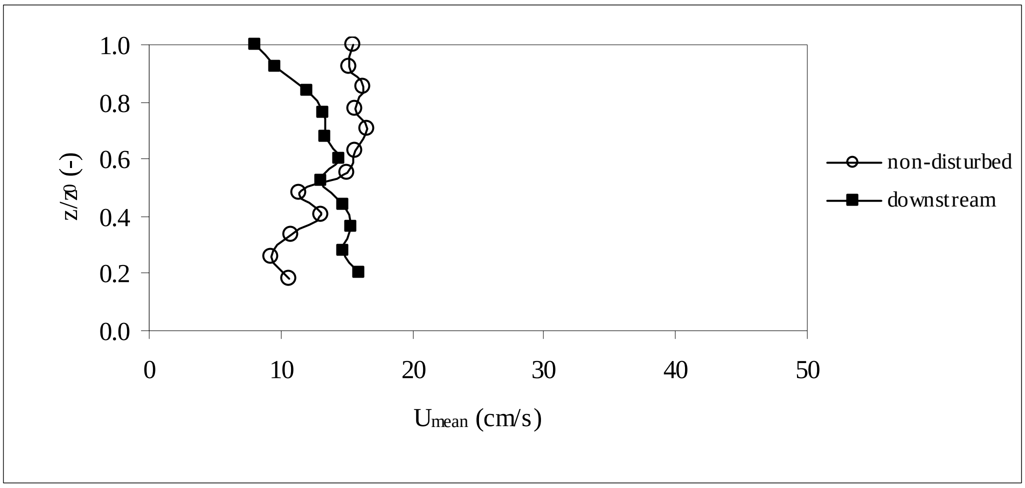

Figure B.4: The measured velocity profile of non-disturbed case and measured velocity profile at the downstream of vegetative element for Experiment no: 4 (Type 1, d=25 cm)

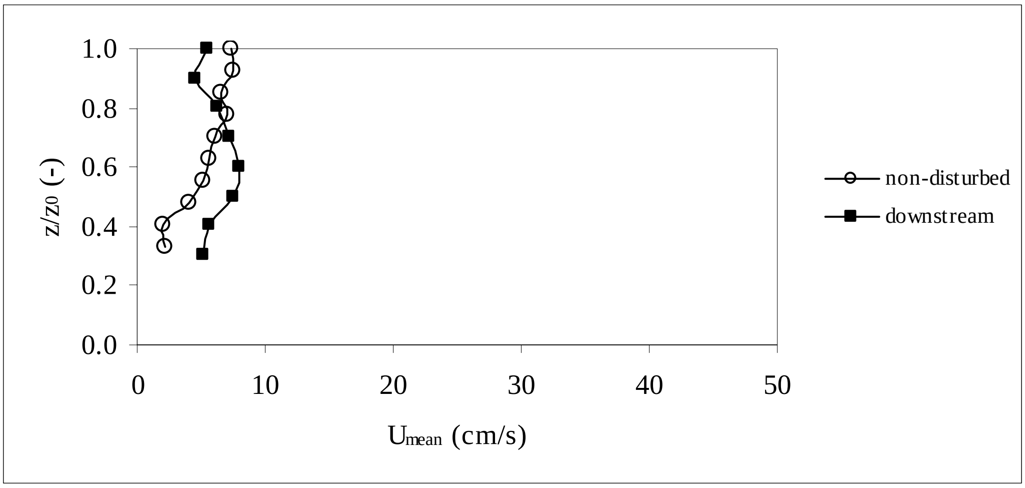

Figure B.5: The measured velocity profile of non-disturbed case and measured velocity profile at the downstream of vegetative element for Experiment no: 5 (Type 1, d=25 cm)

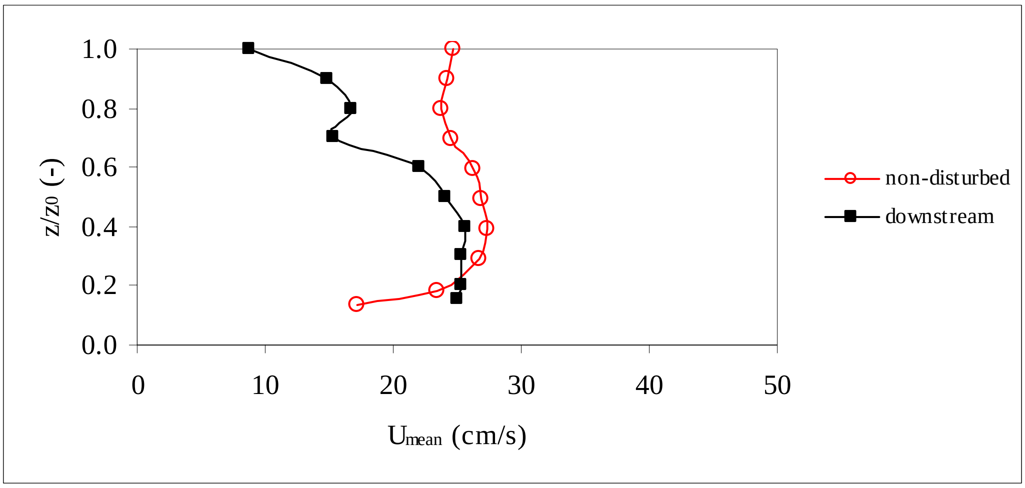

Figure B.6: The measured velocity profile of non-disturbed case and measured velocity profile at the downstream of vegetative element for Experiment no: 6 (Type 1, d=40 cm)

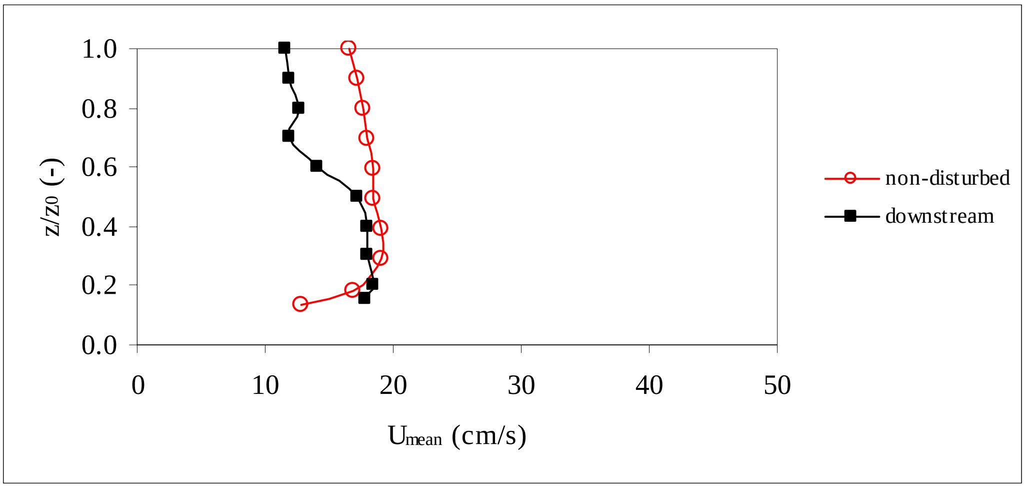

Figure B.7: The measured velocity profile of non-disturbed case and measured velocity profile at the downstream of vegetative element for Experiment no: 7 (Type 1, d=40 cm)

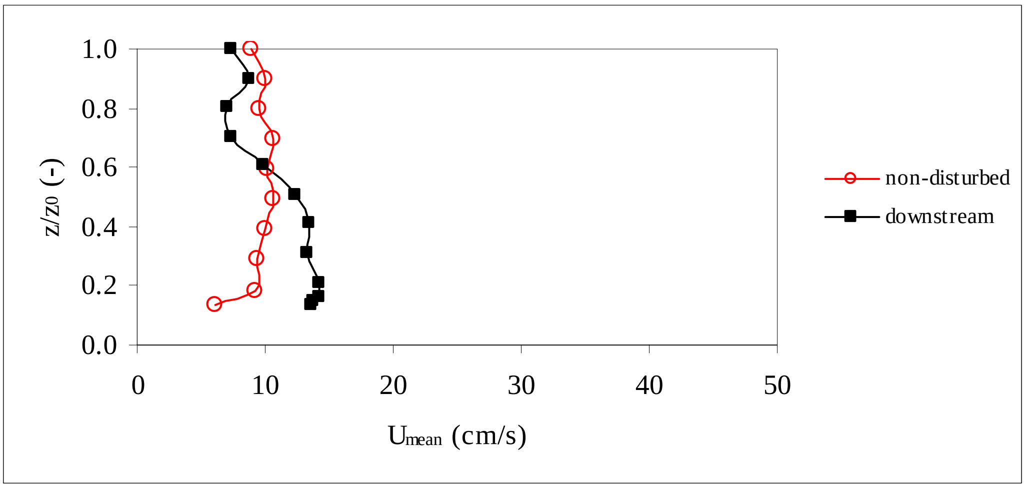

Figure B.8: The measured velocity profile of non-disturbed case and measured velocity profile at the downstream of vegetative element for Experiment no: 8 (Type 1, d=40 cm)

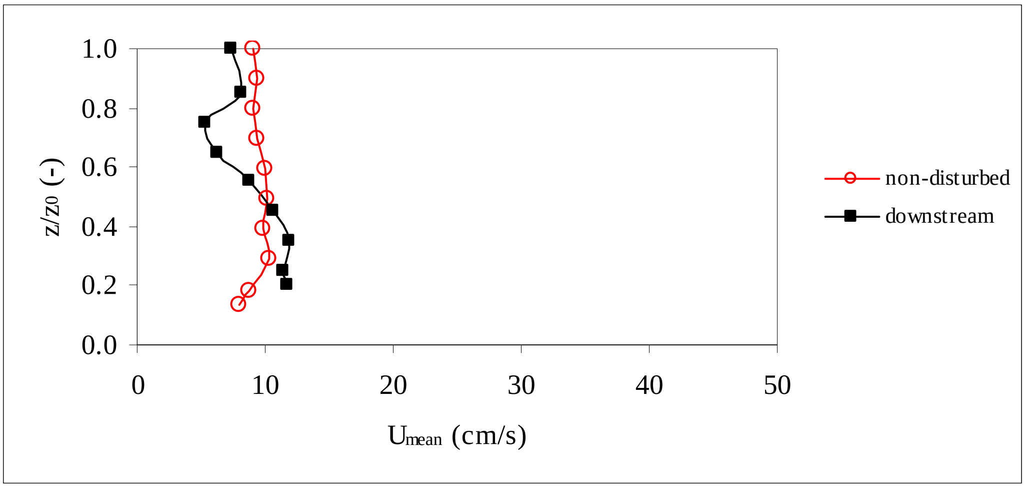

Figure B.9: The measured velocity profile of non-disturbed case and measured velocity profile at the downstream of vegetative element for Experiment no: 9 (Type 1, d=40cm)

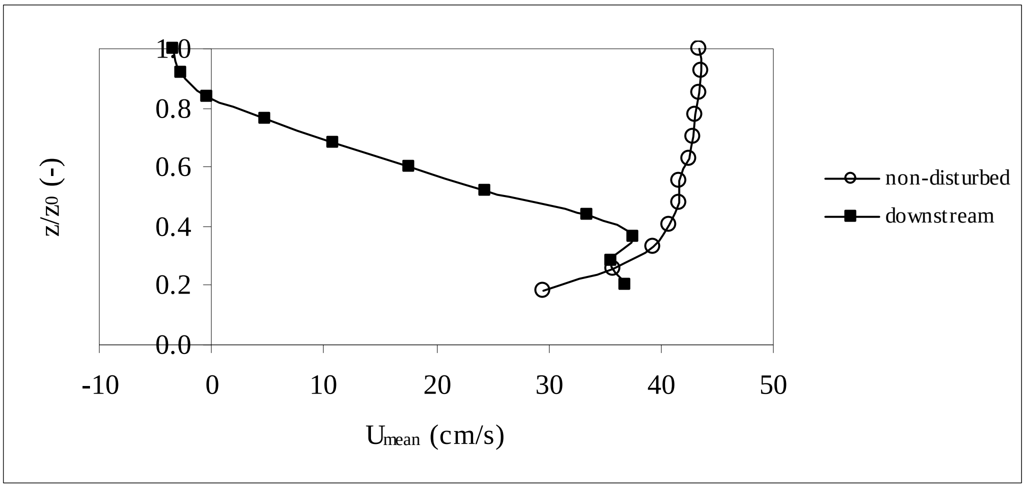

Figure B.10: The measured velocity profile of non-disturbed case and measured velocity profile at the downstream of vegetative element for Experiment no: 11 (Type 2, d=25 cm)

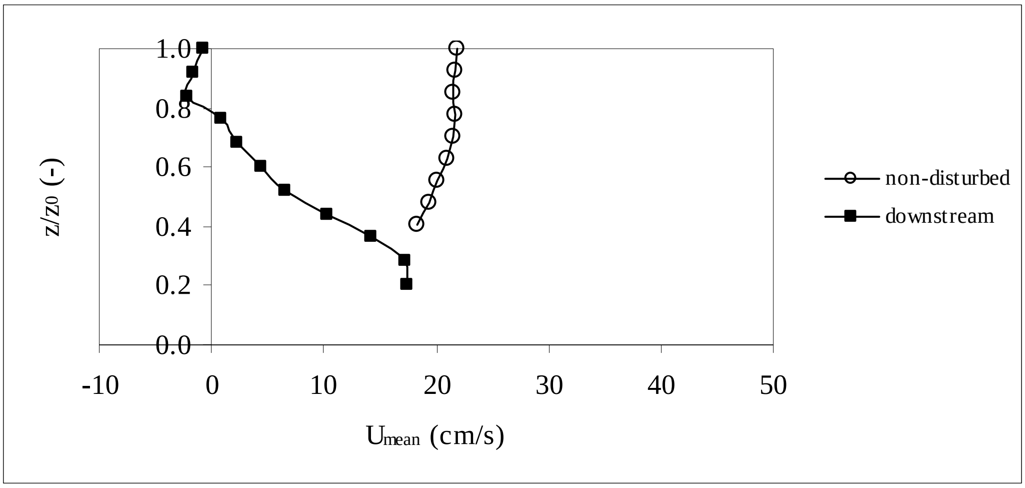

Figure B.11: The measured velocity profile of non-disturbed case and measured velocity profile at the downstream of vegetative element for Experiment no: 12 (Type 2, d=25 cm)

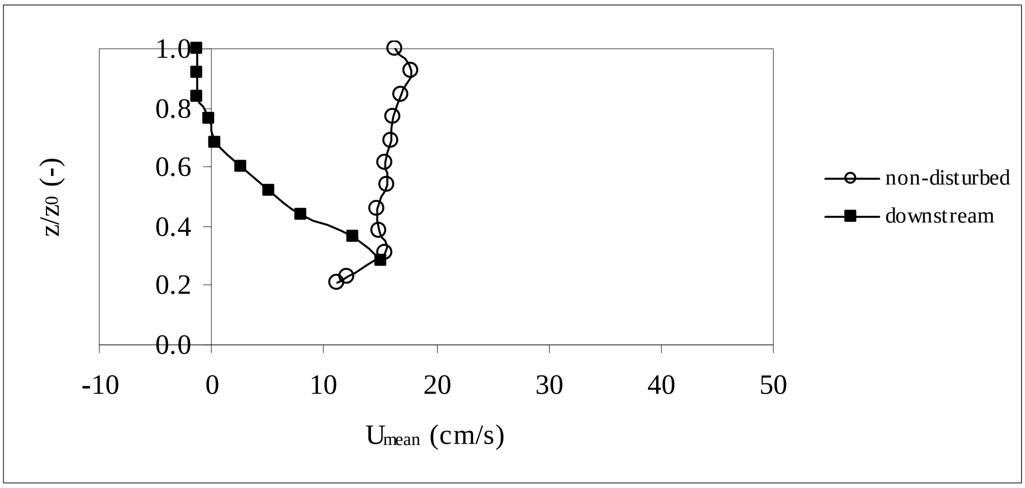

Figure B.12: The measured velocity profile of non-disturbed case and measured velocity profile at the downstream of vegetative element for Experiment no: 13 (Type 2, d=25 cm)

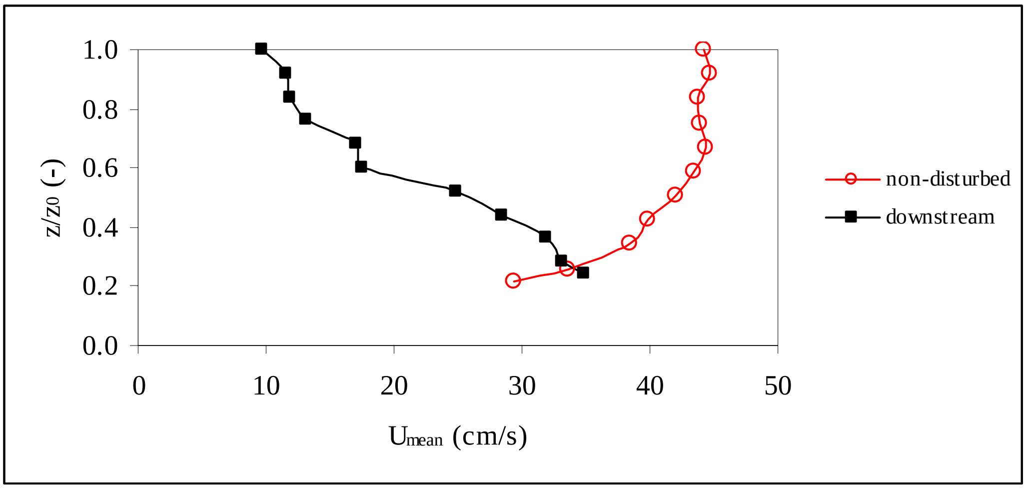

Figure B.13: The measured velocity profile of non-disturbed case and measured velocity profile at the downstream of vegetative element for Experiment no: 15 (Type 3, d=25 cm)

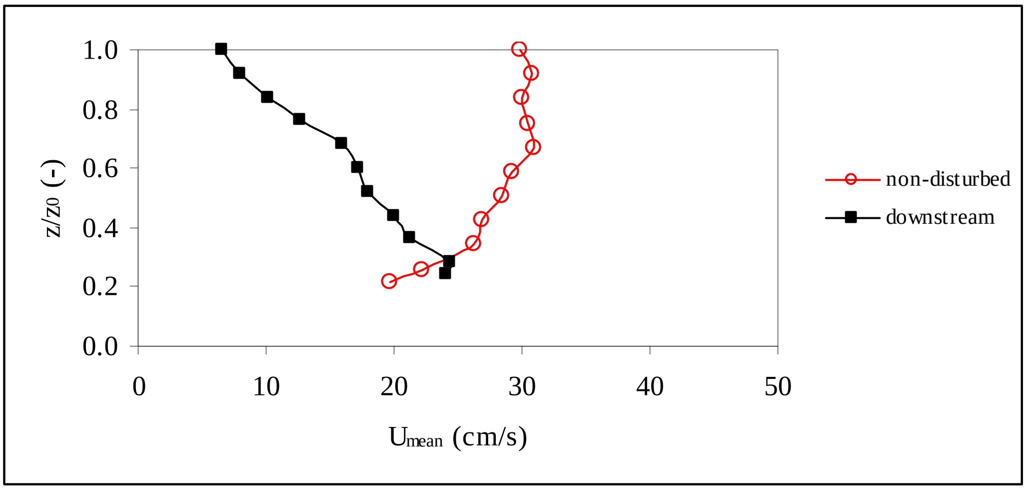

Figure B.14: The measured velocity profile of non-disturbed case and measured velocity profile at the downstream of vegetative element for Experiment no: 16 (Type 3, d=25 cm)

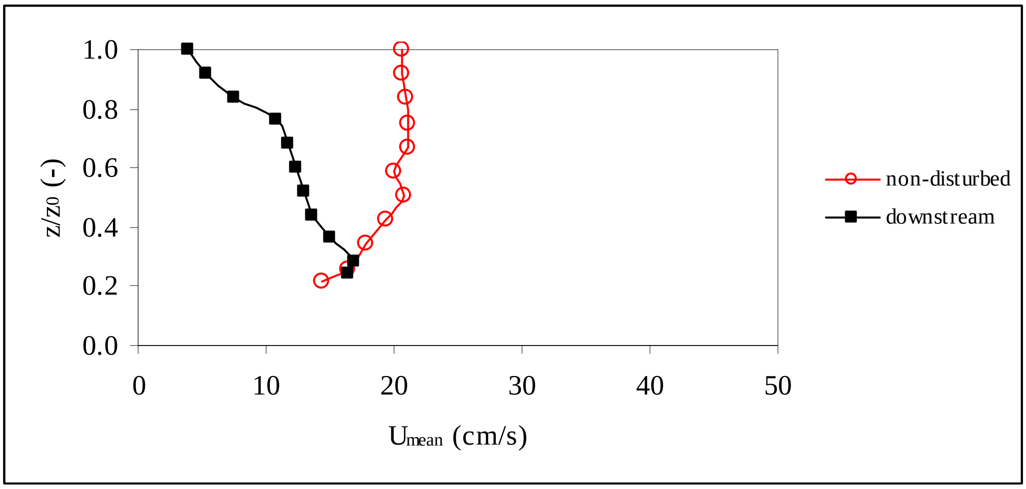

Figure B.15: The measured velocity profile of non-disturbed case and measured velocity profile at the downstream of vegetative element for Experiment no: 17 (Type 3, d=25 cm)

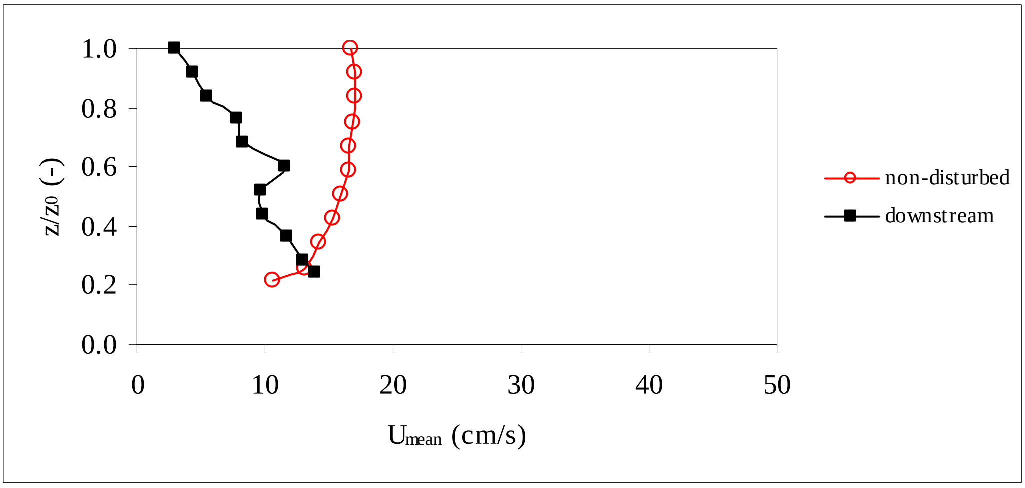

Figure B.16: The measured velocity profile of non-disturbed case and measured velocity profile at the downstream of vegetative element for Experiment no: 18 (Type 3, d=25 cm)

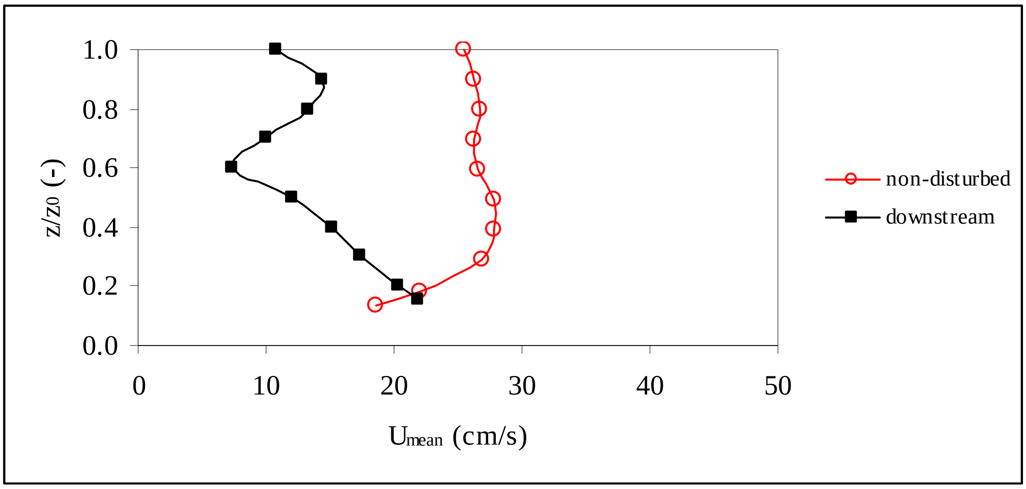

Figure B.17: The measured velocity profile of non-disturbed case and measured velocity profile at the downstream of vegetative element for Experiment no: 19 (Type 3, d=40 cm)

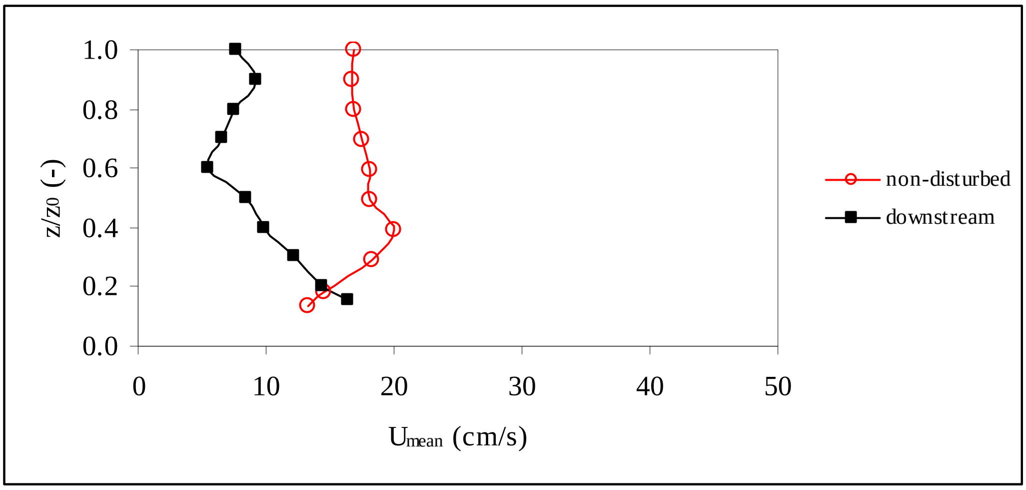

Figure B.18: The measured velocity profile of non-disturbed case and measured velocity profile at the downstream of vegetative element for Experiment no: 20 (Type 3, d=40 cm)

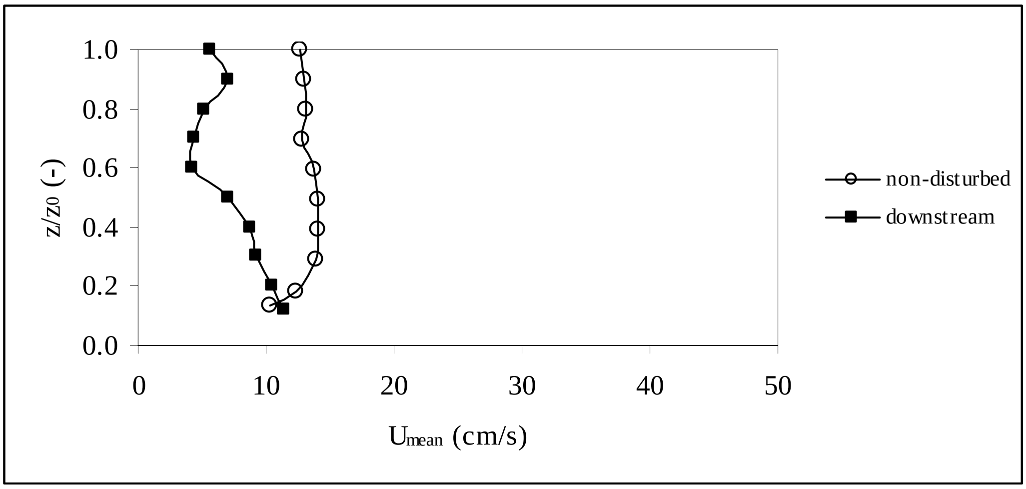

Figure B.19: The measured velocity profile of non-disturbed case and measured velocity profile at the downstream of vegetative element for Experiment no: 21 (Type 3, d=40 cm)

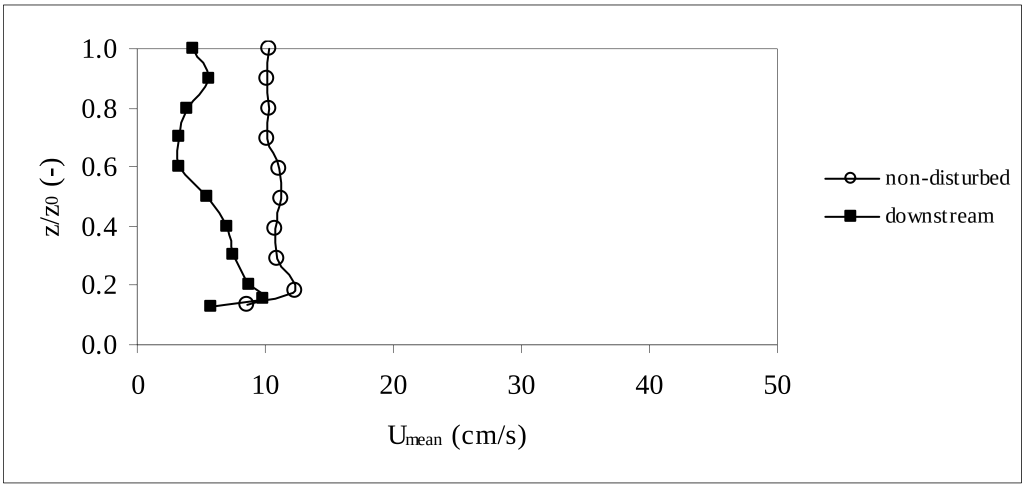

Figure B.20: The measured velocity profile of non-disturbed case and measured velocity profile at the downstream of vegetative element for Experiment no: 22 (Type 3, d=40cm)

APPENDIX C: THE OBTAINED VELOCITY CONTOURS UNDER THE EFFECT OF VEGETATION FOR DIFFERENT EXPERIMENTS

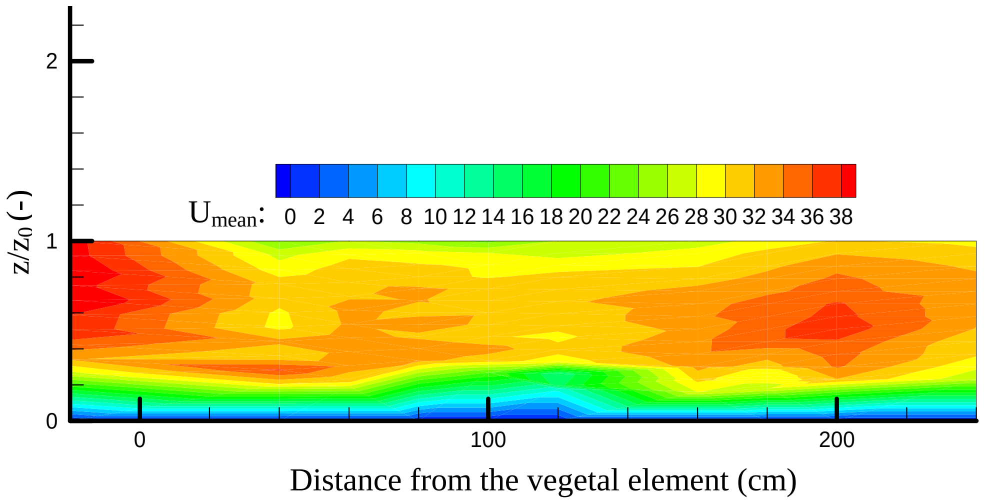

Figure C.1: The obtained velocity contours under the effect of vegetation for Experiment no: 1 (Type 1, d=25 cm)

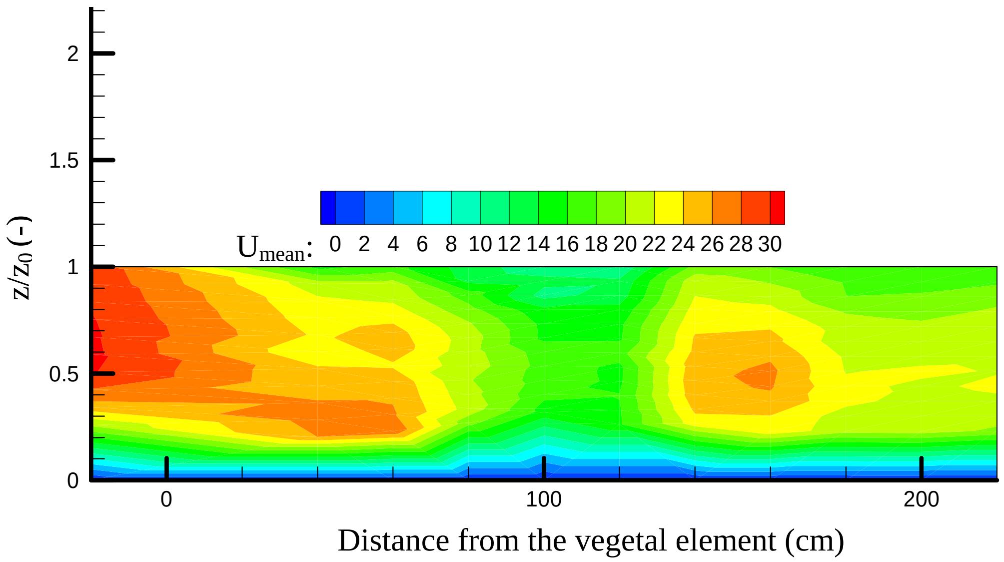

Figure C.2: The obtained velocity contours under the effect of vegetation for Experiment no: 2 (Type 1, d=25 cm)

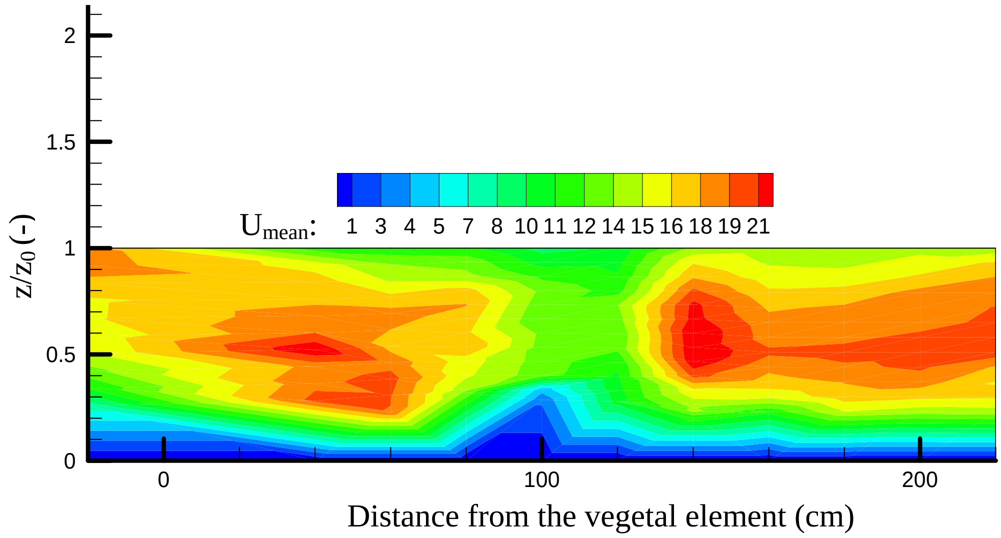

Figure C.3: The obtained velocity contours under the effect of vegetation for Experiment no: 3 (Type 1, d=25 cm)

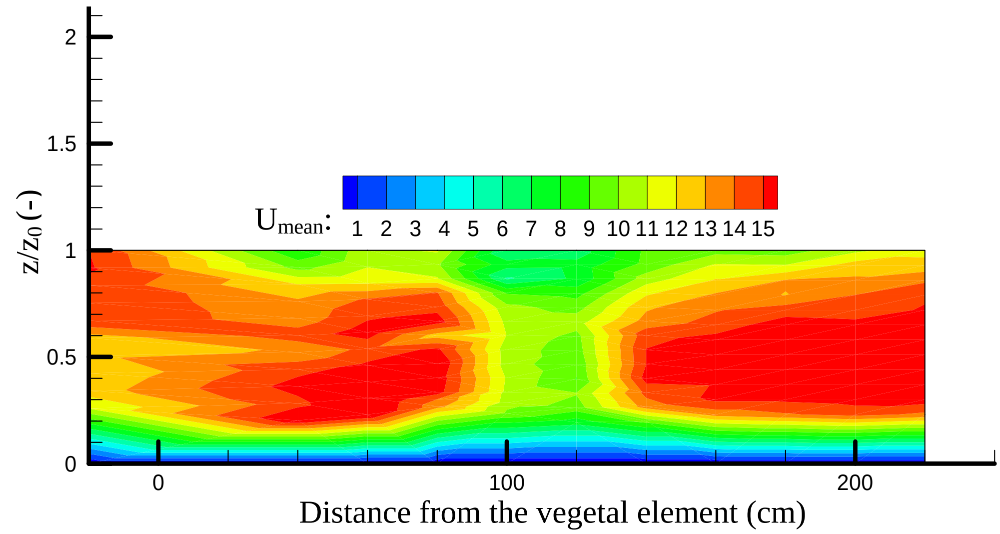

Figure C.4: The obtained velocity contours under the effect of vegetation for Experiment no: 4 (Type 1, d=25 cm)

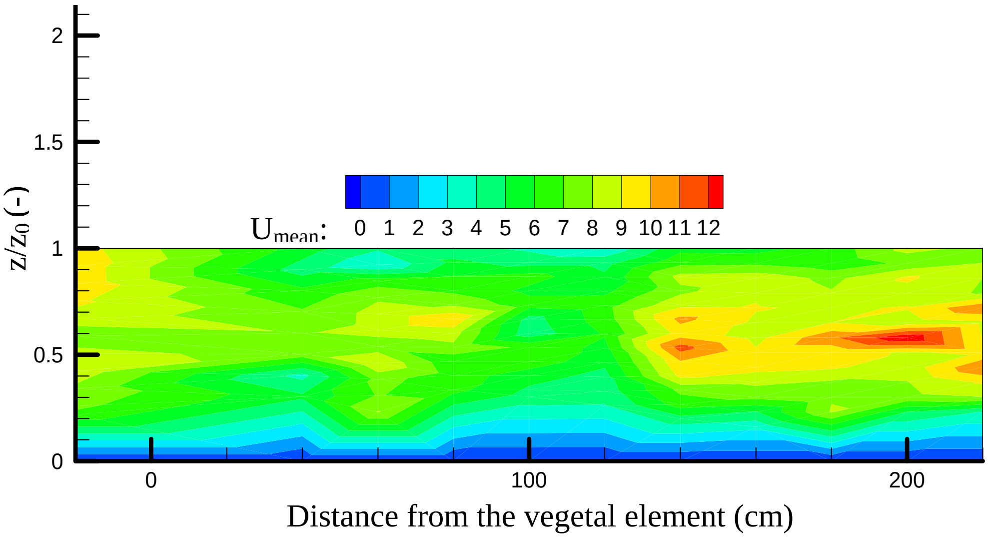

Figure C.5: The obtained velocity contours under the effect of vegetation for Experiment no: 5 (Type 1, d=25 cm)

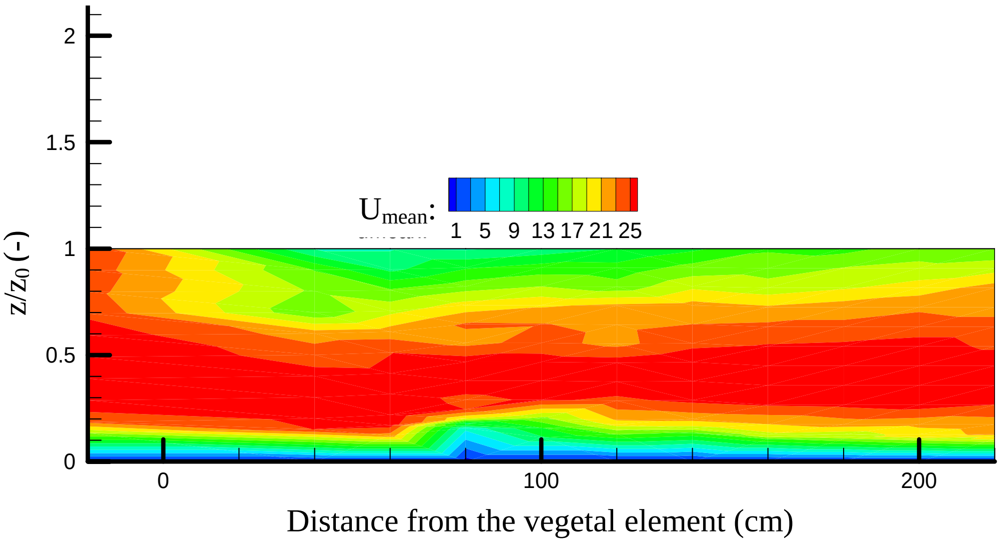

Figure C.6: The obtained velocity contours under the effect of vegetation for Experiment no: 6 (Type 1, d=40 cm)

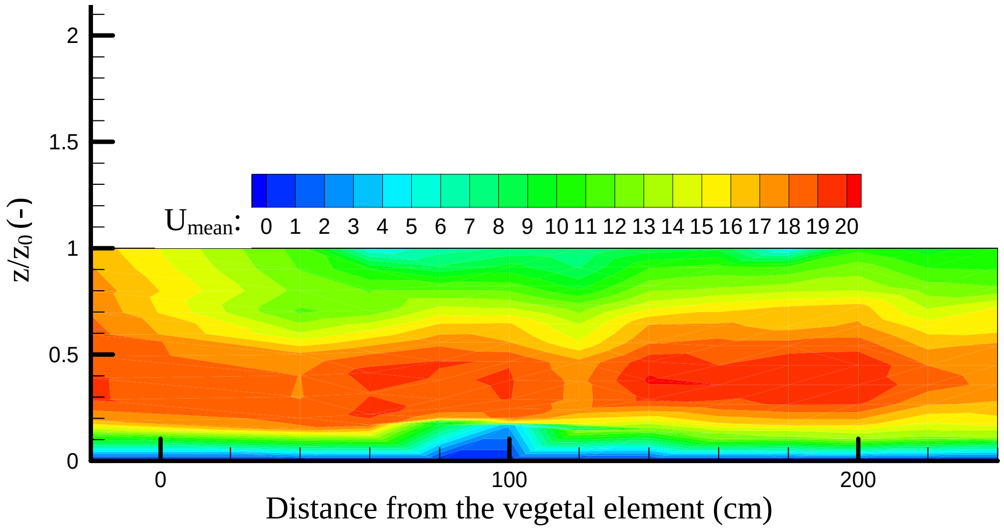

Figure C.7: The obtained velocity contours under the effect of vegetation for Experiment no: 7 (Type 1, d=40 cm)

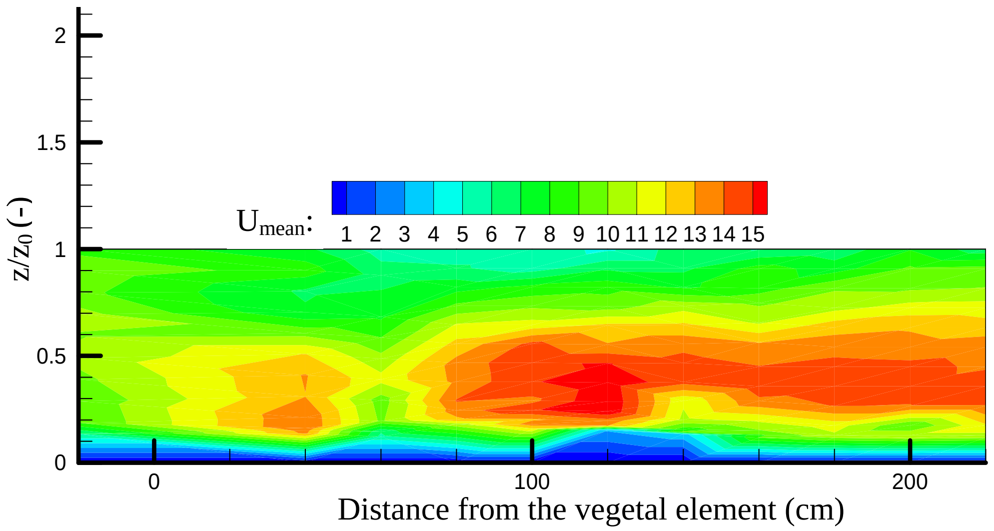

Figure C.8: The obtained velocity contours under the effect of vegetation for Experiment no: 8 (Type 1, d=40 cm)

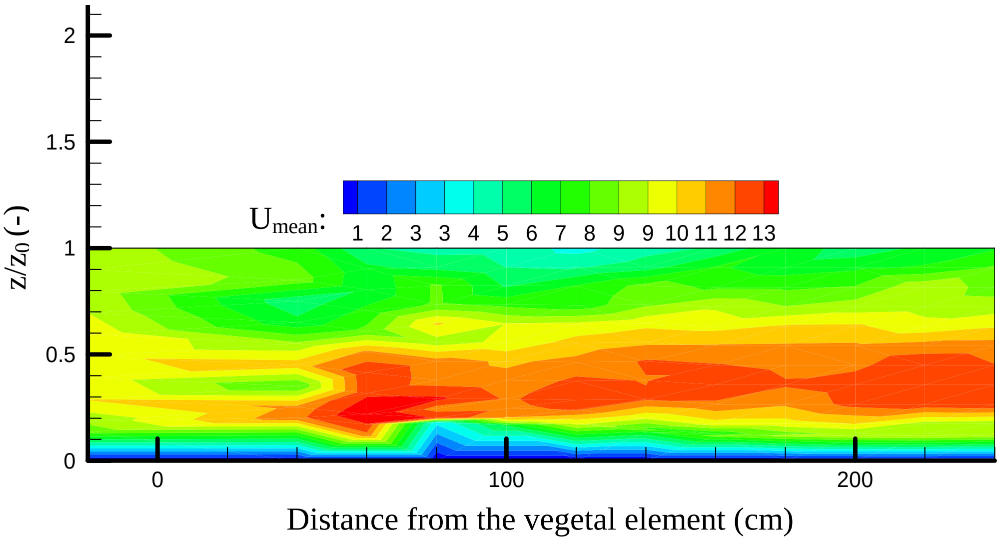

Figure C.9: The obtained velocity contours under the effect of vegetation for Experiment no: 9 (Type 1, d=40 cm)

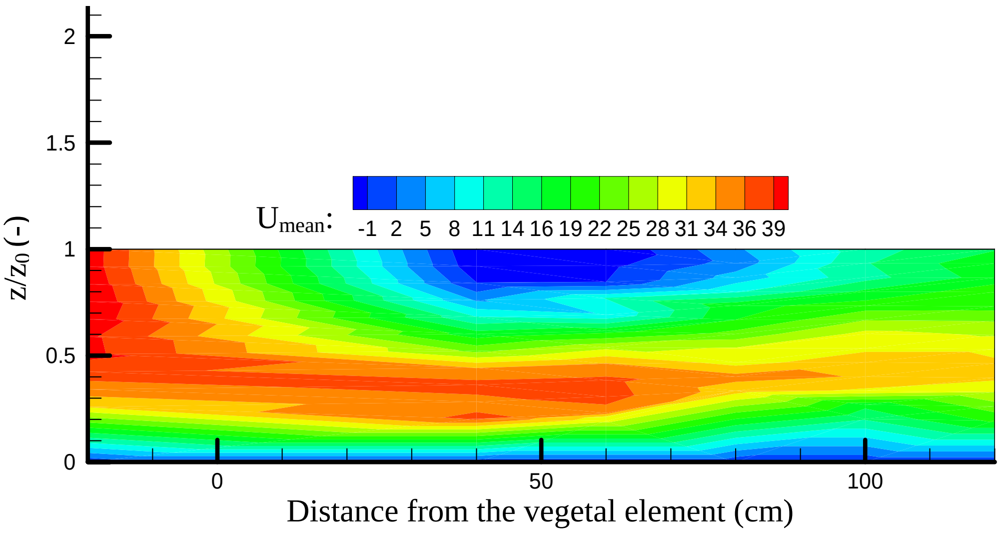

Figure C.10: The obtained velocity contours under the effect of vegetation for Experiment no: 1 (Type 2, d=25 cm)

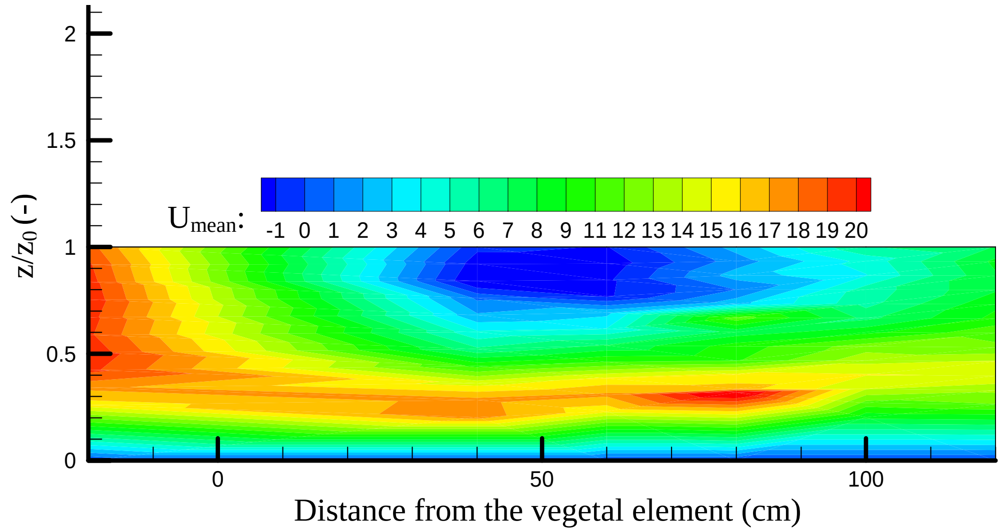

Figure C.11: The obtained velocity contours under the effect of vegetation for Experiment no: 12 (Type 2, d=25 cm)

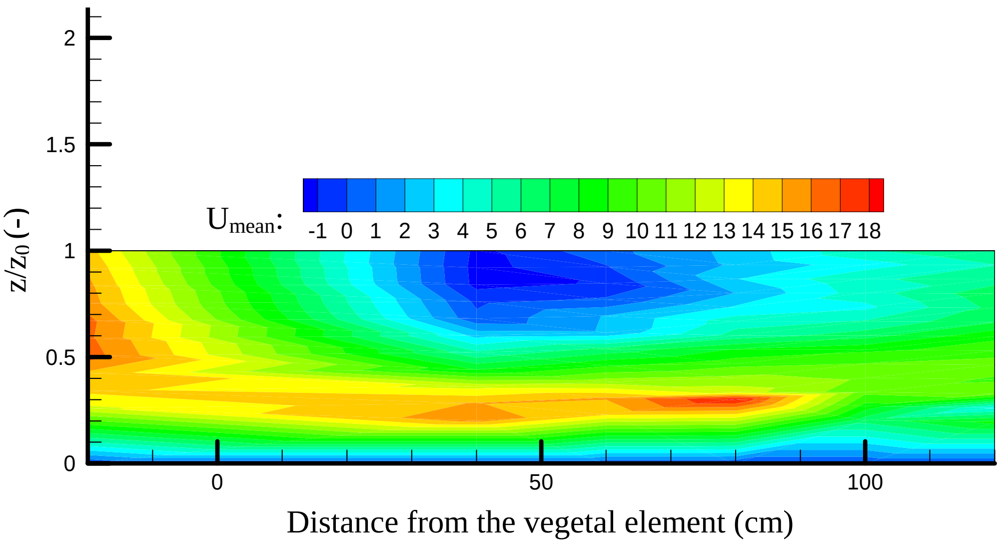

Figure C.12: The obtained velocity contours under the effect of vegetation for Experiment no: 13 (Type 2, d=25 cm)

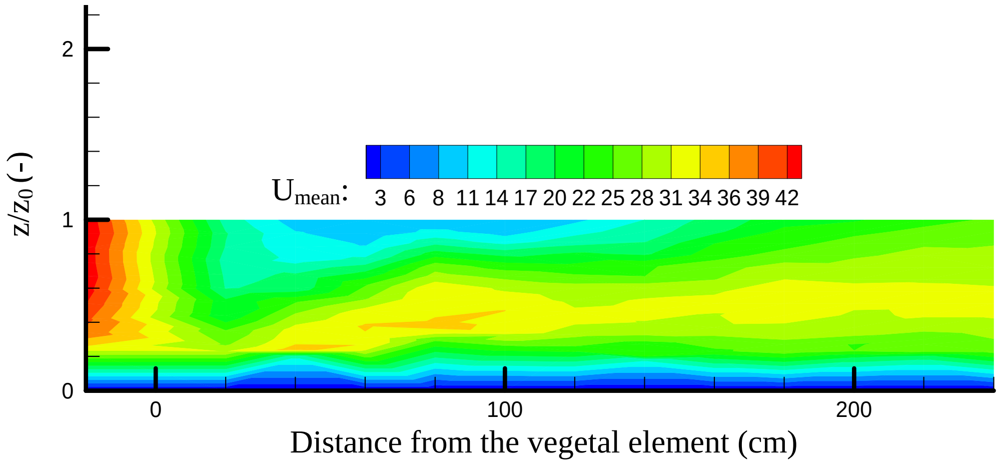

Figure C.13: The obtained velocity contours under the effect of vegetation for Experiment no: 15 (Type 3, d=25 cm)

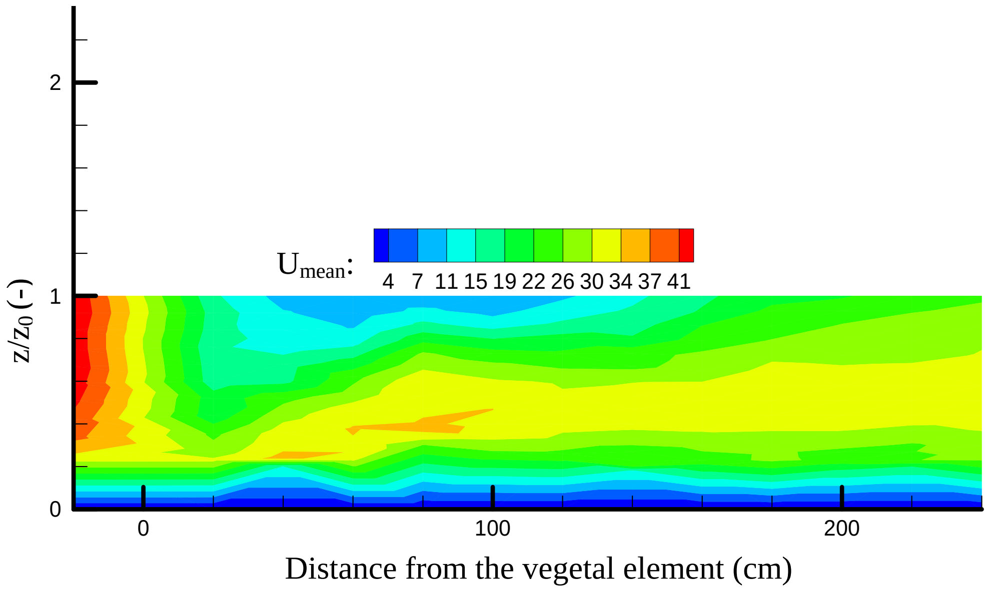

Figure C.14: The obtained velocity contours under the effect of vegetation for Experiment no: 16 (Type 3, d=25 cm)

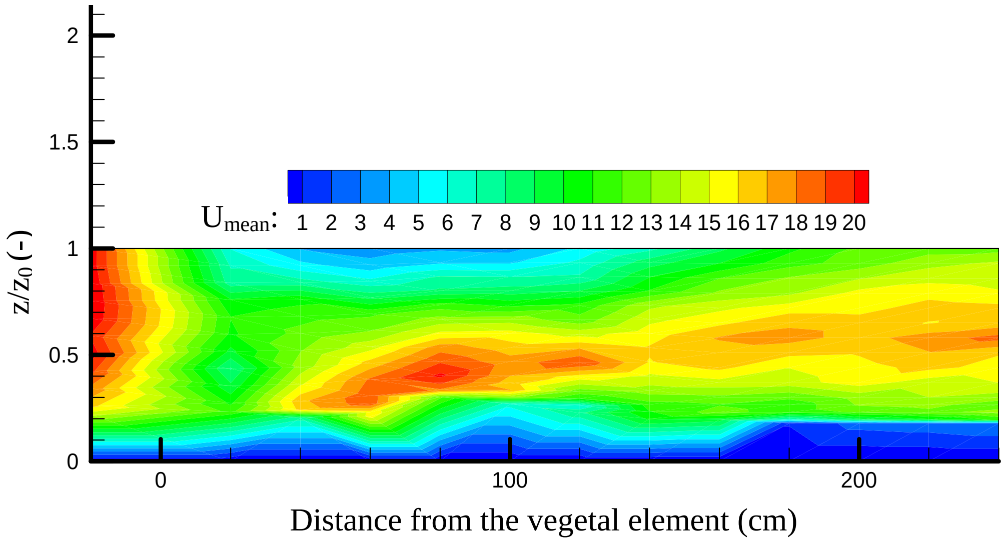

Figure C.15: The obtained velocity contours under the effect of vegetation for Experiment no: 17 (Type 3, d=25 cm)

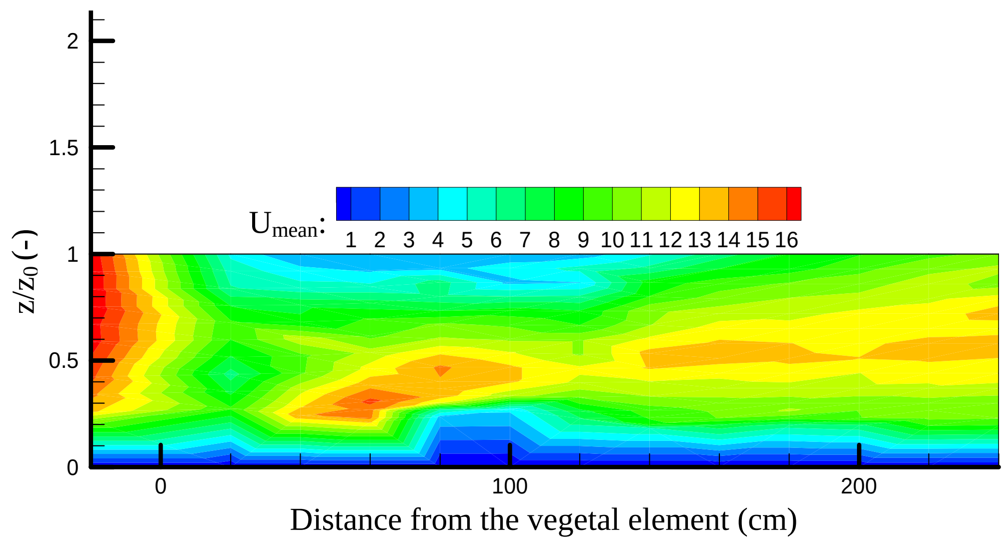

Figure C.16: The obtained velocity contours under the effect of vegetation for Experiment no: 18 (Type 3, d=25 cm)

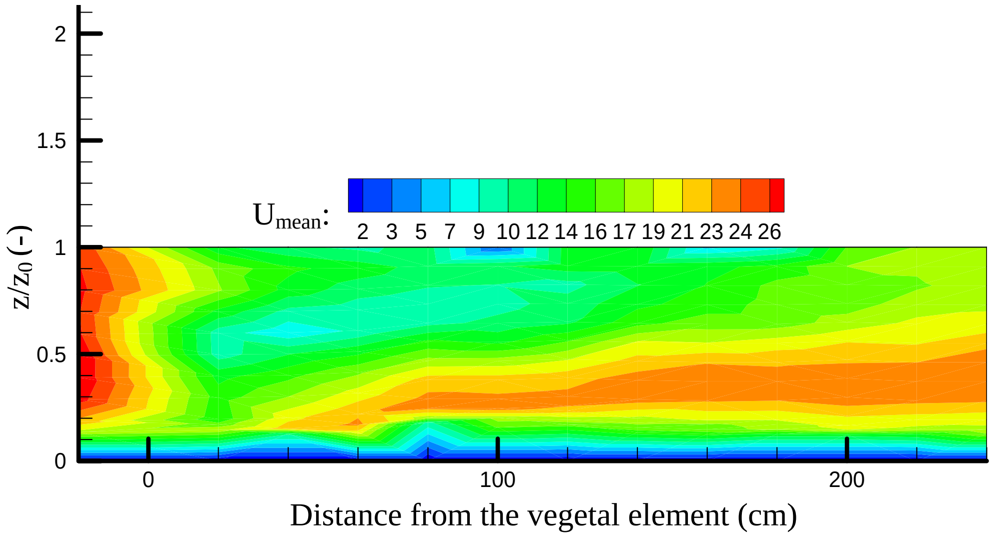

Figure C.17: The obtained velocity contours under the effect of vegetation for Experiment no: 19 (Type 3, d=40 cm)

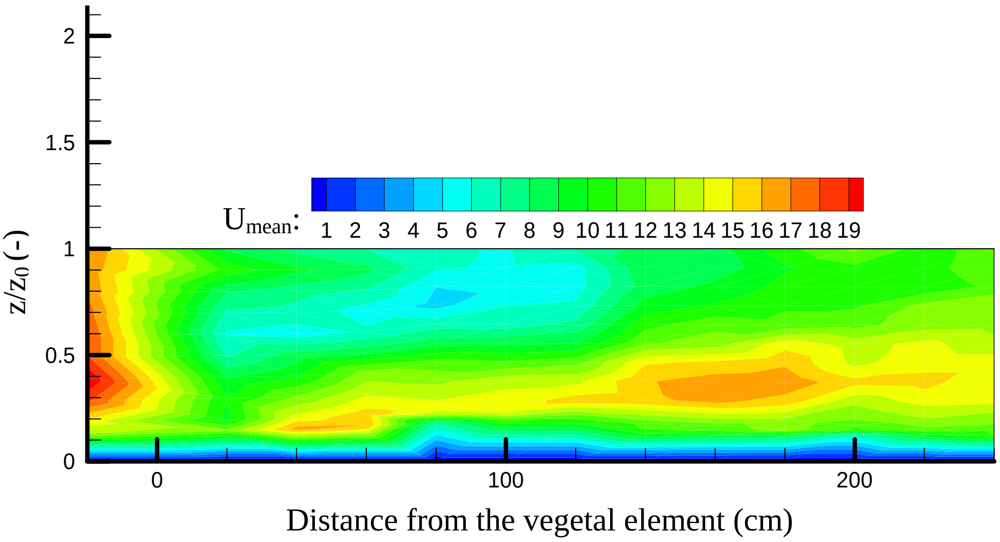

Figure C.18: The obtained velocity contours under the effect of vegetation for Experiment no: 20 (Type 3, d=40 cm)

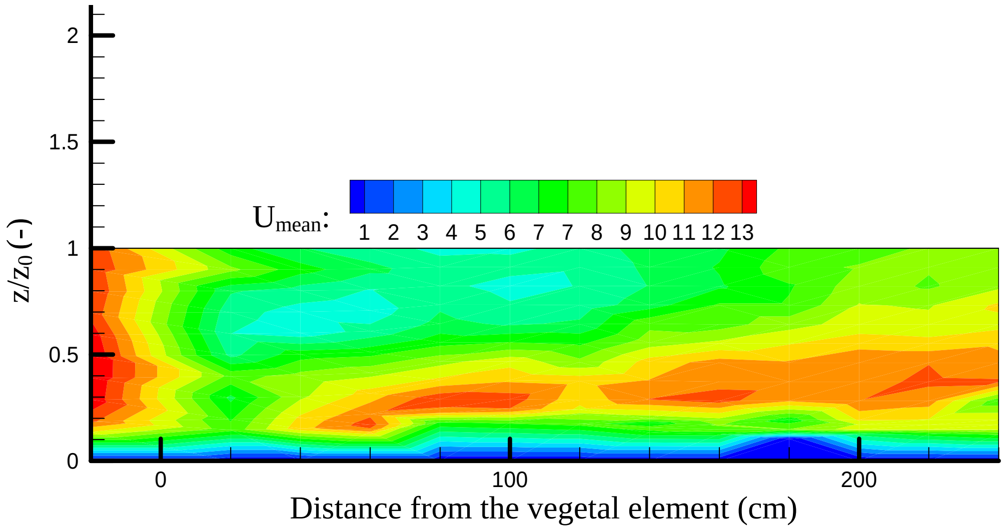

Figure C.19: The obtained velocity contours under the effect of vegetation for Experiment no: 21 (Type 3, d=40 cm)

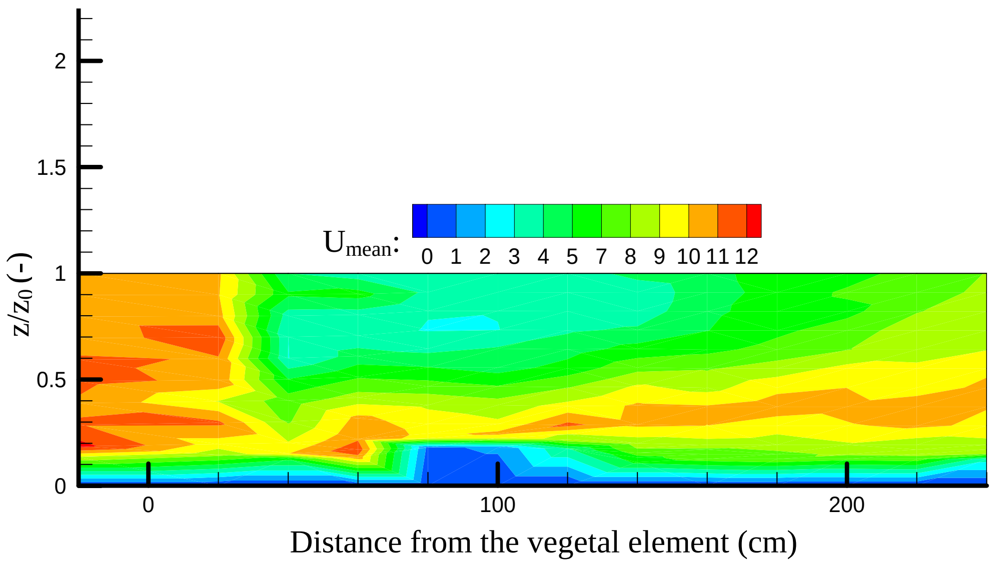

Figure C.20: The obtained velocity contours under the effect of vegetation for Experiment no: 22 (Type 3, d=40 cm)

APPENDIX D: THE MEASURED VELOCITY PROFILES AT THE LOCATIONS OF c300, r300, r320, r360 FOR DIFFERENT EXPERIMENTS

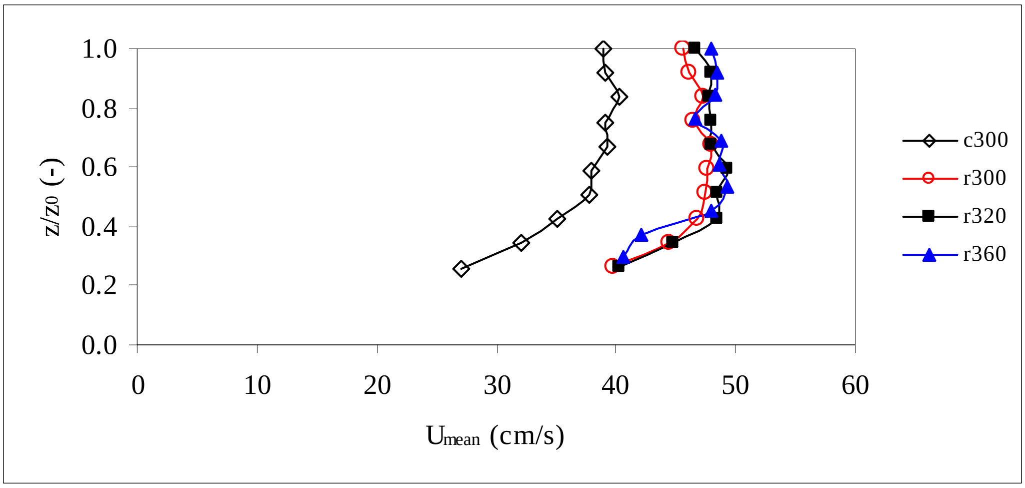

Figure D.1: The measured velocity profiles at the locations of c300, r300, r320, r360 for Experiment no: 1 (Type 1, d=25 cm)

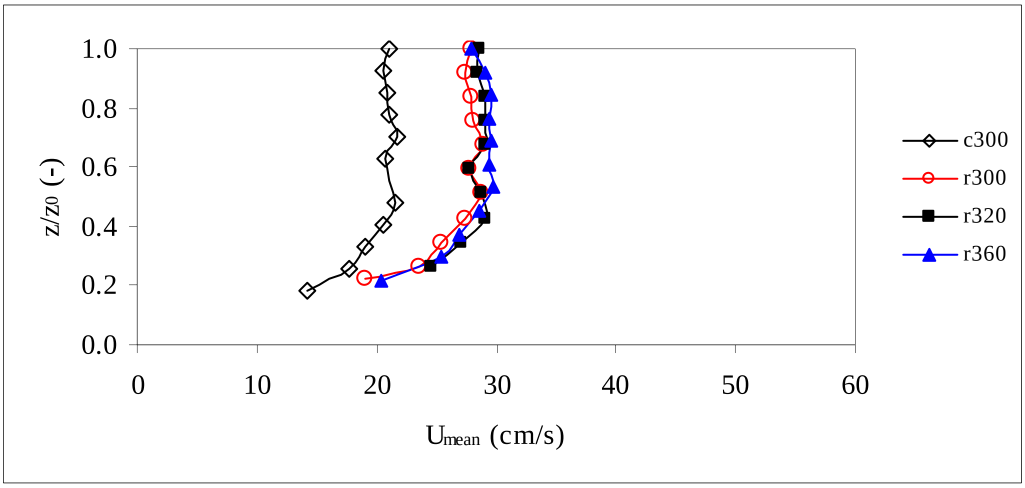

Figure D.2: The measured velocity profiles at the locations of c300, r300, r320, r360 for Experiment no: 2 (Type 1, d=25 cm)

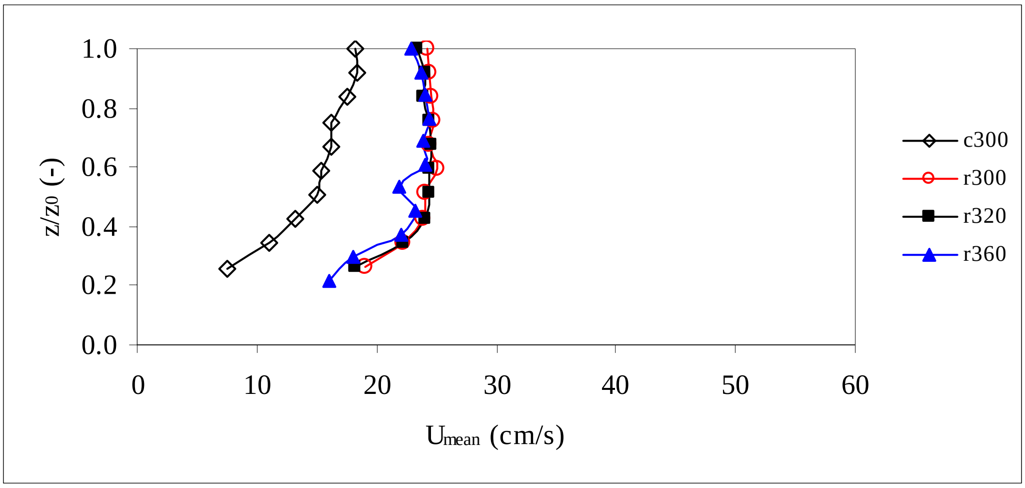

Figure D.3: The measured velocity profiles at the locations of c300, r300, r320, r360 for Experiment no: 3 (Type 1, d=25 cm)

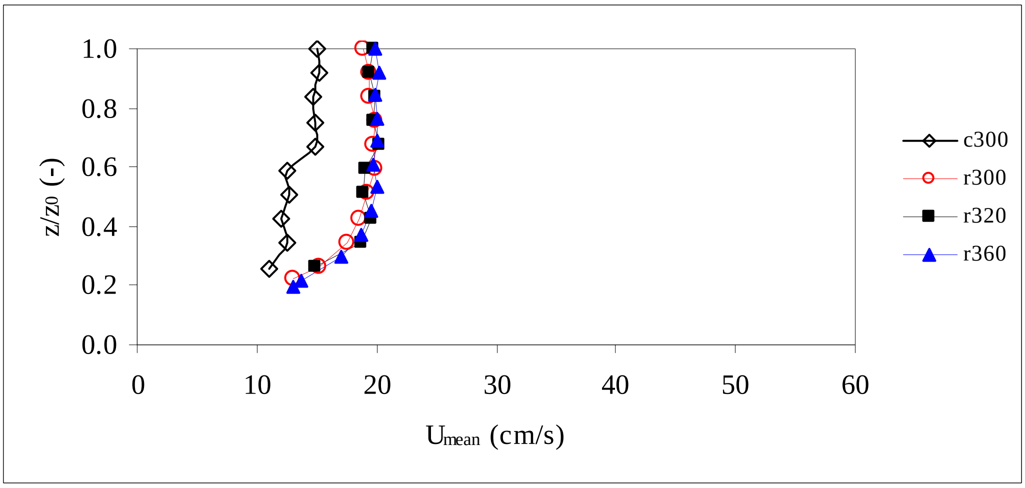

Figure D.4: The measured velocity profiles at the locations of c300, r300, r320, r360 for Experiment no: 4 (Type 1, d=25 cm)

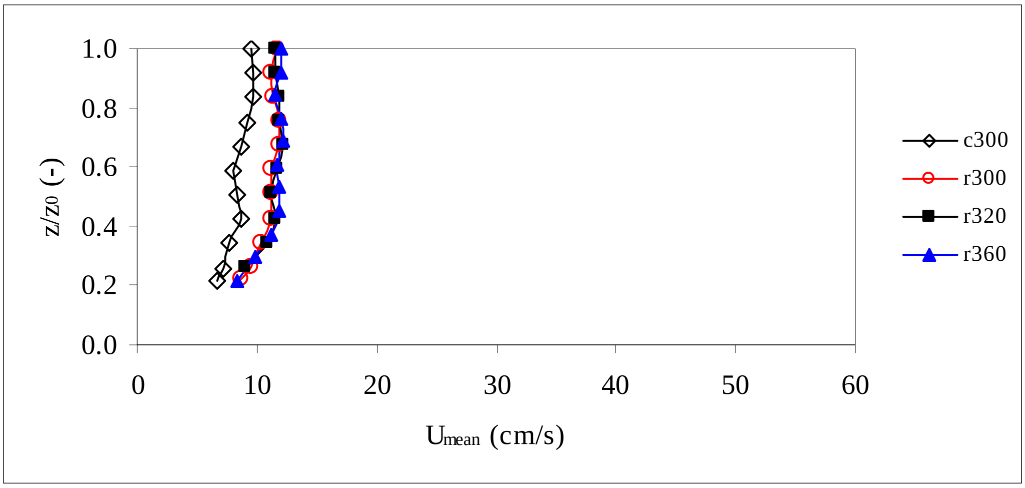

Figure D.5: The measured velocity profiles at the locations of c300, r300, r320, r360 for Experiment no: 5 (Type 1, d=25 cm)

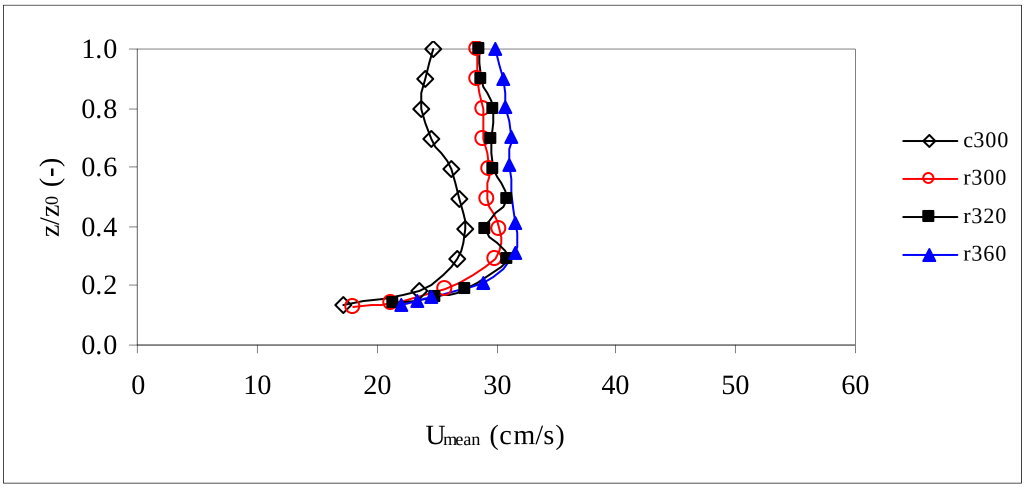

Figure D.6: The measured velocity profiles at the locations of c300, r300, r320, r360 for Experiment no: 6 (Type 1, d=40 cm)

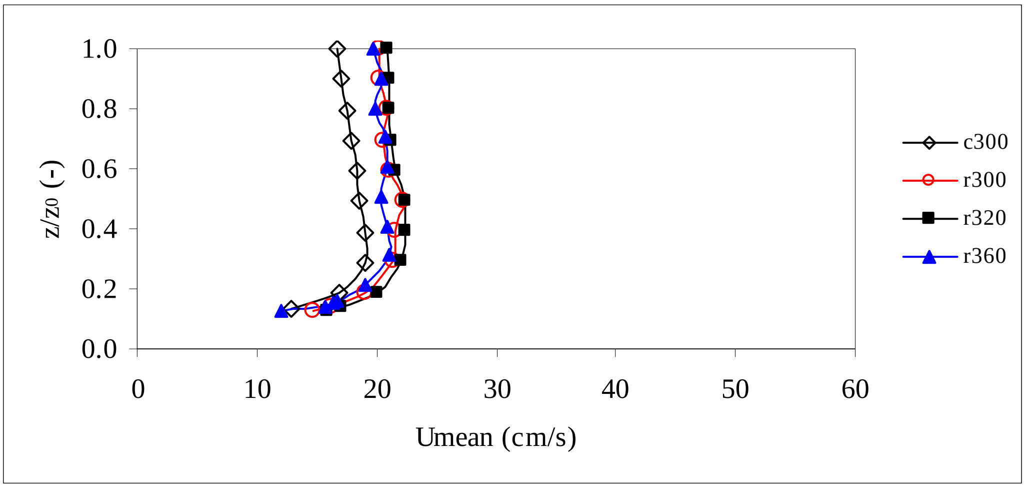

Figure D.7: The measured velocity profiles at the locations of c300, r300, r320, r360 for Experiment no: 7 (Type 1, d=40 cm)

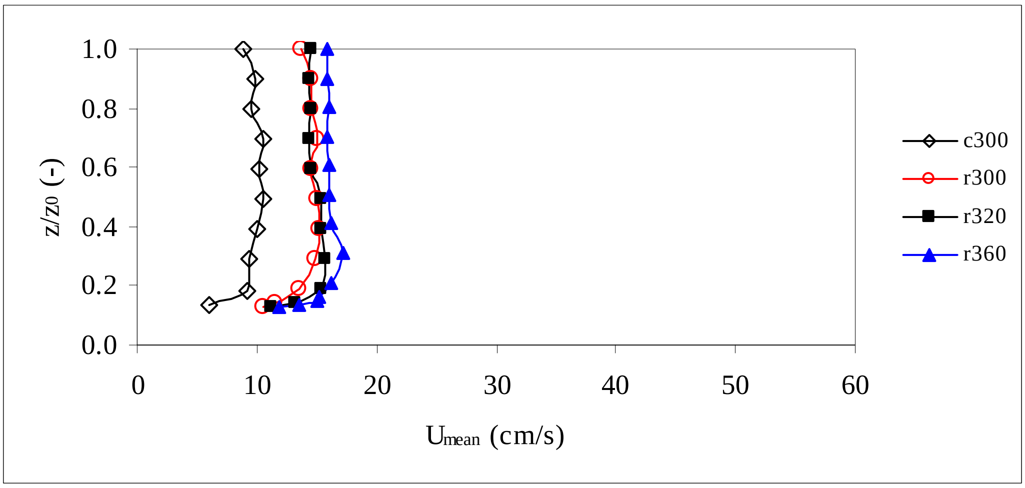

Figure D.8: The measured velocity profiles at the locations of c300, r300, r320, r360 for Experiment no: 8 (Type 1, d=40 cm)

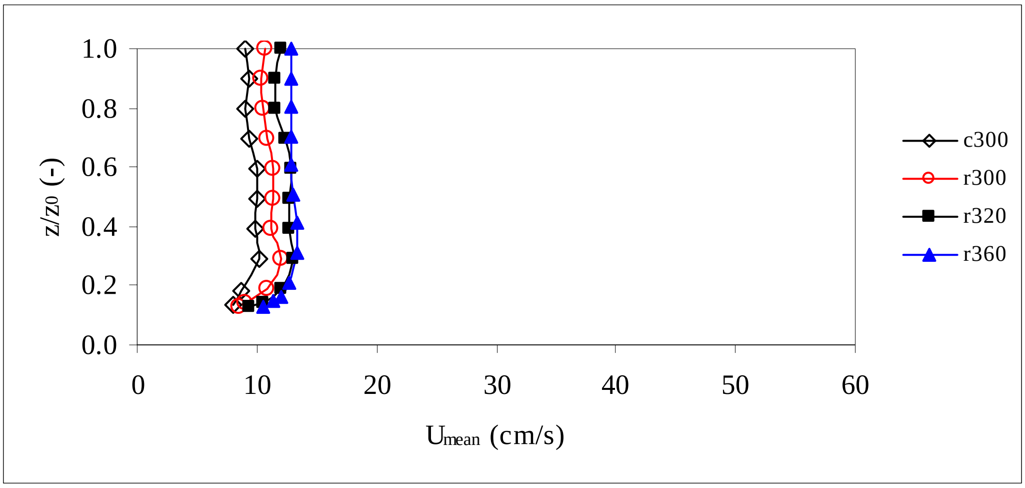

Figure D.9: The measured velocity profiles at the locations of c300, r300, r320, r360 for Experiment no: 1 (Type 1, d=40 cm)

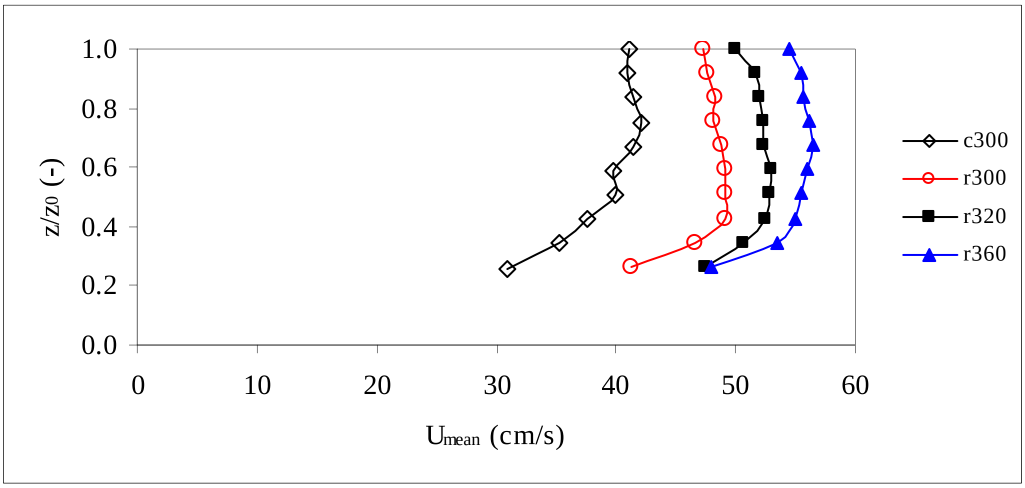

Figure D.10: The measured velocity profiles at the locations of c300, r300, r320, r360 for Experiment no: 11 (Type 2, d=25cm)

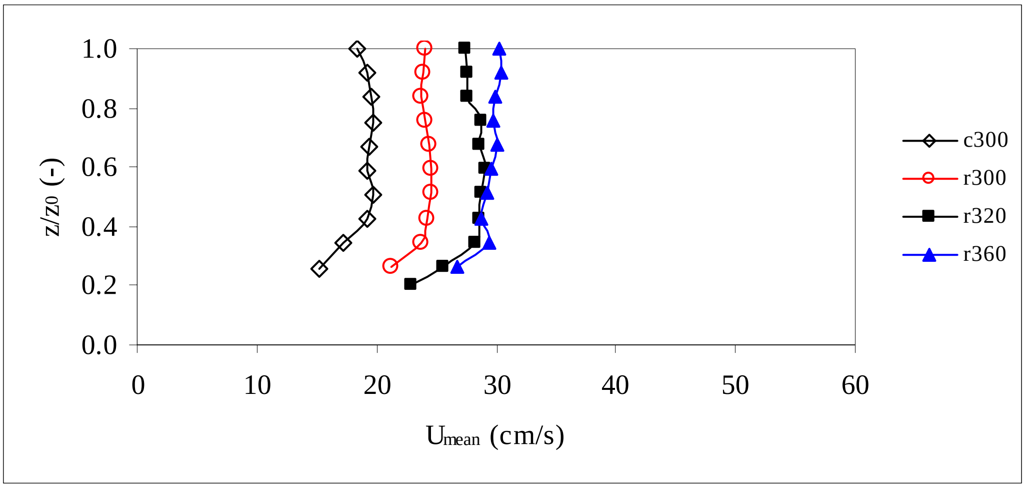

Figure D.11: The measured velocity profiles at the locations of c300, r300, r320, r360 for Experiment no: 12 (Type 2, d=40 cm)

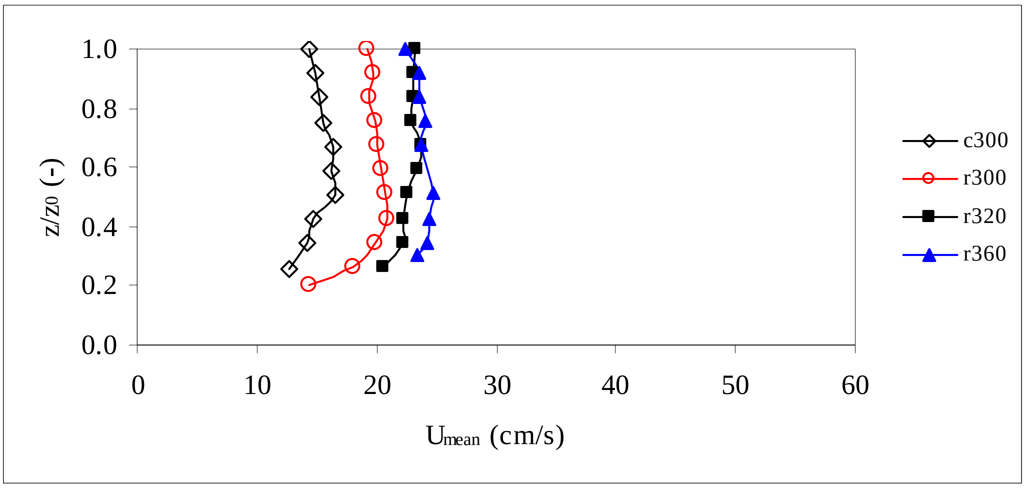

Figure D.12: The measured velocity profiles at the locations of c300, r300, r320, r360 for Experiment no: 13 (Type 2, d=25 cm)

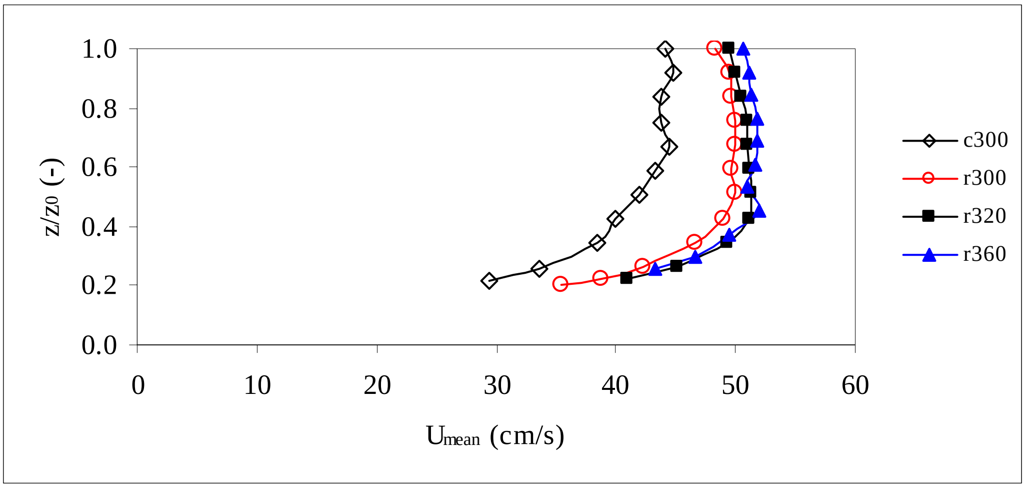

Figure D.13: The measured velocity profiles at the locations of c300, r300, r320, r360 for Experiment no: 15 (Type 3, d=25 cm)

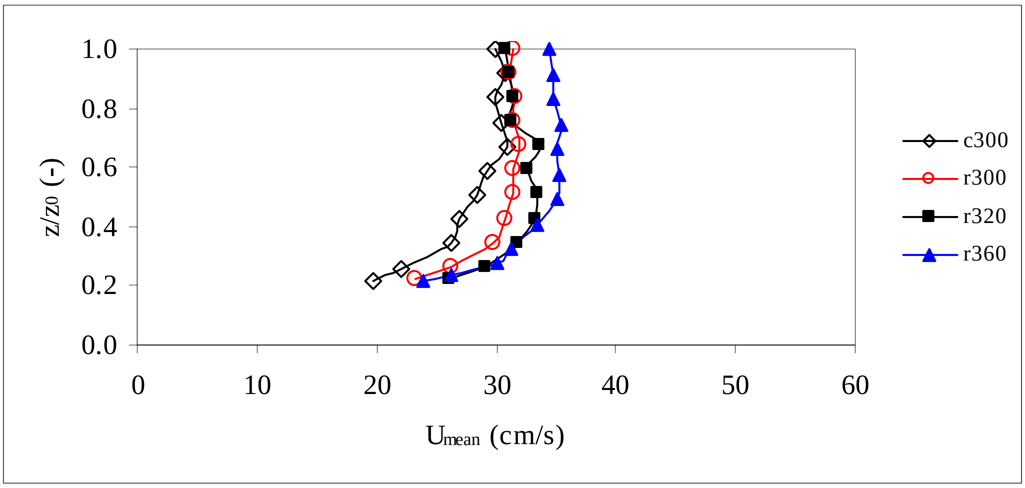

Figure D.14: The measured velocity profiles at the locations of c300, r300, r320, r360 for Experiment no: 16 (Type 3, d=25 cm)

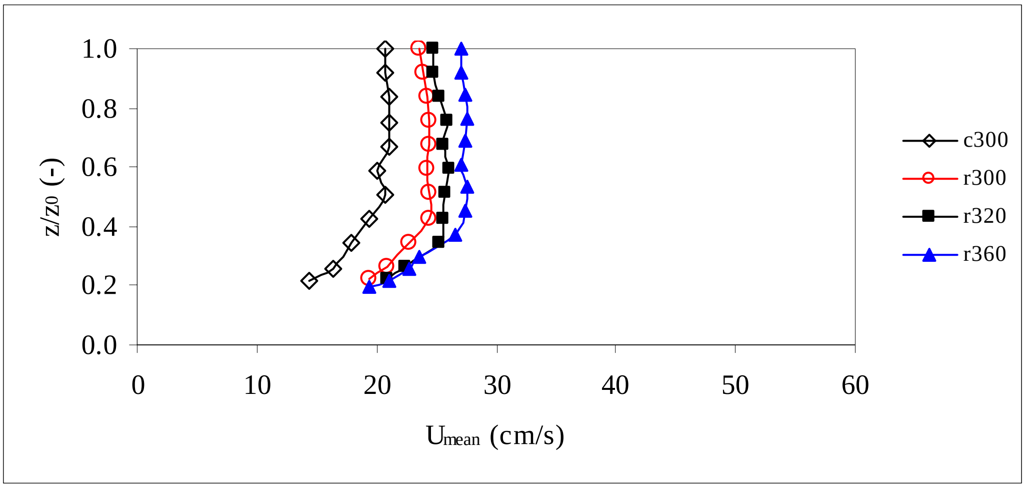

Figure D.15: The measured velocity profiles at the locations of c300, r300, r320, r360 for Experiment no: 17 (Type 3, d=25 cm)

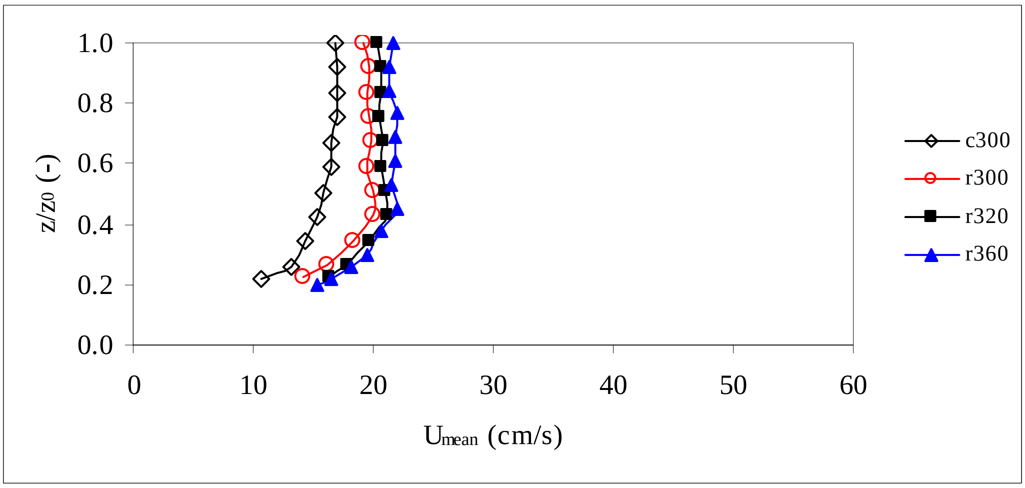

Figure D.16: The measured velocity profiles at the locations of c300, r300, r320, r360 for Experiment no: 18 (Type 3, d=25 cm)

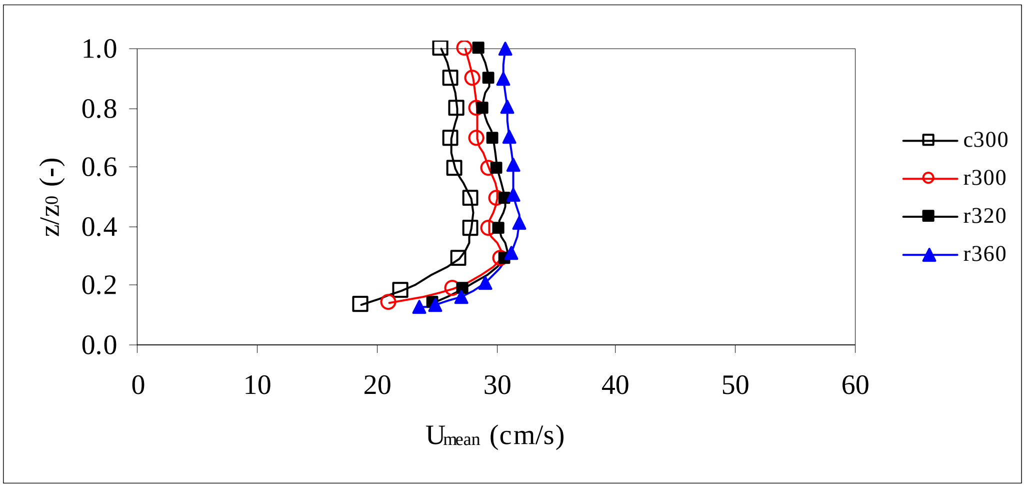

Figure D.17: The measured velocity profiles at the locations of c300, r300, r320, r360 for Experiment no: 19 (Type 3, d=40 cm)

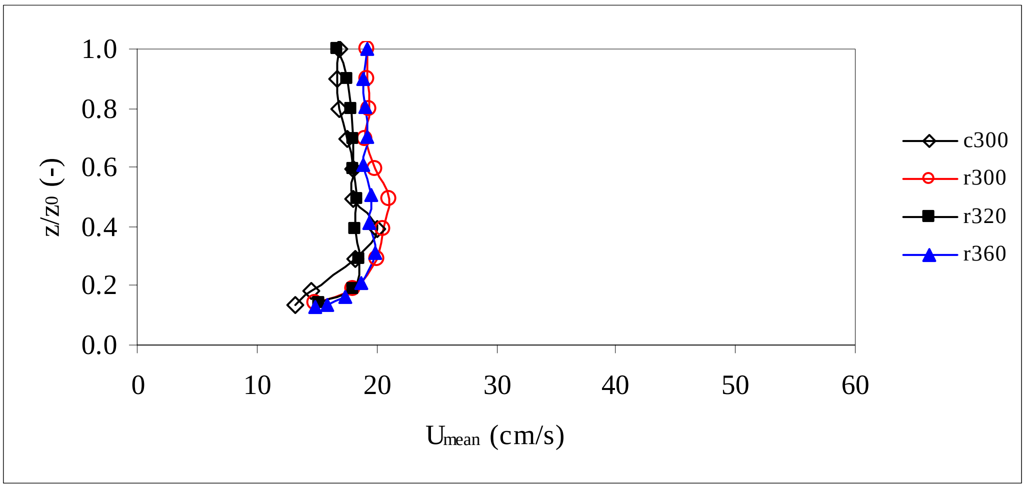

Figure D.18: The measured velocity profiles at the locations of c300, r300, r320, r360 for Experiment no: 20 (Type 3, d=40 cm)

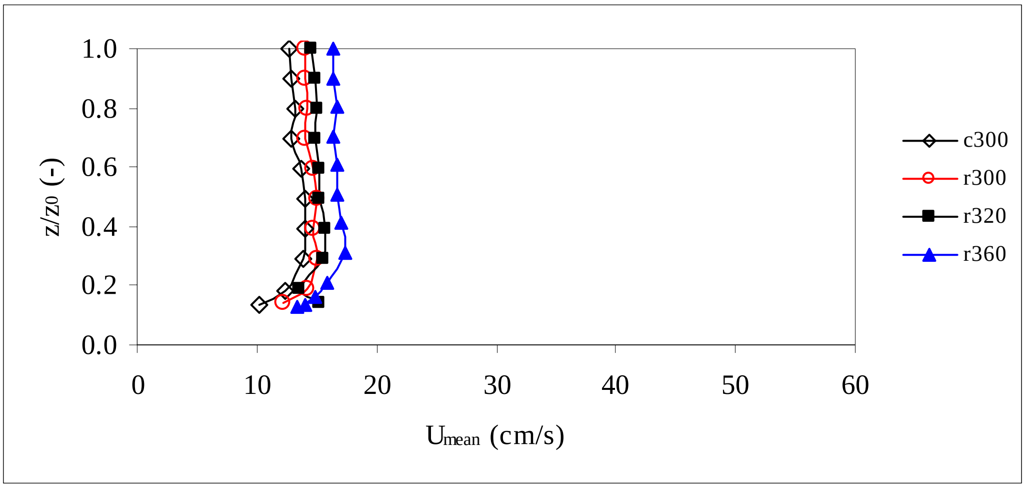

Figure D.19: The measured velocity profiles at the locations of c300, r300, r320, r360 for Experiment no: 21 (Type 3, d=40 cm)

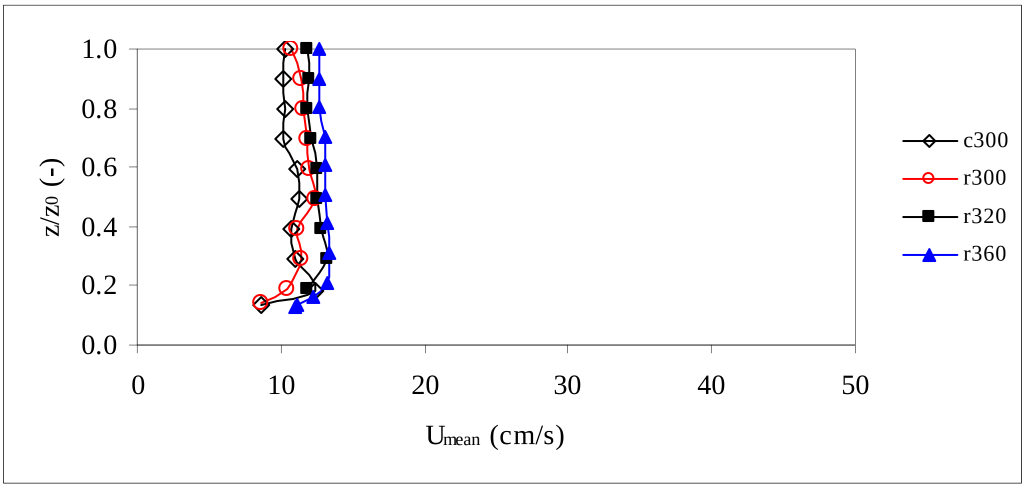

Figure D.1: The measured velocity profiles at the locations of c300, r300, r320, r360 for Experiment no: 1 (Type 1, d=40 cm)

APPENDIX E: VARIATION OF NORMALIZED VEGETATIVE VERTICAL VELOCITY DIFFERENCE PARAMETER WITH RESPECT TO RELATIVE DEPTH FOR DIFFERENT TYPES

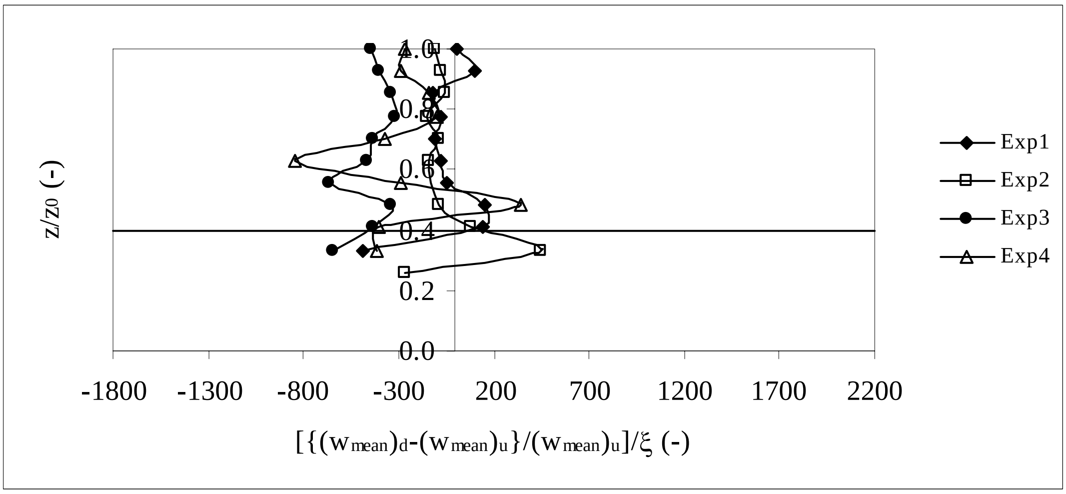

Figure E.1: The variation of normalized vegetative vertical velocity difference parameter with respect to relative depth for Type 1

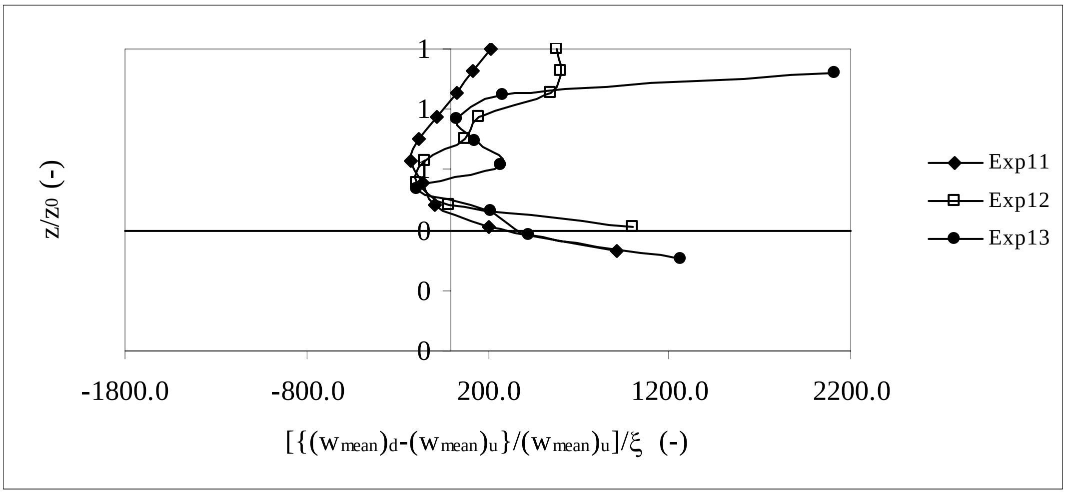

Figure E.2: The variation of normalized vegetative vertical velocity difference parameter with respect to relative depth for Type 2

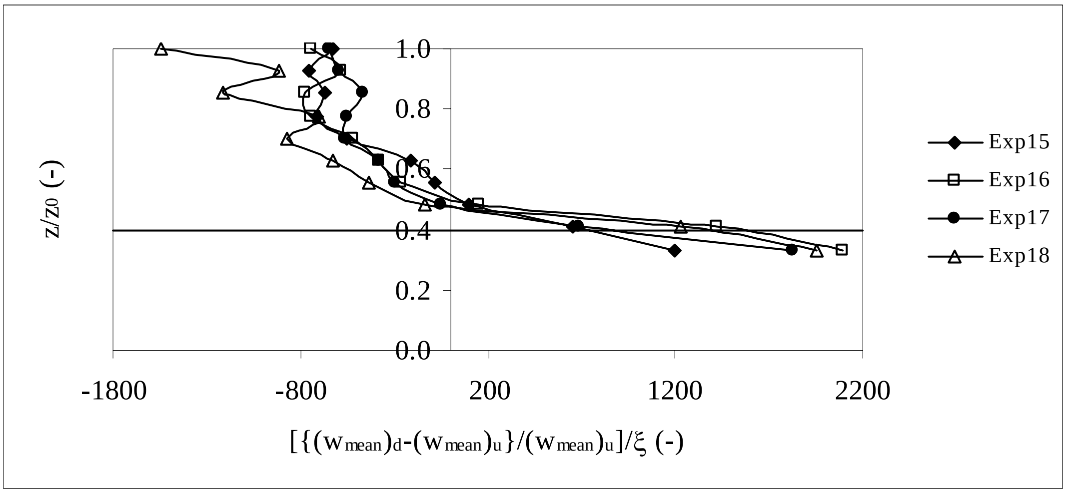

Figure E.3: The variation of normalized vegetative vertical velocity difference parameter with respect to relative depth for Type 3

APPENDIX F: THE VARIATION OF NORMALIZED VEGETATIVE STREAMWISE TURBULENCE INTENSITY PARAMETER WITH RESPECT TO RELATIVE DEPTH FOR DIFFERENT TYPES

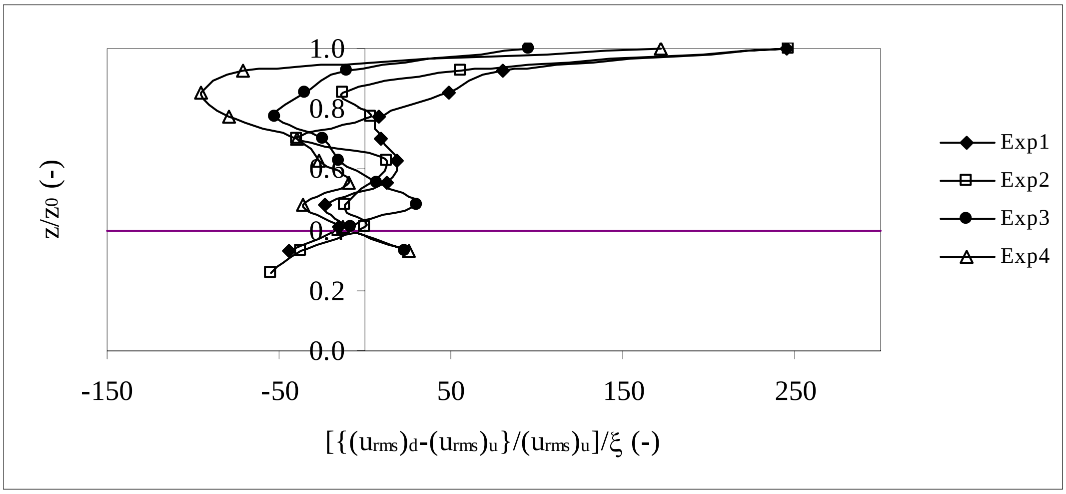

Figure F.1: The variation of normalized vegetative streamwise turbulence intensity parameter with respect to relative depth for Type 1

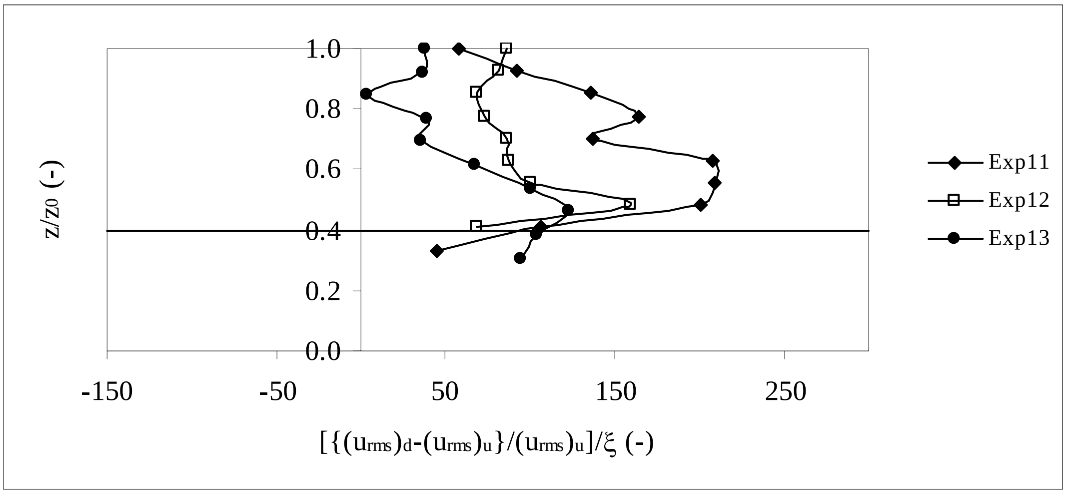

Figure F.2: The variation of normalized vegetative streamwise turbulence intensity parameter with respect to relative depth for Type 2

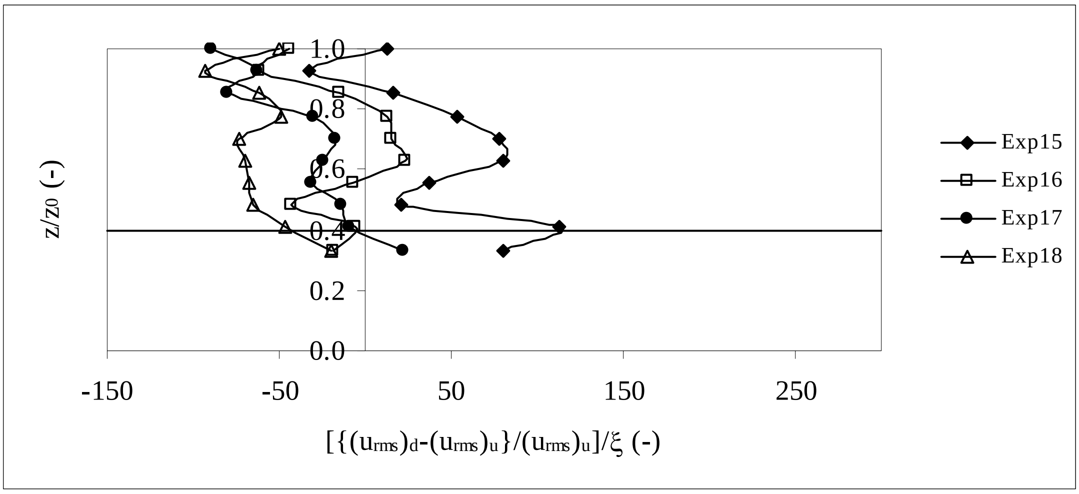

Figure F.3: The variation of normalized vegetative streamwise turbulence intensity parameter with respect to relative depth for Type 3

APPENDIX G: THE VARIATION OF NORMALIZED VEGETATIVE VERTICAL TURBULENCE INTENSITY PARAMETER WITH RESPECT TO RELATIVE DEPTH FOR DIFFERENT TYPES

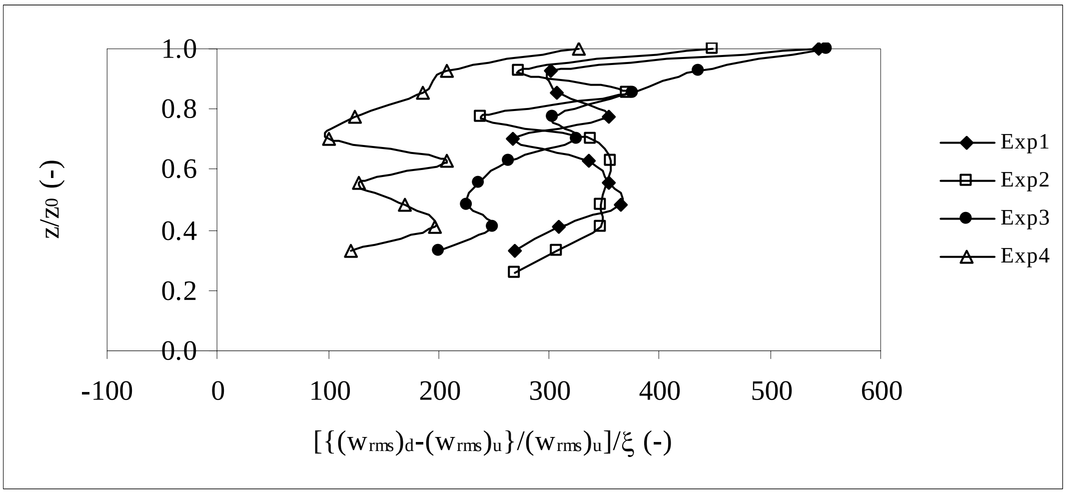

Figure G.1: The variation of normalized vegetative vertical turbulence intensity parameter with respect to relative depth for Type 1

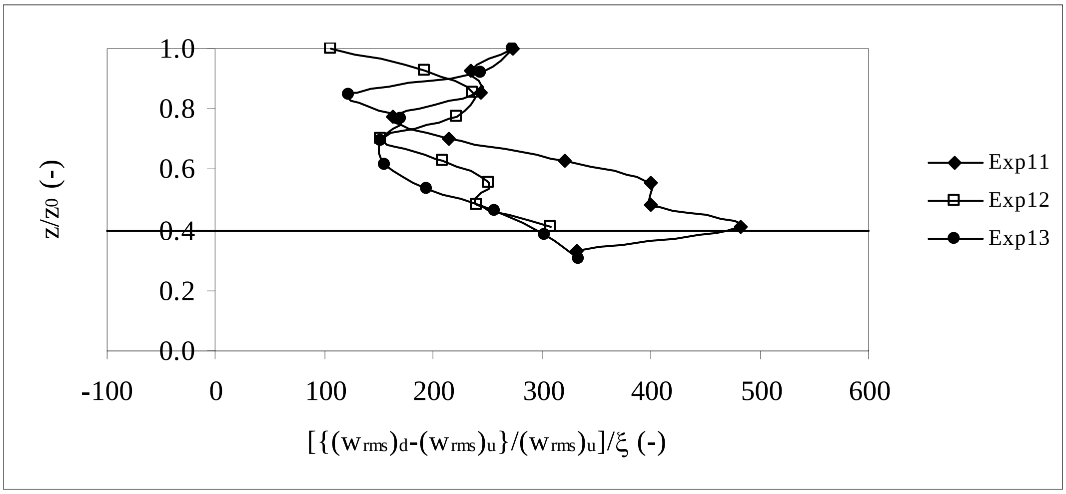

Figure G.2: The variation of normalized vegetative vertical turbulence intensity parameter with respect to relative depth for Type 2

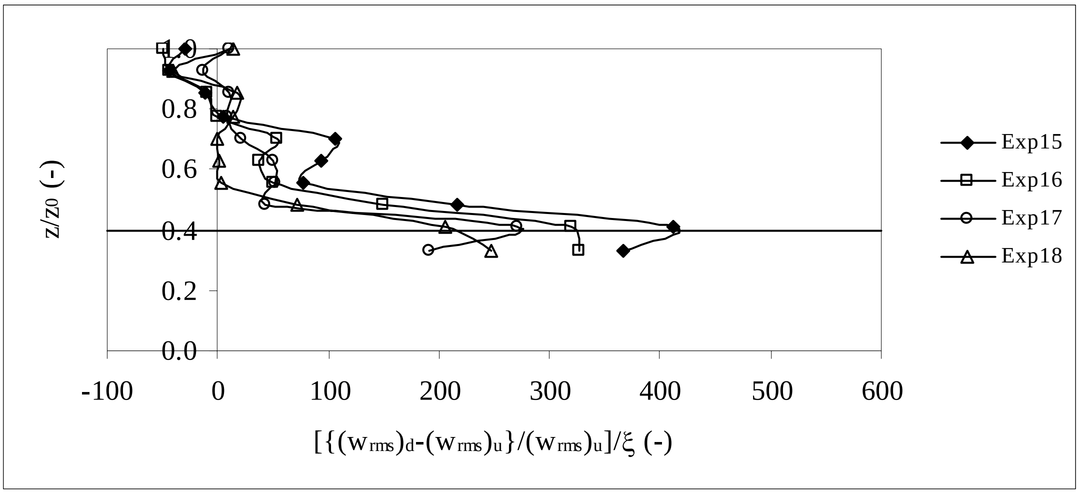

Figure G.3: The variation of normalized vegetative vertical turbulence intensity parameter with respect to relative depth for Type 3

APPENDIX H: THE VARIATION OF NORMALIZED VEGETATIVE TURBULENCE KINETIC ENERGY PARAMETER WITH RESPECT TO RELATIVE DEPTH FOR DIFFERENT TYPES

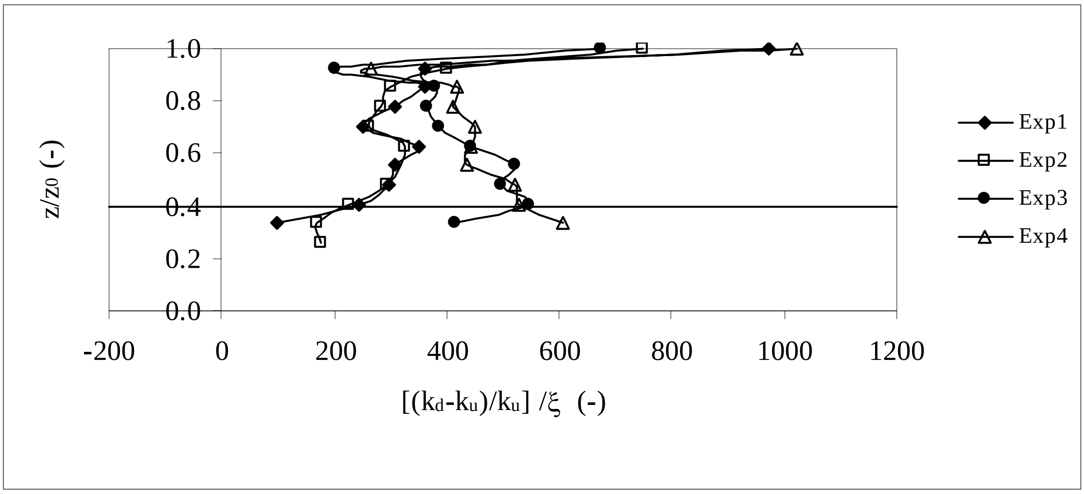

Figure H.1: The variation of normalized vegetative turbulence kinetic energy parameter with respect to relative depth for Type 1

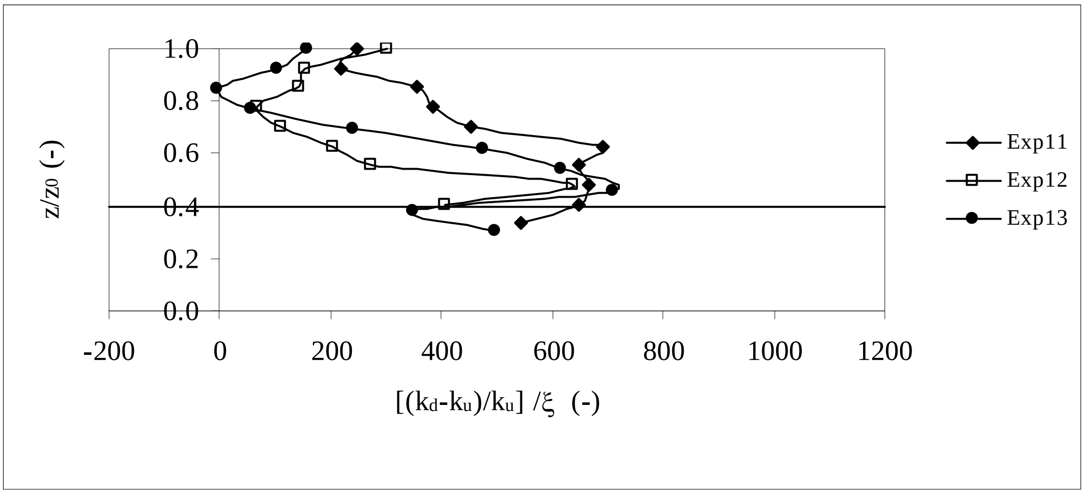

Figure H.2: The variation of normalized vegetative turbulence kinetic energy parameter with respect to relative depth for Type 2

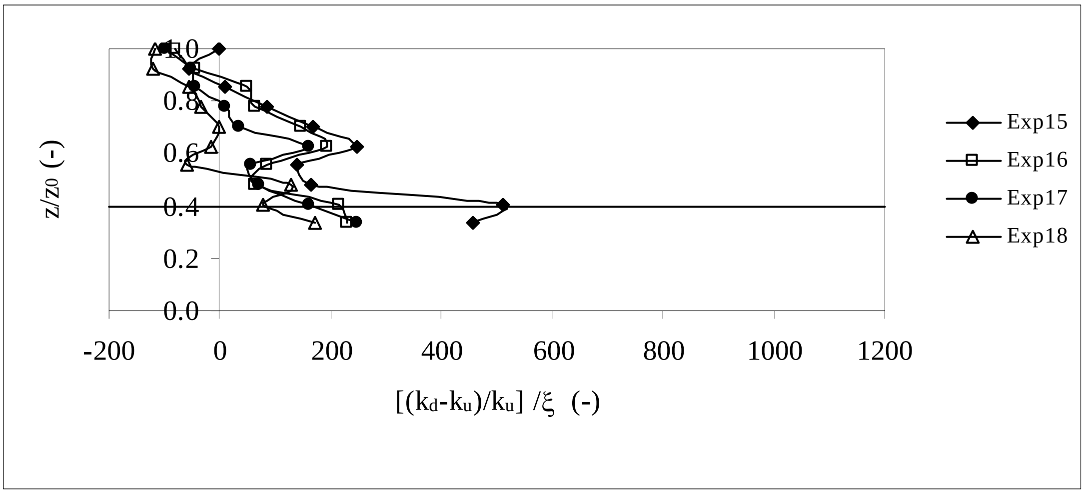

Figure H.3: The variation of normalized vegetative turbulence kinetic energy parameter with respect to relative depth for Type 3

CURRICULUM VITAE

Oral Yağcı was born in 1973 in İzmir. He received a Bachelor of Science degree in Civil Engineering in 1995 and Master of Science degree in Water Engineering in 2000 from Istanbul Technical University. He took a research assistant position at the Department of Civil Engineering in Trakya University for one year. Later on he started to work in the same position in Istanbul Technical University in 1998.

He won a research scholarship from *Scientific and Research Council of Turkey* (TUBITAK) and British Council and studied in Cardiff University for one year. He studied on 3D numerical modeling of a willow vegetated river/floodplain system.

His major research and professional interests are on fluid mechanics, hydraulics, design and stability of coastal structures, wave statistics, wave mechanics, and dynamic oceanography.

He authored 7 international journal papers, 4 papers and abstracts published in international conference proceedings, 5 papers published in national proceedings. He also authored 7 research reports.